

**Water-Soluble Rotaxanes:
Identifying Suitable Building Blocks for Molecular
Daisy Chains**

Inauguraldissertation

zur

Erlangung der Würde eines Doktors der Philosophie

vorgelegt der

Philosophisch-Naturwissenschaftlichen Fakultät

der Universität Basel

von

Sylvie Carolin Drayss-Orth

aus Lorsch, Deutschland

Basel, 2016

Originaldokument gespeichert auf dem Dokumentenserver der Universität Basel

edoc.unibas.ch

Genehmigt von der Philosophisch-Naturwissenschaftlichen Fakultät
auf Antrag von

Prof. Dr. Marcel Mayor

Prof. Dr. Thomas R. Ward

Basel, den 20. September 2016

Prof. Dr. Jörg Schibler
Dekan

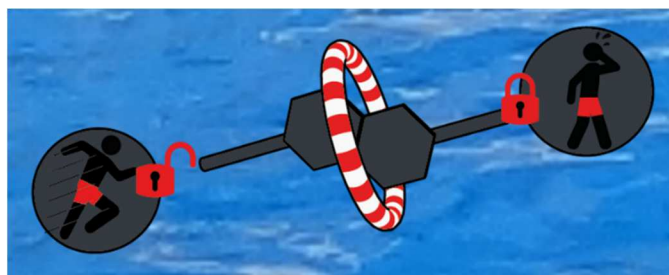
Die Naturforschung lehrt uns die Geschichte der Allmacht, der unergründlichen Weisheit eines unendlich höheren Wesens in seinen Werken und Taten erkennen; unbekannt mit dieser Geschichte kann die Vervollkommung des menschlichen Geistes nicht gedacht werden, ohne sie gelangt seine unsterbliche Seele nicht zum Bewusstsein ihrer Würde und des Ranges, den sie im Weltall einnimmt.

Justus Freiherr von Liebig
(1803 – 1873)

Abstract

Structurally diverse rotaxane-based systems have been investigated extensively for applications as molecular machines and functional nanomaterials. Although the vast majority of functional molecules were assembled and function in organic solvents, to date the most efficient and sophisticated molecular machines are biomolecules which function in aqueous media. Many vital processes, such as protein folding and assembly, rely on hydrophobic interactions and are only possible in aqueous environment. From a supramolecular chemistry perspective, the hydrophobic effect is an appealing driving force for host-guest association as it potentially leads to high complexation affinities and no extra binding sites need to be installed into the respective components. Appealing macrocyclic candidates for the preparation of mechanically interlocked molecules in aqueous media are the synthetically modifiable, water-soluble cyclophanes developed and comprehensively studied by Diederich et al..

The focus of this doctoral thesis was to identify suitable guest molecules for Diederich-type cyclophanes, allowing for the assembly of rotaxanes and also molecular daisy chains. The first part of the thesis describes the investigation of the aggregation behavior of amphiphiles based on OPE guests which are potentially capable of forming molecular daisy chains (Chapter 2). A deeper insight into the system was obtained through a series of rotaxane model compounds, basically relying on the main components of the previously examined amphiphiles (Chapter 3). The investigation of an extended scope of potential guest molecules via ^1H NMR complexation studies resulted in an optimization of the molecular guest design and revealed some important features of suitable candidates (Chapter 4). Based on these results a water-soluble 2,6-disubstituted naphthalene derivative was found to function as (pseudo)rotaxane axle and enabled the isolation and characterization of a [2]rotaxane (Chapter 5). The results obtained throughout this doctoral thesis allow to obtain guidelines for the successful preparation of interlocked molecular daisy chains.



- Chapter 1 provides a general introduction to mechanically interlocked molecules and explains basic conceptual and synthetic principles of rotaxanes and molecular daisy chains by means of introducing the most common recognition motifs, classified by different types of macrocycles, in particular Diederich-type cyclophanes.
- Chapter 2 describes the design, synthesis and aggregation studies of a series of amphiphilic molecules potentially capable of assembling to molecular daisy chains and to function as nanoscale potentiometer. Furthermore, the chapter contains MCBJ conductance measurements of a thiol-terminated amphiphile and attempts to obtain mechanically interlocked aggregates by reaction with bulky stopper molecules.
- Chapter 3 describes the design, synthesis and investigation of the threading behavior of different monostoppered OPE molecules in presence of Diederich cyclophanes via rotaxanation as well as ^1H NMR-based complexation studies.
- Chapter 4 describes the design, synthesis and ^1H NMR spectroscopy-based complexation studies of a series of potential guest molecules for mechanically interlocked molecules, comprising different solubilizing functionalities.
- Chapter 5 describes the assembly, isolation and characterization of a water-soluble rotaxane comprising a 2,6-disubstituted naphthalene axle moiety. Furthermore, a series of naphthalene axle derivatives, differing in their length of solubilizing oligoethylene glycol chains, were investigated in their propensity to react to rotaxanes by applying a modular proof-of-principle analysis strategy.
- Chapter 6 gives a summary of the obtained results of this thesis and provides an outlook.
- Chapter 7 provides the experimental details, including the characterization of all compounds described throughout the thesis.

Table of Contents

1 Introduction.....	1
1.1 Mechanically Interlocked Molecules.....	1
1.2 Rotaxanes and Molecular Daisy Chains.....	3
1.2.1 Molecular Daisy Chains	3
1.2.2 General Approaches to the Construction of Rotaxanes and Molecular Daisy Chains	5
1.3 Recognition Motifs in Rotaxanes and Molecular Daisy Chains	7
1.3.1 Crown Ether.....	8
1.3.2 Cyclodextrins	15
1.3.3 Cucurbiturils	19
1.3.4 Pillar[n]arenes	21
1.3.5 Calix[n]arene	25
1.3.6 Tetralactam based Macrocycles.....	28
1.3.7 Metal-ligand based Macrocycles.....	31
1.3.8 Tetracationic Cyclophanes.....	34
1.3.9 Diederich Cyclophanes	37
2 Towards Molecular [c2]Daisy Chains as Functional Materials	45
2.1 General Molecular Design of Amphiphiles 91-95.....	46
2.2 General Synthetic Approach for Amphiphiles 91-95.....	47
2.3 General Approach for the Aggregation Studies	49
2.3.1 ¹ H NMR Dilution Studies.....	49
2.3.2 DOSY Analysis	51
2.3.3 Fluorescence Spectroscopy	52
2.4 Synthesis and Aggregation Studies of Hydroxyl-substituted Amphiphile 92	53
2.4.1 Synthesis of Monomer 92	53
2.4.2 ¹ H NMR Dilution Studies.....	55
2.4.3 DOSY Analysis	57
2.4.4 Fluorescence Spectroscopy	58
2.5 Synthesis and Aggregation Studies of Acetylene-substituted Amphiphile 93	59
2.5.1 Synthesis of Monomer 93	59
2.5.2 ¹ H NMR Dilution Studies.....	60
2.5.3 DOSY Analysis	62
2.5.4 Fluorescence Spectroscopy	62
2.6 Synthesis and Aggregation Studies of Anthracene-substituted Amphiphile 94	63
2.6.1 Synthesis of Monomer 94	63

2.6.2 ^1H NMR Dilution Studies.....	64
2.6.3 DOSY Analysis	65
2.6.4 Fluorescence Studies.....	65
2.7 Synthesis and Aggregation Studies of <i>S</i> -Acetyl-substituted Amphiphile 95	66
2.7.1 Synthesis of Monomer 95	66
2.7.2 ^1H NMR Dilution Studies.....	68
2.7.3 DOSY Analysis	69
2.7.4 Further Analysis.....	69
2.8 Conductance Studies of Amphiphile 95	70
2.8.1 Mechanically Controllable Break Junction	70
2.8.2 Conductance Measurements	72
2.9 Stoppering of Interlinked Aggregates	73
2.10 Conclusion	76
3 OPE-based Rotaxane Test Systems	77
3.1 Molecular Design of the Rotaxane Building Blocks.....	78
3.2 Syntheses of the Rotaxane Building Blocks.....	79
3.3 Rotaxane Assembly Test Reactions.....	81
3.4 ^1H NMR Host-Guest Studies	84
3.5 Conclusion	89
4 Identifying Suitable Guest Molecules.....	91
4.1 Molecular Design of Guests.....	91
4.2 Syntheses of Guest Molecules.....	92
4.3 ^1H NMR Complexation Studies	93
4.4 Conclusion	101
5 Assembly of [2]Rotaxanes in Water	103
5.1 Introduction.....	103
5.2 Syntheses of Rotaxane Axles.....	105
5.3 Binding Studies	105
5.4 Screening Reactions	107
5.4.1 Reaction Conditions.....	107
5.4.2 Analysis of the Screening Reactions.....	108
5.5 Isolation and Characterization of [2]Rotaxane 170d.....	111
5.5.1 1D and 2D ^1H NMR Experiments	112
5.5.2 Optical Spectroscopy.....	114
5.6 Stability Test	114
5.7 Conclusion	115

6 Summary and Outlook.....	117
7 Experimental Section.....	121
8 Bibliography.....	193
9 Appendix.....	202
9.1 Abbreviations	202
9.2 Contributions.....	205
9.3 Chromatograms of Screening Reactions	206

1 Introduction

1.1 Mechanically Interlocked Molecules

The Nobel Prize in Chemistry awarded jointly to Donald J. Cram, Jean-Marie Lehn, and Charles J. Pederson in 1987 “for their development and use of molecules with structure-specific interactions of high selectivity”, established supramolecular chemistry as one of the most important research fields in today’s chemistry. The “chemistry beyond the molecule”^[1] relies on the noncovalent bonding interactions between molecular subunits or components, such as metal coordination, π - π stacking, donor-acceptor interactions, hydrogen bonding, hydrophobic forces, van der Waals interactions and halogen bonding.^[2] Combining supramolecular chemistry with traditional covalent synthesis allows accessing mechanically interlocked molecules (MIMs). The unique properties of MIMs can be explained by the subtle coordinative/noncovalent interactions and features of associated robust covalent structures and their interplay with each other.^[3] The different components of MIMs are linked together mechanically. Catenanes (Latin for chain) and rotaxanes (*rota* is Latin for wheel, and *axis* is Latin for axle) are the two basic classes in which mechanically interlocked structures are divided in (Figure 1). In contrast to catenanes, which consist of interlinked ring shaped molecules, in rotaxanes one or more rings encircle one or more dumbbell shaped molecules. The number of interlocked components is indicated in bracketed prefixes, e.g. the [2]rotaxane in Figure 1 consists of one macrocycle which encircles one dumbbell unit. As breaking of a covalent bond is required in order to separate the interlocked elements from each other, MIMs are by definition molecules and not supramolecular structures.

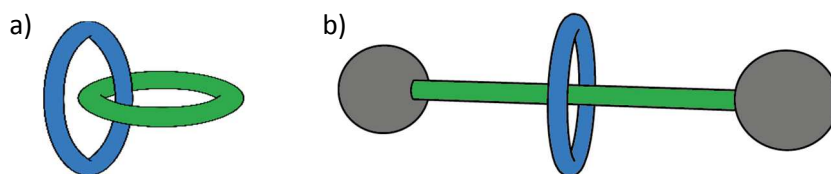


Figure 1. Schematic representation of the two MIM classes; a) catenane, b) rotaxane.^[2]

Whereas both the first catenane^[4] and rotaxane^[5] synthesis relied on statistics, yielding molecules **1** in less than 1% and molecule **2** in 6% (Figure 2), the first directed synthesis of a catenane in 1964 followed a 20 step-protocol.^[6]

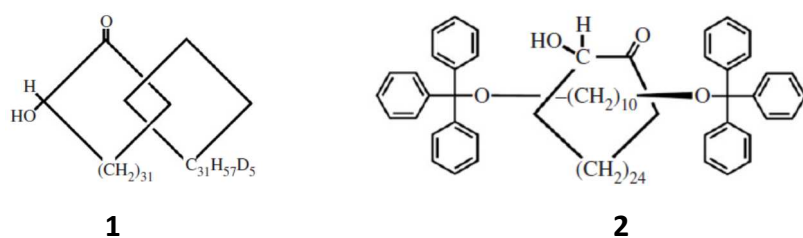


Figure 2. The chemical structures of the first reported catenane (1) and rotaxane (2).^[2]

In 1983 Sauvage and coworkers successfully developed the first noncovalent directed synthesis, based on the coordination of the two catenane components with a transition metal.^[7] The phenanthroline moiety of a closed macrocycle was linked via a Cu(I) ion to another phenanthroline located at the open precursor of the second catenane ring resulting in a preorganization for the final cyclization reaction. The Cu(I) template of metallo-catenane **3** was removed via ligand-exchange with cyanide anions, resulting in catenane **4**.^[8]

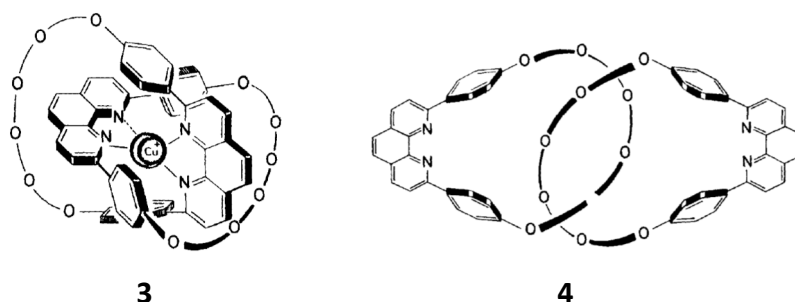


Figure 3. The chemical structure of Sauvage's metallo-catenane **3**^[7] and its demetalated analog **4**^[8].

Initiated by these pioneering results, various recognition motifs for the templated MIM syntheses relying on noncovalent interactions have been explored resulting in a large toolkit (see chapter 1.3). This synthetic advancement inspired chemists to design and synthesize a variety of MIMs with large structural diversity and numerous functions, including artificial switches, molecular muscles and molecular machines in general. Aiming at their integration into larger functional systems, such nanomaterials find potential applications in electronic devices, sensors, smart materials, and drug delivery.^[9]

1.2 Rotaxanes and Molecular Daisy Chains

1.2.1 Molecular Daisy Chains

Molecular daisy chains^[10,11] are a subclass of rotaxanes, conceptually introduced by Stoddart and Williams in 1998.^[10] Consisting of self-complementary monomers, which are able to form chain-like assemblies, reminiscent of daisy flower garlands (Figure 4a). In contrast to rotaxanes, the thread moiety is covalently bound to the ring, resulting in monomers which intermolecularly – rather than intramolecularly – assemble to cyclic or acyclic chains. Bulky stopper groups at the rods' termini prevent dethreading into monomers, converting the supramolecular bonded components into mechanically interlocked molecules. The mechanical bond provides kinetical stability,^[12] whereas stability and molecular weights in unstoppered, interlinked daisy chains are sensitive to the environmental conditions (i.e., concentration, temperature, solvent). The self-complementary monomers are also termed as plerotropic^[10], hermaphroditic^[13] or heteroditopic^[14] in literature. Prefixes indicate the number of interlocked monomers [*n*] and specify their connectivity, in particular if they are assembled as an acyclic [*a*] or cyclic [*c*] chain (Figure 4b and c).

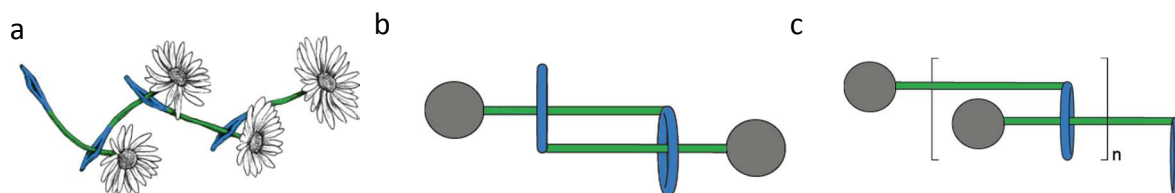


Figure 4. a) Daisy flower garland, b) interlocked [c2]daisy chain, c) interlocked [an]daisy chain.

To date, the majority of the reported daisy chain systems were isolated as discrete cyclic dimers, which seem to be thermodynamically more favorable than their acyclic analogs. In [c2]daisy chains, there are two stabilizing host-guest interactions present, whereas in the [a2]assembly only one stabilizing interaction exists. The free rod and/or the respective macrocycle might undergo unfavorable cohesive and dispersive interactions.^[11]

The increased interest in interlinked [an]daisy chain polymers is due to their unique properties, such as reversibility and responsiveness to stimuli, which makes them ideal candidates for biomedical applications.^[15–17] As the aggregation of polymeric [an]daisy chains is entropically unfavorable,^[18] high monomer concentrations and strong host-guest binding

affinities are crucial, rendering the design and synthesis of monomers challenging. For example, Huang and coworkers discovered that rigid threads are not necessarily the only path to compensate entropic cost of polymerization. In their novel approach, flexible alkyl chains covalently link the host and guest moiety, which, in combination with high monomer concentration, resulted in long polymeric [an]daisy chain fibers (see chapter 1.3.1)^[19] In cyclodextrine-based systems, the linking position of the thread moiety on the cyclodextrin rim also affects the aggregation behavior, ranging between selective dimer-formation and acyclic daisy chains (see chapter 1.3.2).^[20]

[c2]daisy chains are of particular interest for applications as artificial molecular muscles.^[21] Upon actuation, driven by an external stimulus, such as change of pH, metal exchange, variation of the solvent (protic/aprotic or polar/apolar) or oxidation/reduction, bistable [c2]daisy chains can access two different states.^[22] In such molecular muscles, the switching is accompanied by linear motion along the axis' dimension, which results in contraction or extension of the system.

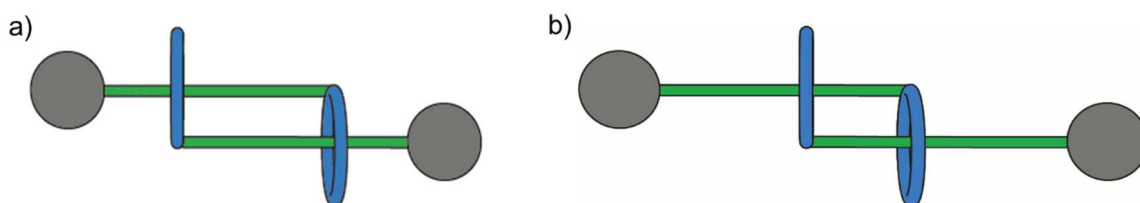
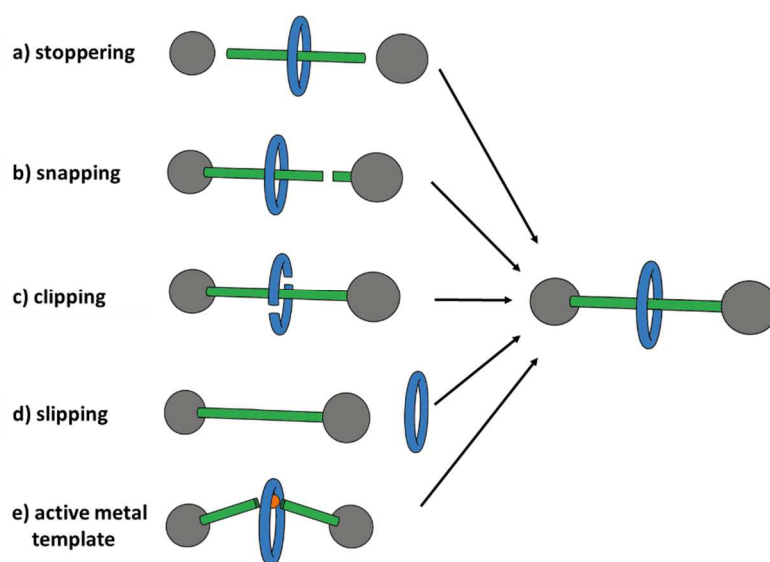


Figure 5. Bistable [c2]daisy chain working as an artificial molecular muscle; a) contracted and b) extended state.

Like muscle fibers, the sacromers, poly[c2]daisy chains consist of numerous switchable units. The addition of all synchronized single nanoscale motions result then in a macroscopic motion. So far, only few muscle-like poly[c2]daisy chains were reported and the majority showed only a low degree of polymerization. In contrast to the previously reported systems bearing 5–11 repeating units,^[23–25] the groups of Buhler and Giuseppone achieved poly[c2]daisy chains of high molecular weight, composed of ~ 3000 repeating units.^[26] The contour lengths of the extended state (15.9 μm) and the contracted system (9.4 μm) differed by remarkable 6.5 μm .

1.2.2 General Approaches to the Construction of Rotaxanes and Molecular Daisy Chains

This subchapter schematically introduces the template-directed synthetic methodologies for rotaxanes^[27] and the corresponding general approaches for the synthesis of molecular daisy chains. Scheme 1a demonstrates the *stopping* method (e.g. chapter 1.3.8), in which the formation of a pseudorotaxane is subsequently followed by the reaction of the two thread termini with bulky stopper molecules.^[28] In the *snapping* mechanism (e.g. chapter 1.3.2) a semirotaxane, consisting of a monostoppered axis encircled by a macrocycle, reacts with a second single stoppered (shorter) axle to a rotaxane.^[29] This strategy is well-suited for the construction of unsymmetrical rotaxanes.

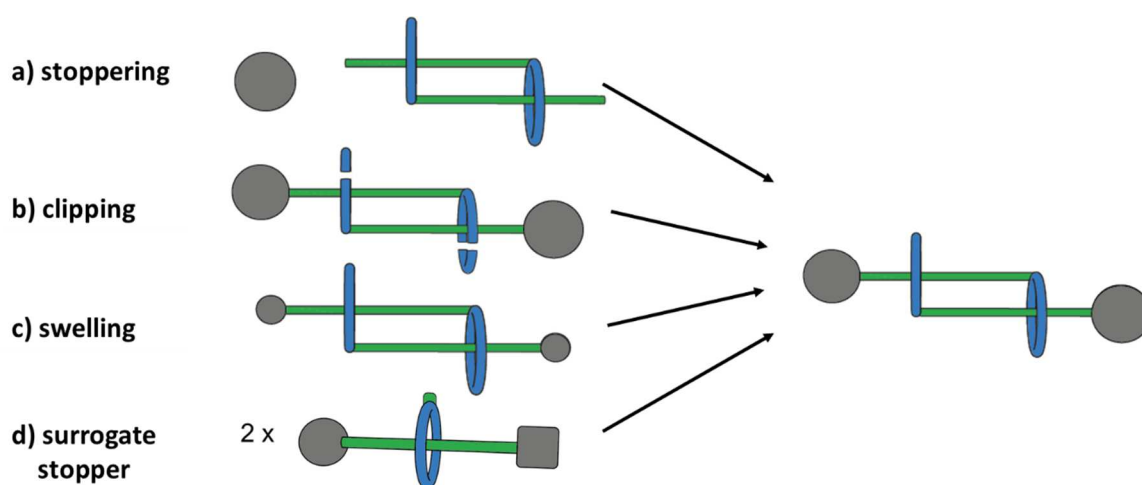


Scheme 1. General approaches to the construction of rotaxanes.^[22]

In the third approach the *clipping* method (e.g. chapter 1.3.8) is exhibited, in which the ring molecule is formed around the dumbbell shaped unit.^[30] If the macrocycle threads over a stopper moiety of the dumbbell, the approach is termed *slipping*.^[31] In order to circumvent the elevated temperature crucial for *slipping*, the dumbbell may comprise small terminal groups, which will be increased in size after the ring encircled the axle.^[32] Scheme 1e demonstrates the *active metal template* approach (e.g. chapter 1.3.6), in which a metal ion in the macrocycle both acts to pre-organize the rotaxane components and catalyzing the formation of the mechanical bond.^[33]

Usually low concentrated reaction solution are employed for the preparation of [c2]daisy chains in order to prevent the formation of acyclic oligomers. The *stopping*^[23] method (e.g.

chapter 1.3.4) as well as the *clipping*^[34] approach (e.g. chapter 1.3.6) are both well-established templated synthetic strategies. Scheme 2c demonstrates the less common used *swelling*^[35] method (e.g. chapter 1.3.1). The terminal groups of the axle are triggered by an external stimulus to transform to bulky stoppers. An alternative method for the preparation of [c2]daisy chains is based on a rotaxane with two different stoppers. One is inert, whereas the other one is reactive, also called a *surrogate stopper*^[36] (e.g. chapter 1.3.1), as it is cleaved off during the reaction with a functional group located at the macrocycle.



Scheme 2. General approaches for the preparation of [c2]daisy chains.

Poly[c2]daisy chains are composed of [c2]daisy chain repeating units, which bear an anchoring group at the thread termini for linkers, connecting the dimers to a polymer (e.g. chapter 1.3.1). As already mentioned in the previous chapter, acyclic polymeric daisy chains are often synthesized statistically in high concentrated solutions. An alternative approach is based on the formation of a semirotaxane, which bears at the macrocycle a thread moiety.^[37] This moiety reacts with the unstoppered terminus of the semirotaxane axle, resulting in acyclic daisy chains (see chapter 1.3.1).

1.3 Recognition Motifs in Rotaxanes and Molecular Daisy Chains

In this subchapter the most common recognition motifs employed for the construction of rotaxanes and molecular daisy chains are introduced and classified by different macrocycle types. The characteristic structural features as well as the general complexation behavior of each cavitant with its typical guest molecules is explained briefly. Furthermore, this chapter gives a rough overview about the state of the art and seizes basic conceptual and synthetic principles of the mechanically bonded molecules by means of selected examples. The different recognition motifs are mainly discussed on the basis of the more specialized and advanced daisy chain systems.

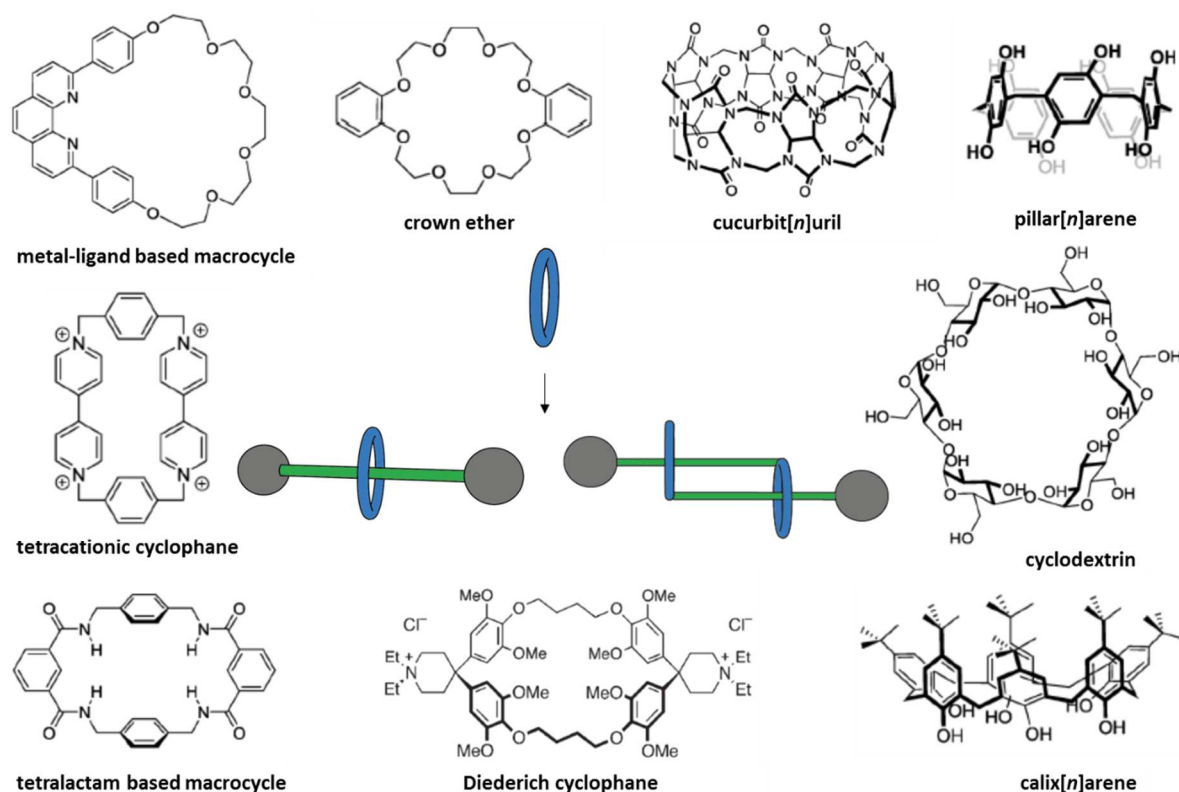


Figure 6. Common macrocycles used for rotaxane and daisy chain preparation.

1.3.1 Crown Ether

The discovery of crown ethers and their ability to bind metal ions by Pederson in 1967^[38] has contributed essentially to the development of supramolecular chemistry. The cyclic ethers, usually bridged by ethylene units, were employed as macrocycle components in numerous mechanically interlocked systems. Dibenzo-24-crown-8 (DB24C8), benzo-21-crown-7 (B21C7), bis(*m*-phenylene)-32-crown-10 (BMP32C10) (Figure 7) and their corresponding substituted derivatives, are the most prevalent crown ether hosts in MIMs, binding organic nitrogen cations such as (di)benzylammonium or viologen cations. The main molecular interactions are attributed to C-H...O hydrogen bonding and N⁺...O electrostatic interactions between organic guests and the cyclic ethers as well as π - π stacking interactions between aromatic units of host and guest.

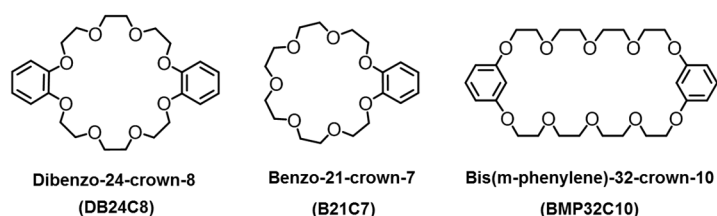


Figure 7. Most relevant crown ethers for the synthesis of interlocked molecules.

Stoddart and Williams introduced the daisy chain terminology in 1998, when they reported the X-ray structure of a [c2]daisy chain obtained by the assembly of monomer **5** comprising a DB24C8 macrocycle and a benzylammonium thread unit.^[10] The early investigations of this novel system^[39] already approached important conceptual aspects influencing the molecular daisy chain systems, such as solvent polarity and character, temperature, monomer concentration, chain propagation and isomerism in aggregates.

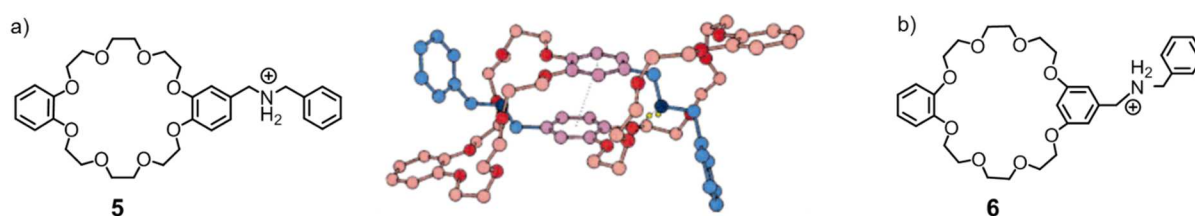


Figure 8. a) The monomeric unit (**5**) and the corresponding crystal structure showing the first molecular daisy chain as a cyclic dimer;^[10] b) [25]crown-8 analogue (**6**)^[39] of monomer **5**.

The rather simple ^1H NMR spectrum of **5** in CD_3SOCD_3 , in which all signals could be assigned, remarkably contrasted the complicated spectrum of the same compound in CD_3CN , indicating daisy chain formation in the latter, less polar solvent. In CD_3SOCD_3 solvation of the ammonium center occurred preferentially by hydrogen bonding with the solvent, whereas in CD_3CN the cationic thread is encircled by the crown ether, resulting in [c2]daisy chains as the most favorable species. In CD_3CN , monomeric species were observed only at elevated temperature (358 K) and high dilution (0.026 mM). Furthermore, aggregation could be hindered by deprotonation of the ammonium center, while reprotonation promoted the association again. An important finding was the presence of diastereoisomeric dimers in solution, which also contributed to the complicated ^1H NMR spectrum in CD_3CN . Further investigations revealed the presence of two different species with the ratio 5:1, strongly indicating the presence of the enantiomers with C_2 symmetry and the centrosymmetric (C_i) meso species shown in Figure 9.

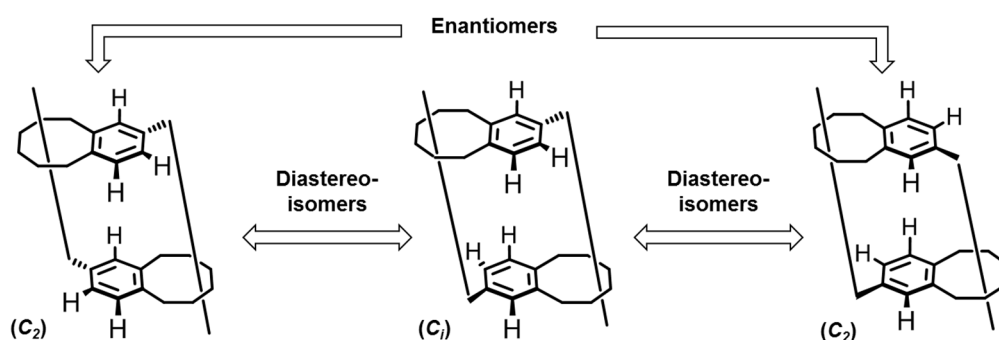


Figure 9. Schematic representation of the three stereoisomers which can form upon dimerization of monomer **5**.

In attempt to circumvent the formation of diastereoisomers, the more symmetrical monomer **6**, which comprised a [25]crown-8-based macrocycle, was synthesized and studied. Acyclic trimeric [a3]daisy chains were observed in CD_3CN upon exceeding a concentration of 1 M, which the authors attributed to the weaker interaction of the secondary ammonium with DB25C8.

In 1987, Stoddart and coworkers demonstrated that the larger crown ether BMP32C10 binds paraquat in acetone.^[40] On the basis of this host-guest recognition, Gibson and coworkers synthesized monomer **7**, which undergoes chain propagation resulting in linear fibers with up to 50 repetition units in a 2 M solution in CD_3COCD_3 .^[41] The aggregation number n , was

calculated based on ^1H NMR dilution studies and further evidence for polymerization were given by the measurement of the glass transition temperature and differential scanning calorimetry.

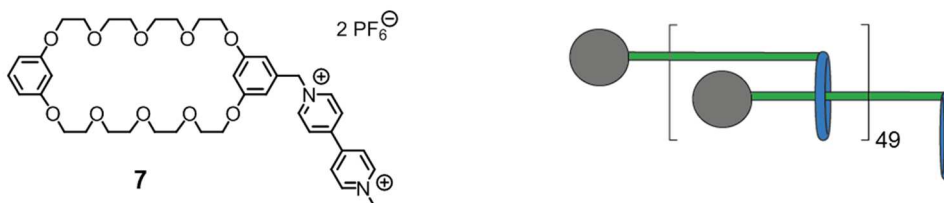
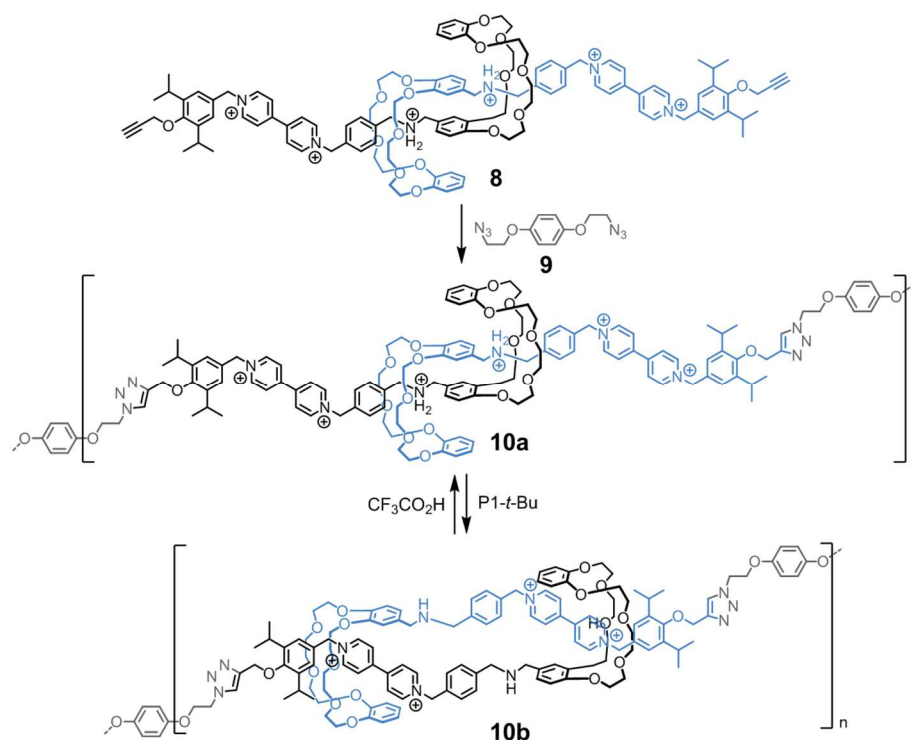


Figure 10. Hermaphroditic monomer **50**, which assembles to linear polymers in acetone.^[41]

The recognition motif between crown ethers and secondary ammonium and paraquat, respectively, is often exploited in aprotic solvents to create mechanically interlocked molecules that respond to pH changes.^[22] Employing DB24C8 in such a pH triggerable system, the macrocycle has a stronger affinity to the secondary ammonium ion than to paraquat, and therefore predominantly binds the ammonium motif. Upon addition of base, the secondary ammonium is deprotonated and hence the strength of hydrogen bonding interaction with the macrocycle decreases. The crown ether migrates to the permanent cation paraquat and stabilizes the charged unit also via hydrogen bonding and π -associated donor-acceptor interactions. The system can be switched back to the primary state by reprotonation of the amine moiety. Scheme 3 shows an artificial molecular muscle system developed by Stoddart and coworkers, in which monomers are aggregated to form interlinked [c2]daisy chains (**8**), driven by DB24C8/ammonium recognition.^[24,25] The terminal propargyl group react with the symmetrical azide functionalized linker **9** to oligomers, which contain up to 11 repetitive units. Similar to single [c2]daisy chain dimers, the change of pH value ensues migration of the macrocycle along the molecular axis in the oligomer and leads to a length variation between the elongated (**10a**) and the contracted state (**10b**) of 48%.



Scheme 3. Acid/base switchable [c2]daisy chain polymer in the elongated (**10a**) and contracted state (**10b**).^[24,25]

In 2007, Huang and coworkers demonstrated that secondary dialkylammonium salts can be bound by the smaller crown ether B21C7 with even higher affinity in acetone (up to $K_a = 1.0 \times 10^3 \text{ M}^{-1}$) compared to the larger DB24C8 cavity (up to $K_a = 0.3 \times 10^3 \text{ M}^{-1}$).^[42] The first B21C7-based hermaphroditic monomer (**11**), which assembles to [c2]daisy chains in acetone, was prepared by the same research group.^[43] The investigation of the chemically driven reversible threading and dethreading revealed the system to be dual-responsive, not only towards pH changes, but also towards controlled addition and removal of potassium ions. In the presence of an equimolar amount of KPF_6 the polyether ring is occupied by K^+ and therefore daisy chain formation is suppressed. Expanding the distance between crown ether and the ammonium site with the help of a flexible alkyl chain, afforded polymeric structures.^[19]

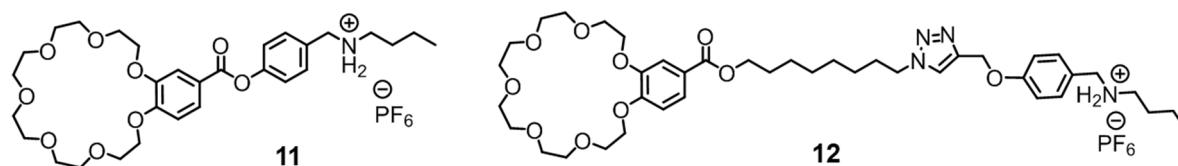


Figure 11. Daisy chain monomers comprising the B21C7/ dialkylammonium recognition motif found by Huang and coworkers. **11**^[43] favorably forms dimers, whereas analogue **12**^[19] polymerizes in solution.

A supramolecular network gel was obtained from the fibers by adding Pd(II) as a crosslinker, which binds the 1,2,3-triazol unit in the polymer backbone (Figure 12).^[44] The viscosity of the system could be triggered by acid/base, addition of the competing crown-ether guest K⁺ and heating/cooling.

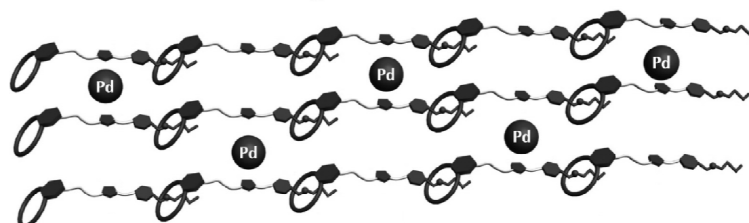
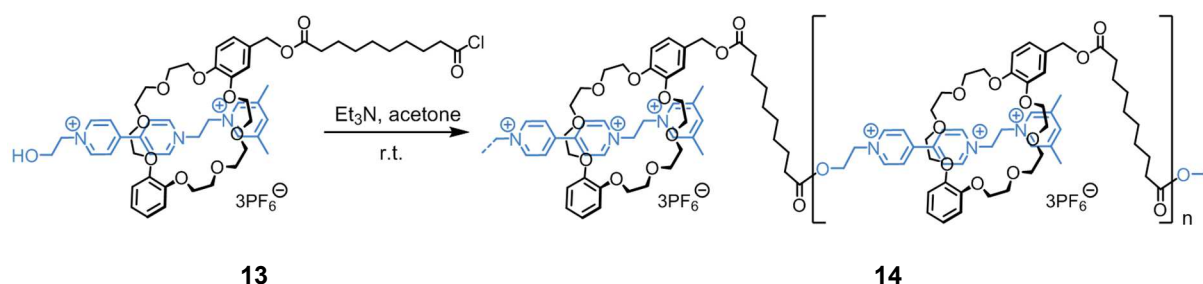


Figure 12. Schematic representation of the formation of cross-linked supramolecular polymer comprising monomer **12** with Pd(II) as crosslinker.^[44]

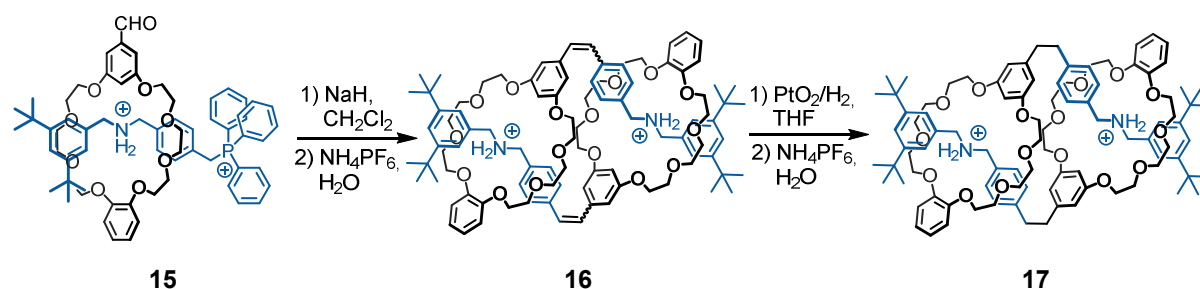
Flexibility of the thread helped to overcome the formation of thermodynamically favored [c2]daisy chains, which is a premise in order to achieve the formation of acyclic polymers. The *threading-followed-by-polymerization* synthetic strategy, reported by Huang and coworkers, is based on the flexible semirotaxane (**13**).^[45] Compound **13** comprises a 1,2-bis(pyridinium)ethane unit, bound by a DB24C8 macrocycle, which is substituted with a flexible C8-alkyl chain. The acetyl chloride functionality polycondensates with the hydroxyl group of the monostoppered axle to a linear, mechanically interlocked polymer (**14**) containing approximately 45 repeating units.



Scheme 4. Threading-followed-by-polymerization approach based on the polycondensation of the bifunctional pseudorotaxane **13**.^[45]

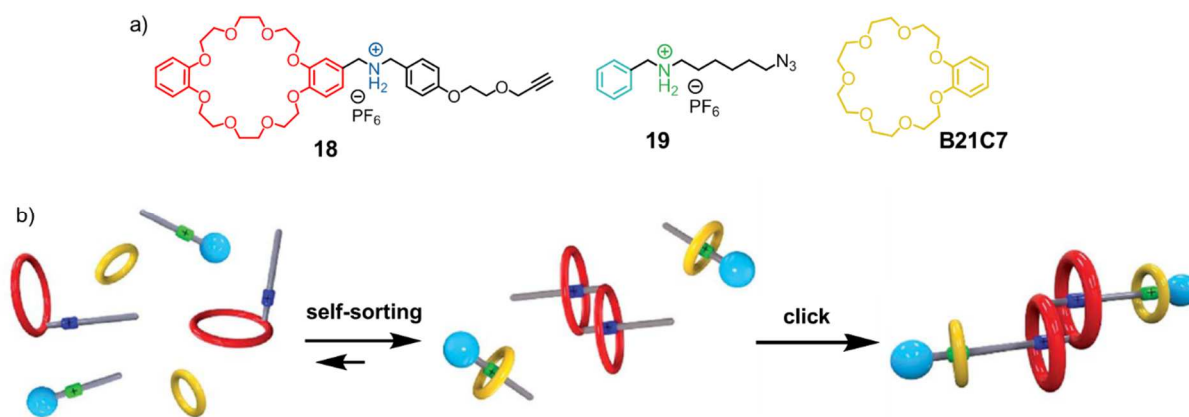
Based on a similar binding motif, Stoddart and coworkers developed the *surrogate stopper* procedure for the preparation of [c2]daisy chains.^[46] A rotaxane, bearing both an inert stopper and a triphenylphosphonium group as a reactive stopper, reacts to daisy chains without losing

the interlocked character during the transformation. The triphenylphosphonium group undergoes an intermolecular Wittig reaction with the aldehyde functionality attached to the 25-crown-8 ether and forms a stilbenoid linked daisy chain as a mixture of cis and trans isomers. The dethreading of the by sodium hydride deprotonated binding site is hindered during the Wittig reaction. At a reaction concentration of 5 mM [c2]daisy chains (**16**) were afforded in 50% yield. The C=C double bond could be hydrogenation in the last step.



Scheme 5. [c2]Daisy chain synthesized via the surrogate stopper method starting from a [2]rotaxane.^[46]

Very recently, Tian and coworkers utilized the crown ethers DB24C8 and B21C7 for size-dependent self-sorting and afforded the construction of a hetero[4]rotaxane in 50% yield (Scheme 6).^[47] The structural complex product was prepared by a facile one-pot synthesis, in which the three starting materials self-sorted into an [c2]daisy chain and a semi[2]rotaxane, respectively. The interlinked compounds were connected to the hetero[4]rotaxane via mild copper(I)-catalyzed alkyne-azide cycloaddition (CuAAC).^[48–50] The thread moiety of **18** was employed as a selective site which can only be bound by the macrocycle DB24C8, but not by B21C7. The dialkylammonium site in axle **19** was favorably complexed by the smaller macrocycle B21C7, which has a higher affinity for ammonium ions than DB24C8. Hence, axle **19** does not affect the daisy chain formation of **18**, which has been shown by ¹H NMR measurements.



Scheme 6. One-pot synthesis of a hetero[4]rotaxane by employing a self-sorting strategy.^[47]

The versatility of crown ethers in daisy chains is also shown in the *threading-followed-by-swelling* method, in which an external trigger causes size increase of reactive terminal axle groups, as reported by Chiu and coworkers.^[35] The symmetrical macrocycle of monomer **20**, bearing a pyridyl unit, was chosen to prevent diastereomer formation, observed in preliminary experiments, despite lower binding affinity towards dibenzylammonium ions in CD_3CN ($K_a = 40 \text{ M}^{-1}$) and a rather low yield. Heating a 11 mM solution of hermaphroditic monomer **20** in chloroform/acetonitrile 10:1 at 40 °C for 120 hours afforded 77% yield of the interlocked [c2]daisy chain. The elevated temperature promoted the transformation of the cyclopropane end groups into the much bulkier cycloheptadiene stoppers.

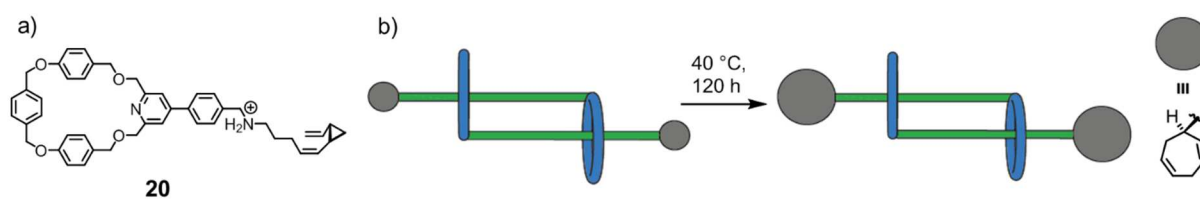


Figure 13. a) Hermaphroditic daisy chain monomer **20**, b) the reactive end groups of the interlinked aggregate react to bulky cycloheptadiene stoppers, resulting in interlocked [c2]daisy chains.^[35]

1.3.2 Cyclodextrins

Cyclodextrins (CDs) are macrocycles consisting of cyclic 1→4 α -linked D-(+)-glucopyranose units. The homologous series of CDs is distinguished by the number of incorporated oligosaccharide, normally comprising 6 (α -CD), 7 (β -CD) or 8 (γ -CD) units, which defines the ring size. The numerous hydrophilic groups are generally directed to the outer sphere resulting in a hydrophobic cavity, which exhibits a truncated, funnel-like shape with primary hydroxyl groups at the narrow site and secondary hydroxyl substituents at the wide rim.^[51]

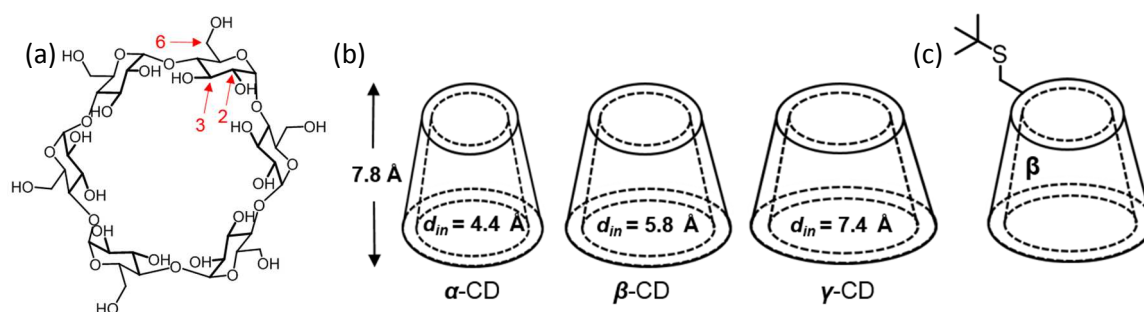


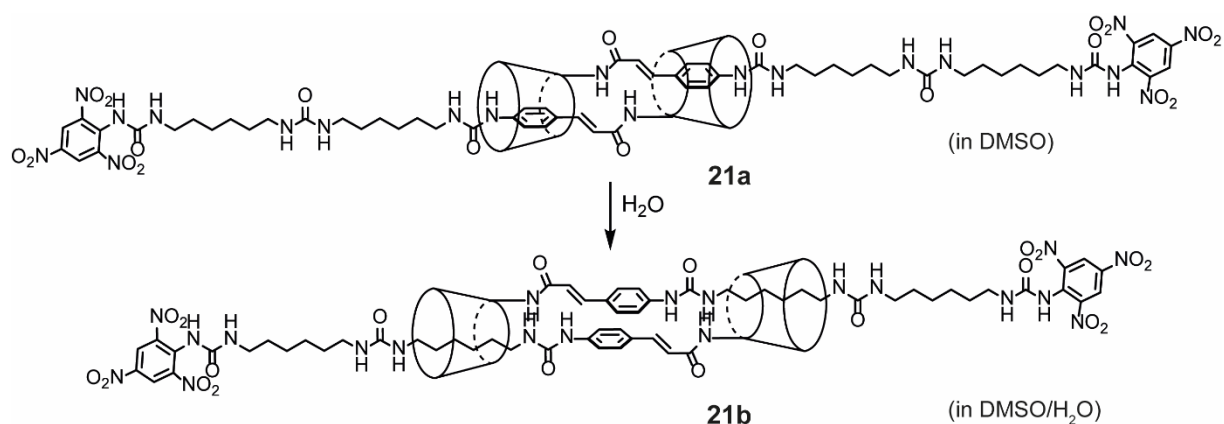
Figure 14. a) Chemical structure of α -cyclodextrine, b) the schematic representation of α - β - γ -cyclodextrine with their cavity width and corresponding internal diameters,^[51] and c) the schematic structure of the first daisy chain monomer.

In 1982, Hirotsu, Fujita and Tabushi were the first who observed the intermolecular inclusion of monofunctionalized cyclodextrins^[52] and hence by definition the first daisy chain, although the terminology was introduced later.^[10] The β -cyclodextrin was functionalized with a *tert*-butylthiol group, resulting in the formation of dimers, trimers and also oligomers at high concentrations in aqueous medium.^[52]

In general, hydrophobic organic molecules form strong inclusion complexes with CDs in aqueous medium driven by hydrophobic interactions (K_a values in water between 10^2 M^{-1} and 10^5 M^{-1})^[51]. As observed in multiple rotaxane-based examples, many linear molecules, can be employed as guests in the syntheses of cyclodextrine-based MIMs, sufficient hydrophobicity and appropriate diameter size provided.^[27] Alkyl chains substituted with polar solubilizing groups, such as $[\text{R}(\text{CH}_2)_n\text{R}']^{m+}$ ($m = 0-2$, R or R' = pyrazine, bipyridine, amino, amido or carboxylic groups) are commonly used as thread molecules.

In [c2]daisy chain muscle **21** reported by Harada et al., an amido moiety is located adjacent to a cinnamoyl group, the main binding site for the α -CD, in dimethyl sulfoxide. Upon addition

of water, the α -CD ring moves to the adjacent hexamethylene chain in order to shield it from the more polar solvent, resulting in a contraction of the system.^[53]



Scheme 7. Solvent-switchable molecular muscle **21** with the cinnamoyl group and the hexamethylene chains as recognition sites.^[53]

Cinnamamide is also harnessed as guest in another interesting system developed in the Harada group.^[20] Monofunctionalized CD rings are permeated by *N*-methyl cinnamamide from the narrower rim, although entering from both sides should be possible, as affirmed by molecular models with unmodified CDs. Taking this phenomenon into account, depending on the linking position at the CD ring, either cyclic dimers or acyclic oligomers are favored (Figure 15). [c2]daisy chains (**22a**) were constructed, in case of the linkage at position 6, whereas linkage at the wider rim in 3-position afforded oligomeric [a12]daisy chains (**22b**).

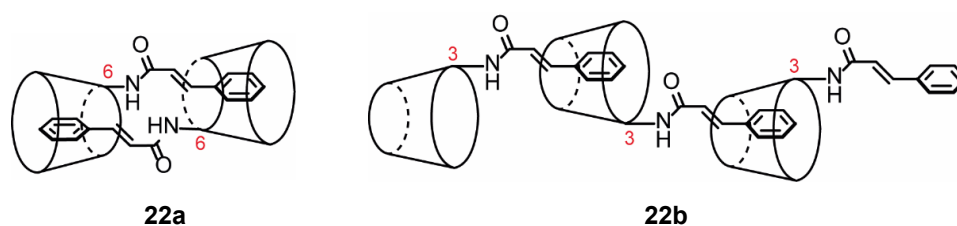


Figure 15. [c2]daisy chain of 6-cinnamonyl α -CDs, and [a12]daisy chain of 3-cinnamonyl α -CDs.^[20]

Very recently, Harada and coworkers reported a novel kind of molecular muscle.^[54] The cyclodextrine-based [c2]daisy chain repeating units are linked by four-armed polyethylene glycol chains affording wet- as well as dry-type gel artificial molecular muscles (**23**). Upon ultraviolet irradiation, the numerous photo-responsive azobenzene guests undergo a

conformational change and the macroscopic gels bend towards the light source. The fast-responsive dry-type gel was even used as a crane arm to lift an object.

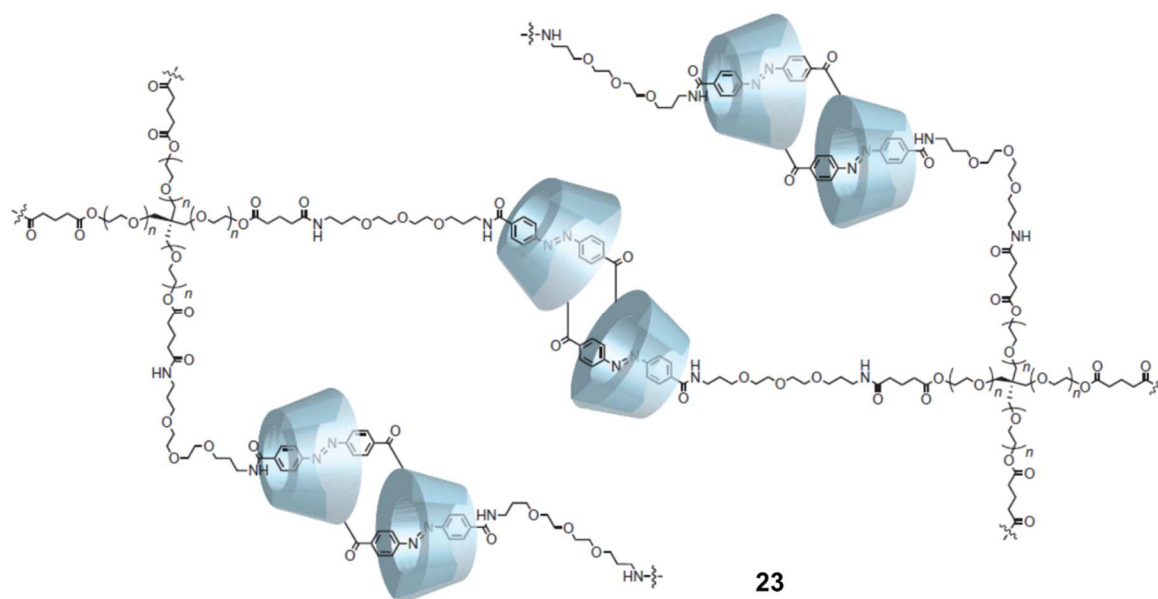
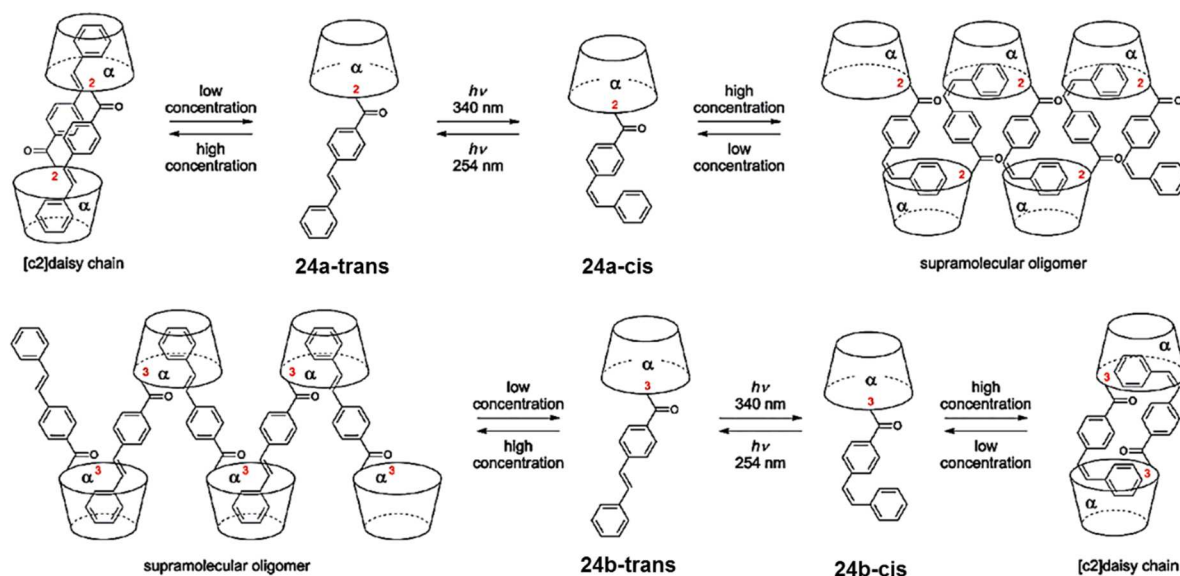


Figure 16. Chemical structure of a polymeric [c2]daisy chain gel working as artificial molecular muscles.^[54]

The geometrical features of the thread also control the aggregation behavior of daisy chain monomers (Scheme 8). The *trans*-stilbene functionalized α -CD monomer **24a-trans** forms dimeric daisy chains. Photoirradiation with $\lambda = 340$ nm leads to its *cis*-isomer (**24a-cis**), which forms acyclic oligomeric daisy chains at high concentrations. 2D NMR and diffusion coefficient studies revealed the same reversible photo-triggerable aggregation behavior in 3-substituted derivatives **24b**, however with the opposite result. Conclusively, the aggregation behavior of both the 2- and 3-substituted monomeric units can conveniently be accessed and controlled by external physical input.



Scheme 8. Schematic illustration of the photo-triggered aggregation behavior of stilbene functionalized α -cyclodextrins, dependent on the *cis*- or respectively *trans*-configuration and on the linkage position of the stilbene thread. Reprinted from reference.^[11]

Most of the CD-based mechanically interlocked rotaxanes or daisy chains were synthesized via the *stopping* approach. As stable inclusion complexes are solely formed in aqueous or highly polar media, the bulky molecules for the subsequent capping reaction have to be soluble in polar solvents. Many daisy chains, in particular α -CD based systems, contain a primary amine moiety used as anchor group for bulky stoppers, with which they react under basic conditions via aromatic substitution (**25** and **26**)^[53,55] or condensation (**27**)^[56] to mechanically interlocked molecules. (Figure 17).

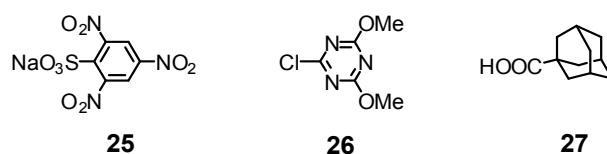
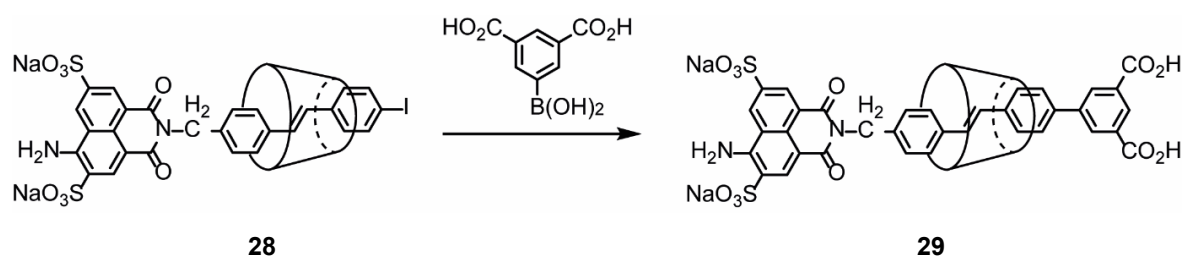


Figure 17. Examples for bulky stopper molecules applied for α -CD based MIM syntheses.

But also Suzuki couplings^[57], which work efficiently in aqueous media, turned out to be a powerful method for interlocking cyclodextrine-based systems. For example in the so-called *snapping* approach, inclusion complex **28**, already stoppered at one end of the thread, reacts in the rotaxation step with 5-boronoisophthalic acid.^[58]



Scheme 9. Snapping approach for the synthesis of rotaxane **29** based on the Suzuki coupling reaction.^[58]

Similarly, Anderson and coworkers comprehensively explored the behavior of organic semiconductors encapsulated with cyclodextrin rings. In most cases, the supramolecular (poly)-pseudorotaxanes were prevented from dethreading by stoppering via aqueous Suzuki^[57] reaction. Remarkably, the “insulated molecular wires” showed increasing fluorescence quantum yields, electroluminescence efficiencies, and chemical stabilities compared to the free, unshielded semiconductors.^[59–65]

1.3.3 Cucurbiturils

Cucurbit[*n*]urils (CB[*n*]) are water-soluble macromolecules consisting of *n* glycoluril units that are linked by methylene groups in the acid-catalyzed condensation reaction of glycoluril and formaldehyde at high temperatures. The most common CB[*n*]-based hosts in supramolecular chemistry are CB[6], CB[7] and CB[8].

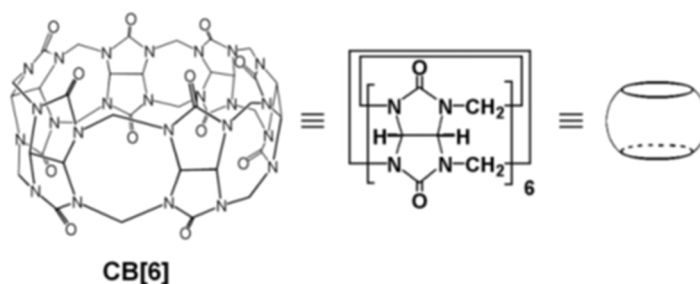
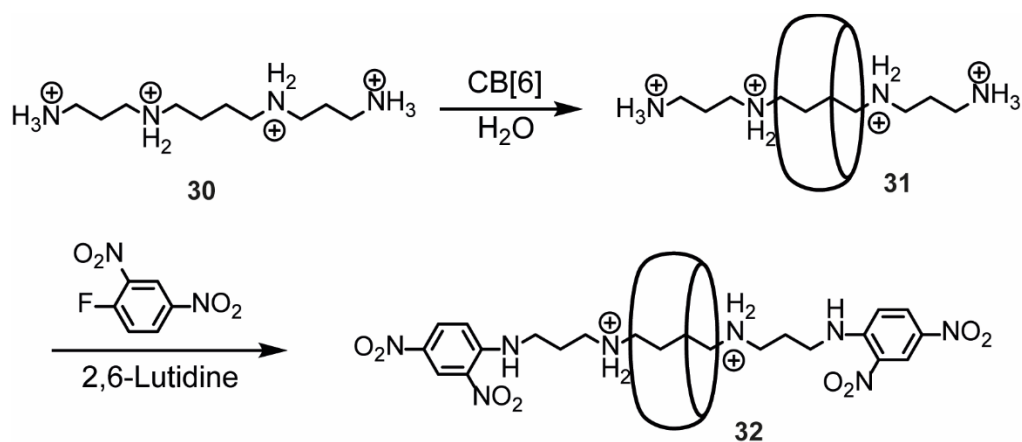


Figure 18. Structure and schematic representation of cucurbit[6]uril.^[66]

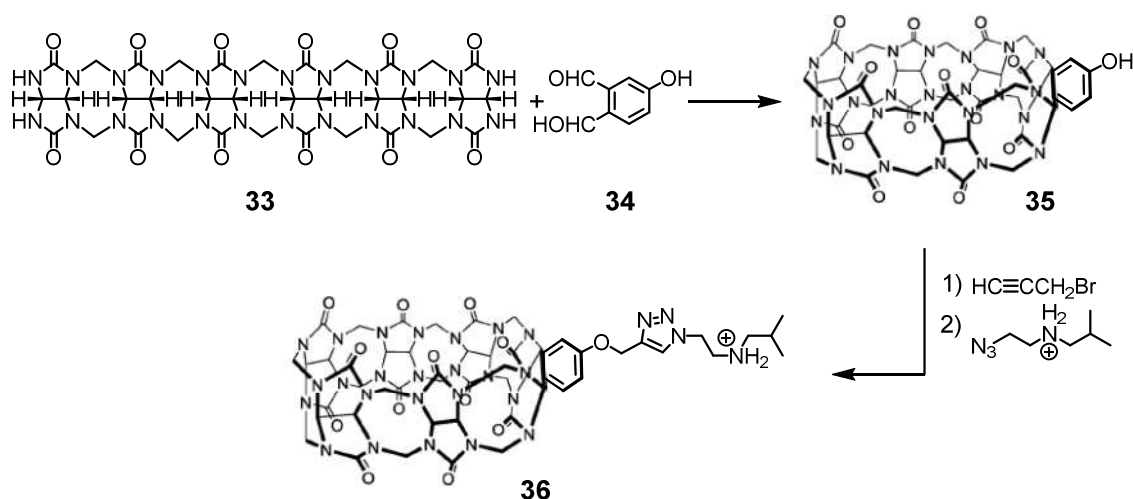
Similar to cyclodextrins, CBs comprise an inner hydrophobic cavity, allowing the formation of inclusion complexes with hydrophobic guests. The remarkably strong (K_a values in water up to 10^{12} M^{-1}) and unique guest encapsulation properties are not only based on the hydrophobic effect, but also on the existence of polar carbonyl groups at the symmetrical cavity rim. The carbonyl groups allow the binding of ions and other molecule via charge-dipole and hydrogen-

bonding interactions.^[66] These interactions are also present in the first cucurbituril-based rotaxane, reported by Kim in 1996.^[67] A K_a value of 10^7 M^{-1} in water for the inclusion complex of the guest spermine and host CB[6] was obtained (Scheme 10).



Scheme 10. Synthesis of the first cucurbituril rotaxane based on the CB[6]/spermine recognition motif.^[67]

By developing a protocol for the synthesis of monofunctionalized cucurbit[6]uril derivatives, Isaacs and coworkers promoted cucurbituril-based daisy chain formation.^[68] The phenol substituent at the CB[6] macrocycle **35** was obtained via condensation of the methylene bridged glycoluril hexamer **33** with phthalaldehyde derivative **34**. Subsequent reaction with propargyl bromide led to a propargyloxy moiety enabling a CuAAC reaction in water to yield monomer **36**.



Scheme 11. Synthesis of a monofunctionalized CB[6] derivative which self-assembles in water to interlinked [c2] daisy chains.^[68]

Monomer **36** forms intermolecular inclusion complexes through its isobutyl ammonium group, resulting in predominantly cyclic dimeric [c2]daisy chains, revealed by diffusion

measurements (DOSY) and molecular models. The comparatively weak association constant (K_a) of $3 \cdot 10^4 \text{ M}^{-1}$ between CB[6] and the isobutyl ammonium group in water allowed reversible triggering of the aggregation behavior via a chemical stimulus in form of either a competing guests (butandiammonium) or host (CB[8]).

1.3.4 Pillar[n]arenes

This relatively novel type of molecular macrocycles is composed of n hydroquinone units mutually linked by methylene bridges at para position. Since the discovery of pillararenes by Ogoshi et al. in 2008^[69], the complexation properties of pillar[5]arenes have been extensively investigated and widely used for the synthesis of functional systems, whereas the homologues consisting of $n = 6$ and 7 hydroquinone moieties have been rarely analyzed. With an inner diameter of about 5 Å,^[69] pillar[5]arenes feature a cavity size comparable to β -cyclodextrins.

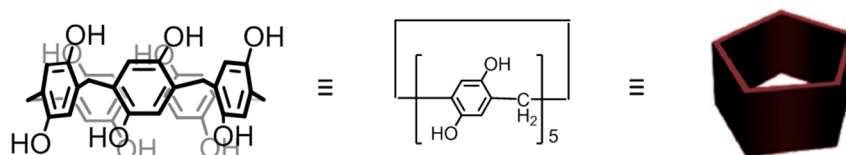
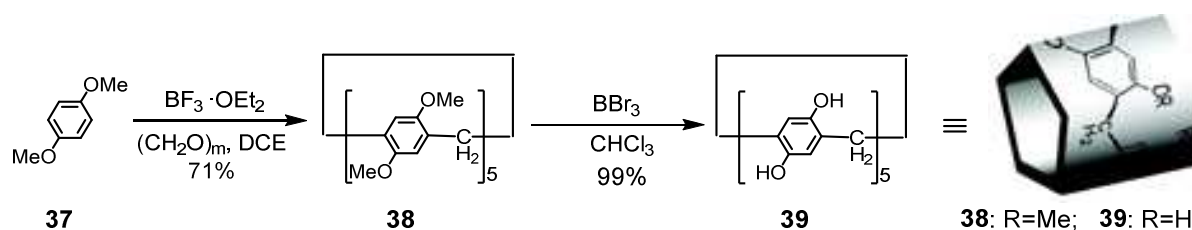


Figure 19. Structure of pillar[5]arene (left) and two different corresponding schematic representations.^[70]

Compared to cucurbiturils, which in general exhibit similar molecular recognition properties to pillararenes, the latter are relatively easy to functionalize with different functional groups and moieties at the cavity rim. For example, the primarily reported per-hydroxylated pillar[5]arene **39** was synthesized via Friedel Crafts alkylation^[71] of 1,4-dimethoxybenzene **37** followed by the demethylation of pillar[5]arene **38** using borontribromide (Scheme 12). In contrast to the highly crystalline macrocycle **38**, the per-hydroxylated pillar[5]arene **39** is well soluble in methanol, acetone, acetonitrile, dimethylformamide and dimethyl sulfoxide.



Scheme 12. Optimized synthetic pathway of the first reported per-methoxylated and per-hydroxylated pillar[5]arenes **38** and **39**^[72] as well as their schematic representation.^[73]

The π electron-abundant cavity render the highly symmetrical and rigid pillararenes ideal hosts for electron-deficient guest molecules,^[74] such as paraquat and pyridinium derivatives, imidazolium cations, bis(imidazolium) dications and secondary ammonium ions (Figure 20).^[27]

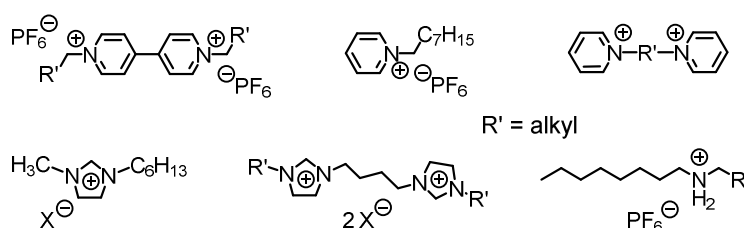
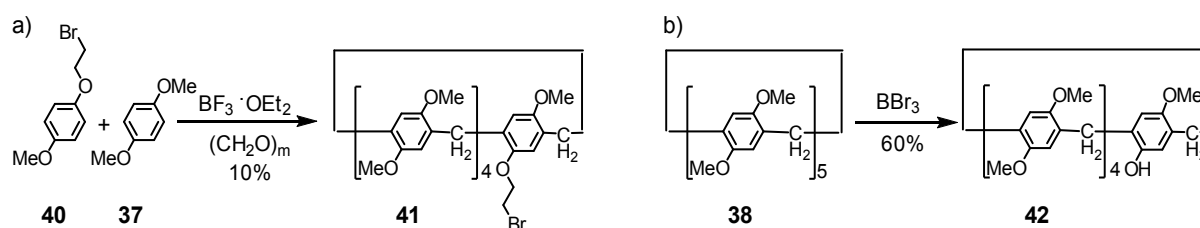


Figure 20. Typical guest molecules for pillar[5]arenes.^[27]

Typically, pillar[5]arenes form 1:1 inclusion complexes with K_a values between 10^2 and 10^4 M^{-1} in solvents such as methanol, DMSO, chloroform or acetone. Complexation is mainly driven by host-guest charge-transfer interaction and C-H $\cdots\pi$ interaction, which is the weakest kind of hydrogen bonding.^[70] Association constants up to 10^5 M^{-1} were measured for a water-soluble pillar[5]arene containing ten negatively charged carboxylate groups and 1,4-bis(pyridinium)butane derivative guests in aqueous phosphate buffer solution.^[75] The water-soluble pillar[5]arene developed by Hou and co-workers comprises neutral amino groups at the cavity rim and binds linear diacids in neutral, alkaline and acidic environment.^[76] Huang and co-workers prepared a cationic pillar[5]arene with ten trimethylammonium groups which encapsulates sodium 1-octanesulfate in water mainly driven by hydrophobic effects and electrostatic interactions.^[77]

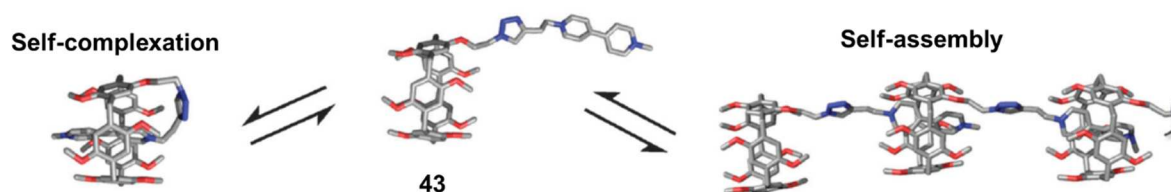
Concerning monofunctionalization of the macrocycle, a premise for daisy chain synthesis, two different approaches are well established (Scheme 13).^[78] The substituent, in this case a bromoethoxy handle, is introduced into the pillararene backbone via co-cyclization (approach a) of 1,4-dimethoxybenzene **37** and its corresponding derivative **40**.^[79] Approach b) relies on

the deprotection of one alkoxy group of the per-methoxylated pillararene **38** and hence allows for the addition of new functionality at the cavitand.^[80]



Scheme 13. The two established synthetic approaches for the monofunctionalization of per-methoxylated pillar[5]arenes: a) co-cyclization; b) deprotection^[79,80]

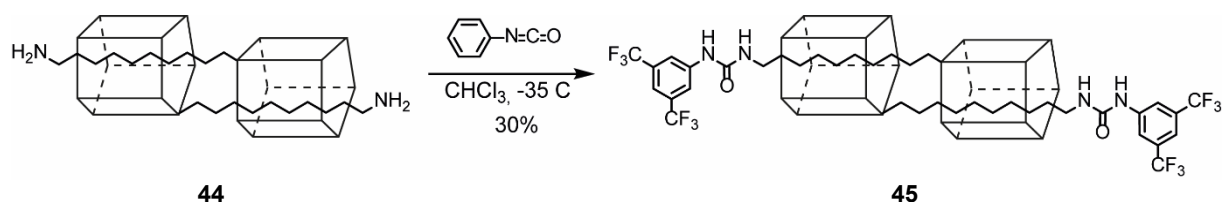
Employing approach a), Huang and co-workers prepared an octyl monofunctionalized dimethoxybenzene pillar[5]arene which aggregates at high concentration (up to 768 mM) to linear polymeric daisy chain pseudorotaxanes.^[81] Scanning electron microscopy revealed the existence of fibers with a diameter of 9.5 μm . Concentration-dependent oligomer and polymer formation was also achieved with Stoddart's system (Scheme 14) comprising a viologen thread (**43**).^[74] In dilute solution (0.1 mM) the functionalized pillar[5]arene forms intramolecular complexes (Scheme 14), whereas a polymeric organogel was obtained at concentrations higher than 25 mM. Strong complexation was indicated by the high K_a value of $1.3 \times 10^5 \text{ M}^{-1}$ in dichloromethane obtained via fluorescence quenching experiments. Charge-transfer bands resulting from the encapsulation of the electron-deficient guest into the electron-abundant cavity were observed in the UV/Vis spectra, accompanied with a color change.



Scheme 14. Molecular modelled structure of the intramolecular (left) self-complexation in dilute solution and intermolecular oligomerization (right) at high concentration of the viologen-functionalized pillar[5]arene **43**.^[74]

In 2012, Huang and co-workers synthesized an interlocked [c2]daisy chain (**45**) by stoppering an amine functionalized daisy chain pseudorotaxane (Scheme 15).^[82] The preparation was

based on the X-ray structure of analogue bromodecyloxy copillar[5]arene. The authors concluded that the formation of cyclic dimeric aggregates is facilitated by the dispersive features of the C₁₀ alkyl chains.^[83] The bromine atom was substituted by a primary amine group via Gabriel^[84] reaction and the double threaded aggregate (**44**) was then stoppered with bis(trifluoromethyl)phenyl isocyanate.



Scheme 15. Synthesis of the interlocked pillar[5]arene based molecular [c2]daisy chain **45**.^[82]

In pure chloroform-*d*3, the pillar[5]arene rings of **45** are located near the urea-linked stopper, the system is present in its contracted state with a total length of 31 Å (Figure 21). In turn, the system is extended to 37 Å in pure DMSO-*d*6, where the macrocycle was found to encircle the middle of the alkyl chain. By varying the percentage of the two different solvents and hence the polarity of the solvent system, the length of the [c2]daisy chain can be changed to intermediate states. As there are no distinct favored binding sites for the pillararene macrocycles within the thread, length variation can take place continuously. The system is therefore acting as a molecular spring.

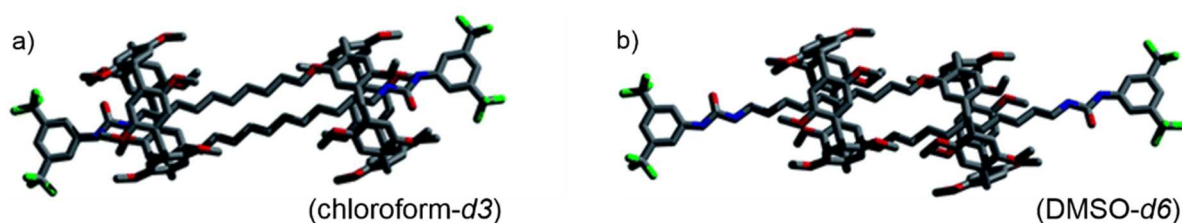


Figure 21. Molecular model of the solvent-driven length variation of [c2]daisy chain **45**; a) contracted state in chloroform-*d*3, and b) extended state in DMSO-*d*6.^[82]

Further development of the system incorporates the integration of terpyridine moieties at the thread termini.^[85] The tridentate ligand works as a linker to connect [c2]daisy chain units via complexation with iron ions resulting in a supramolecular polymer (Figure 22). Filamentous fibers of the solvent responsive metallo-polymer **46** with a length of up to 40 μm and a diameter of 10 nm were observed with SEM and TEM measurements. The solvent-dependent

integrated motion within polymer **46** was investigated by dynamic light scattering experiments, revealing a considerably higher hydrodynamic radius in pure DMSO ($r_H = 254$ nm) than in pure chloroform ($r_H = 104$ nm). The authors attribute this finding predominantly to the system's extension and only secondarily to a potential increase of r_H due to swelling of the fibers.

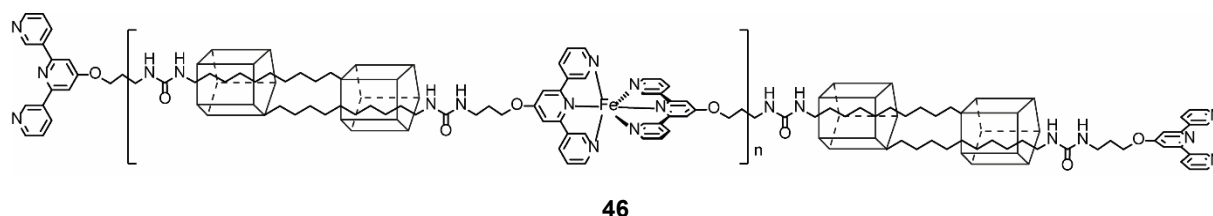


Figure 22. Contracted state of the solvent-switchable supramolecular metallo-polymer **46** consisting of [c2]daisy chain units.^[85]

1.3.5 Calix[*n*]arene

Calix[*n*]arenes are structurally related to pillar[*n*]arenes as both macrocycles contain methylene bridged aromatic units. Whereas the rigid pillararenes comprise hydroquinone units, in calixarenes substituted phenols, resorcinols or pyrogallols are linked together (Figure 23), resulting in vase-shaped cavities. Due to the relatively free rotation about the σ -bonds of the methylene groups different conformational states can be adopted. The conformation strongly depends on the number *n* of repeating units, the substituents located at the benzene cores and their substitution pattern. Typically, in phenol-based calix[4]arenes all hydroxyl groups are oriented intra-annular interacting via hydrogen bonding and adopt the so called cone conformation. In other possible types of conformers the substituents are either oriented alternating or form a partial cone.

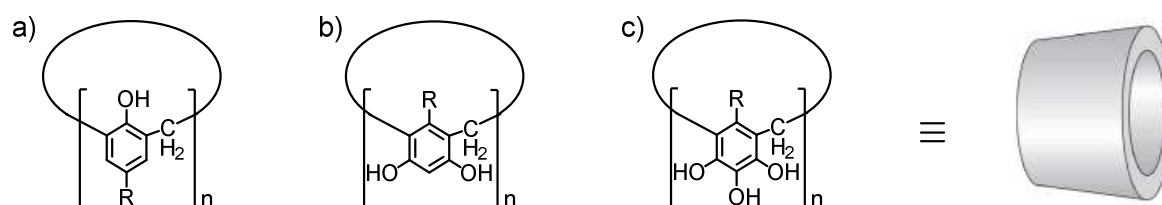
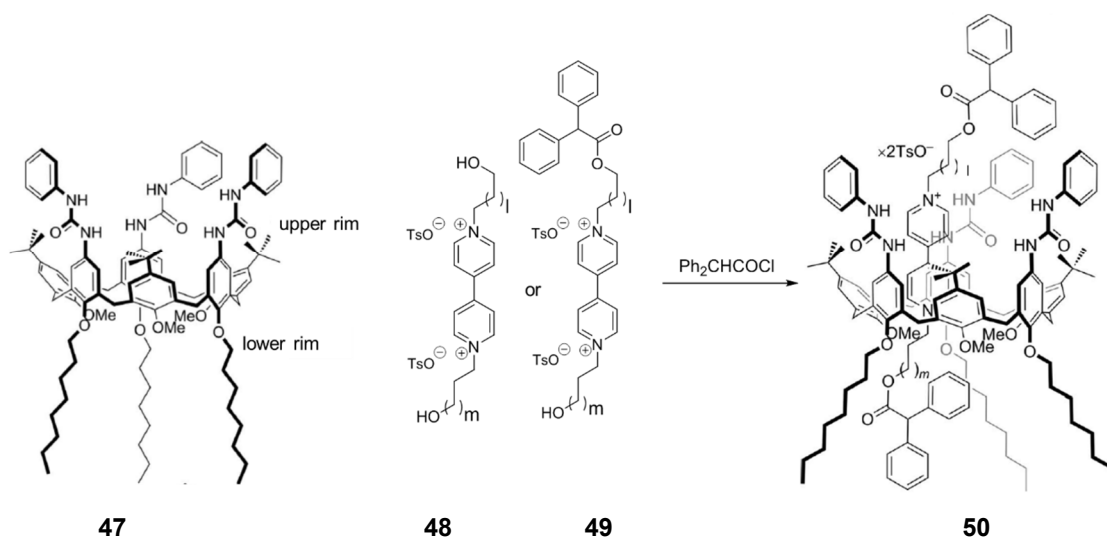


Figure 23. Structures of three kinds of calix[*n*]arenes derived from a) phenol b) resorcinol or c) pyrogallol. The cavity of calix[*n*]arenes typically resembles the shape of a vase.

In general, calix[*n*]arenes have received less attention as macrocyclic components in the synthesis of mechanically interlocked molecules. However, one of the few examples for rotaxanes preparation based on calix[*n*]arenes is a collaboration of the Arduini, Credi, Venturi and Secchi groups.^[86–88] The electron rich cavity of the tris(*N*-phenyl-ureido)calix[6]arene **47** allowed the encapsulation of *N,N'*-dialky viologen-based axles **48** and **49** (Scheme 16). In 2000, the symmetrical [2]rotaxane **50** with *l* = *m* = 10 methylene units was reported as the first rotaxane containing a calixarene macrocycle.^[86] Through X-ray analysis of the corresponding [2]pseudorotaxane analogue with *l* = *m* = 6, the authors identified aromatic π - π donor-acceptor interactions, hydrogen bonding and C-H \cdots π interactions as main stabilization forces between host and guest. Another important finding was the complexation of the guest's counteranions via hydrogen bonding with the ureidic NH fragments of the host. The ensuing publication in 2004^[87] focused on the effects of the nature of counteranions on both the stability of the complexes and the rate of the threading process. The binding constant K_a in dichloromethane of host **47** with the tosylate salt of the unstoppered axle **48** ($6 \times 10^6 \text{ M}^{-1}$) and the monostoppered analog **49** with *l* = *m* = 6 ($3 \times 10^6 \text{ M}^{-1}$), respectively, were higher than the corresponding hexafluorophosphate salt of the symmetric axle ($0.8 \times 10^6 \text{ M}^{-1}$). Stopped-flow experiments, more precisely monitoring the absorption changes upon rapid mixing of host **47** with the axles, revealed threading rate constants *k* of the tosylate salts more than two orders of magnitude higher than the hexafluorophosphate salt of the unstoppered axle. The obtained results on stability and kinetics clearly indicated that the in low polar solvents strongly pairing anions are components of the complex and contribute to its stabilization.^[87]



Scheme 16. Synthesis of rotaxane **50** comprising the ureido *N*-phenyl substituted calix[6]arene macrocycle **47** and the diphenyl acetate stoppered viologen axle **48/49**, optionally symmetric ($l = m$) or unsymmetric ($l \neq m$).^[86–88]

Very recently in 2016, the synthesis and characterization of the analogue unsymmetrical rotaxane, in which the linker alkyl chains between the stoppers and the viologen moiety of the axle are different in length ($l \neq m$) (Scheme 16) was published by the same collaboration.^[88] The preferential formation of rotaxanes with the shorter span (l) close to the upper calix[6]arene rim and the longer span (m) oriented to the lower rim was observed. The oriented rotaxanes were investigated with the aim to gain information whether reduction of the biphenyl core, and hence weakening the host-guest interaction, induces movement within the rotaxane. However, no significant indication for the shuttling of the macrocycle upon reduction was observed by the combination of spectroelectrochemistry and electron paramagnetic resonance (EPR) measurements.

The formation of calix[*n*]arene based molecular daisy chains were observed from monomeric structures comprising both a cyclodextrine binding motif and a calix[4]arene unit (Figure 24).^[89] To the latter macrocycle four polyethylene glycol chains were attached forming the “lower” rim. Calix[4]arene was further functionalized at the “upper” rim with an amine group working as linker between the cyclodextrine and a naphthalene based chromophore. Dependent on the chromophore’s substitution pattern and the functional groups, either intramolecular (**51a**) or intermolecular (**51b**) recognition was in form of vesicles or poly[*n*]daisy chain fibers, respectively.

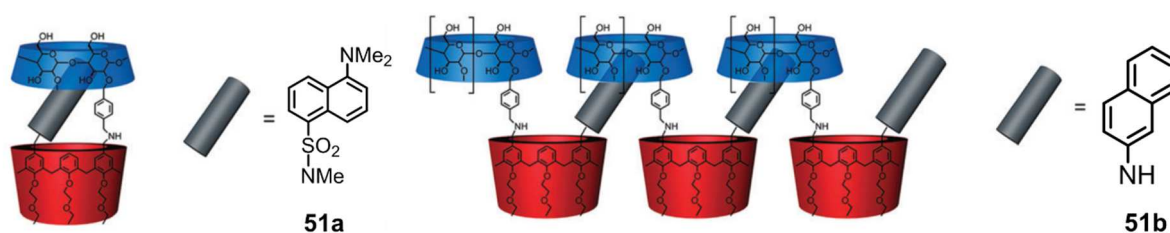


Figure 24. Schematic representation of the merged monomeric structures forming either intramolecular (**51a**) or intermolecular (**51b**) inclusion complexes. Reprinted from reference.^[11]

1.3.6 Tetralactam based Macrocycles

The first tetralactam based macrocycles, as components in catenanes, were reported independently by Vögtle^[90] and Hunter^[91] in 1992. The macrocycles comprised isophthaloyl diamide groups and diarylmethane moieties which provide recognition sites with hydrogen-bonding and π - π interaction capabilities. Profiting from the strong affinity of tetralactam macrocycles toward inorganic and organic anions in apolar solvents, the first anion-templated rotaxane synthesis was developed by Vögtle and coworkers.^[92] A phenoxide anion was linked via hydrogen bonding to the isophthalamide motif of the host and subsequently reacted as supramolecular nucleophile (**52**) with a benzylic monostoppered axle affording rotaxane **53** in 95% yield. In contrast to Vögtle's rotaxane, in the templated rotaxane preparation reported by Schalley and coworkers the phenoxide was not consumed (**54**).^[93] A pseudorotaxanes comprising the templating anion was stoppered at the amine functionalized axle termini remote from the phenoxide motif.

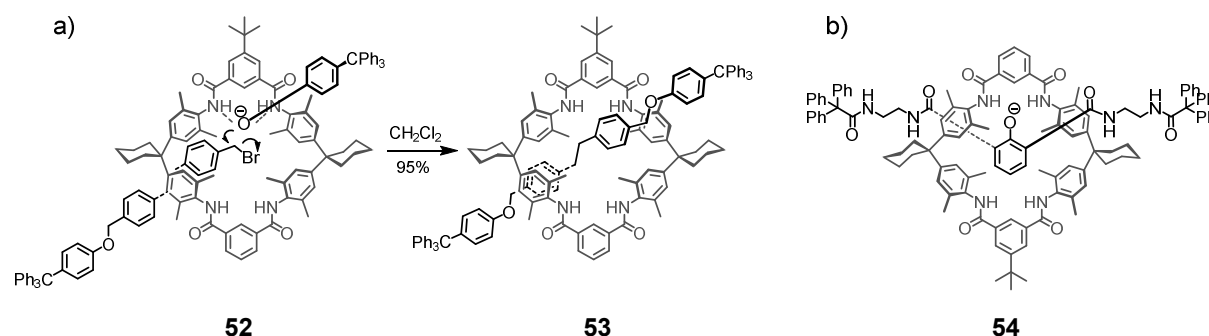


Figure 25. Phenoxide templated rotaxane syntheses with diarylmethane tetralactam macrocycles, a) Vögtle's approach in which the template is consumed, b) Schalley's templated rotaxane.

The Beer group developed a strategy for halide ion templated rotaxane synthesis based on tetralactam macrocycles.^[94] Figure 26 exhibits a molecular [c2]daisy chain (**55**) based on this chloride template concept.^[95] By applying the clipping strategy in the last step, the preorganized pseudorotaxane was transformed into the interlocked daisy chain. In general, the isophthalamide motif in tetralactam based macrocycles provides an anion binding site and saturates the halide ion's coordination sphere. The isophthalamide moieties in daisy chain **55** coordinate the chloride counter anion of the methylpyridinium axle moiety in noncompetitive solvents, such as dichloromethane. Hydroquinone building blocks form the macrocycles' cavity walls and allow π - π donor-acceptor interaction with the pyridine unit. Adjacent

polyethylene glycol chains work both as hydrogen bonding sites for the thread molecule and as linker to terminal alkene units. The vinyl units enable the clipping approach via Grubbs ring-closing metathesis^[96], which is typically applied in the halide templated rotaxane synthesis.

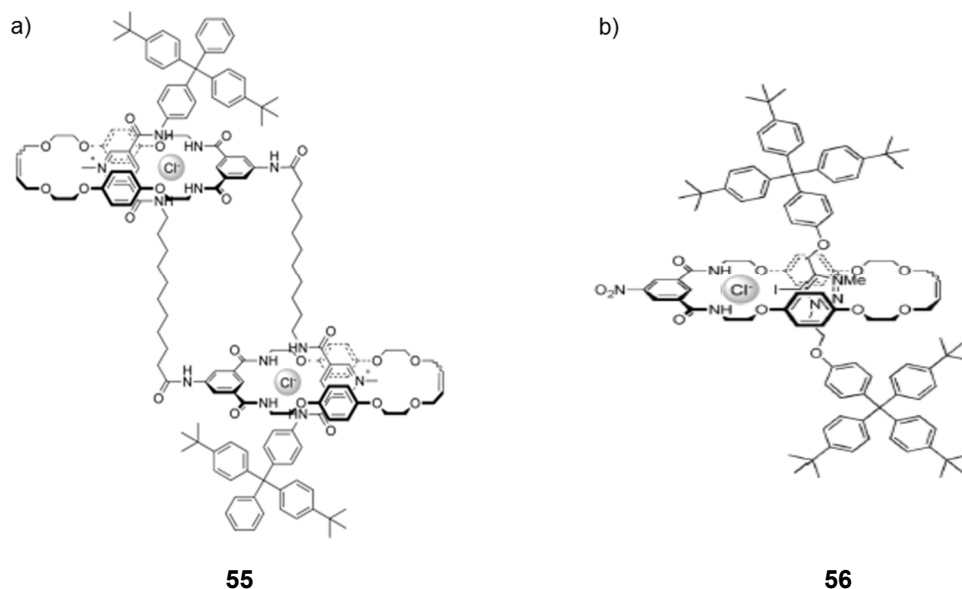
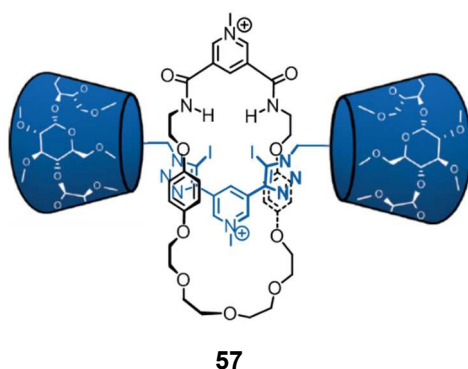


Figure 26. MIMs synthesized by harnessing a chloride templating approach. a) ringclosing metathesis of an pseudorotaxane comprising a pyridinium chloride ion pair resulted in [c2]daisy chain **55**,^[95] b) rotaxane **56** contains an iodotriazolium chloride ion pair.^[97]

The macrocycle's design also permits the construction of rotaxanes with other cationic threads, like imidazolium^[98], triazolium^[99] and even iodotriazolium^[97]. The latter coordinates to halide anions by means of a halogen bond. For example, iodotriazolium rotaxane **56** exhibits a high selectivity for iodide anions ($K_a = 2.2 \times 10^3 \text{ M}^{-1}$) even in competitive aqueous (10% D₂O) solvent mixtures.

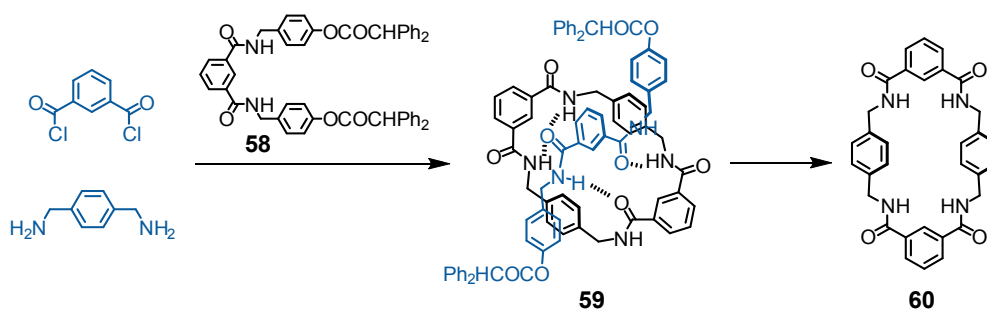
With the recently published rotaxane **57** anion sensing was afforded even in pure D₂O.^[100] The halogen-bonding axle comprises a pyridinium motif with two adjacent iodotriazolium units functioning as halogen-bonding recognition site. Employing permethylated β -cyclodextrin stoppers render the rotaxane water-soluble. ¹H NMR titration studies with rotaxane **57** in D₂O revealed binding of iodide with remarkably high affinity ($K_a = 2.2 \times 10^3 \text{ M}^{-1}$).



57

Scheme 17. The two last steps of the water-soluble anion sensing rotaxane **57** synthesis.^[100]

Another important type of tetralactam macrocycles comprising benzamide moieties was developed by Leigh and coworkers. The first tetralactam macrocycles with benzamide was synthesized in a yield of 28% via rotaxane formation in 1996.^[101] Isophthaloyl dichloride and *p*-xylylenediamine were slowly added to a solution which contained the hydrogen-bonding template axle **58** with terminal ester linked stopper units. Isolation of the desired macrocycle **60** was achieved by disassembly of the thread via ester hydrolysis. A higher yield (62%) could be obtained by harnessing a glycylglycine dipeptide axle which exhibits complementary binding sites to the tetralactam macrocycle.^[102]



Scheme 18. Tetralactam macrocycle **60** synthesis via rotaxane **59** formation.^[101]

The rigid fumaramide motif, which forms four hydrogen bonds with the macrocycle without any distortion, turned out to be an even better template for the hydrogen-bonding mediated rotaxane synthesis, as a yield up to 97% was obtained for rotaxane **61** (Figure 27).^[103] The powerful recognition motif of the amide macrocycle with fumaramide or the less strongly binding succinamide as well as peptide based axles was applied in various artificial molecular machines^[104], like shuttles^[105], switches^[106] and molecular ratchets^[107].

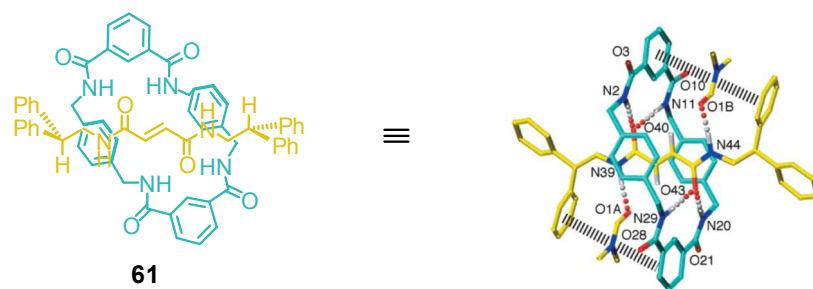


Figure 27. Tetralactam based rotaxane **61** with fumaramide axle and corresponding X-ray structure.^[103]

1.3.7 Metal-ligand based Macrocycles

A powerful strategy for the preparation of interlocked molecules is exhibited by the transitionmetal templated synthesis. Similar to the anion templated rotaxane synthesis developed by Beer and coworkers, a metal ion preorganises the macrocycle and axle component for the rotaxation step. The first metal-ligand controlled rotaxane preparation was reported in 1991 by Gibson and coworkers.^[108] Macrocycle and axle both comprised a disubstituted 1,10-phenanthroline ligand which assembled to a pseudorotaxane via a tetracoordinate copper(I) complex. After stoppering, the template was removed via an amberlite-CN resin. Sauvage and coworkers applied the same recognition motif for the coordination driven assembly of a molecular [c2]daisy chain (**62**). The phenyl units in the 2- and 9-position of the 2,9-diphenyl-1,10-phenanthroline (dpp) moiety of the macrocycle were connected through a benzene bridged glycol chain. The benzene-moiety also served as anchor motif for the linear thread moiety. Upon addition of a stoichiometric amount of tetrakis(acetonitrile)copper(I) hexafluorophosphate in $\text{CH}_3\text{CN}/\text{CH}_2\text{Cl}_2$ 1:1 the hermaphroditic monomers assembled via complexation to interlinked double-threaded daisy chains **62** at room temperature.

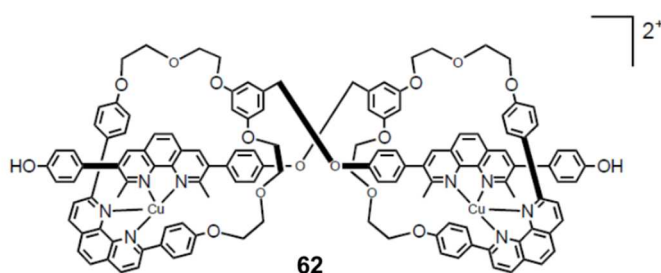
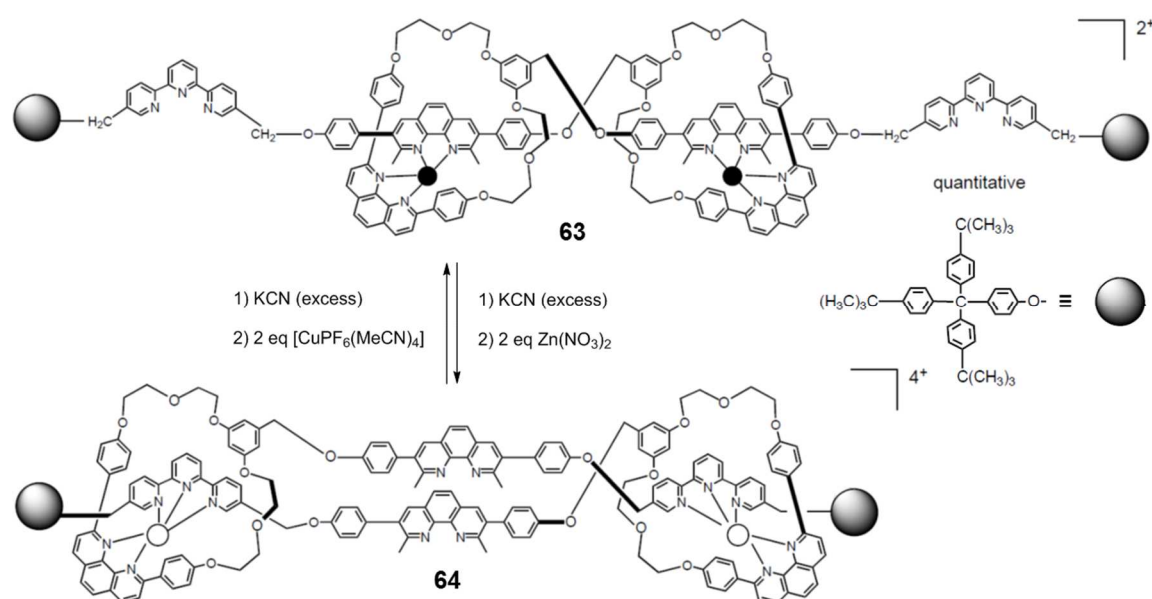


Figure 28. Molecular [c2]daisy chain assembled via Cu(I) template approach.^[109]

In the year 2000, Sauvage introduced the concept of stimuli triggered artificial molecular muscles based on this kind of dimeric supermolecules.^[21] A second metal binding site, a terpyridine ligand, monofunctionalized with a bulky stopper group was attached to the interlinked molecule **62** resulting in the interlocked [c2]daisy chain **63**. Contraction of the molecular system to 27% could be induced chemically by metal exchange with an excess of cyanide ligand and subsequent Zn(II) phenanthroline-terpyridine complex **64** formation (Scheme 19).



Scheme 19. Extended (**63**) and contracted (**64**) conformation of the first artificial molecular muscle. The muscle-like actuation could be triggered chemically upon Cu(I)/Zn(II) exchange.^[21]

Leigh and Goldup developed a conceptually novel approach for rotaxane synthesis based on an *active metal* template.^[33] The transition metal, endotopically bound to the macrocycle, both arranges the rotaxane components and mediate the formation of the mechanical bond as a catalyst. The new strategy allows preparation of rotaxanes in high yield and requires only a metal binding site on the macrocycle. A well investigated exemplary reaction for the *active metal* strategy^[110,111] is the Cu-catalyzed alkyne-azide cycloaddition (CuAAC). Rotaxane **65**, comprising a pyridine-based macrocycle as wheel component, was afforded in 94% yield with stoichiometric amount of [Cu(CH₃CN)₄(PF₆)]. Using the copper source in catalytic amounts afforded rotaxane **65** in 82% yield after three hours. Increasing the ration of macrocycle to Cu(I) to 10:1 resulted in the formation of [3]rotaxane **66** as byproduct. This observation

indicates that under these conditions the mechanism of the CuAAC reaction involves a reactive intermediate that features at least two metal ions (Figure 29).

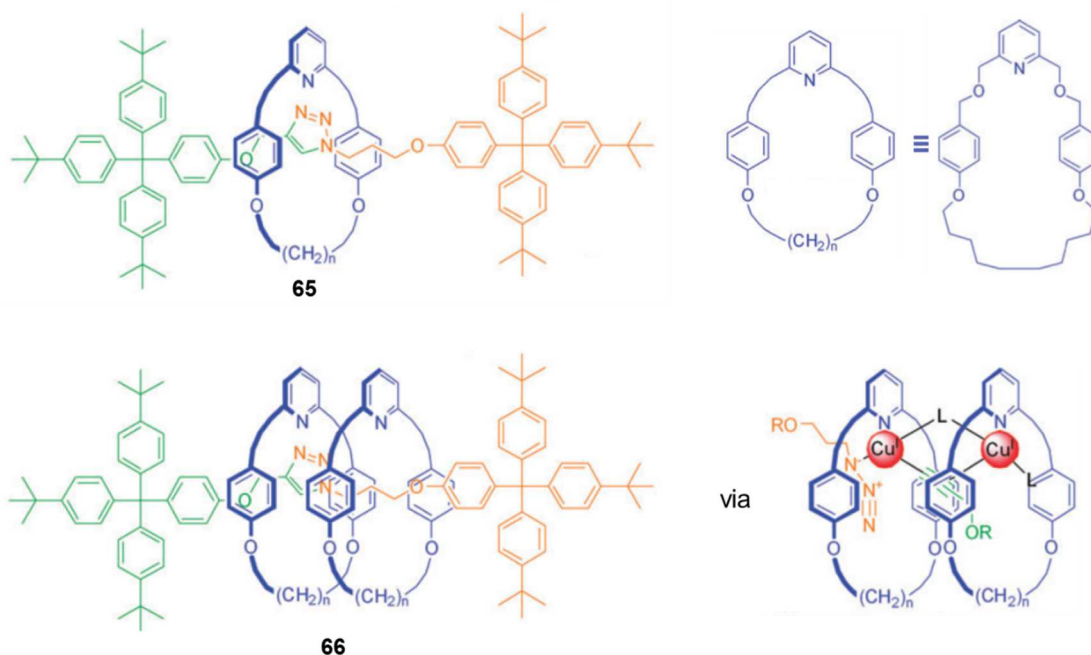


Figure 29. [2]Rotaxane **65** synthesized via active metal template strategy with a pyridine-based macrocycle as catalyst site. The formation of [3]rotaxane **66** as a byproduct provided some insight into the mechanism of the CuAAC reaction.^[111]

Other active metal template reactions have been adopted for the preparation of interlocked molecules, such as the Pd(II) oxidative Heck cross-coupling reaction.^[112]

1.3. 8 Tetracationic Cyclophanes

Cram and Steinberg established the term *cyclophane* in 1951 for compounds consisting of an arene motif in which two positions are bridged by an aliphatic chain, forming a cycle.^[113] Among the countless cyclophanes synthesized to date, a well-established example is the tetracationic cyclobis(paraquat-*p*-phenylene) (CBPQT⁴⁺), initially reported by the group of Stoddart in 1988 (Figure 30).^[114] Due to the violet blue color of its corresponding radical cation, which can be formed upon one-electron reduction, it is also called “blue box”.

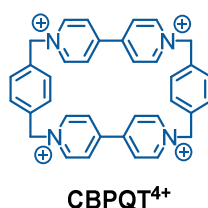
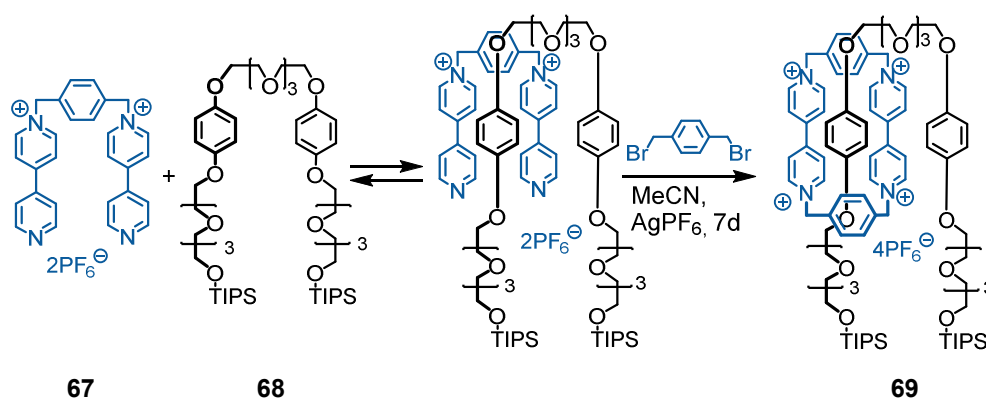


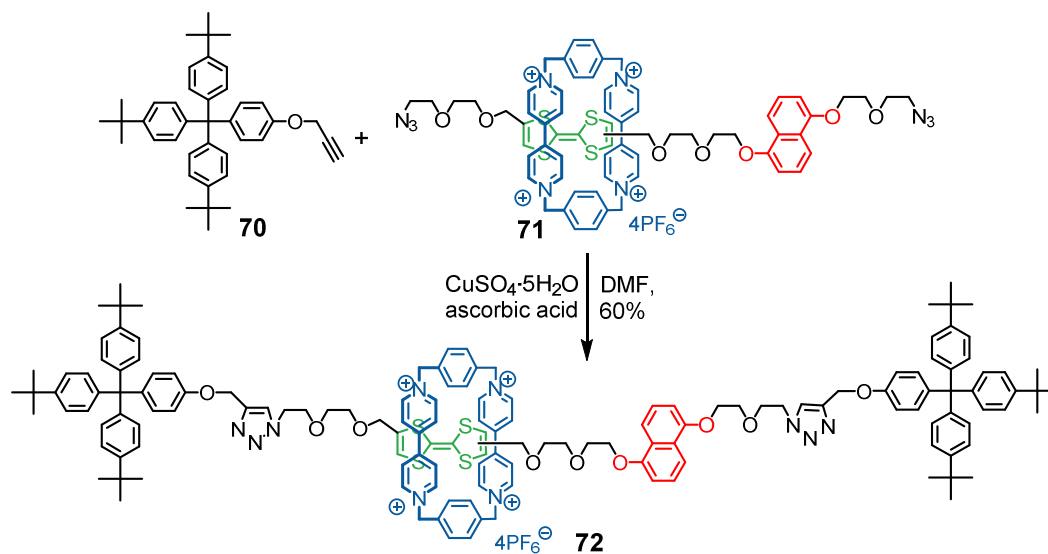
Figure 30. Structure of the tetracationic cyclophane cyclobis(paraquat-*p*-phenylene).^[114]

The π -electron deficient cavity binds a variety of π -electron rich guests, such as hydroquinone, tetrathiafulvalene (TTF) or 1,5-dioxynaphthalene (DNP). As the tetracationic cyclophane is easily attacked by reducing agents, bases and nucleophiles,^[27] CBPQT⁴⁺ is typically prepared either by the clipping method using 1,4-bis(bromomethyl)benzene and the bispyridinium dication **67**, or by the mild CuAAC reaction. Scheme 20 shows the first rotaxane preparation based on CBPQT⁴⁺.^[115] The macrocycle precursor **67** interacts with the anisole motif of axle **68**. The preorganized components then reacts with 1,4-bis(bromomethyl)benzene to afford rotaxane **69** as a deep-orange colored product after 7 days in 32% yield.



Scheme 20. Formation of the first CBPQT⁴⁺-based rotaxane.^[115]

Employing the CuAAC reaction as stoppering method proved to be an efficient strategy for the preparation of switchable donor/acceptor rotaxanes. Stoddart introduced this approach with the synthesis of the bistable rotaxane **72** (Scheme 21), bearing an CBPQT⁴⁺ encircled TTF unit (green) and a free DNP motif (red).^[116] The azide termini of pseudorotaxane **71** react with the propargyl moiety of stopper **70** in the presence of the catalyst system Cu(II)sulfate/reducing agent ascorbic acid affording **72** in a yield of 60%.



Scheme 21. Synthesis of the bistable CBPQT⁴⁺-based rotaxane **72** using the CuAAC reaction. Blue: CBPQT⁴⁺ cyclophane, green: TTF unit, red: DNP moiety. ^[116]

Upon one- or two-electron oxidation of TTF, CBPQT⁴⁺ is electrostatically repelled and moves directly to the competing DNP unit. In turn, reduction back to electroneutral TTF leads to migration of the macrocycle back to the original position. The same principle was utilized for an advanced bistable [3]rotaxane system (**73**), bearing CBPQT⁴⁺ rings.^[117] The palindromic interlocked molecule has two TTF and two naphthalene (NP) recognition sites for the two macrocycles, which are functionalized with a disulfide tether. The disulfide moieties self-assemble to monolayers on the gold surfaces of an array of flexible atomic force microscope (AFM) microcantilevers. The resulting coated surfaces consisted each of 6 billion [3]rotaxanes. The locations of the two rings along the rotaxane axle could be controlled precisely either by chemical stimuli, oxidation with tri(*p*-bromophenyl)-amminium hexafluoroantimonate and reduction with Zn powder, or electrochemically using the potential of the working electrode in a cyclic voltammetry (CV) setup. The inter-ring distance changing in each [3]rotaxane from

4.2 to 1.4 nm and vice versa ensues reversible up and down bending of the attached AFM cantilevers 5 orders of magnitude larger in size.

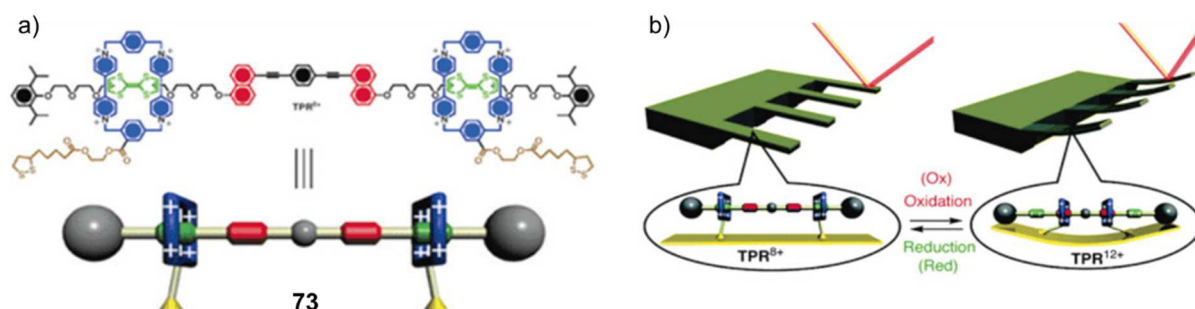
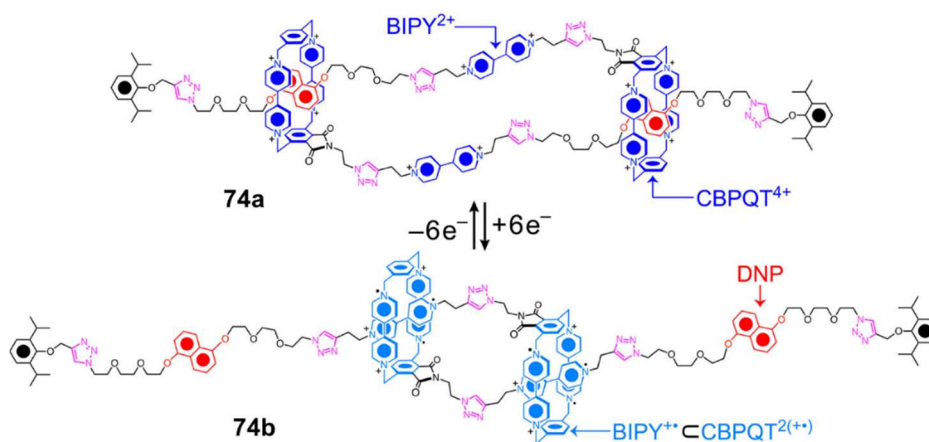


Figure 31. a) Chemical structure of the switchable palindromic [3]rotaxane **73** bearing a disulfide tether on the macrocycle; b) the redox driven mechanical switching of the bistable rotaxanes bends and releases the AFM cantilever reversibly.^[117]

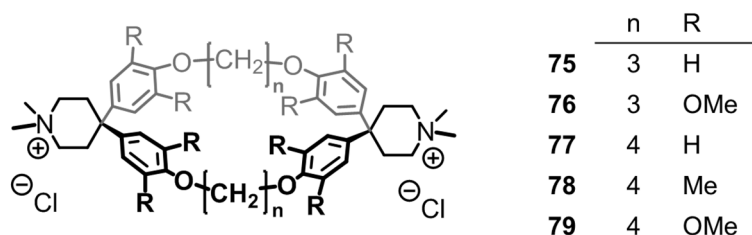
A related redox-switchable molecular muscle is exhibited by [c2]daisy chain **74**, one member of a family of related cyclic and acyclic daisy chains isolated from a one-pot click reaction in low yield (9%).^[12] The system, developed by Stoddart and coworkers, comprises a bipyridinium (BIPY²⁺) motif and a DNP unit, which is encircled by a CBPQT⁴⁺ ring (**74a**). Coulombic repulsion between the tetracationic macrocycle and BIPY²⁺ prevents association between the two motifs. However, under reducing conditions, all six of the bipyridinium radical cations, including the four CBPQT²⁽⁺⁺⁾ units of the macrocycle and the two axle BIPY⁺ units, generated by one-electron reduction, become associated through spin-pairing interactions, causing an extension of the system (**74b**). The electrochemically actuated muscle behavior could be investigated by cyclic voltammetry and spectroelectrochemistry.



Scheme 22. Electrochemically driven actuation of [c2]daisy chain **74**, where CBPQT⁴⁺ encircles the DNP site in the contracted state (**74a**) and spin-pairing interactions associate CBPQT²⁽⁺⁺⁾ with the reduced BIPY⁺ motif in the extended state (**74b**).^[12,22]

1.3.9 Diederich Cyclophanes

Starting in the 1980s,^[118] Diederich and coworkers developed a wide variety of cyclophanes and comprehensively investigated their complexation behavior with aromatic guests. The simple, symmetrical cyclophanes **75-79** are soluble in pure water and allow for rather easy synthetic modification.^[119]



The hosts comprise quaternary ammonium centers, which provide water-solubility at neutral pH values and are located remote from the binding site.^[120,121] The diphenylmethane moieties are linked by dioxalkane chains of variable chain length, which affords different cavity sizes. X-ray structures show that the lone pairs of the four ether oxygen atoms in the bond to the alkyl chain linker are oriented outwards, which enhances the hydrophobic character of the binding site. Methyl or methoxy substituents ortho to the bridging dioxalkane ethers increase the cavity depth. The distance between two meta hydrogens in cyclophane **75** is ~ 4.3 Å, whereas the hydrogen atoms of two *m*-methyl groups in **78** are ~ 6.0 Å apart.^[122] The deepest cavity, with a distance between the *m*-methoxy groups of ~ 8.1 Å, is formed by cyclophane **76**. The X-ray structure (Figure 32) demonstrates that each methoxy substituent is aligned in the plane of the phenyl ring to which it is attached.^[123] The methyl and methoxy substituents affect also the torsional angles about the aryl ether C-O bonds and hence influence the macrocyclic conformation. The torsion angles in the unsubstituted cyclophane are close to 0° . In contrast to that, the torsion angles are close to 90° in the methyl/methoxy-substituted macrocycles and the first CH₂ group of every ether bridge is either twisted inwards or outwards from the cavity.

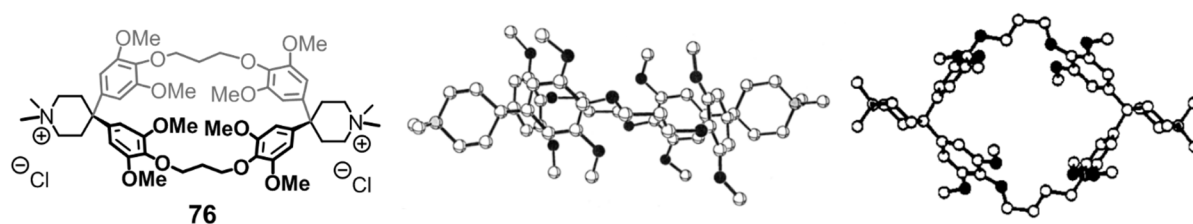


Figure 32. Molecular structure of cyclophane **76** and two different perspectives of the corresponding X-ray crystal structure. The diiodide counteranions are omitted for clarity.^[122,123]

Diederich-type cyclophanes were found to form 1:1 inclusion complexes with aromatic guests in protic solvents. The X-ray crystal structure of cyclophane **80**, the tertiary amine precursor of **75**, with an enclosed benzene guest demonstrates that the cyclophane adopts a rectangular conformation, in which the four electron-rich aromatic rings act as cavity walls. Cyclophanes **75-79** form complexes with 1,4-disubstituted benzene substrates, whereas the larger cyclophanes, with $n = 4$ CH₂ bridging units also complex 2,6-disubstituted naphthalene guests.

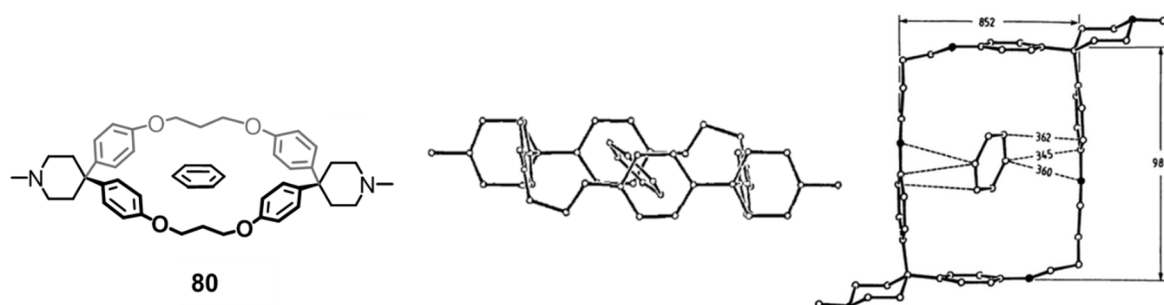


Figure 33. X-ray crystal structure and skeletal structure of a benzene inclusion complex with cyclophane **80**.^[121]

¹H NMR complexation studies strongly indicate that both 1,4-substituted benzene and 2,6-substituted naphthalene substrates generally prefer an axial-type inclusion geometry upon complexation in the liquid phase. The aromatic guest protons point directly into the π -cloud of the aromatic cavity walls, in an edge-to-face and π -offset fashion. Furthermore, in this geometry the substituents X and Y are oriented into solution (Figure 34), which is in particular favorable for highly solvating, polar groups.

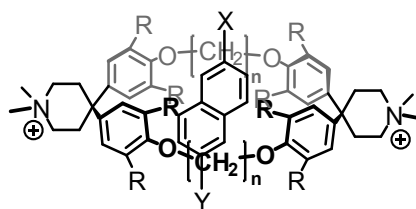


Figure 34. Axial inclusion of an aromatic substrate with the substituents X and Y pointing outwards from the cavity.

An important aspect for the host-guest complexation in aqueous media involves the potential self-association of the host and/or guest molecules, leading to structures similar to micellar systems. In order to avoid interference of the complexation equilibrium by additional self-aggregation equilibria, complexation studies should be performed in a concentration regime below the critical aggregation concentration (*cac*) of the involved compounds. In this series of

cyclophanes the highest critical aggregation concentration in water exhibit the methoxy substituted macrocycles **76** and **79** (both 1×10^{-2} M). Methyl groups even caused a more favorable self-aggregation than in the case of the unsubstituted cyclophane. The *cac* of **78**, bearing eight methyl groups was $<2 \times 10^{-5}$ M, whereas the critical value for **77** was determined as 1.6×10^{-4} M. The low *cac* values of **77** and **78** in pure D₂O were the reason why Diederich and coworkers investigated the binding properties of the different cyclophanes mainly in D₂O/CD₃OD (60:40 v/v), a solvent mixture in which no self-association was observed and hence the determined binding constants with different guests were comparable.

Van't Hoff analysis revealed an enthalpically driven complexation, the entropic contribution to the Gibbs free energy turned out to be lower. This finding proofed that the complexation is driven by a nonclassical hydrophobic effect, rather than by the entropically driven classical hydrophobic effect.

Association constants in D₂O and/or D₂O/CD₃OD (60:40 v/v) of hosts **75-79** and a variety of 1,4-disubstituted benzene and 2,6-disubstituted naphthalene guest were determined by ¹H NMR titration experiments. Table 1 exhibits K_a values, as well as free energies ΔG° of complexation with *p*-dimethoxybenzene and *p*-benzodinitrile, as exemplary guests featuring electron-donating and respectively withdrawing substituents. Regarding the K_a values of the C₃-bridged cyclophanes in D₂O, electron donor-acceptor interactions have an immense influence on the binding properties. For both hosts **75** and **76**, the affinity between the electron-rich cavity and the electron-deficient guest *p*-benzodinitrile is much higher than the binding to the substrate with electron-donating tendency. In case of the unsubstituted cyclophane **75**, ΔG° for complexation with the electron-rich guest is even positive. In turn, the same cyclophane provides the highest binding affinity for the electron-accepting *p*-benzodinitrile.

Concerning the larger hosts, Table 1 shows that octamethyl cyclophane **78** is the best binder. The sequence is followed by the octamethoxy derivative **79** and then the unsubstituted host **77**. The effect of electron donor-acceptor interactions is most pronounced in the complexation behavior of octamethyl cyclophane **78**. In case of the methoxy cyclophane **79**, the tendency is negligible. In pure D₂O, the electron-rich guest *p*-dimethoxybenzene is even stronger complexed than the electron-accepting substrate *p*-benzodinitrile.

Table 1. Association constants K_a and free energies of complexation ΔG° at 293K for complexes of cyclophanes **75-79** with 1,4-disubstituted benzene guests, each two bearing electron donating (D) or accepting (A) substituents X and Y, in D₂O and D₂O/CD₃O (60/40 v/v). Complexation-induced upfield shifts $\Delta\delta_{\text{sat}}$ calculated for saturation binding of guest protons. ^[122,123]

host	R	n	X, Y	K_a in D ₂ O, M ⁻¹	K_a in D ₂ O/CD ₃ O (60/40 v/v), M ⁻¹	ΔG° , kcal mol ⁻¹	$\Delta\delta_{\text{sat}}$ H _{guest} , ppm
75	H	3	OMe (D)	< 85	-	< 2.6	-1.83
75	H	3	CN (A)	1520	-	-4.3	-2.13
76	OMe	3	OMe (D)	371	-	-3.45	-2.19
76	OMe	3	CN (A)	1020	-	-4.04	-2.24
77	H	4	OMe (D)	-	95	-2.66	-
77	H	4	CN (A)	-	140	-2.89	-
78	Me	4	OMe (D)	-	580	-3.72	-
78	Me	4	CN (A)	-	1580	-4.29	-
79	OMe	4	OMe (D)	-	340	-3.41	-
79	OMe	4	CN (A)	-	390	-3.48	-
79	OMe	4	OMe (D)	10200	-	-5.38	-2.03
79	OMe	4	CN (A)	7830	-	-5.23	-2.09

Table 1 demonstrates that the guests' complexation-induced upfield shifts at saturation are around 2 ppm in pure D₂O, almost independent of the binding strength.

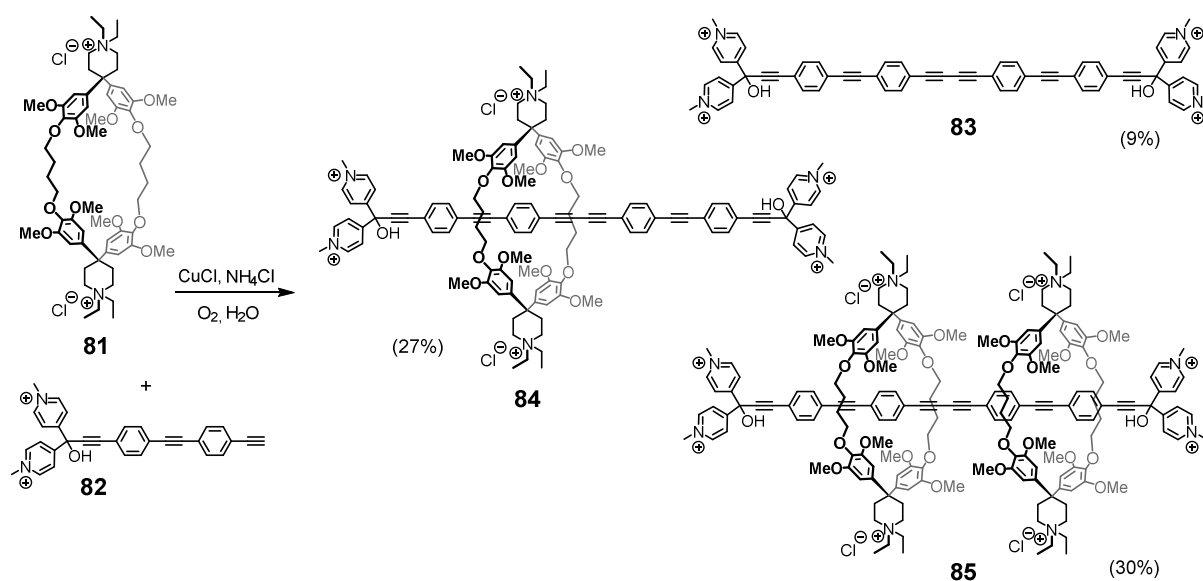
Evaluation of the complexation strength with the in protic solvents low-soluble naphthalene guests proved to be more difficult. Only few accurate association constants and thermodynamic data could be determined, such as the values for host **79** with 2,6-dimethoxynaphthalene ($K_a = 4490 \text{ M}^{-1}$ and $\Delta G^\circ = -4.90 \text{ kcal mol}^{-1}$) and **79** with 2,6-dicyanonaphthalene ($K_a = 7160 \text{ M}^{-1}$ and $\Delta G^\circ = -5.17 \text{ kcal mol}^{-1}$) in D₂O/CD₃OD (60:40 v/v). In general, the measured association constants of octamethyl host **78** with a series of different 2,6-disubstituted naphthalene derivatives in pure CD₃OD followed the electron-donor-acceptor theory. The measured K_a values are considerably lower than the association for the same host-guest couples in the binary solvent mixture.

In none of the electronic absorption spectra of the solution complexes a charge-transfer band was observed. Compared to the spectra of free guests, the spectra of cyclophanes **76-79**

threaded with benzene or naphthalene derivatives, only exhibit small bathochromic shifts (2-4 nm), band broadening and weak hypochromicity.

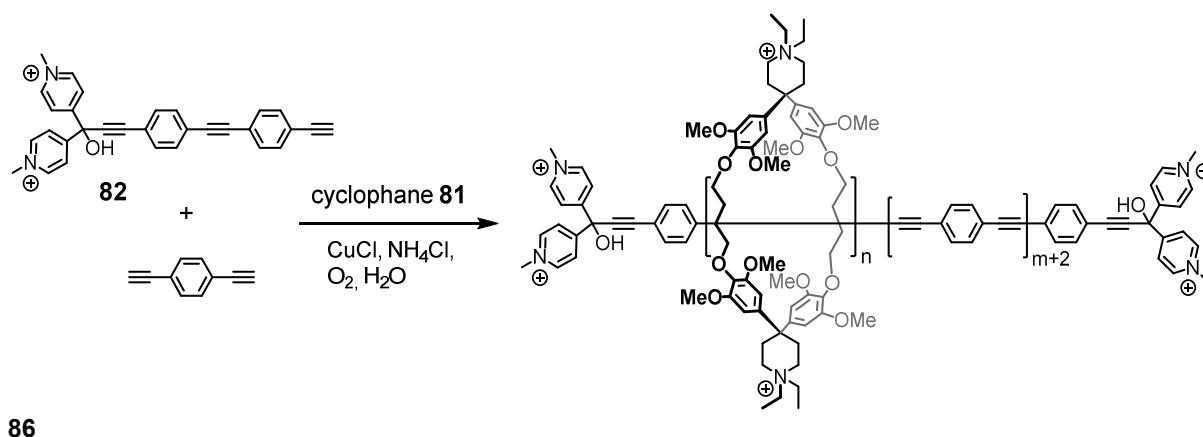
The group of Benson investigated the complexation strength of octamethoxy cyclophane **79** with monosubstituted naphthalene guests via fluorescence quenching titration.^[124] Formation of host-guest exciplexes upon photoexcitation were found for complexes of **79** with 1- and respectively 2-methylnaphthalene. Bulky substituents and electron-deficient guests turned out to hinder exciplex generation, as for example neither 1-cyanonaphthalene nor the 2-substituted analogue aromatic showed this behavior. The association constants for **79** complexing 1- and 2-methylnaphthalene were determined as $1.6 \times 10^3 \text{ M}^{-1}$ and $1.3 \times 10^5 \text{ M}^{-1}$ respectively. Interestingly, the substitution at the 1-position of naphthalene seems to be unfavorable for complexation, as the binding constants for 1-methylnaphthalene ($K_a = 1.6 \times 10^3 \text{ M}^{-1}$) and 1-cyanonaphthalene ($K_a = 2.1 \times 10^4 \text{ M}^{-1}$) are significantly lower.

On their approach to the insulation of long conjugated π -systems via polyrotaxane formation, Anderson and coworkers used Diederich-type cyclophanes as well as cyclodextrins^[60,63-65] as protective macrocycles of a water-soluble molecular axle. The octamethoxy-substituted cyclophane **81** presents the bis(*N*-ethylpiperidinium) analogue to cyclophane **79**.^[125] Anderson varied the last two synthetic steps from originally basic *N*-acetyl hydrolysis and subsequent Eschweiler-Clarke methylation^[126,127] to reduction of *N*-acetyl with DIBAL-*H*, followed by quaternization with ethyl iodide.^[128] Harnessing the hydrophobic effect as driving force is appealing due to the hydrophobic character of the conjugated oligophenylene ethynylene (OPE) axle. ¹H NMR titrations and Job plot analysis confirmed the formation of stable 1:1 complexes between host **81** and axle **82** in water with an association constant of $K_a = 4.3 \times 10^4 \text{ M}^{-1}$. The rotaxation step, an aqueous Glaser coupling^[129,130] of a 1:1 mixture of **81** and **82** gave after purification a product mixture containing 30% [3]rotaxane **85**, 27% [2]rotaxane **84** and 9% dumbbell **83**.



Scheme 23. Insulation of the π -conjugated backbone of an OPE by rotaxane synthesis in water.^[125,128]

Although the reaction was repeated with varying concentration ratios of the starting materials, the percentage of cyclophane incorporated into rotaxane was never greater than 56%. Interestingly, the reaction with 2,6-di-*O*-methyl- β -cyclodextrin as an alternative host with a high affinity for **82** ($K_a = 2.7 \times 10^4 \text{ M}^{-1}$), did not afford any rotaxane. A likely explanation for affording low or no rotaxane yield in both cases, might be found in the huge excess of ammonium chloride (2000 eq) and copper(I) chloride (667 eq) used for the coupling reaction. The cyclodextrin cavity entrance might have been blocked by complexation of copper(I) cations with the cyclodextrin's hydroxyl groups, whereas some of the cyclophane might have been precipitated as the salt of a chlorocuprate anion. Another given conjecture was kinetically slower coupling of the encircled axle. The synthesis of longer polyrotaxanes (**86**) in the presence of 1,4-diethynylbenzene afforded only the incorporation of up to two units, probably due to precipitation of formed diethynylbenzene oligomers or elongated axle **82**.



Scheme 24. Synthesis of a poly-rotaxane **86**.^[128]

Measurements of fluorescence spectra revealed an increase of the kinetic stability of the excited state and hindered quenching in the presence of cyclophane. Rotaxanes **84** and **85** showed a 1.8 times higher fluorescence emission compared to the free dumbbell **83**. Emission enhancement was also observed for a related rotaxane system (**87**) with an anionic naphthalene stopper moiety.^[131] [3]rotaxane **87** was afforded in 35% yield under the same reaction conditions as rotaxanes **84** and **85**. Remarkable was the strong binding strength of the corresponding anion stoppered OPE axle with cyclophane **81** ($K_a = 4.5 \times 10^6 \text{ M}^{-1}$).

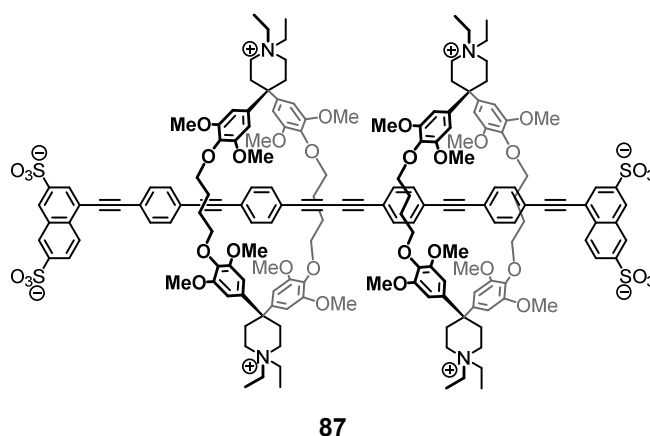
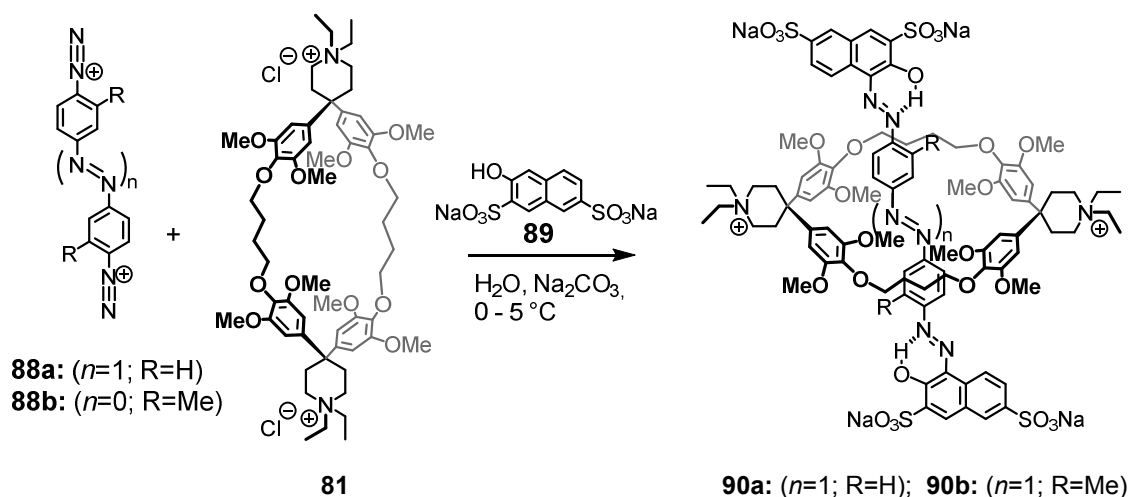


Figure 35. Anion-stoppered OPE-rotaxane.^[131]

Besides preparing rotaxanes with OPEs, Anderson and coworkers also protected the chromophore of azo dyes by rotaxanation with cyclophane **81**.^[132] Diazonium salts **88a** and **88b** were synthesized from their corresponding amine in presence of sodium nitrite, before cyclophane **81** and stopper **89** were subsequently added. Rotaxanes **90a** and **90b** were isolated in 46 and 40% yield, respectively. Interestingly, no free dumbbell, but some by-product due to dediazotization was obtained. Harnessing α - and β -cyclodextrins as macrocycles resulted in considerably lower yields and also more complicated ^1H NMR spectra caused by the unsymmetrical CD rims.



Scheme 25. Synthesis of water-soluble Diederich cyclophane-based azo-dye rotaxanes.^[132]

In 2013, Rotzler et al. reported the synthesis of an amphiphilic daisy chain monomer and investigated the aggregation behavior in polar solvent.^[133] The design profited to a large extent from Andersons' OPE-based rotaxanes with water-soluble Diederich cyclophane hosts.^[125,128] Rotzler et al. functionalized the periphery of an *N,N*-ethylated analogue of Diederich cyclophane **75** with a unfunctionalized OPE rod, affording monomer **91**.

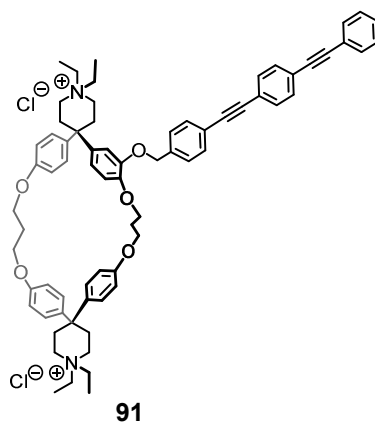


Figure 36. Unsubstituted amphiphilic daisy chain monomer **91**.

Association was observed already at very low concentrations (i.e. 10^{-6} mM). Concentration-dependent 1H NMR shift experiments in combination with diffusion studies indicated the presence of mainly [c2]daisy chains up to a concentration of 1 mM and higher oligomers above this concentration.

2 Towards Molecular [c2]Daisy Chains as Functional Materials

Inspired by the beautiful pseudo-rotaxane concept of Sauvage,^[21,109] our group designed organic molecular structures which are suitable for the formation of molecular daisy chains. These supermolecules, in particular in form of polymers, are appealing candidates to realize a major aim of material science – precise alteration of a systems' macroscopic physical output induced by a controlled change in the molecular level.

Artificial molecular muscles and also single molecular potentiometers^[134] are examples for systems which fulfil this objective of functional materials. In contrast to molecular muscles, where length variation (physical output) is triggered by changes in electrochemical potential or pH (input), in a molecular potentiometer mechanically induced length alteration (input) results in a change of conductivity (physical output).

Encouraged by the initial results of Rotzler's unsubstituted amphiphile **91**, indicating [c2]daisy chain formation at concentrations below 1 mM,^[133] the aim was to advance the proof-of-principle system and to construct a molecular potentiometer (Figure 37). Introduction of a terminal thiol group on the OPE rod allows [c2]daisy chains to be anchored to gold electrodes in a mechanically controllable break junction (MCBJ)^[135,136]. Acetyl was chosen as protecting group for the thiophenol (**95**) in order to prevent the formation of disulfides, but on the other hand allowing facile deprotection *in situ* in presence of tetrabutylammonium hydroxide.^[137] Conductance through the resulting bimolecular junction is expected due to intermolecular π - π stacking between the two complexed OPE rods of the daisy chain dimer.^[138] Mechanical alteration of the distance between the two electrodes and hence the change in π -overlapping surface is expected to afford a variation in conductance.

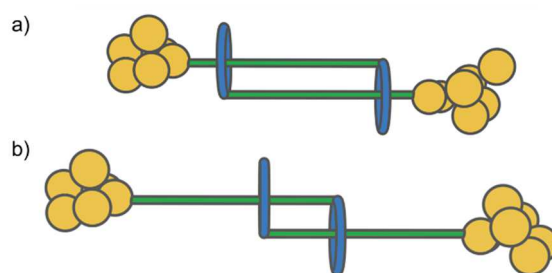


Figure 37. Schematic representation of a [c2]daisy chain fixed between the two gold electrodes of a mechanically controlled break junction. a) high conductance state; b) low conductance state due to less π -overlapping surface.

A further objective was to get a deeper insight into the aggregation behavior of the amphiphilic OPE-cyclophane system and to capture the daisy chain aggregates affording mechanically interlocked molecules. Therefore, a series of derivatives (**92-95**) with different functionalities (Figure 38) was prepared relying on the basic structure of amphiphile **91**.

The hydroxyl group and the free acetylene group in amphiphiles **92** and **93** were introduced with the objective of providing a reactive group for attaching a potential stopper molecule. A feasible approach might be a substitution reaction at the hydroxyl functionality of **92**. In principle, the acetylene allows for the application of different coupling types, such as Glaser^[129,130] coupling or CuAAC^[48,49] *click* chemistry. Both reaction types are applicable in water, which is an important premise for trapping the aggregates formed by **93** in aqueous medium. Monomer **94**, comprising a bulky anthracene moiety linked by a benzylic ether, was prepared as a nonthreading reference compound, especially for DOSY experiments. Furthermore, the conceivable influence of the OPE substituent's electronic properties on the aggregation was of interest.

2.1 General Molecular Design of Amphiphiles 91-95

Monomers **91-95** are composed of two major parts, the hydrophobic OPE rod and the water-soluble Diederich-type cyclophane comprising a hydrophobic cavity interior. Similarly to the design of the preceding Diederich cyclophanes (see Chapter 1.3.9), two diphenylmethane units function as rigid spacers and cavity walls. One of the in total four phenyl rings is monofunctionalized with a hydroxyl group employed as an anchor group for the OPE rod. The diphenylmethane units are bridged by a dioxapropane chain, defining the cavity size. Chloride was chosen as the counterion since dichloride cyclophanes exhibit the highest solubility in water.^[120] The OPE rod was linked to the monofunctionalized cyclophane via a benzyl ether moiety, which gives the system the necessary flexibility to find an ideal spatial arrangement for threading the rigid OPE rod into the cyclophane cavity.

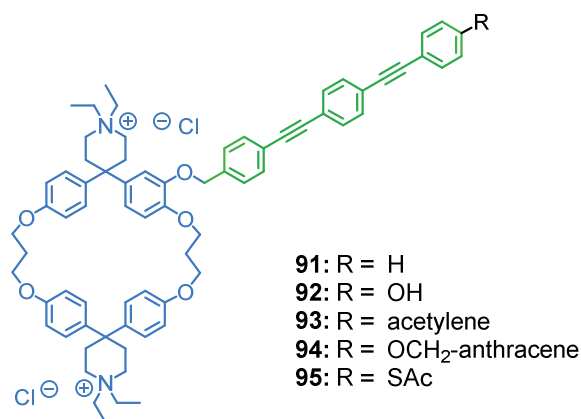
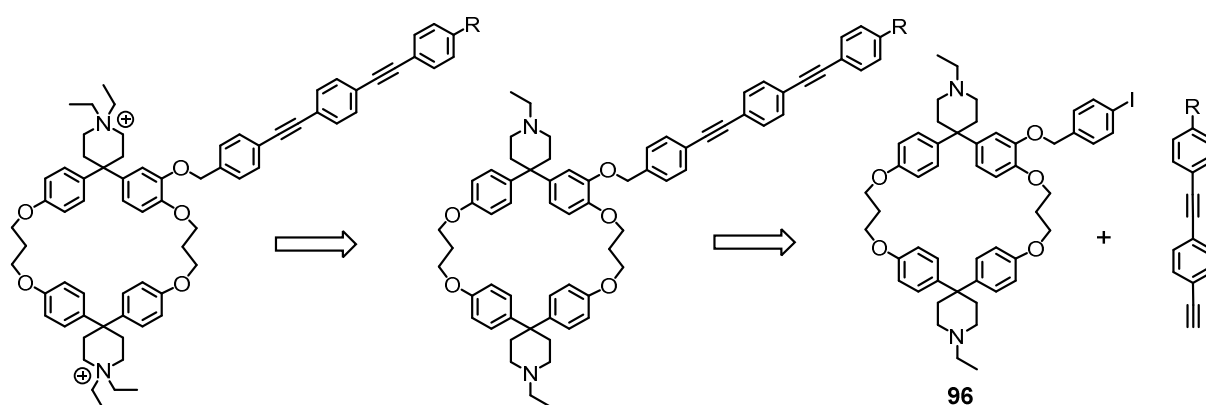


Figure 38. Synthesized and characterized derivatives **92-95** originated from the unsubstituted amphiphile **91**^[133]

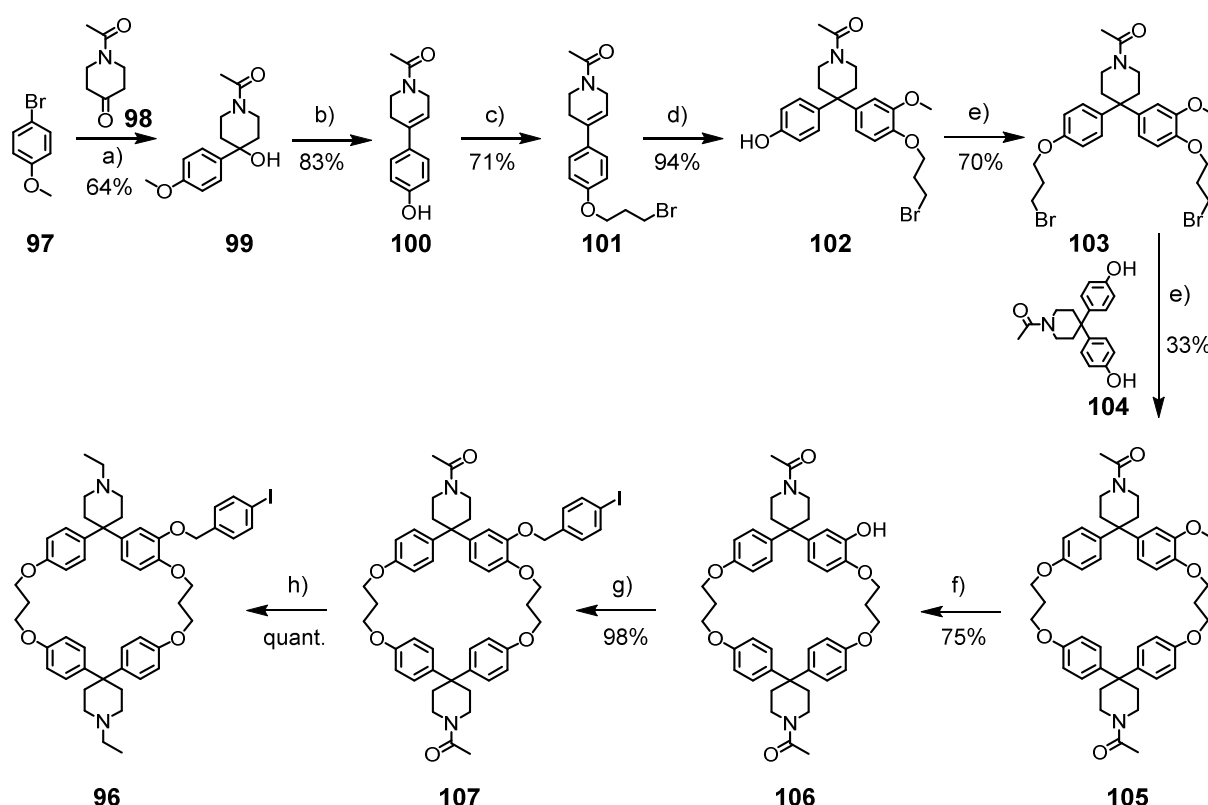
2.2 General Synthetic Approach for Amphiphiles 91-95

Amphiphiles **92-95** were prepared in accordance to the synthetic procedure for **91** developed by Rotzler et al.. The OPE rod, consisting of two phenylene ethynylene units, was coupled to the benzyl linker of the *N*-ethyl cyclophane **96** via Sonogashira cross-coupling^[139]. Attachment of the OPE in a late stage of the synthesis allows facile alteration of the substitution pattern of the rod. Introduction of the amphiphilic character via quaternization with iodoethane was performed in the last synthetic step, avoiding Sonogashira cross-coupling with an organic salt and potential solubility issues.



Scheme 26. Retrosynthetic strategy towards amphiphiles **91-95**.

The synthetic protocol towards building block **96**, developed by Rotzler et al.^[133] was inspired by the previously reported synthetic routes towards monofunctionalized Diederich-type cyclophanes.^[120,121,140–142] The procedure composed of nine consecutive steps starting with a Grignard reaction^[143,144] of 4-bromoanisole (**97**) and *N*-acetyl-piperidin-4-one (**98**). The reaction is followed by deprotection of the methoxy group and elimination of the alcohol in one step using boron tribromide. Both reactions allowed for gram scale batches since chromatographic purification was not required. Alkylation of phenol **100** with 1,3-dibromopropane was followed by a Friedel-Crafts-type reaction of guaiacol and compound **101** in presence of boron trifluoride diethyl etherate. After nine days reaction duration, compound **102** was obtained alongside 9% of a regioisomer. The undesired isomer was removed by high performance liquid chromatography (HPLC) after the introduction of the second alkyl chain. The key step towards benzyl-substituted cyclophane **96** was the intermolecular cyclization reaction of **103** with bisphenol **104**, which was performed under dilute conditions (2.9 mM). After purification via column chromatography monofunctionalized cyclophane **105** was obtained in 33% yield.



Scheme 27. Assembly of the macrocyclic building block of amphiphiles **91-95**. a) Mg, THF, reflux, 1.5 h, then *N*-acetyl-piperidin-4-one, THF, rt, 4 h; b) BBr₃, CH₂Cl₂, reflux, 3 h; c) 1,3-dibromopropane, K₂CO₃, MeCN, reflux, 5 h; d) guaiacol, BF₃·OEt₂, CH₂Cl₂, rt, 9 d; e) 1,3-dibromopropane, K₂CO₃, acetone, reflux, 20 h; f) Cs₂CO₃, acetonitrile, reflux, 20 h; e) sodium thiomethoxide, DMF, 160°C, 6 h; f) 4-iodobenzyl bromide, Cs₂CO₃, DMF, 85°C, 20 h; g) LiAlH₄, CH₂Cl₂, -10°C, 5 min, then DIBAL-*H*, CH₂Cl₂, 0°C 40 min.

For the selective cleavage of the methoxy group without opening the ring via cleavage of dioxapropene chains, nucleophilic demethylation with sodium thiomethoxide turned out to be the method of choice. The reaction required water-free conditions, inert atmosphere and high temperature in order to avoid ring opening and ensure full conversion. The benzyl linker was attached to the phenol group of **105** in a S_N2 reaction with 4-iodobenzyl bromide in presence of cesium carbonate. In the subsequent reduction of cyclophane **106** with DIBAL-*H* according to Rotzler et al.^[133] partial cleavage of the benzyl ether and *N*-deacetylation were observed. Side reactions could be prevented by treating the *N*-acetyl cyclophane **107** with 4.0 equivalents of $LiAlH_4$ at $-10\text{ }^\circ\text{C}$ for five minutes, before 2.2 equivalents of DIBAL-*H* were added to the reaction at $0\text{ }^\circ\text{C}$. The macrocyclic building block **96** for amphiphiles **91-95** could be obtained quantitatively.

The preparation of the functionalized OPE building blocks, as well as the final assembly towards the amphiphilic monomers will be described individually for each target molecule in following sections.

2.3 General Approach for the Aggregation Studies

Based on the proof-of-principle publication^[133] the aggregation behavior of the four novel amphiphiles **92-95** were investigated by applying similar analytical techniques. The association constant K_a , as well as the aggregation number N were obtained by concentration dependent ^1H NMR titration studies, whereas diffusion ordered spectroscopy (DOSY) measurements provided information about the size of the aggregates. Qualitative comparison of fluorescence emission spectra recorded in solvents of high polarity with those in low polarity gave an indication about the self-complexation behavior in different environments.

2.3.1 ^1H NMR Dilution Studies

In line with previous publications the self-aggregation behavior of molecule **91**^[133] as well as the derivatives **92-95** was investigated by performing ^1H NMR dilution studies. Starting with a concentrated stock solution in D_2O/CD_3OD (60:40 v/v) a dilution series of each amphiphile was prepared and ^1H NMR spectra were recorded after every dilution step at constant

temperature. Comparison of the spectra revealed signal broadening and additionally a concentration-dependent change of the observed chemical shift δ_{obs} . This parameter is composed of the sums of the individual chemical shift of the monomer (δ_{mon}) and all the present aggregates (δ_{agg}) (equation 1):

$$\delta_{obs} = \delta_{mon}(C_{mon}/C_{tot}) + \delta_{agg1}(C_{agg1}/C_{tot}) + \delta_{agg2}(C_{agg2}/C_{tot}) + \dots \quad (1)$$

The critical aggregation concentration (cac), indicating the concentration at which the predominant aggregate changes to another, can be determined with the plot of δ_{obs} versus the reciprocal of the total concentration C_{tot} . For instance, the cac from the transition of dimer to higher aggregates was determined as 1 mM for amphiphile **91**.

The association constant K_a and the aggregation number N were obtained by applying the following linear expression^[133,145]:

$$\ln[C_{tot}(|\delta_{obs}-\delta_{mon}|)] = N \ln[C_{tot}(|\delta_{agg}-\delta_{obs}|)] + \ln K_a + \ln N - (N-1)\ln(|\delta_{agg}-\delta_{mon}|) \quad (2)$$

Equation (2) was based on the simplification considering only one equilibrium for each aggregate and concentration range. For all equilibria the same association constant was assumed ($K_{a1} = K_{a2} = K_{a3}$ etc.). The two unknown parameters δ_{mon} and δ_{agg} were approximated by plotting δ_{obs} versus C_{tot} and δ_{obs} versus $1/C_{tot}$, respectively, and extrapolating to the intercept with the y-axis (see exemplary chapter 2.3.2). Fitting a straight line with the plots of $\ln[C_{tot}(|\delta_{obs}-\delta_{mon}|)]$ vs. $\ln[C_{tot}(|\delta_{agg}-\delta_{obs}|)]$ gave a slope (N) and an intercept with which K_a could be calculated. The dilution studies were performed three times for each derivative, if not indicated otherwise.

2.3.2 DOSY Analysis

Assuming a similar aggregation behavior to amphiphiles **91**, the formation of predominantly dimeric daisy chains was also expected for derivatives **92-94** at low concentrations.

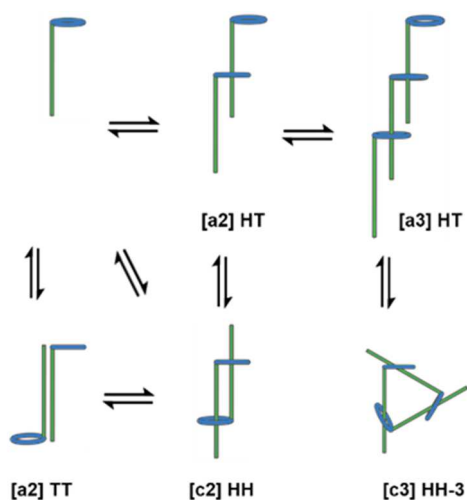


Figure 39. Possible dimeric and trimeric aggregates formed by amphiphiles **91-94** in polar solvents.

Monomer **91** can aggregate to three different dimers: 1) the acyclic head-tail **[a2] HT** daisy chain and also the first propagation step towards polymers, 2) the head-head threaded cyclic and thermodynamically favored dimer **[c2] HH** or 3) the unthreaded **[a2] TT** aggregate. As the OPE rods of the latter do not thread the cyclophane cavity no release of high energy water can take place as it is usually the case upon complexation driven by a nonclassical hydrophobic effect. For the following aggregates (*N*-mers) mechanically interlinked compounds can only be acyclic or cyclic, as exemplary demonstrated for trimers (**[a3] HT** and **[c3] HH-3**). Micellar or multiple stacked aggregates are possible as unthreaded version.

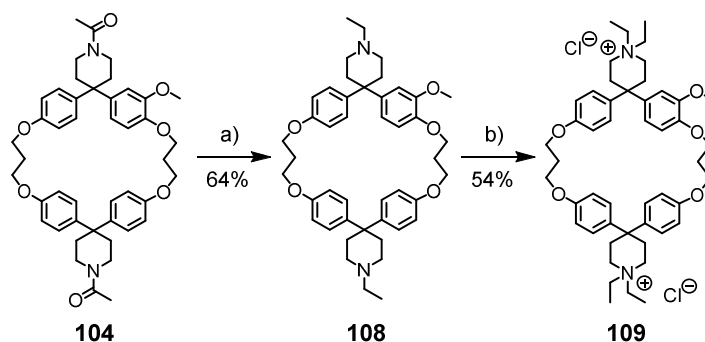
By performing diffusion ordered ^1H NMR (DOSY) measurements in a concentration range where predominantly dimerization was expected, the size of the aggregate and hence the type of dimer was estimated. However, a direct comparison of the obtained diffusion coefficient D_{agg} with the one of the monomer (D_{mon}) was not feasible. Due to instrumental limits the concentration range in which monomer can be observed in the $\text{D}_2\text{O}/\text{CD}_3\text{OD}$ (60:40 v/v) could not be reached by ^1H NMR experiments. Therefore, the monomethoxy-functionalized cyclophane lacking the OPE moiety was synthesized as a reference compound. The

determined diffusion coefficient D_{ref} was used to estimate the ratio of aggregate volume V_{agg} to monomer volume V_{mon} by the following expression:^[133]

$$\frac{V_{agg}}{V_{mon}} = \frac{(D_{agg}/D_{ref})^3}{M_{mon}/M_{ref}} \quad (3)$$

with M_{mon} and M_{ref} exhibiting the molecular weight of the monomeric amphiphile and the reference compound, respectively.

Reference cyclophane **109** was synthesized starting from cyclophane **104** in two steps (Scheme 28). The *N*-acetyl unit of **104** was reduced by applying a previously reported procedure with boron-tetrahydrofuran complex as reductant affording **108** in 64% yield. The tertiary amine was then alkylated using iodoethane. Purification by column chromatography with a mixture of acetone: 1 M aq. ammonium chloride: acetonitrile (7:1:1 v/v), Soxhlet extraction and ion exchange chromatography yielded **109** in 54% yield.



Scheme 28. Synthesis of reference compound **109**. a) $\text{BH}_3 \cdot \text{THF}$, THF reflux, 18 h, then H_2SO_4 , EtOH, reflux, 1 h; b) iodoethane, CH_2Cl_2 , rt, 24 h, then ion exchange (DOWEX 1X8, Cl^-).

2.3.3 Fluorescence Spectroscopy

The influence of the hydrophobic effect on the aggregation tendency of amphiphiles **92-95** was investigated qualitatively by recording fluorescence emission spectra. In highly polar protic solvents, such as the mixture of water/methanol (3:2 v/v), aggregation was expected. In turn, in the less polar and aprotic acetonitrile, a solvent in which the amphiphilic monomers were still soluble, a significantly lower tendency for association was anticipated. This behavior potentially leads to a reduced emission of the aggregated, threaded rod, compared to the free

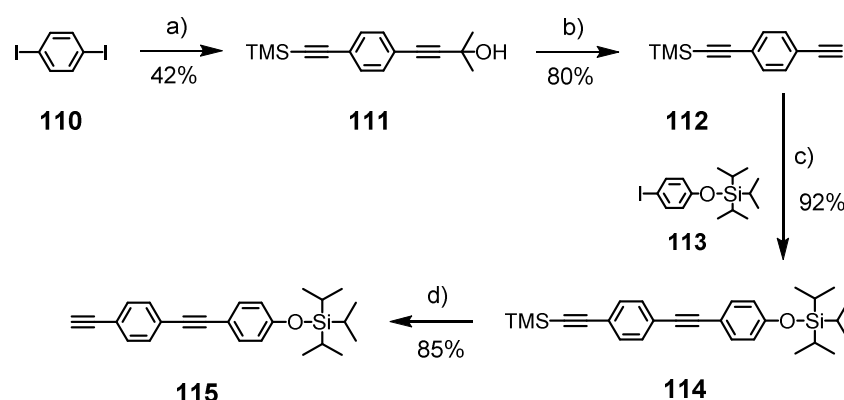
OPE unit. The shielding effect of the macrocycle was expected to be more pronounced in a more protic water/methanol mixture than in aprotic and less polar acetonitrile. Excitation at the absorption wavelength of the characteristic π - π^* transition of the OPE moiety (between 321 and 328 nm) was applied for measuring the fluorescence spectra.

2.4 Synthesis and Aggregation Studies of Hydroxyl-substituted Amphiphile 92

2.4.1 Synthesis of Monomer 92

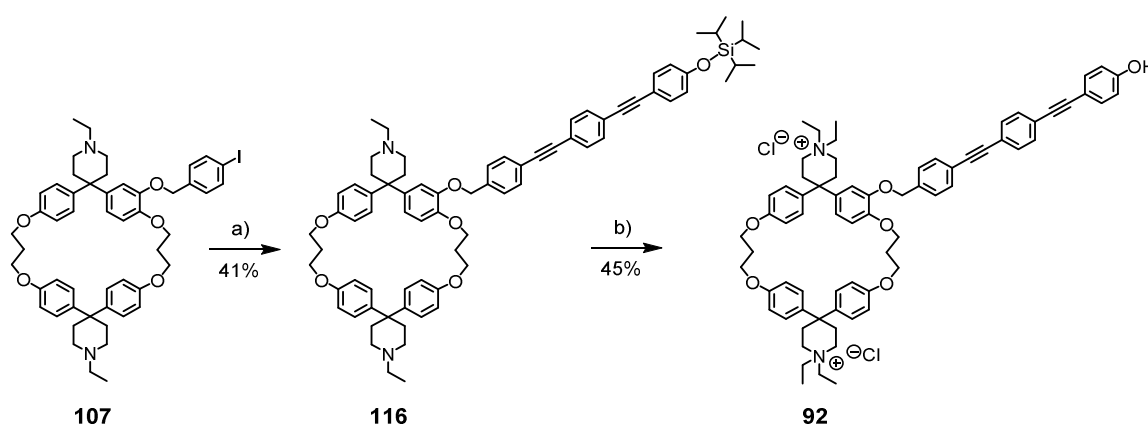
The hydroxyl group of the amphiphile's OPE building block was protected by a triisopropylsilyl (TIPS) group (**110**) in order to avoid the alkylation of the OH group under the basic conditions of the quaternization step. The protecting group was then cleaved off in the final step.

Building block **110** was synthesized starting from 1,4-diiodobenzene. Acetylenes with orthogonal protecting groups, trimethylsilyl (TMS) and dimethylpropargyl alcohol (HOP) were introduced via statistical Sonogashira cross-coupling reaction yielding **111** in a yield of 42%.^[133] Selective removal of the HOP protecting group with sodium hydride afforded component **112**,^[146] which was then coupled with (4-iodophenoxy)triisopropylsilane **113** under standard Sonogashira reaction conditions obtaining **114** in 92% yield. The TMS protecting group of component **114** was selectively cleaved off with potassium carbonate in methanol affording OPE building **115** in 85% yield.



Scheme 29. Synthesis of the TIPS-protected oligophenylene-ethynylene building block **115**. a) $\text{PdCl}_2(\text{PPh}_3)_2$, CuI , DIPA, THF, rt, 1.) TMS-acetylene, 4 h, 2.) 2-methyl-3-butyn-2-ol, rt 16 h; b) NaOH , toluene, 80°C , 45 min; c) **113**, $\text{PdCl}_2(\text{PPh}_3)_2$, CuI , DIPA, THF, 60°C , 3 h; d) K_2CO_3 , MeOH, rt, 2 h.

OPE building block **115** was attached to iodobenzyl cyclophane **96** via Sonogashira cross-coupling using catalyst bis(dibenzylideneacetone)palladium(0) ($\text{Pd}(\text{dba})_2$) in combination with triphenylphosphine as it had been employed for the final assembly of unsubstituted amphiphile **91**.^[133] The resulting precursor **116** was alkylated with an excess (1600 eq) of freshly distilled iodoethane in presence of 5 eq of base potassium carbonate. The base turned out to be crucial for full conversion to the alkylated product. After 40 h stirring in the dark at room temperature, the combined analysis method composed of high-performance liquid chromatography and electrospray ionization mass spectrometry (HPLC-ESI-MS) measurement indicated completion of the reaction and the remaining iodoethane was removed *in vacuo*. The resulting pale yellow solid was taken up in methanol in order to filter off the major part of excess potassium carbonate. Using dry methanol was essential to avoid cleavage of the TIPS protecting group. The HPLC-ESI-MS chromatogram showed the double charged hydroxyl amphiphile **92** as the main product ($m/z = 527$) besides a signal with $m/z = 541$, most likely corresponding to the *O*-ethylated analogue product formed from some TIPS-deprotected compound during the alkylation with iodoethane. Amphiphile was isolated by applying reverse-phase column chromatography. It turned out that addition of 5% 1 M aq. NH_4Cl to the neutral eluent consisting of 95% acetonitrile and 5% water was crucial for eluting the target compound. Assuming counter-anion exchange from iodide to chloride upon during the chromatographic purification with ammonium chloride, the desired amphiphile was obtained in 45% yield.



Scheme 30. Final assembly of amphiphile **92**. a) OPE **115**, $\text{Pd}(\text{dba})_2$, PPh_3 , CuI , THF, DIPA, rt, 8 h; b) 1.) EtI , K_2CO_3 , rt, 40 h, 2.) aq. NH_4Cl .

2.4.2 ^1H NMR Dilution Studies

Figure 39 demonstrates the ^1H NMR spectra of amphiphile **92** of different concentrations (0.13 mM – 8.0 mM) recorded in $\text{D}_2\text{O}/\text{CD}_3\text{OD}$ (60:40 v/v). Most striking are the peak broadening as well as the change of the observed chemical shifts δ_{obs} with increasing concentrations. The highest change of δ_{obs} was observed for the two different signals of the OPE protons in “the middle” phenyl unit of the rod, which were assigned by 2D NMR spectra in CD_3CN . The protons correspond to the chemical shift at 7.45 ppm and 7.32 ppm, respectively, in the spectrum recorded at 8.0 mM.

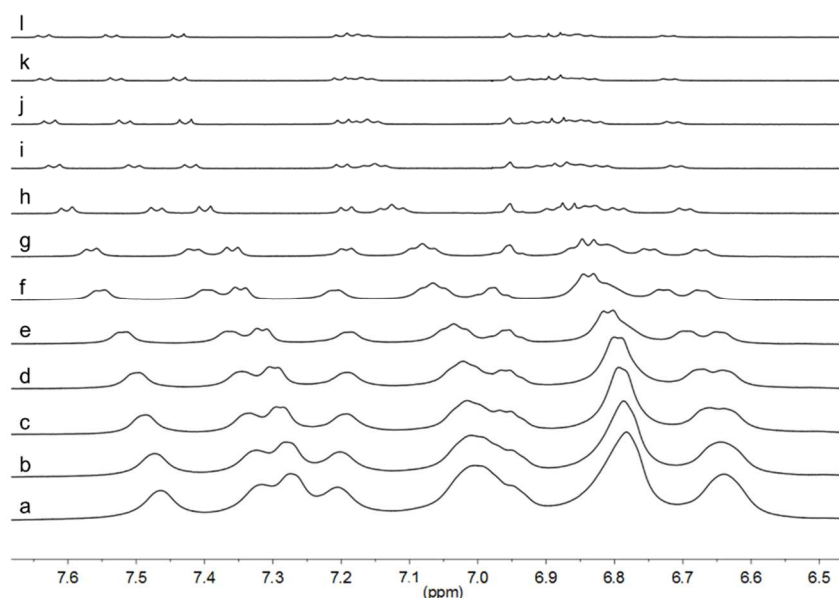


Figure 40. Stacked ^1H NMR spectra of the aromatic region of monomer **92** recorded in $\text{D}_2\text{O}/\text{CD}_3\text{OD}$ (60:40 v/v) at 298 K on a 500 MHz NMR spectrometer. a) 8.0 mM; b) 6.0 mM; c) 4.0 mM; d) 3.0 mM; e) 2.0 mM; f) 1.5 mM; g) 1.0 mM; h) 0.5 mM; i) 0.33 mM; j) 0.25 mM; k) 0.19 mM; l) 0.13 mM.

By way of comparison, ^1H NMR spectra of **92** were also recorded in acetonitrile- d_3 (Figure 40). The spectra are well-resolved, whereas peak-broadening and changes in the chemical shifts are lacking. These observations confirmed that no or only minor aggregation takes place in the aprotic, less polar solvent.

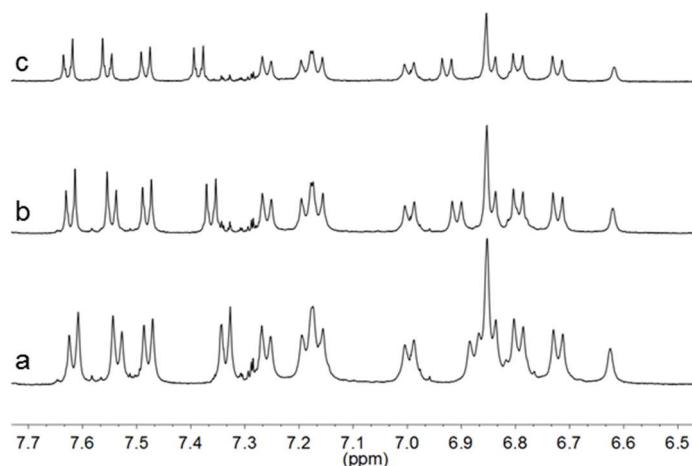


Figure 41. Stacked ^1H NMR spectra of the aromatic region of monomer **92** recorded in acetonitrile- d_3 at 298 K on a 500 MHz NMR spectrometer. a) 2.4 mm; b) 1.2 mm; c) 0.6 mm.

Applying the analysis method for the determination of the aggregation number N and the association constant K_a , introduced in chapter 2.2.1, δ_{obs} was plotted against C_{tot} and $1/C_{\text{tot}}$, respectively (see Figure 41 exemplary for one dilution series and for the most strongly shifting ^1H NMR signal). Linear regression of the data points in the respective linear ranges was used to estimate δ_{mon} (7.57 ppm) and δ_{agg} (7.31 ppm) respectively, as the intercepts with the y-axis.

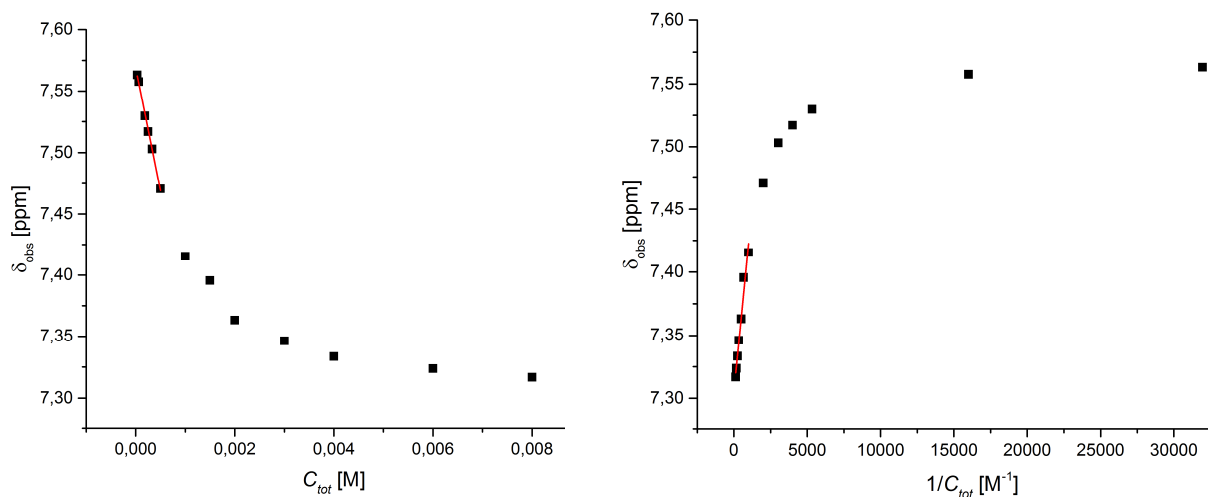


Figure 42. Plot of the observed chemical shift δ_{obs} versus the total concentration C_{tot} (left graph) and versus the inverse total concentration $1/C_{\text{tot}}$ (right graph). Linear regression gave δ_{mon} and δ_{agg} , respectively.

The cac of **92** and the other derivatives could not be determined. The method was not reliable as the data quality at low concentration was insufficient due to the detection limit of the NMR spectrometer.

By plotting $\ln[C_{tot}(|\delta_{obs}-\delta_{mon}|)]$ vs. $\ln[C_{tot}(|\delta_{agg}-\delta_{obs}|)]$ and utilizing linear regression a straight line was obtained. The slope corresponded to the aggregation number $N = 2.26$ (~ 2). With the intercept and equation (2) the association constant K_a was calculated. The three ^1H NMR dilution study series gave K_a values of $8.1 \times 10^3 \text{ M}^{-1}$, $5.4 \times 10^3 \text{ M}^{-1}$ and $7.6 \times 10^5 \text{ M}^{-1}$, respectively, for the most shifting peak (at 7.32 ppm in a 8.0 mM solution). Consequently, the association strength of the hydroxyl-substituted, electron-rich amphiphile **92** turned out to be lower than the one for the unsubstituted monomer **91**, confirming the EDA theory.

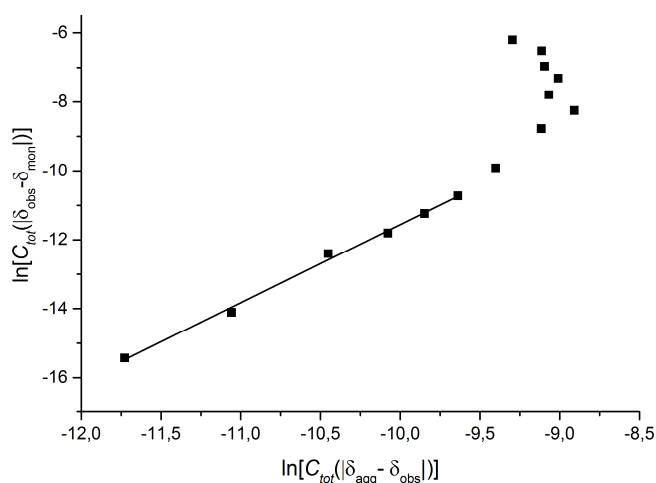


Figure 43: Plot of $\ln[C_{tot}(|\delta_{obs}-\delta_{mon}|)]$ vs. $\ln[C_{tot}(|\delta_{agg}-\delta_{obs}|)]$. The straight line represents linear regression from which the aggregation number N and the association constant K_a were estimated.

2.4.3 DOSY Analysis

Diffusion ordered spectroscopy measurements of amphiphile **92** were performed in $\text{D}_2\text{O}/\text{CD}_3\text{OD}$ (60:40 v/v) with a 0.2 mm sample, a concentration regime in which dimers were expected as predominant aggregates. By using the obtained diffusion coefficient D ($1.23 \times 10^{-10} \text{ m}^2 \text{ s}^{-1}$) and equation (3), the volume of the aggregate was estimated to be 1.41 times larger than the corresponding volume of the monomer. This finding strongly indicated mainly the formation cyclic, double threaded daisy chain dimers (**[c2] HH**) under these conditions.

2.4.4 Fluorescence Spectroscopy

UV and fluorescence spectra of amphiphile **92** were recorded in the binary solvent mixture water/methanol (60:40 v/v) as well as in acetonitrile. The maxima of the two almost identical UV spectra were observed for both cases at a wavelength of $\lambda = 326$ nm, corresponding to the π - π^* transition of the OPE rod. For recording the emission spectra, compound **92** was excited at 326 nm in both solvent systems. The huge difference in the intensity and hence the fluorescence quenching in the more polar system is striking. The maximum intensity in water/methanol is only 3.4% of the corresponding emission in acetonitrile at the same concentration, strongly indicating formation of inclusion complexes in the polar solvent mixture.

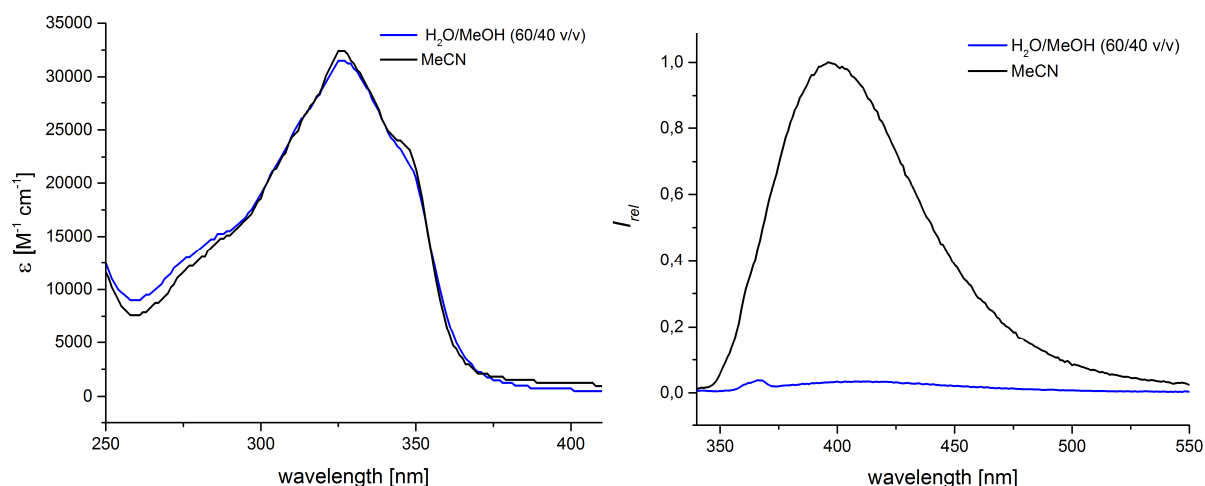
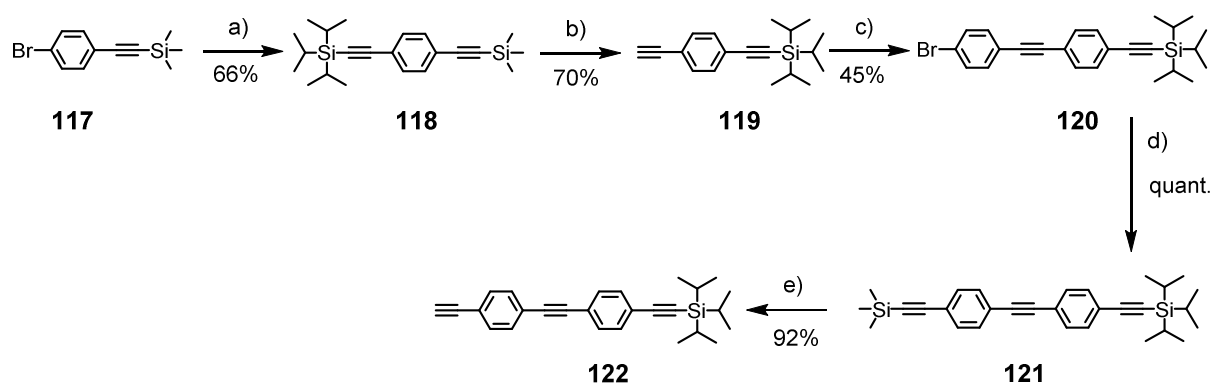


Figure 44. Absorption (left) and relative emission (right) spectra of amphiphile **92** in H₂O/MeOH (60:40 v/v) (blue) and MeCN (black), respectively. The two emission spectra were recorded at a concentration of 4.0×10^{-4} mM.

2.5 Synthesis and Aggregation Studies of Acetylene-substituted Amphiphile **93**2.5.1 Synthesis of Monomer **93**

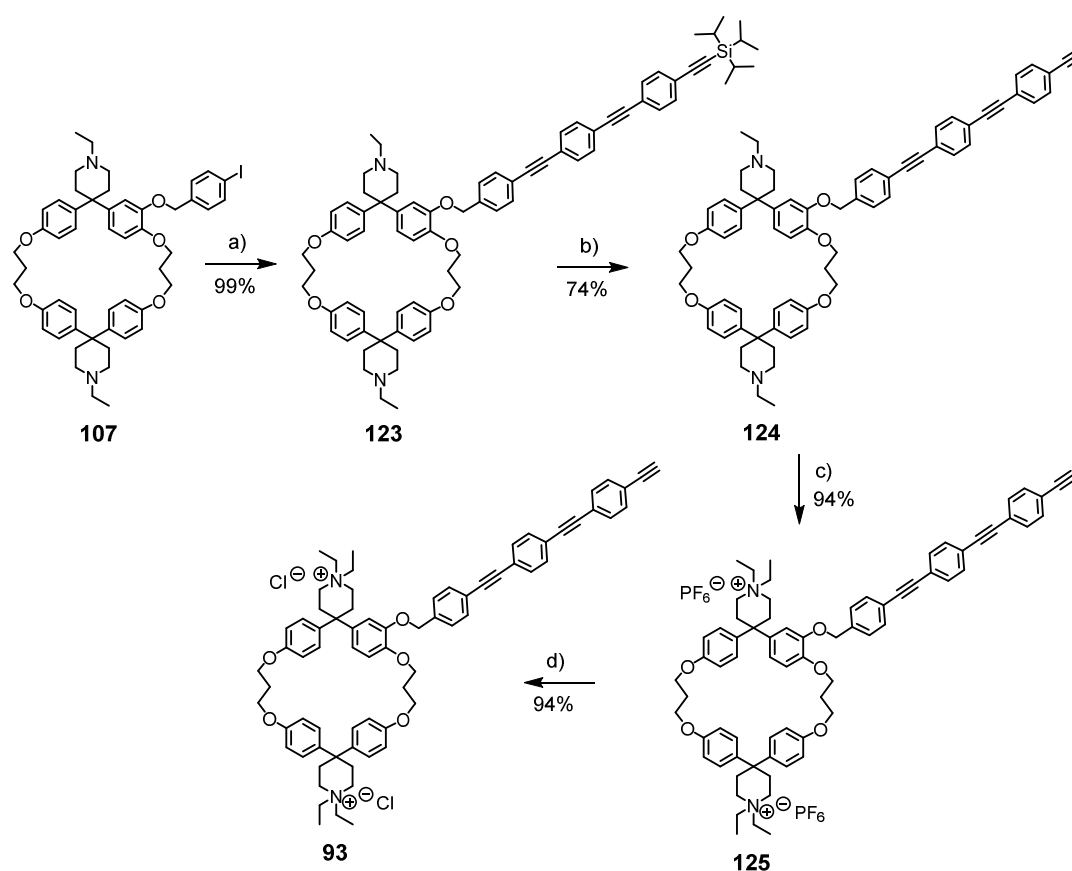
In the final assembly of **93** (Scheme 32), the OPE moiety **122** was attached to the macrocyclic building block **96** via Sonogashira cross-coupling reaction. The second acetylene unit of **122** was protected by a TIPS group. The first synthetic step towards OPE moiety **122** (Scheme 31) composed the introduction of the TIPS-acetylene (TIPSA) functionality to the commercially available (4-bromophenylethynyl)trimethylsilane **117** by a standard Sonogashira cross-coupling protocol. Purification via column chromatography afforded OPE precursor **118** in 66% yield, which was then deprotected with potassium carbonate in methanol to selectively cleave off the trimethylsilyl group. The second phenyl moiety was attached via a second Sonogashira cross-coupling affording the bromo-substituted compound **120**. After chromatographic purification, **120** was coupled to TMS-acetylene (TMSA), giving a quantitative yield of compound **121**. **121** was desilylated under basic conditions in methanol affording OPE moiety **122** in 92% yield.



Scheme 31. Synthesis of the TIPS-protected oligophenylene-ethynylene building block **122**. a) TIPSA, PdCl₂(PPh₃)₂, CuI, NEt₃, THF, 70 °C, 3 h; b) K₂CO₃, CH₂Cl₂, MeOH, rt, 6 h; c) 1-bromo-4-iodobenzene, PdCl₂(PPh₃)₂, CuI, DIPA, THF, rt, 6 h; d) TMSA, PdCl₂(PPh₃)₂, CuI, DIPA, THF, 60 °C, 3 h; e) K₂CO₃, MeOH, rt, 3 h.

The Sonogashira cross-coupling of cyclophane **96** with OPE moiety **122** was performed with tetrakis(triphenylphosphine)palladium(0). Product **123** was afforded in 99% yield after purification via column chromatography. TIPS was cleaved off with the fluoride source tetrabutylammonium fluoride (TBAF) as reagent, yielding compound **124** in 74%. Furthermore, deprotection before alkylation prevented the challenging chromatographic

separation of the alkylated, amphiphilic product from tetrabutyl ammonium, which tends to be eluted together with the cyclophane moiety. Amine **124** was alkylated to yield the quaternary ammonium compound **125** by applying similar reaction conditions as used for the alkylation of derivative **92**. After 34 hours reaction duration, the recorded LC-ESI-MS chromatogram indicated full conversion to the *N,N'*-ethylated product. The hexafluorophosphate salt **125** was isolated in 94% yield by subjecting the dried, crude reaction mixture to an aqueous solution of potassium hexafluorophosphate and subsequent extraction with dichloromethane. Applying chloride ion exchange chromatography afforded the target compound **93** in 94%.



Scheme 32. Synthetic steps towards amphiphile **93**. a) OPE **122**, $Pd(PPh_3)_4$, CuI, THF, DIPA, rt, 18 h; b) TBAF, THF, rt, 45 min; c) 1.) Etl, K_2CO_3 , dark, rt, 34 h; 2.) KPF_6 , CH_2Cl_2 ; d) DOWEX 1X8, Cl^- .

2.5.2 1H NMR Dilution Studies

Regarding the 1H NMR spectra of **93** in D_2O/CD_3OD (60:40 v/v) at different monomer concentrations (Figure 45), evidence for aggregation, such as signal broadening at higher concentrations and changes in the chemical shift δ_{obs} are clearly visible. In contrast, the

recorded ^1H NMR spectra of **93** in CD_2Cl_2 show sharp signals and lack any sign of aggregation (Figure 46). Similar to the aggregation studies of hydroxyl-substituted amphiphile **92**, three dilution series were performed in $\text{D}_2\text{O}/\text{CD}_3\text{OD}$ (60:40 v/v) and with the most strongly shifting signal the aggregation number N as well as the association constant K_a was determined. The signal chosen for the evaluation of the studies was the OPE signal at $\delta = 7.27$ ppm in the 8 mm solution. Employing the linear regression method (see exemplary plots in Chapter 2.3.2), K_a values of $3.6 \times 10^5 \text{ M}^{-1}$, $1.1 \times 10^5 \text{ M}^{-1}$ and $9.9 \times 10^5 \text{ M}^{-1}$ were obtained. However, the three determined aggregation numbers $N = 2.8$, 2.7 and 3.0 indicated trimers as major species in the utilized concentration range.

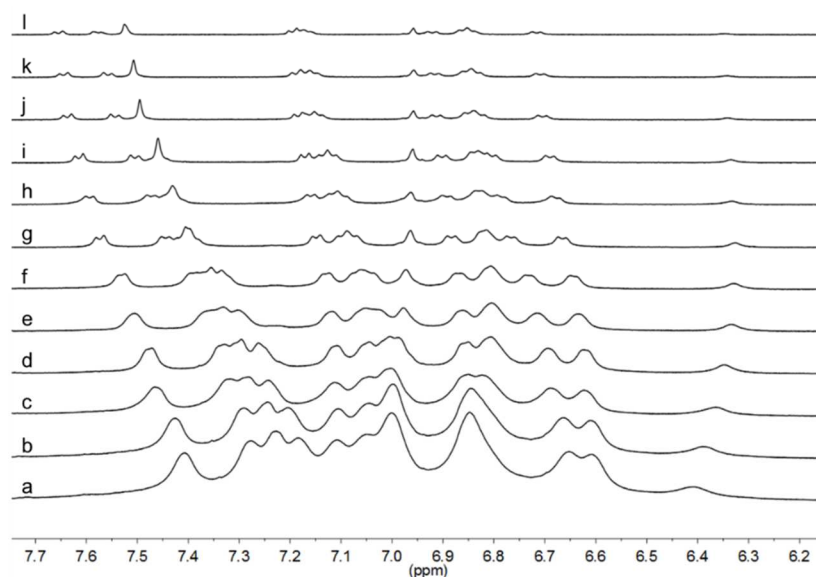


Figure 45. Stacked ^1H NMR spectra of the aromatic region of amphiphile **93** recorded in $\text{D}_2\text{O}/\text{CD}_3\text{OD}$ (60:40 v/v) at 298 K on a 500 MHz NMR spectrometer. a) 8.0 mm; b) 6.0 mm; c) 4.0 mm; d) 3.0 mm; e) 2.0 mm; f) 1.5 mm; g) 1.0 mm; h) 0.75 mm; i) 0.5 mm; j) 0.33 mm; k) 0.25 mm; l) 0.18 mm.

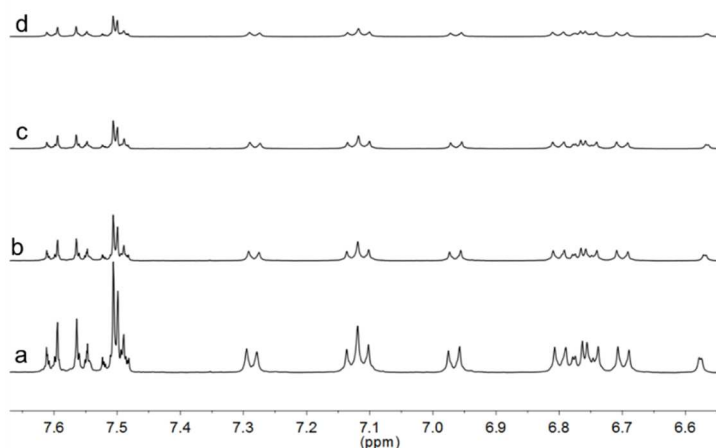


Figure 46. Stacked ^1H NMR spectra of the aromatic region of monomer **93** recorded in CD_2Cl_2 at 298 K on a 500 MHz NMR spectrometer. a) 4.0 mm; b) 2.0 mm; c) 1.0 mm; d) 0.5 mm.

2.5.3 DOSY Analysis

The diffusion coefficient in the protic, polar solvent mixture D_2O/CD_3OD (60:40 v/v) corresponding to the aggregates of **93** in the 0.2 mm sample was determined as $D = 1.20 \times 10^{-10} \text{ m}^2 \text{ s}^{-1}$. This parameter revealed to be very similar to the corresponding diffusion coefficient of amphiphile **92** ($D = 1.23 \times 10^{-10} \text{ m}^2 \text{ s}^{-1}$). Also the ratio of aggregate volume (V_{agg}) to monomer volume (V_{mon}) of 1.42, estimated by employing equation (3), turned out to be almost identical with the ratio obtained for **92** (1.41). These ratios rather implicated the presence of [c2]daisy chains, which however stands in contrast to the determined aggregation number N of **93**.

2.5.4 Fluorescence Spectroscopy

In line with the qualitative fluorescence studies of **92**, the UV and fluorescence spectra of amphiphile **93** were recorded in water/methanol (60:40 v/v) as well as in acetonitrile. The maximum wavelength ($\lambda = 328 \text{ nm}$) in the UV spectrum in acetonitrile (Figure 47, left) was used as excitation wavelength of both recorded emission spectra. In contrast to the fluorescence spectra of **92**, which showed a great difference in emission intensity, the fluorescence quenching in the protic, more polar solvent mixture is much less distinct for **93**. The reason for this unexpected result, which appeared to be contradicting the high association constant of **93** in the range of 10^5 M^{-1} , was not further investigated.

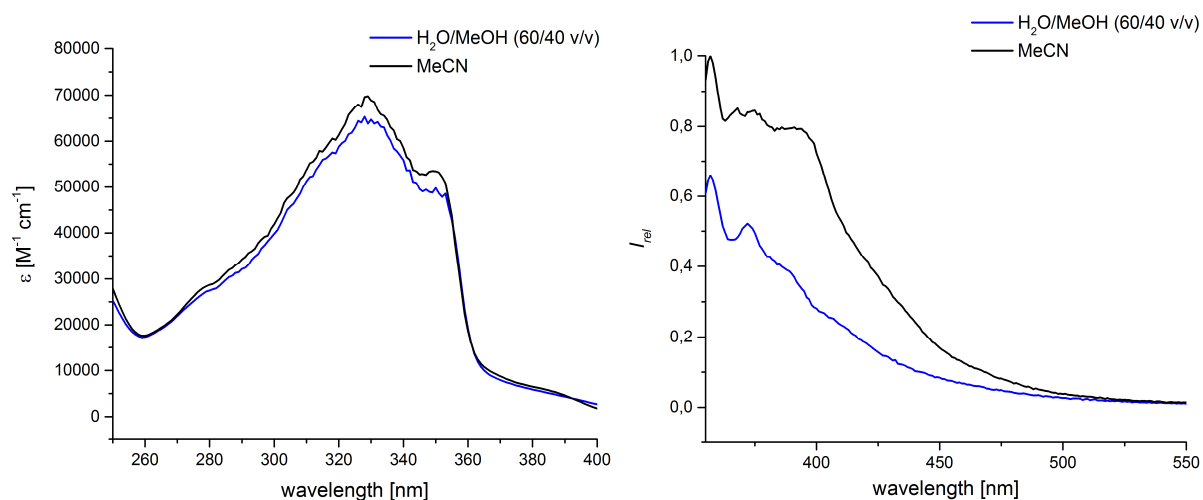
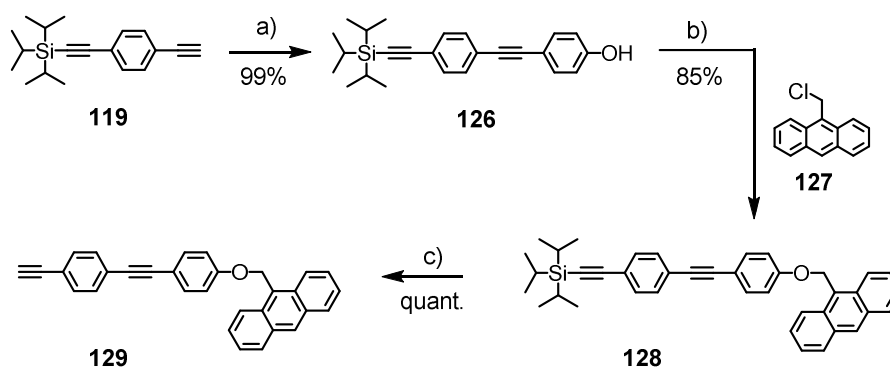


Figure 47. Absorption (left) and relative emission (right) spectra of amphiphile **93** in $H_2O/MeOH$ (60:40 v/v) (blue) and MeCN (black), respectively. Both emission spectra were recorded at a concentration of $6.0 \times 10^{-5} \text{ mm}$.

2.6 Synthesis and Aggregation Studies of Anthracene-substituted Amphiphile **94**

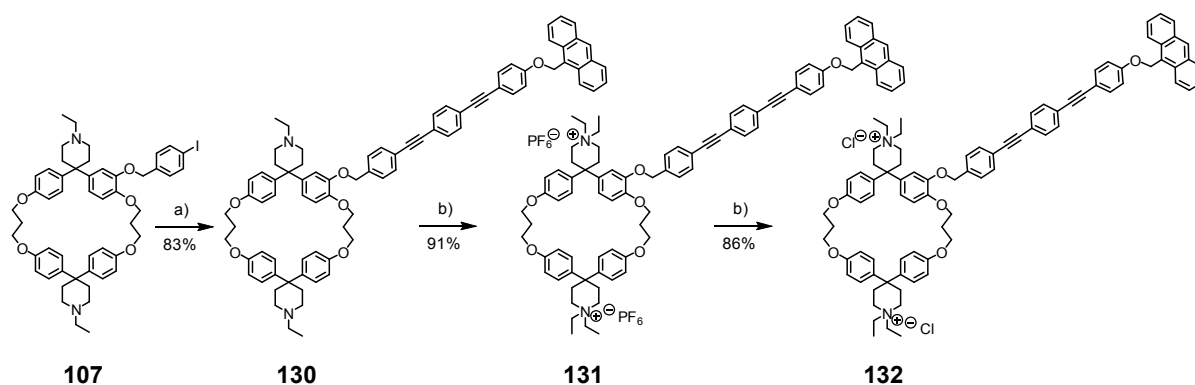
2.6.1 Synthesis of Monomer **94**

OPE moiety **129** was prepared starting with a standard Sonogashira cross-coupling reaction of TIPS-protected precursor **119** with 4-iodophenol, affording phenol-OPE **126** in 99% yield. The anthracene component was then introduced via nucleophilic substitution reaction at OPE **128** with 9-chloromethyl anthracene (**127**) under basic reaction conditions. In the last step, the TIPS protecting group was removed by utilizing TBAF in THF resulting in quantitative yield of **129**.



Scheme 33. Synthesis of OPE moiety **129**. a) 4-iodophenol, Pd(PPh₃)₂Cl₂, CuI, DIPA, THF, 60 °C, 6 h; b) NaOH, MeCN, 5 h; c) TBAF, THF, rt, 1 h.

Similar to the synthesis of the free acetylene-substituted amphiphile **93**, for the assembly of OPE **129** with cyclophane **96** tetrakis(triphenylphosphine)palladium(0) was employed as catalyst for the Sonogashira cross-coupling reaction. After purification by column chromatography, amine **130** was obtained in 83% yield. Alkylation with iodoethane in presence of potassium carbonate and subsequent subjection to potassium hexafluorophosphate afforded **131** in 91% yield. Compound **94** was obtained after ion exchange from hexafluorophosphate to chloride in 86% yield.



Scheme 34. Assembly of amphiphile **94**. a) OPE **129**, Pd(PPh₃)₄, CuI, THF, DIPA, rt, 18 h; b) 1.) EtI, K₂CO₃, dark, rt, 24 h; 2.) KPF₆, CH₂Cl₂; c) DOWEX 1X8, Cl⁻.

2.6.2 ¹H NMR Dilution Studies

Figure 48 shows the aromatic region as well as the signal corresponding to the bridging CH₂ unit adjacent to the anthracene moiety of the ¹H NMR spectra of PF₆⁻ salt **131** in CD₂Cl₂ at different concentrations.

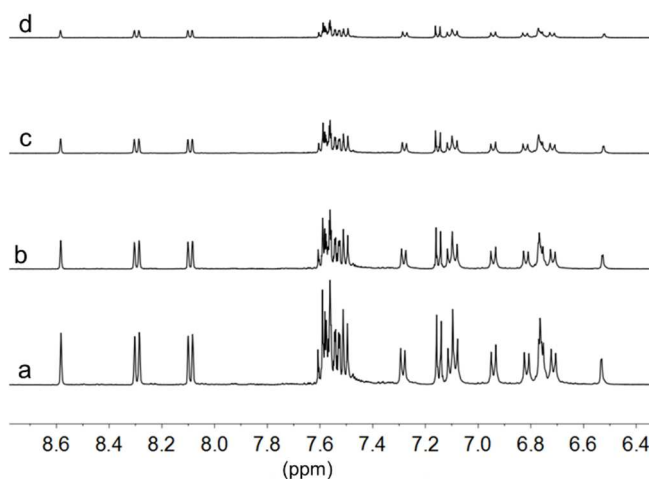


Figure 48. Stacked ¹H NMR spectra of the aromatic region of monomer **131** recorded in CD₂Cl₂ at 298 K on a 500 MHz NMR spectrometer. a) 4.0 mM; b) 2.0 mM; c) 1.0 mM; d) 0.5 mM.

Regarding the ¹H NMR spectra of the same compound as chloride salt in D₂O/CD₃OD (60:40 v/v) at identical concentrations (Figure 49, left), the difference to the spectra in CD₂Cl₂ and also to the corresponding ones in pure CD₃OD (Figure 49, right) is striking. Whereas the spectra recorded in CD₂Cl₂ and even in pure CD₃OD show sharp signals and no peak

broadening with increasing concentration, the influence of D₂O causes an immense peak broadening making assignment of the signals impossible. Already at a concentration of 0.5 mM signals appeared very broad and could hardly distinguished from the spectrum baseline. The behavior is most likely attributed to unspecific intermolecular aggregation of the hydrophobic rod and anthracene stopper.

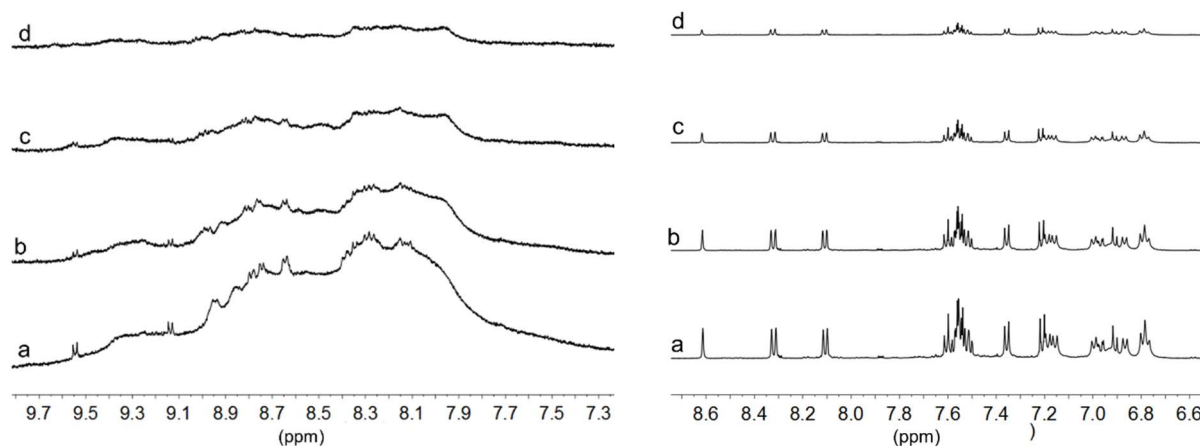


Figure 49. Stacked ¹H NMR spectra of the aromatic region of monomer **94** recorded in D₂O/CD₃OD (60:40 v/v) (left) and pure CD₃OD (right) at 298 K on a 500 MHz NMR spectrometer. a) 4.0 mM; b) 2.0 mM; c) 1.0 mM; d) 0.5 mM.

2.6.3 DOSY Analysis

Due to the absence of distinct signals, DOSY analysis was not feasible. The anthracene stoppered monomer **94** was hence not suitable as geometry-dependent DOSY reference compound for aggregates formed in the protic, binary solvent mixture.

2.6.4 Fluorescence Studies

The absorption spectrum of **94** of the OPE moiety shows a significantly lower emission in H₂O/MeOH (60:40 v/v) compared to the spectrum in MeCN, standing in contrast to the previous systems. Emission spectra in the two different solvent systems were recorded at a concentration of 9.0×10^{-4} mM and the excitation wavelength for both cases was $\lambda = 327$ nm. The fluorescence quenching in the protic, more polar H₂O/MeOH mixture might be assigned to π -stacking of the anthracene moieties already observed in the ¹H NMR dilution studies.

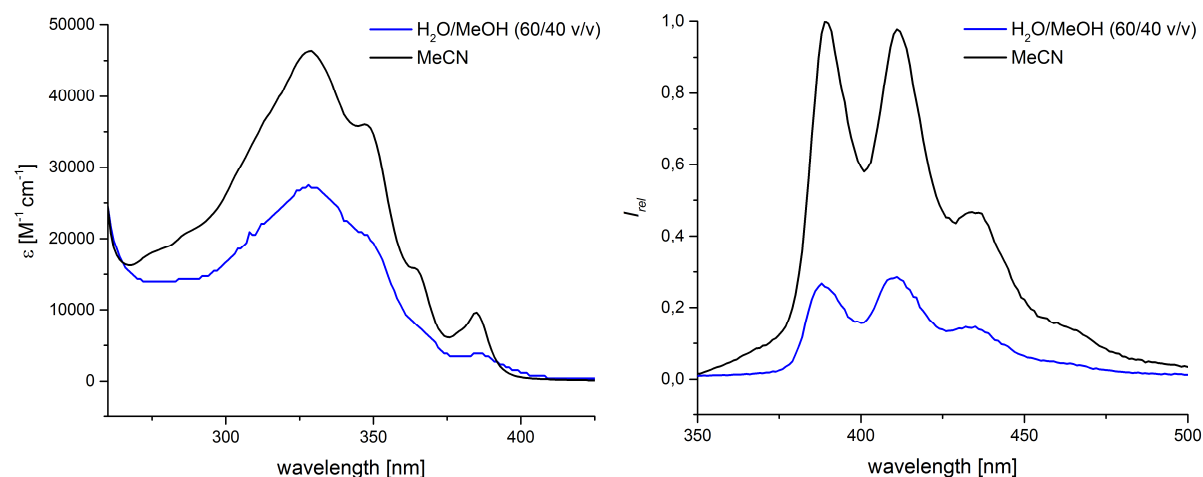


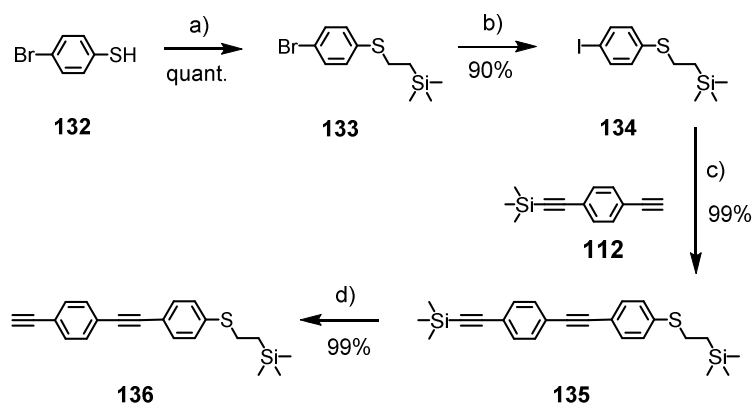
Figure 50. Absorption (left) and relative emission (right) spectra of amphiphile **94** in H₂O/MeOH (60:40 v/v) (blue) and MeCN (black), respectively. Both emission spectra were recorded at a concentration of 9.0×10^{-4} mM.

2.7 Synthesis and Aggregation Studies of *S*-Acetyl-substituted Amphiphile **95**

2.7.1 Synthesis of Monomer **95**

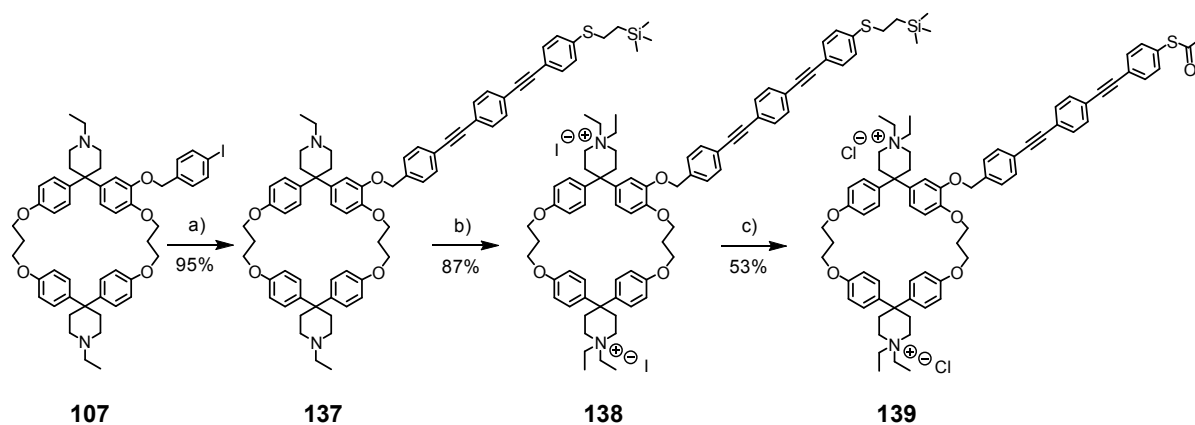
In regard to the instability of the *S*-acetyl group in presence of nucleophilic bases, such as potassium carbonate, which is used in the quaternization step, the OPE moiety was protected by the trimethylsilyl ethyl protecting group. A transprotection reaction was performed in the final step towards the *S*-acetyl substituted monomer **95**.

4-bromothiophenol (**132**) reacted in a radical addition reaction with vinyltrimethylsilane to the trimethylsilyl ethyl protected thiol (SEtTMS) **133**, using azobis(isobutyronitril) (AIBN) as radical initiator.^[147] The quantitatively isolated compound **133** was transformed into the more reactive iodine derivative **134** by employing *tert*-butyl lithium for lithium halogen exchange and subsequent quenching with molecular iodine.^[148] OPE building block **112** was coupled to the protected thiol **134** via Sonogashira reaction, affording compound **135** in 99% yield after chromatographic purification. OPE **136** was obtained by selective removal of the acetylene-TMS protecting group at -78 °C in presence of TBAF.



Scheme 35. Synthesis of the SETMS oligophenylene-ethynylene building block **136**. a) vinyltrimethylsilane, AIBN, 95 °C, 24 h, quant.; b) 1.) *t*BuLi, Et₂O, -70 °C, 40 min, 2.) I₂, Et₂O, -70 °C, 10 min, then 0 °C, 30 min; c) **112**, PdCl₂(PPh₃)₂, CuI, DIPA, THF, 40 °C, 5 h; d) TBAF, THF, -78 °C, 1 h.

OPE **136** was attached to cyclophane **96** via Sonogashira cross-coupling, affording compound **137** in 95% yield. Iodide salt **138** was obtained by quaternization of amine **137**. After removing excess iodoethane and potassium carbonate, **138** was directly used for the transprotection reaction. In the first step, the trimethylsilyl ethyl protecting group was removed by utilizing TBAF at room temperature, followed by the reprotection of the thiolate with acetyl chloride at -10 °C. It turned out, that even for the purification by reverse-phase column chromatography addition of ammonium chloride was crucial for eluting **95**, as it was also the case for the purification of hydroxyl-substituted amphiphile **92**. Three purification cycles were necessary, until tetrabutyl ammonium could be entirely removed. Other inorganic fluoride sources, such as potassium or silver fluoride or silver tetrafluoro borate did not work as deprotecting reagent for this system. Centrifugation in water revealed to be a suitable method to separate the poorly water-soluble target compound **95** from the well-soluble eluate component ammonium chloride, affording amphiphile **95** in 53% yield.



Scheme 36. Last synthetic steps towards amphiphile **95**. a) OPE **136**, Pd(PPh₃)₄, CuI, THF, DIPA, rt, 18 h; b) EtI, K₂CO₃, dark, rt, 72 h; c) 1.) TBAF, THF, rt, 45 min; 2.) AcCl, THF, -10 °C, 2 h.

2.7.2 ¹H NMR Dilution Studies

The recorded ¹H NMR spectra of the *S*-acetyl substituted amphiphile in D₂O/CD₃OD (60:40 v/v) (Figure 51) exhibit more pronounced signal broadening, than derivatives **92** and **93**, which might indicate a stronger aggregation tendency. For example, the spectra at the concentration 8.0 mM and 6.0 mM, respectively, could not be used for evaluation. However, the determined association constant revealed to be relatively low, with $K_a = 2.3 \times 10^3 \text{ M}^{-1}$. The aggregation number was obtained as $N = 2.2$.

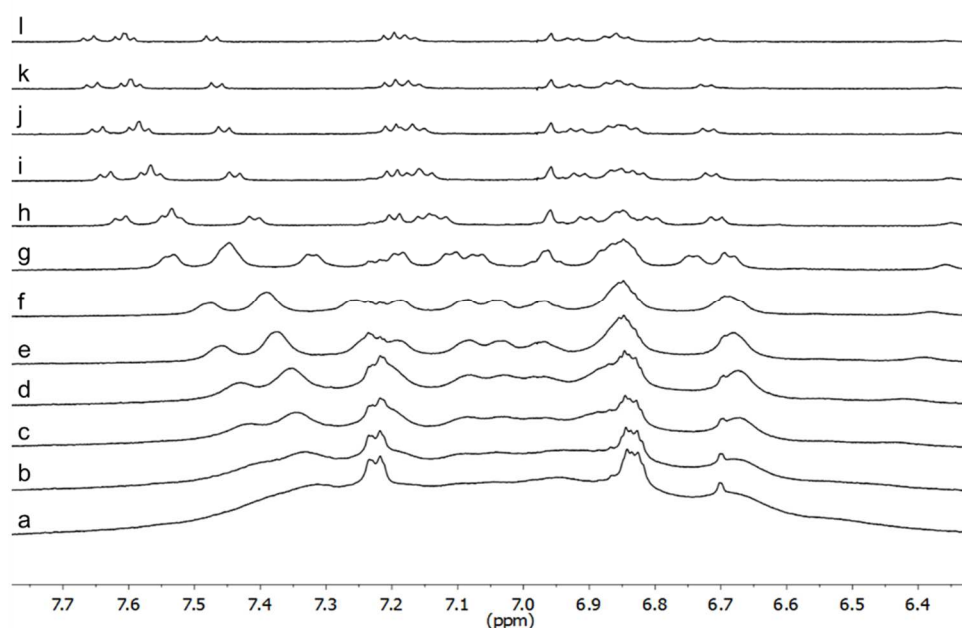


Figure 51. Stacked ¹H NMR spectra of the aromatic region of monomer **93** recorded in D₂O/CD₃OD (60:40 v/v) at 298 K on a 500 MHz NMR spectrometer. a) 8.0 mM; b) 6.0 mM; c) 4.0 mM; d) 3.0 mM; e) 2.0 mM; f) 1.5 mM; g) 1.0 mM; h) 0.5 mM; i) 0.33 mM; j) 0.25 mM; k) 0.19 mM; l) 0.13 mM.

2.7.3 DOSY Analysis

Performing diffusion studies in D₂O/CD₃OD (60:40 v/v) with amphiphile **95** at 0.2 mM gave a diffusion coefficient of $D = 1.25 \times 10^{-10} \text{ m}^2 \text{ s}^{-1}$. Applying equation (3) resulted in an aggregate volume (V_{agg}) to monomer volume (V_{mon}) ratio of 1.27, which is lower than the corresponding values for **92** ($V_{agg}/V_{mon} = 1.41$) and **93** ($V_{agg}/V_{mon} = 1.42$), but still indicates the presence of [c2]daisy chains rather than monomer in the measured solution.

2.7.4 Further Analysis

Amphiphile **95** could not be satisfactorily characterized by ¹³C NMR spectroscopy and neither by fluorescence spectroscopy in different solvents due to decomposition of the sample. The cleavage of the benzylic ether linker leads to a mixture of compounds with different characteristic fluorescence properties, rendering emission spectroscopy analysis insignificant. The definite reason for the cleavage of the benzylic ether linker is not clear, but a possible explanation might be photocatalytic decomposition, which is known from pyrene-^[149] and anthracene-based^[150] benzylic systems comprising an adjacent carbonyl group. Resynthesis of **95** proved to be very challenging. In some attempts, incomplete cleavage of the SETMS protecting group was observed, demanding more than three equivalents of TBAF, which render the already troublesome purification more challenging. In another effort, *S*-ethyl-functionalized amphiphile was obtained as main product. Fortunately, a fraction containing pure amphiphile **95** was directly given to the group of Michel Calame at the University of Basel, enabling conductance measurements of **95** in an MCBJ setup.

2.8 Conductance Studies of Amphiphile 95

2.8.1 Mechanically Controllable Break Junction

As already briefly described in the beginning of Chapter 2, the aim was to mount an interlinked [c2]daisy chain comprising thiophenol anchoring groups between the electrodes of a mechanically controllable break junction (MCBJ) and measure the distance-dependent conductance through the supermolecule. The idea was originally inspired by the discovery of Wu et al. that charge transport can occur through two molecules interacting via intermolecular π - π stacking.^[138] Monofunctionalized thiol OPE **139** was investigated in the MCBJ and exhibited an unexpectedly high conductance. Since **139** comprises only one anchoring group for the gold electrodes, the observed conductance was attributed to π - π stacking of the phenyl units (Figure 52).

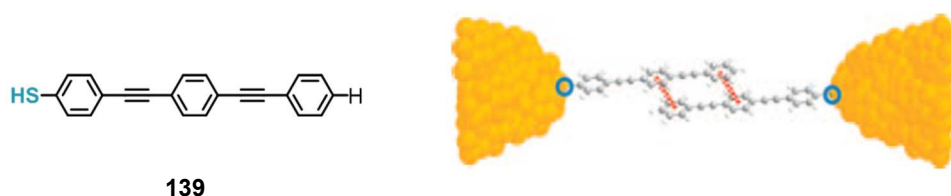


Figure 52. Monothiol OPE **139** (left) mounted as stacked dimer between two gold electrodes of a MCBJ (right).

Figure 53 demonstrates a typical MCBJ setup:^[151] an atomic wire with a constriction in the middle is placed on a pushing rod with two counter supports. By bending the substrate (T) when moving the rod upwards, the wire is stretched until it finally breaks resulting in two atomic-scale metallic contacts. As the distance between the nano-electrodes is only few Ångstroms, tunneling current through space is observed in a nonbridged MCBJ^[152] as shown in Figure 54 a.^[138] The conductance decreases exponentially with increasing distance between the contacts.

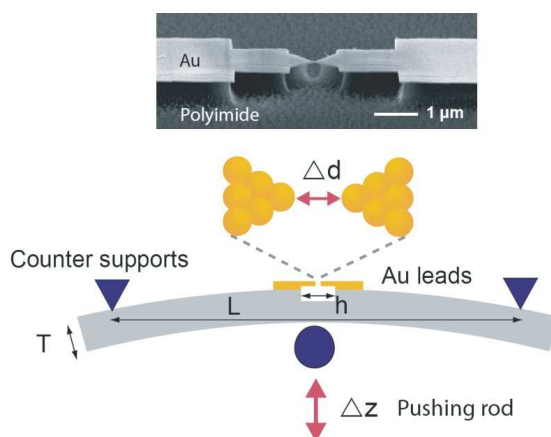


Figure 53. Schematic representation of a MCBJ setup.^[151]

Molecules can be deposited into the junction either in solution or by evaporation. As soon as a conducting molecule bridges the electrodes, the corresponding conductance (G)/distance (z) curve shows a plateau and a peak in the logarithmic histogram $N_{\log G}(\log G)$ can be observed (Figure 54, b).^[138]

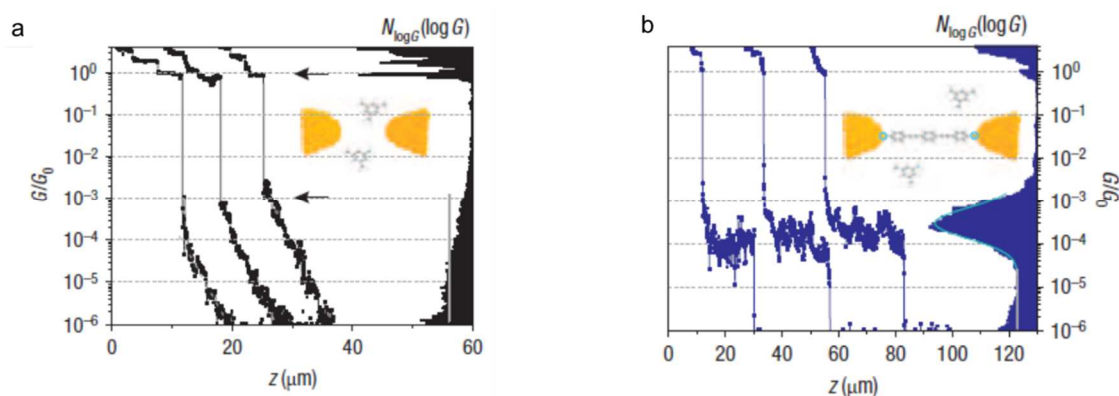


Figure 54. Typical conductance (G)/distance (z) curves and logarithmic histogram $N_{\log G}(\log G)$ corresponding to a nonbridged MCBJ (a) and to a junction with a mounted, conducting molecule (b).^[138]

The junction can also be closed again, allowing minute repetition of the conductance measurements for several hundred times and hence a statistical data set.

2.8.2 Conductance Measurements

Investigations of amphiphile **95** in an MCBJ setup were performed by Anton Vladyka in the group of Michel Calame at the University of Basel.

A 0.2 mM sample of monomer **95** in H₂O/MeOH (60/40 v/v) was used for the conductance experiments in the MCBJ. The acetyl protecting group of the thiophenol anchors were removed *in situ* by tetrabutylammonium hydroxide (TBAH) under argon atmosphere. The applied bias voltage of 0.1 V was kept constant, while 250 traces were recorded. Figure 55 demonstrates the obtained G/z curves (a) and the corresponding logarithmic histogram $N_{\log G}(\log G)$ (b), unfortunately both lacking a clear sign for the incorporation of a conducting molecule into the MCBJ.

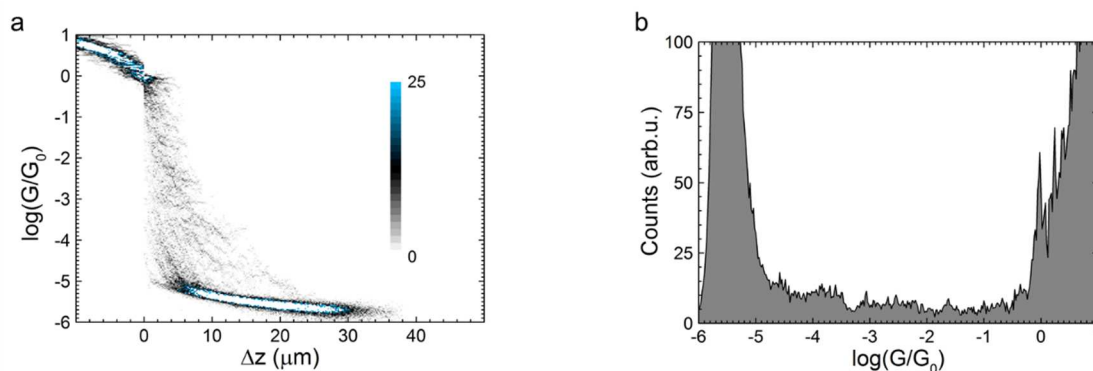


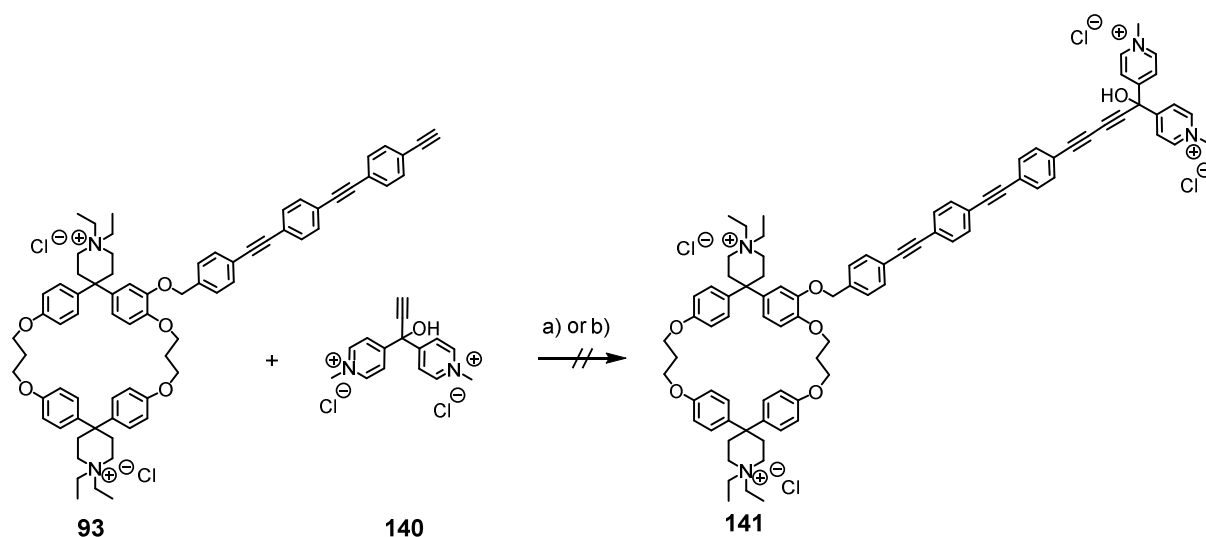
Figure 55. G/z curves (a) and corresponding logarithmic histogram $N_{\log G}(\log G)$ (b) of measurements performed with amphiphile **95** in a MCBJ setup.

An explanation for the obtained result might be that in [c2]daisy chains π - π stacking and hence charge transport between the OPE rods is hindered. Another likely reason for the absence of a conductance plateau might be acyclic daisy chains or unthreaded, micellar-like aggregates as predominant species rather than the cyclic, dimeric daisy chains. Such aggregates are not capable to bridge the MCBJ nanoelectrodes as a single, conducting (super)molecule.

2.9 Stopping of Interlinked Aggregates

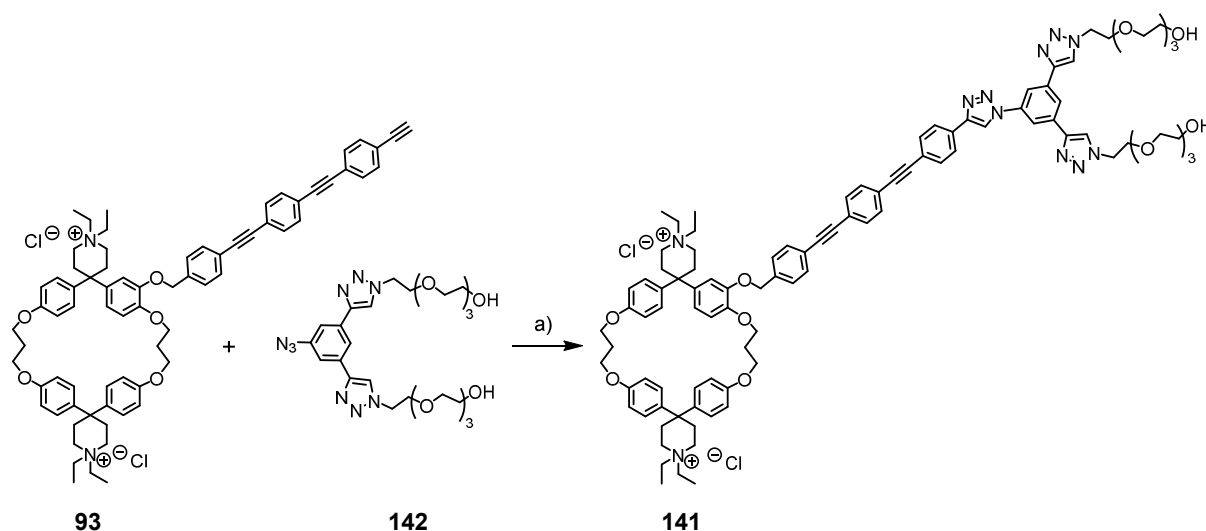
The aggregates of the hydroxyl- and respectively acetylene-substituted amphiphiles **92** and **93** were intended to be trapped by reaction with a bulky stopper molecule. Preliminary experiments with 9-(chloromethyl)anthracene as stopper under basic conditions revealed that a nucleophilic substitution reaction at the phenol moiety of **92** is not feasible in the required H₂O/MeOH solvent mixture most likely due to the insolubility of the stopper in this environment. However, the protic polar solvent is crucial for complexation driven by the hydrophobic effect.

Therefore, the in aqueous media applicable Glaser^[129,130] coupling as well as azide-alkyne *click* chemistry were employed as stoppering reaction and hence should give further insight into the aggregation behavior of the amphiphilic monomers in general. The terminal acetylene functionality of **93** can potentially react with the free acetylene of the water-soluble stopper **140**, which was developed by Anderson et al..^[125] **140** was synthesized according to a slightly modified protocol which was previously reported.^[128] Preliminary studies revealed that employing the coupling conditions utilized by Anderson^[128] with 10 equivalents of stopper **140** was not feasible for our system (Scheme 37). The large excess (200 eq) of the salts copper(I) chloride and ammonium chloride rendered the reaction controls by HPLC-ESI-MS as well as direct injection ESI-MS impractical. In the resulting spectra of low intensity only starting material was identified after 60 hours of reaction duration. Conversion of amphiphile **93** was also not observed by using copper(II) acetate (0.2 eq) and piperidine (2.0 eq) as an alternative catalyst system.^[153]



Scheme 37. Attempt to trap the aggregates of amphiphile **93** in H₂O/MeOH (60/40 v/v) by using Glaser coupling reactions a) and b): a) CuCl, NH₄Cl, air, rt, 60 h; b) Cu(CO₂CH₃)₂, piperidine, air, rt, 48 h.

Another attempt to trap the aggregates of **93** was made by using the azide-functionalized, water-soluble stopper **142**, designed and synthesized by Yves Aeschi, in a copper-catalyzed azide-alkyne cycloaddition (*click* reaction) (Scheme 38). A 0.55 mM solution of monomer **93** in H₂O/MeOH (60/40 v/v) was subjected to excess (1.5 eq) stopper **142** and stoichiometric amounts of copper(II) sulfate and reductant L(+)-ascorbic acid sodium salt. After 1.5 hours reaction duration at room temperature, full conversion of **93** towards a single product was observed by HPLC-ESI-MS (Figure 56).



Scheme 38. Attempt to trap aggregates of **93** via *click* reaction resulted in the formation the stoppered monomer **143** as exclusive product. a) CuSO₄, Na-ascorbate, H₂O/MeOH (60/40 v/v), rt, 1.5 h.

The total ion chromatogram (T.I.C.) as well as the UV chromatogram exhibit two main signals, which correspond to the unreacted excess amount of stopper **142** ($t_R = 6.25$ min) and the stoppered monomer **143** ($t_R = 8.90$ min). The latter signal comprised m/z values of 835 and 557 which were assigned, also in accordance to the observed isotopic patterns, to the doubly positive charged product **143** and its protonated, triply charged form. In case of a stoppered dimer, a signal for the fivefold charged species ($m/z = 668$) would be expected due to statistical protonation of the stopper moieties. However, the chromatogram did not contain a relevant signal with this m/z value. A quadruply charged species, corresponding to the stoppered, unprotonated dimer (also $m/z = 835$), could only be observed in low intensity by high-resolution ESI-MS measurements of the crude reaction mixture. The dimer might have been formed only as a gas-phase aggregate of two stoppered monomers.

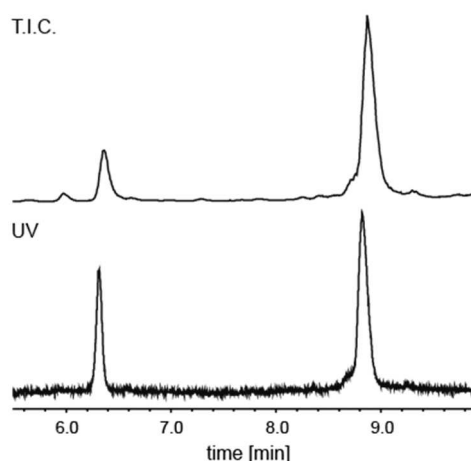


Figure 56. Total ion chromatogram (T.I.C.) (top) and UV chromatogram (bottom) obtained by HPLC-ESI-MS analysis of the crude *click* reaction mixture of **93** with stopper **142**. The signal at $t_R = 6.25$ min corresponds to stopper **142** and the larger signal at $t_R = 8.90$ min was identified to correspond to the stoppered monomer **143**.

The results lead to the assumption that unthreaded, stacked dimers ([a2] TT), which would be in accordance with the DOSY analyses, or unthreaded micellar-like aggregates rather than the expected [c2]daisy chains are the predominant species in protic polar solutions.

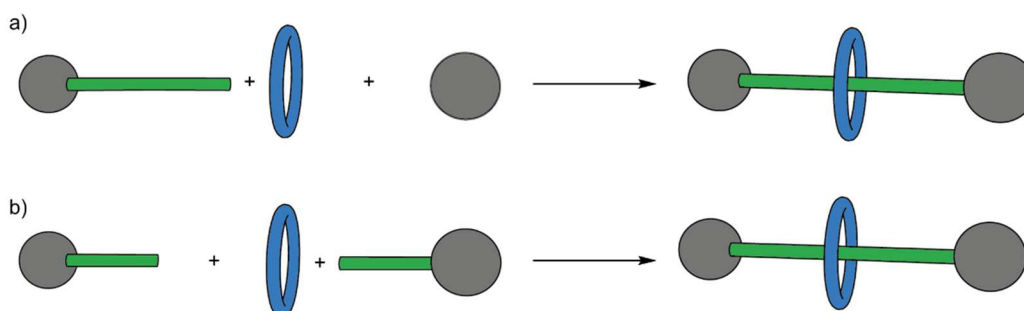
2.10 Conclusion

The aggregation behavior of the successfully synthesized and characterized amphiphiles **92-95** was investigated by means of $^1\text{H-NMR}$ titration studies, DOSY experiments and by qualitative evaluation of emission spectra. The obtained results of these investigations clearly indicated aggregation in protic, polar solvent driven by a hydrophobic effect. Furthermore, the size and hence the shape of the aggregates in low concentrated solution was estimated. Unfortunately, only stoppered monomer could be trapped. The the m/z vale attributed to stoppered dimer was only observed in traces by HR-ESI-MS measurements, presumably formed in the gas-phase during the evaporation process as aggregate of two stoppered monomers. This finding stands also in accordance with the conductance measurements of amphiphile **95** in a MCBJ setup, since a conductance plateau, indicating inserted [c2]daisy chains between the two electrodes, was not observed. Conclusively, the presence of unthreaded, micellar-like species in protic, polar solvent turned out to be very likely. Further pursuing the objective to build mechanically interlocked molecules for potential application in material science demands a deeper insight into the complex aggregation behavior of our systems. As a consequence, basic investigations to prove inclusion of the OPE into the cyclophane cavity turned out to be crucial (Chapter 3).

3 OPE-based Rotaxane Test Systems

The syntheses of rotaxanes based on monostoppered OPEs was chosen as a test system to shed light on the threading behavior of the rod into the cavity of Diederich-type cyclophanes driven by a hydrophobic effect. The amphiphilic molecular systems described in Chapter 2, combining an OPE-rod with a macrocycle in an amphiphilic molecule, turned out to lack inclusion complexation in protic, polar solvent and hence formation of interlinked daisy chain aggregates (Chapter 2.8.3).

Performing rotaxane synthesis with the two separate components of the amphiphilic system allows facile proof of threading. The supposed inclusion complexes of monostoppered rod molecule and cyclophane can be potentially transformed into a mechanically interlocked molecule by a reaction with a bulky stopper molecule. This strategy renders the direct detection of the products possible. Scheme 39 demonstrates the two approaches employed as proof-of-principle systems for rotaxane synthesis. Approach a) incorporates the reaction of a monostoppered OPE with a bulky stopper in presence of cyclophane, whereas in approach b) the OPE is divided into two shorter moieties, both stoppered on one terminus.



Scheme 39. Schematic representation of the two employed approaches (a and b) for preparing rotaxanes based on monostoppered OPEs.

In addition, ^1H NMR host-guest complexation studies were performed in order to get further insight into the aggregation behavior of Diederich cyclophanes with different guests.

3.1 Molecular Design of the Rotaxane Building Blocks

The convenient and efficient copper mediated *click* chemistry, already employed in the stoppering reaction of acetylene-substituted amphiphile **93**, was chosen as reaction to assemble the relevant rotaxane components. Within the performed test series, different combinations of OPEs, comprising a terminal acetylene moiety, and azide-functionalized compounds were investigated in their ability to form rotaxanes with cyclophane **81**. Therefore, two different terminal acetylene-functionalized OPEs (**144** and **145**), varying in the number of ethynylene-phenylene units (Figure 57), were prepared for the test series. Since it was concluded from the aggregation studies of amphiphiles **91-95** (Chapter 2) that intermolecular interactions of the OPE moieties appear to be predominant over intracavitary complexation, OPEs **144** and **145** were shortened to two and one phenylene-ethynylene unit respectively in order to reduce the hydrophobic surface. Both OPEs were stoppered on one terminus and rendered soluble in aqueous medium by the tetraethylene glycol chains of the stopper. Furthermore, one azide-functionalized OPE (**146**), comprising two phenylene units and the water-soluble stopper, as well as the two stopper molecules **142** and **147** were synthesized as complementary rotaxane components.

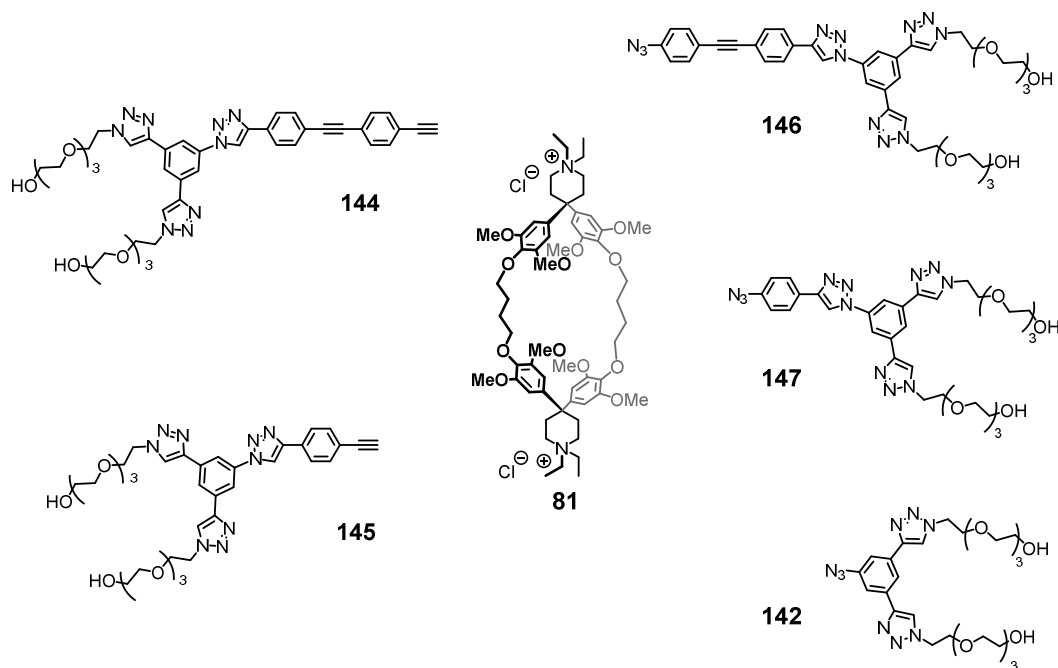
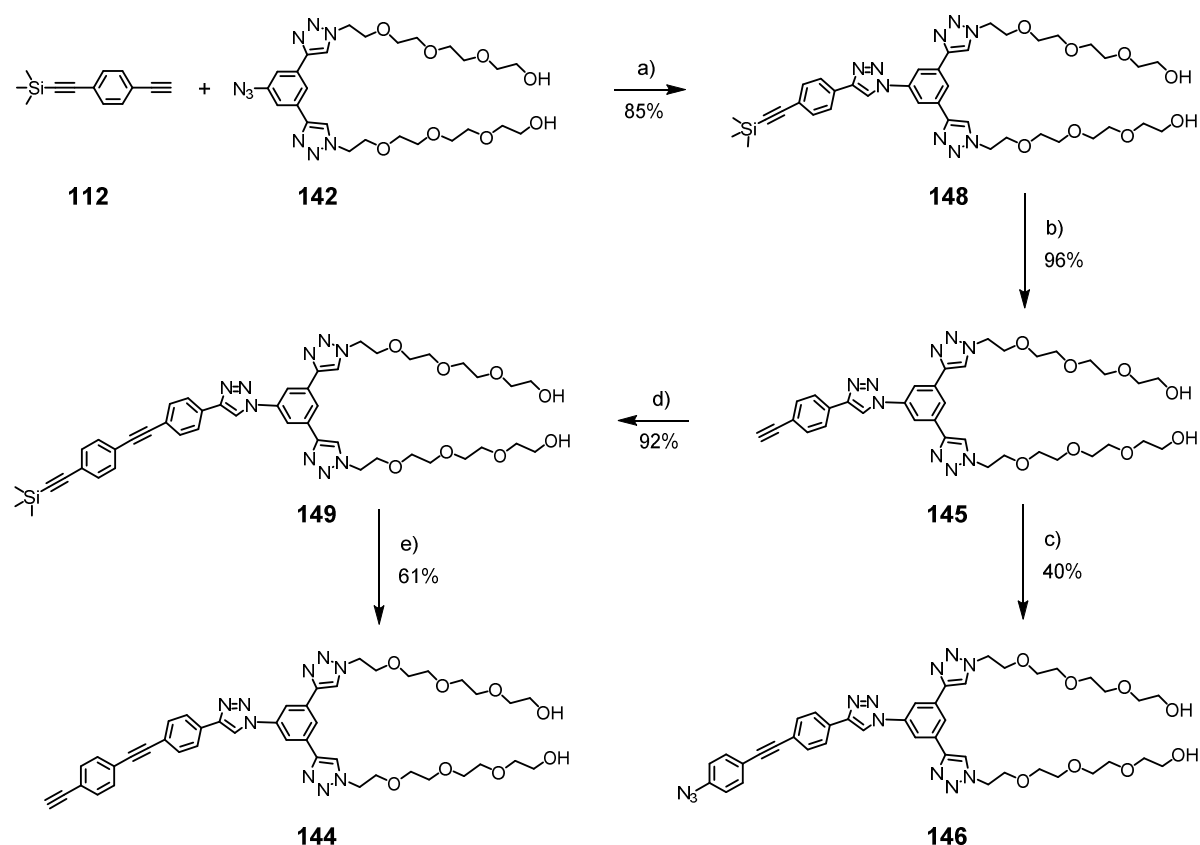


Figure 57. Building blocks for the OPE-based rotaxane test system with cyclophane **81** as macrocyclic component.

The cyclophane moiety of amphiphiles **91-95** was replaced by the octamethoxy-decorated cyclophane **81**, comprising a larger (C₄) alkyl chain bridged cavity than the former (C₃) macrocyclic system. The chosen cyclophane **81** exhibits a deeper cavity and also higher binding affinity towards aromatic guests compared to the C₃-bridged (**75** and **76**) as well as undecorated C₄-bridged (**77**) derivatives (Table 1, Chapter 1.3.9).^[122]

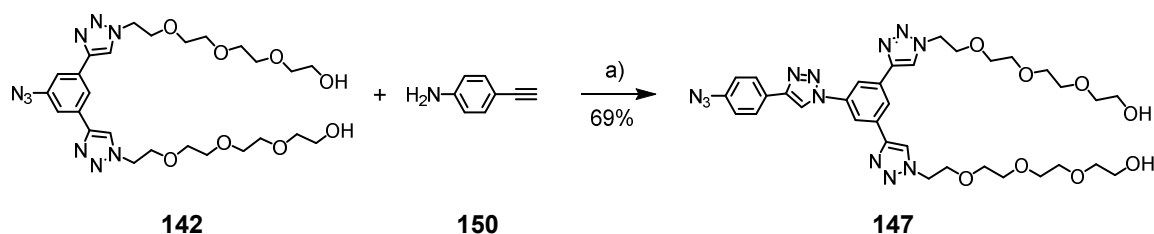
3.2 Syntheses of the Rotaxane Building Blocks

The preparation of the hydrophilic, monostoppered OPEs is mainly based on the stepwise attachment of ethynylene-phenylene units to the stopper molecule (**142**). The short terminal acetylene compound **145** was obtained in two steps, starting with a copper(I)-catalyzed cycloaddition of **112** to stopper **142**, affording **148** in 85% yield. Cleavage of the trimethylsilyl protecting group in presence of potassium hydroxide and methanol afforded compound **145** in a yield of 96% from which the longer OPEs **144** and **146** were both prepared via standard Sonogashira cross-coupling reaction. Using 1-azido-4-iodobenzene as reactant afforded the azide-functionalized OPE **146**, whereas by employing (4-iodophenyl-ethynyl)trimethylsilane the terminal acetylene analogue **144** could be isolated after desilylation.



Scheme 40. Syntheses of hydrophilic OPEs **145**, **146** and **147**. a) $[\text{Cu}(\text{CH}_3\text{CN})_4]\text{PF}_6$, TBTA, acetone, rt, 18 h; b) KOH, MeOH, acetone, rt, 1 h; c) 1-azido-4-iodobenzene, $\text{Pd}(\text{PPh}_3)_2\text{Cl}_2$, CuI, THF, DIPA, rt, 18 h; d) (4-iodophenylethynyl)trimethylsilane, $\text{Pd}(\text{PPh}_3)_2\text{Cl}_2$, CuI, THF, DIPA, rt, 18 h; e) KOH, MeOH, acetone, rt, 1 h.

The elongated azide-functionalized stopper **147** was prepared starting from 4-ethynylaniline (**150**), which was coupled to stopper **142** via CuAAC reaction. The amine was then subsequently transformed to an azide by a Sandmeyer reaction,^[154,155] affording the product in an overall yield of 69%.



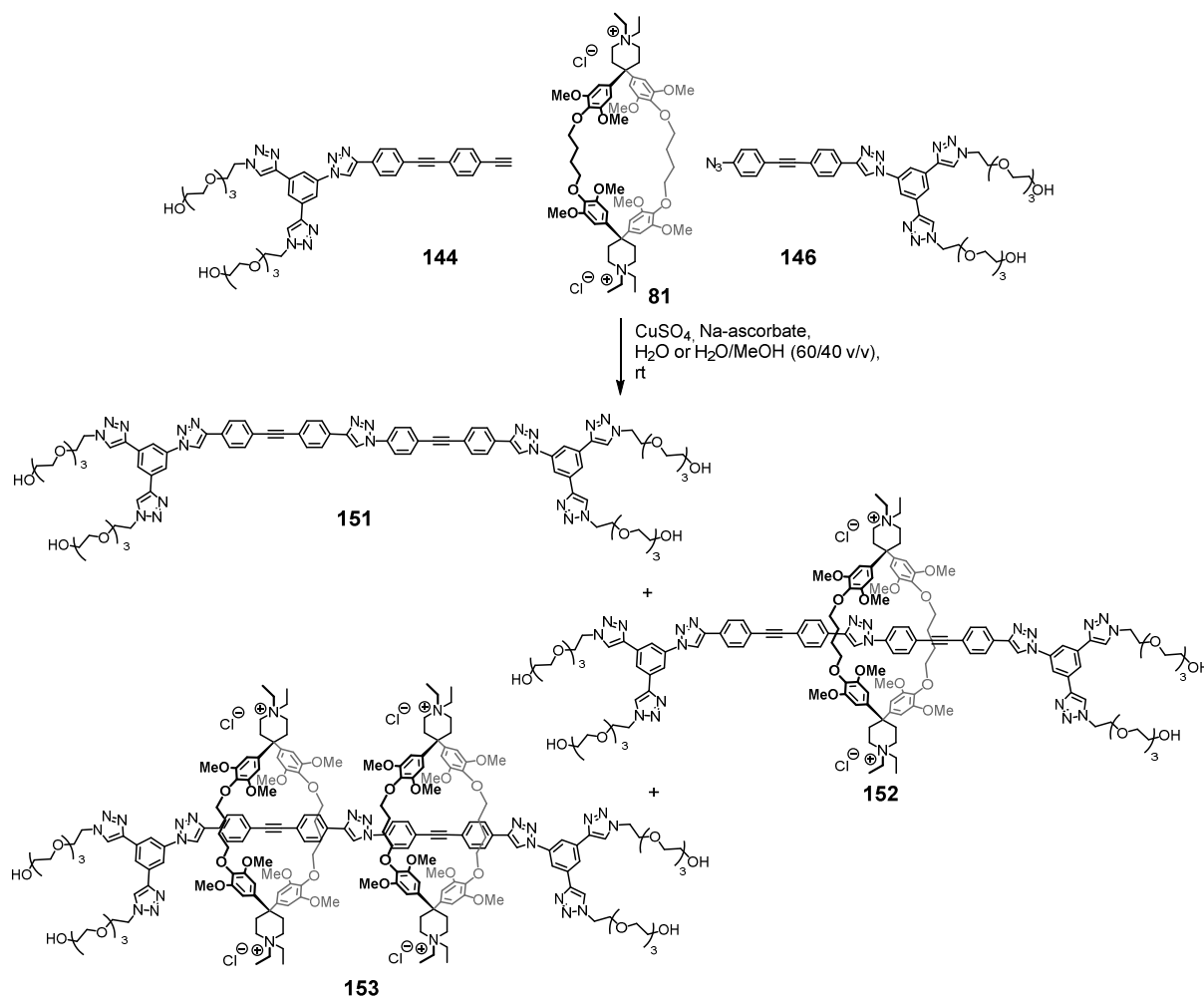
Scheme 41. Synthesis of water-soluble stopper **147**. a) 1.) $[\text{Cu}(\text{CH}_3\text{CN})_4]\text{PF}_6$, TBTA, acetonitrile, 30 °C, 55 h; 2.) NaNO_2 , NaN_3 , aq. HCl, 0 °C, then rt, 1 h.

Cyclophane **81** was prepared by Yves Aeschi according to a slightly modified procedure reported by Anderson et al..^[128]

3.3 Rotaxane Assembly Test Reactions

The acetylene- and azide-functionalized building blocks were each used in a concentration of 1.0 mM. As the formation of a [3]rotaxane comprising two macrocycles is possible for the test systems containing the longer OPEs **144** and **146** (Scheme 42), 2.0 eq of cyclophane **81** were employed. Higher cyclophane concentration is expected to shift the chemical equilibrium towards higher concentrations of inclusion complexes. The reactions were performed in the two different solvent systems water and water/methanol (60/40 v/v). While the hydrophobic effect is expected to be more pronounced in pure water, the rotaxane components exhibit a higher solubility in a solvent mixture additionally comprising methanol, which eliminates potential solubility issues. 0.5 eq of a combination of copper(II) sulfate and L(+)-ascorbic acid sodium salt was employed as Cu(I)-source for the CuAAC reaction. Qualitative reaction control was conducted by HPLC-ESI-MS. Samples were taken and analyzed, until no changes in the corresponding chromatograms were observed.

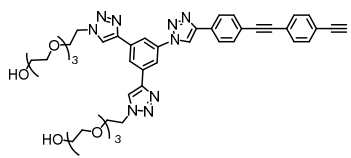
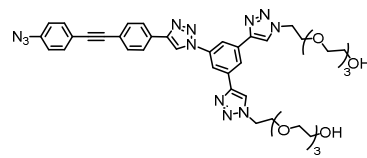
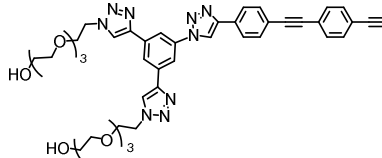
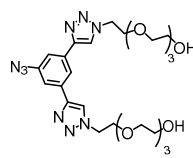
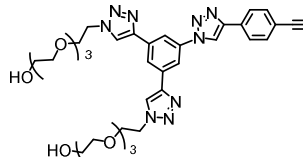
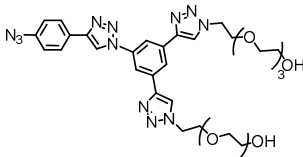
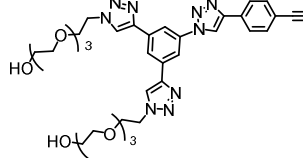
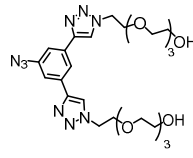
Scheme 42 shows an exemplary reaction between the longer OPE **144** and azide-functionalized compound **146**. The rod-shaped molecules can undergo cycloaddition, either as unthreaded molecules or in form of their threaded inclusion complexes. The former results in a dumbbell-shaped molecule (**151**) while the latter ensues either [2]rotaxane (**152**) or [3]rotaxane (**153**) formation.



Scheme 42. Formation of dumbbell **151**, [2]rotaxane **152** and [3]rotaxane **153** via CuAAC as an exemplary reaction for the OPE-based rotaxane test system.

Table 2 demonstrates the different reactant combinations and the corresponding results in terms of conversion of starting materials as well as rotaxane formation. A quantitative analysis based on the UV chromatograms obtained by HPLC-ESI-MS measurements turned out to be inapplicable since a signal corresponding to rotaxane was never observed in an intensity which allows for integration. However, due to the ionic character of the cyclophane, the macrocycle itself and also the rotaxanes were well-detectable by ESI-MS, enabling a qualitative proof of rotaxane formation. While the shorter compounds **142**, **145** and **147** lead to signals of decent intensity in the MS chromatograms, the signal intensity of the corresponding compounds **144** and **146** decrease dramatically with increasing number of phenylene units. The observations is most likely explainable by the decreased water-solubility and a lower tendency for ionization.

Table 2. Test reactions with different combinations of OPEs (**144** and **145**) and azide-functionalized molecules (**142**, **146** and **147**) in water as well as in water/methanol (60/40 v/v). All reactions were performed in presence of 2.0 equivalents of cyclophane **81** and 0.5 equivalents of copper(II)sulfate as well as L(+)-ascorbic acid sodium salt.

#	OPE	Azide	Conversion	Rotaxane*
1	 144	 146	H ₂ O: incomplete	H ₂ O: traces
			H ₂ O/MeOH: incomplete	H ₂ O/MeOH: no rotaxane
2	 144	 142	H ₂ O: incomplete	H ₂ O: traces
			H ₂ O/MeOH: incomplete	H ₂ O/MeOH: traces
3	 145	 147	H ₂ O: full conversion	H ₂ O: no rotaxane
			H ₂ O/MeOH: incomplete	H ₂ O/MeOH: no rotaxane
4	 145	 142	H ₂ O: incomplete	H ₂ O: no rotaxane
			H ₂ O/MeOH: incomplete	H ₂ O/MeOH: no rotaxane

*The molecule ion (M) refers to the corresponding [2]rotaxane; a [3]rotaxane was not observed in neither of the test reactions.

Regarding Table 2, one of the most striking results is the incomplete conversion of starting materials towards dumbbell or rotaxane in almost every test reaction. This observation indicates that the catalyst system became inactive, before the complete starting material could be converted. Furthermore, the influence of the solvent system on conversion or respectively rotaxane formation seems to be negligible. Instead, the number of ethynylene-phenylene units appears to be an important factor. Most obvious is that test reactions with

OPE **144** (entry 1 and 2) exhibit formation of [2]rotaxanes, whereas in none of the test reactions with the shorter OPE **145** (entry 3 and 4) conversion towards rotaxane was found. The observed results lead to the assumption that, in case of inclusion complexation, the terminal acetylene was sterically hindered by the encircling cyclophane and hence the reaction site was blocked. However, rotaxanes were in general only found in traces, whereas in each test reaction predominantly the unthreaded rod-shaped compounds reacted in a click reaction, resulting in mainly dumbbell formation.

3.4 ^1H NMR Host-Guest Studies

The threading behavior of OPE molecules **144**, **145** and **147** was additionally analyzed by ^1H NMR host-guest studies. ^1H NMR spectra of 1:1 mixtures of cyclophane (host) and OPE (guest) were recorded and the observed chemical shift (δ_{obs}) of the guest and host protons were compared to δ_{obs} values obtained by measuring solutions solely containing host or guest. In line with the rotaxanation test reactions, the measurements were performed in D_2O as well as in $\text{D}_2\text{O}/\text{MeOD}$ (60/40 v/v). Host protons are designated by a grey dot, whereas the relevant guest protons are labelled with letters and shifts are indicated by arrows. Based on the inclusion complexation studies published by the Diederich group^[122] (see exemplary Table 1, Chapter 1.3.9) an upfield change of around -2 ppm in the observed chemical shift (δ_{obs}) can be expected for guest protons in case of saturated threading of the substrate. The reliability of the chosen simplified complexation studies was tested in advance with dimethyl terephthalate (**154**), which according to literature^[122] exhibits a high affinity for cyclophane **81** with an association constant of $K_a = 1.2 \times 10^5 \text{ M}^{-1}$ in D_2O . Indeed, a change of $\Delta\delta_{\text{obs}} = -1.89$ ppm was observed for the aromatic protons of dimethyl terephthalate in presence of **81** in D_2O (Scheme 58, left). In compliance with Diederich's results,^[122] the host protons show a rather small downfield shift upon complexation. The corresponding study in the binary solvent mixture resulted in a shift of $\Delta\delta_{\text{obs}} = -0.64$ ppm. Important to mention is the unknown impurity of cyclophane which can be observed in the spectra as a small signal close to the cyclophane signal. While the corresponding peak for cyclophane **81** shifts upon inclusion complexation, the signal of the impurity does not shift, indicating that it is not involved in complexation. However, a positive side-effect of performing inclusion

complexation studies with the symmetrical, octamethoxy-decorated cyclophane **81** is the simple aromatic region of the ^1H NMR spectrum, comprising only a singlet signal.

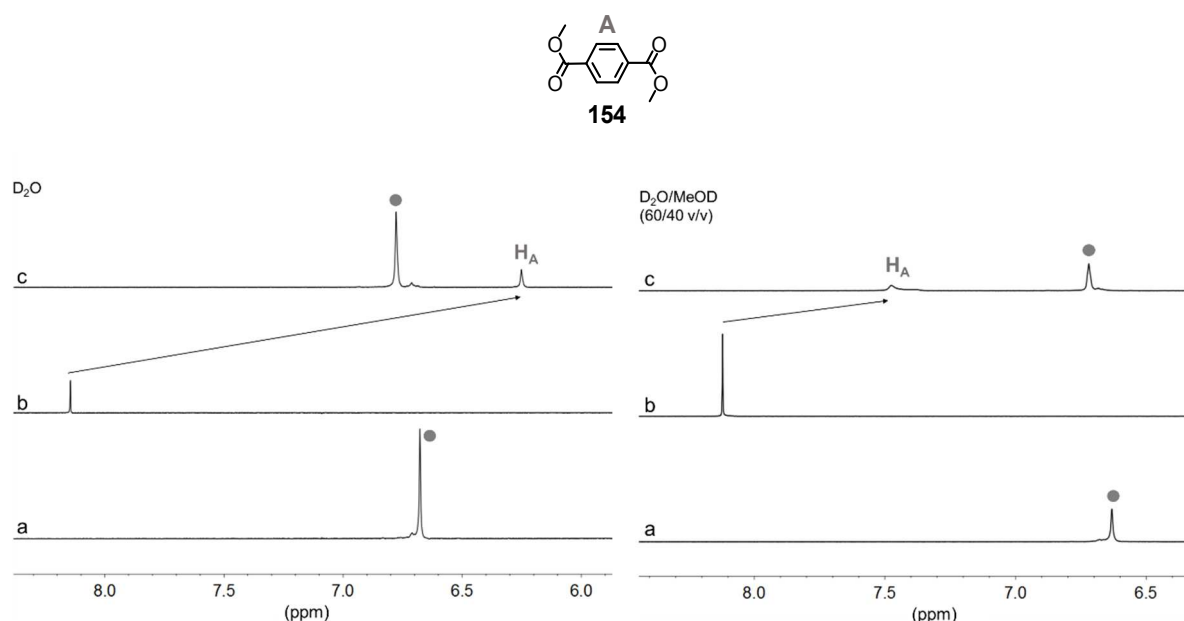


Figure 58. Aromatic region of ^1H NMR spectra in D_2O (left) and $\text{D}_2\text{O}/\text{MeOD}$ (60/40 v/v) (right) of cyclophane **81** only (a), dimethyl terephthalate **154** (b) and a 1:1 mixture of both compounds each in a concentration of 0.5 mM (c).

With the objective to gain further information about the threading behavior of amphiphiles **92-95**, similar inclusion complexation studies were performed with the smaller, mono-methoxylated cyclophane **109**, which was originally prepared as DOSY reference compound. The aromatic protons of dimethyl terephthalate exhibit a comparable change of chemical shift ($\Delta\delta_{\text{obs}} = -0.71$ ppm) in D_2O (Figure 59, left) as in presence of cyclophane **81** in $\text{D}_2\text{O}/\text{MeOD}$. However, Figure 59 (right) clearly shows that the aromatic protons of dimethyl terephthalate hardly shift in presence of the smaller macrocycle **109** in the binary solvent mixture and hence almost no guest complexation occurs.

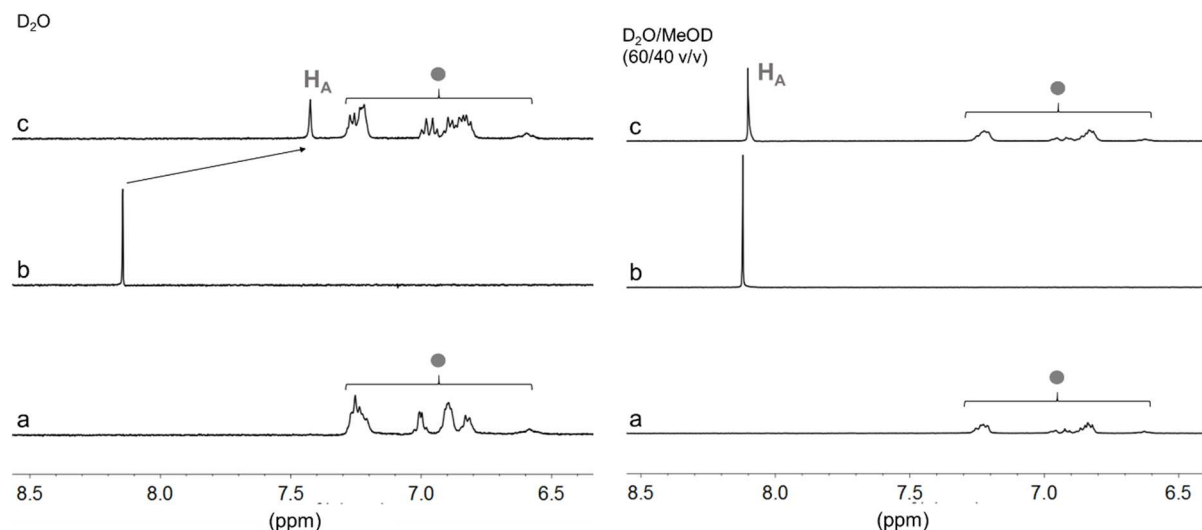


Figure 59. Aromatic region of ¹H NMR spectra in D₂O (left) and D₂O/MeOD (60/40 v/v) (right) of cyclophane **109** only (a), dimethyl terephthalate (b) and a 1:1 mixture of both compounds each in a concentration of 0.5 mM (c).

The complexation experiments with OPE **145**, revealed a rather small upfield shift of the phenylene protons A and B (Figure 60 and 61). Interestingly, $\Delta\delta_{\text{obs}}$ of protons A and B is larger in D₂O/MeOD (-0.42 ppm for both signals) than in D₂O (-0.21 and -0.27 ppm). In turn, the signals corresponding to protons C and D exhibit a downfield shift of $\Delta\delta_{\text{obs}} = +0.48$ and +0.44 ppm in D₂O, which might be induced by unspecific aggregation. Furthermore, the inconsistent shifts of triazole protons in the two different solvents imply a complex aggregation behavior of OPE **145**, especially since control experiments with stopper **142** did not show any change in the observed chemical shift in presence of cyclophane.

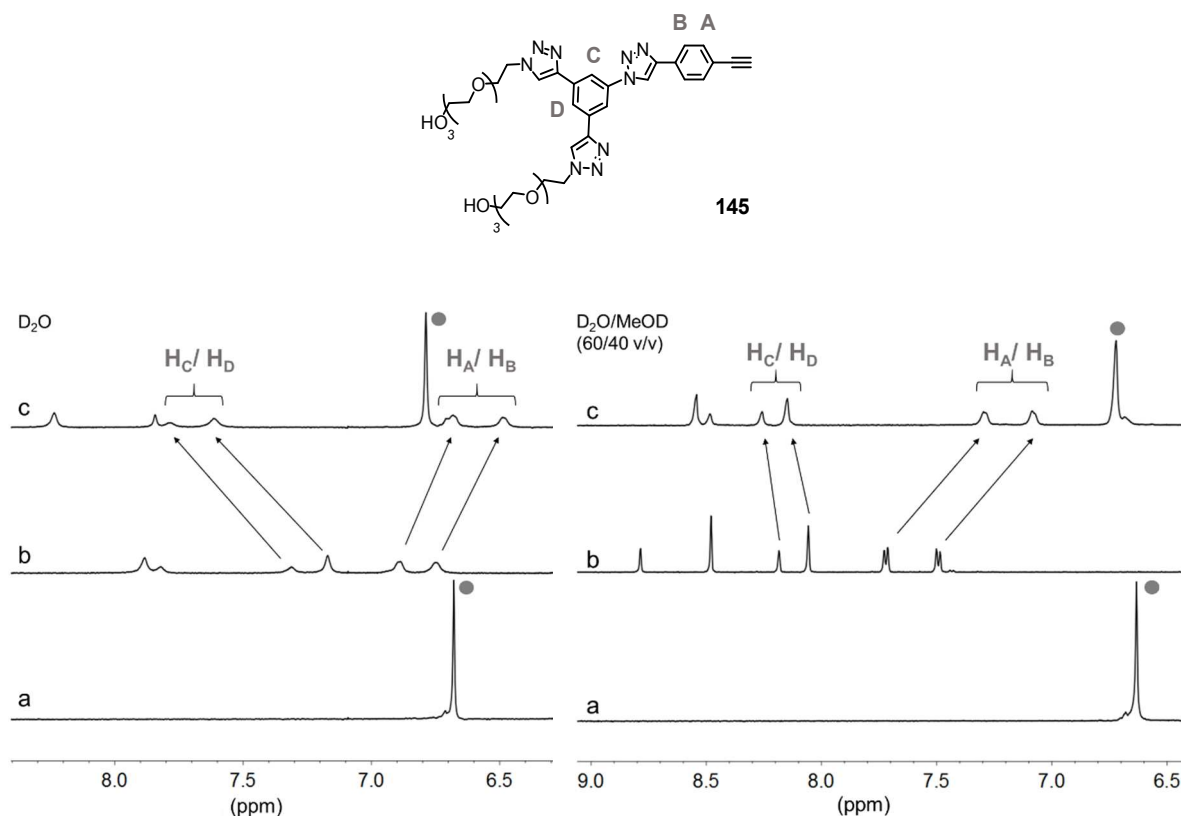


Figure 60. Aromatic region of ^1H NMR spectra in D_2O (left) and $\text{D}_2\text{O}/\text{MeOD}$ (60/40 v/v) (right) of cyclophane **81** only (a), short OPE **145** (b) and a 1:1 mixture of both compounds each in a concentration of 0.5 mM (c).

Regarding the corresponding spectra of OPE **145** in presence of cyclophane **109**, the absence of a change in the chemical shift is striking, especially in the binary solvent mixture where the relevant signals of the two different molecules do not overlap.

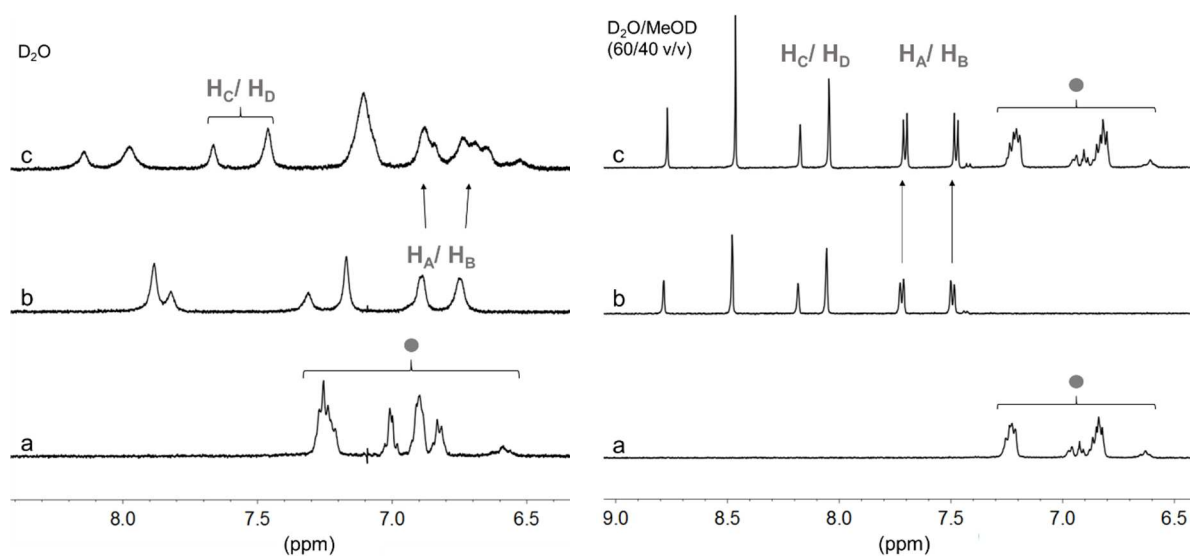


Figure 61. Aromatic region of ^1H NMR spectra in D_2O (left) and $\text{D}_2\text{O}/\text{MeOD}$ (60/40 v/v) (right) of cyclophane **109** only (a), short OPE **145** (b) and a 1:1 mixture of both compounds each in a concentration of 0.5 mM (c).

Figure 62 demonstrates the ^1H NMR experiments with the longer OPE **146** and cyclophane **81** as an example of the inclusion-complexation studies with both longer OPEs (**144** and **146**) and both macrocycles in the two solvent systems. All recorded spectra in D_2O of the guests resembled the ones in Figure 62, in which the signals can hardly be distinguished from the signal noise. Furthermore, the singlet corresponding to the aromatic host proton does not exhibit a change in the chemical shift. Similar results were obtained in $\text{D}_2\text{O}/\text{MeOD}$, in which the very broad guest peaks of low intensity are slightly better visible. Obviously, the water-soluble stopper moiety of the OPEs did not compensate for the insolubility of the hydrophobic phenylene-ethynylene units in both solvent systems, and neither complexation by the cyclophane rendered the guests well soluble. The very broad signals strongly indicate unspecific hydrophobic intermolecular interactions of the guest molecules, which potentially also hinders threading.

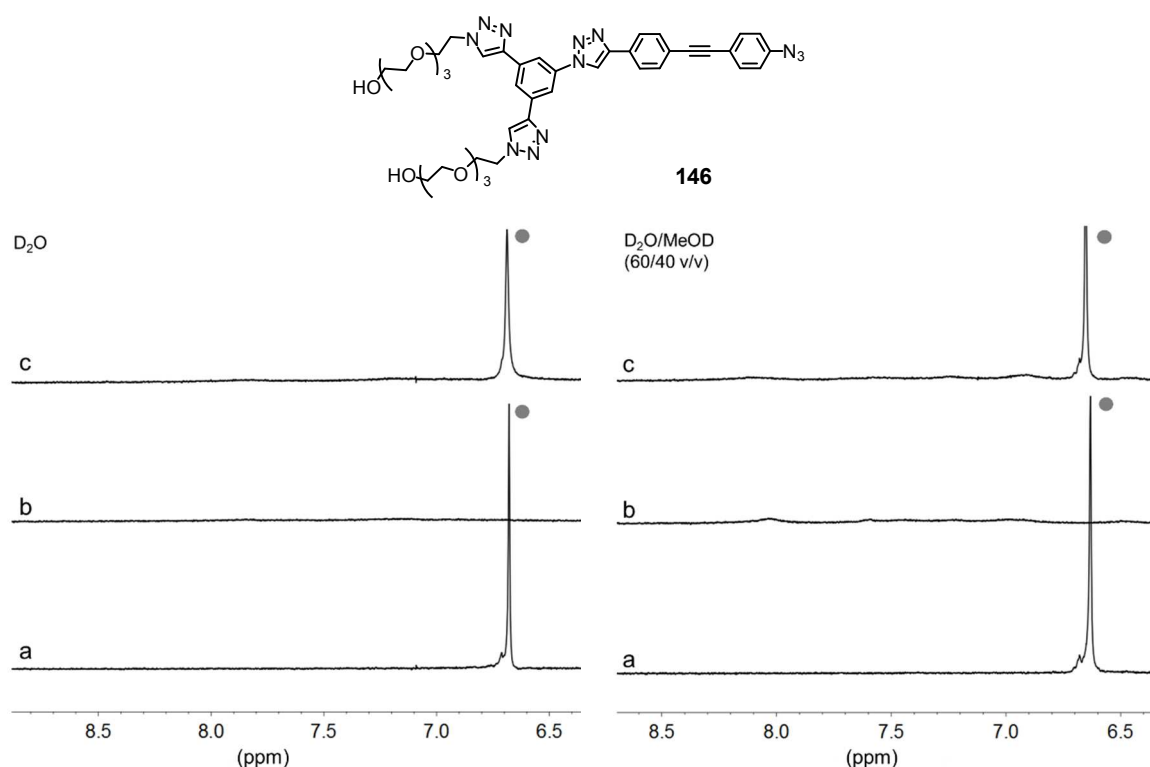


Figure 62. Aromatic region of ^1H NMR spectra in D_2O (left) and $\text{D}_2\text{O}/\text{MeOD}$ (60/40 v/v) (right) of cyclophane **81** only (a), azide-functionalized OPE **146** (b) and a 1:1 mixture of both compounds each in a concentration of 0.5 mM (c).

3.5 Conclusion

The performed test reactions clearly demonstrated the impracticability of the short OPE **145** to react to rotaxanes, whereas traces of the mechanically interlocked molecules were observed in case of OPEs **144** and **146**. ^1H NMR aggregation studies corroborated the assumption that inclusion-complexes of cyclophanes **81** and **109** are not the predominant species and rather unspecific aggregation occurs in protic polar solvents.

In regard to the investigated amphiphiles **92-95** in Chapter 2, composed of a undecorated cyclophane moiety linked by a C_3 chain and different OPE rods, the results of this chapter in addition with the inability to obtain interlocked species allow to conclude that most likely these amphiphiles did not form interlinked [c2]daisy chains. The nature of the cyclophane cavity turned out to be only one factor influencing the intracavitary complexation. Moreover, hydrophobic interactions of the lipophilic OPE moieties revealed to be prevalent over the desired aggregation modes. Consequently, the rod-shaped moiety of the daisy chain monomer requires to be redesigned. Functionalization with solubilizing groups appears to be promising in order to overcome threading issues.

4 Identifying Suitable Guest Molecules

4.1 Molecular Design of Guests

With the objective to identify a suitable guest moiety for amphiphilic daisy chain monomers, potential substrates were screened in their ability to form inclusion-complexes with Diederich-type cyclophanes (**81** and **109**) in protic polar solvents. Two classes of aromatic compounds were investigated (Figure 63). The first class was derived from the unfunctionalized OPE moiety of amphiphiles **91-95**. OPE molecules composed of three and respectively two phenyl units, substituted with differing numbers of solubilizing carboxylate-groups were prepared as potential guest molecules (**155**, **156** and **157**). The second class was based on an aromatic core unit substituted with water-solubility providing tetraethylene glycol chains (**158** and **159**). Naphthalene was chosen in compliance with the high affinity of cyclophane **81** towards naphthalene substrates in protic polar solvents, examined by the Diederich group.^[122]

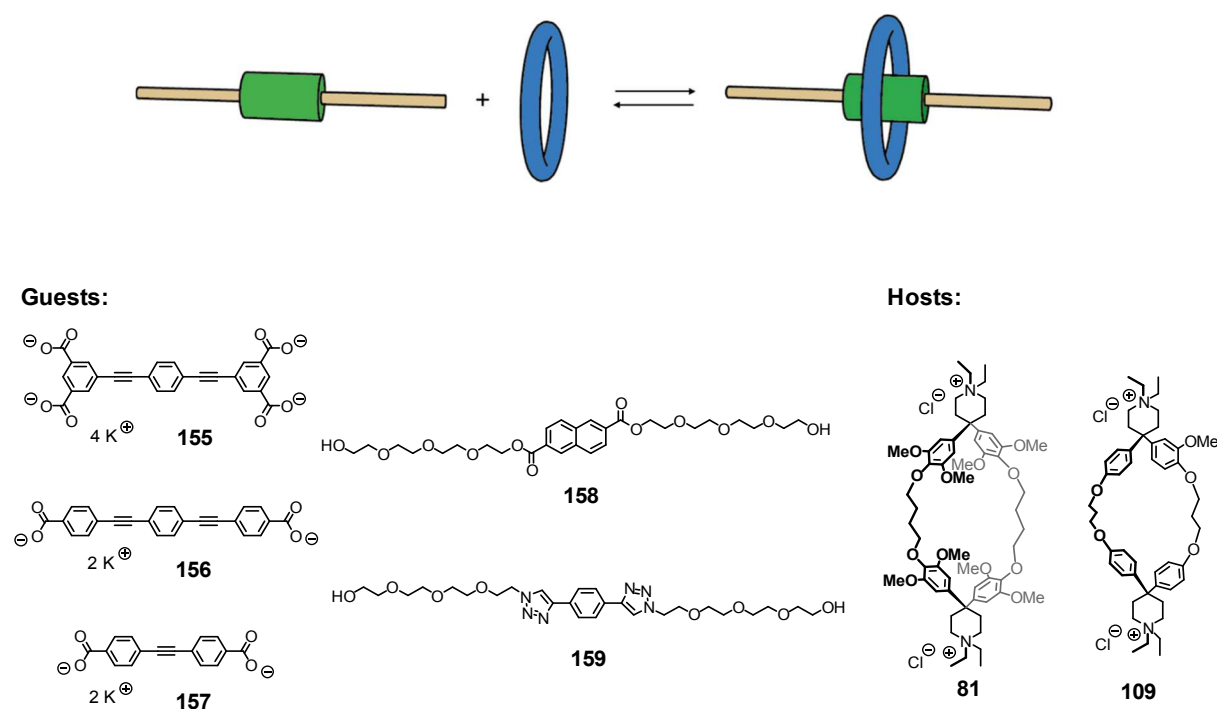
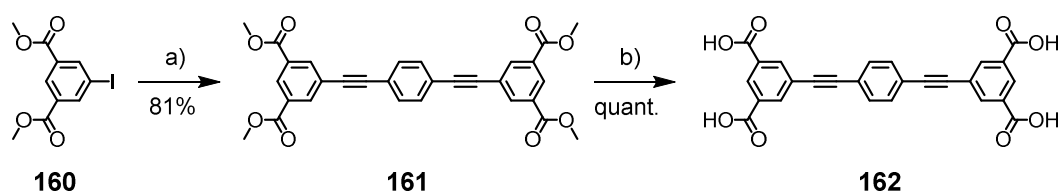


Figure 63. Schematic representation of host-guest inclusion-complexation (top) and investigated potential guest molecules for hosts **81** and **109** (bottom).

Triazole moieties were attached to a benzene ring in order to investigate, if Diederich-type cyclophanes are capable to encircle the *click* cycloaddition product. Especially in regard to further plans of using CuAAC for preparing mechanically interlocked molecules in general and also for the synthesis of amphiphilic daisy chain monomers by introducing the molecular guest moiety to a macrocycle. Furthermore, both compounds, **158** and **159**, revealed to be synthetically well-accessible.

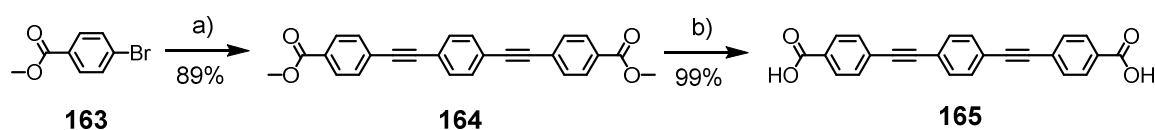
4.2 Syntheses of Guest Molecules

The quadruply carboxylate-functionalized OPE **162** was prepared in two synthetic steps starting from dimethyl 5-iodoisophthalate and 1,4-diethynylbenzene (Scheme 43). The two commercially available compounds reacted via Sonogashira cross-coupling to OPE **161**. The methyl esters were then hydrolyzed under basic conditions following a previously reported protocol.^[156] Protonation with aqueous hydrochloric acid afforded OPE **162** in quantitative yield and also allowed the characterization of the product in organic solvent.



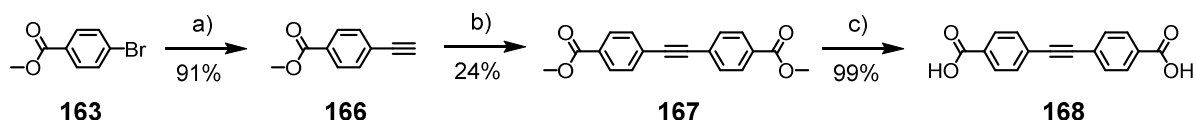
Scheme 43. Synthesis of OPE **162**. a) 1,4-diethynylbenzene, Pd(PPh₃)₂Cl₂, CuI, THF, DIPA, 60 °C, 18 h; b) 1.) aq. KOH, THF/MeOH (50/50 v/v), 90 °C, 4 h, 2.) aq. HCl, rt, quant.

OPE **165**, comprising two carboxylate groups, was synthesized according to the same approach than the analogue OPE **162** (Scheme 44). Two equivalents of the commercially available methyl 4-bromobenzoate (**163**) were coupled to 1,4-diethynylbenzene affording the ester-functionalized OPE **164** in 89% yield. Basic ester hydrolysis was performed and OPE **165** was obtained by protonation with hydrochloric acid.



Scheme 44. Synthesis of OPE **165**. a) 1,4-diethynylbenzene, Pd(PPh₃)₂Cl₂, CuI, THF, DIPA, 60 °C, 18 h; b) 1.) aq. KOH, THF/MeOH (4/1 v/v), 90 °C, 4 h, 2.) aq. HCl, rt.

The bromine of methyl 4-bromobenzoate (**163**) was substituted with trimethylsilyl acetylene (TMSA) by applying a standard Sonogashira cross-coupling protocol. Subsequent desilylation in presence of potassium carbonate afforded the terminal acetylene-functionalized compound **166** in a yield of 91%.^[157] **166** reacted with another equivalent of methyl 4-bromobenzoate to OPE **167**, which was then transformed to the carboxylate-functionalized OPE **168** following a previously published procedure.^[158]



Scheme 45. Synthesis of OPE **168**. a) 1.) TMSA, Pd(PPh₃)₂Cl₂, CuI, THF, DIPA, 60 °C, 4 h, 2.) K₂CO₃, MeOH, DCM, rt, 1 h; b) methyl 4-bromobenzoate, Pd(PPh₃)₂Cl₂, CuI, THF, DIPA, 60 °C, 18 h; c) 1.) aq. KOH, EtOH/H₂O (9/1 v/v), 35 °C, 1.5 h, 2.) aq. HCl, rt.

The potential guest molecules **158** and **159** were prepared by Yves Aeschi. Compound **158** was obtained via transesterification of 2,6-naphthalenedicarboxylic acid dimethyl ester with tetraethylene glycol. The solubilizing ethylene glycol chains of molecule **159** were attached to 1,4-diethynylbenzene via CuAAC.

4.3 ¹H NMR Complexation Studies

The convenient analysis method based on ¹H NMR experiments, already introduced and employed in Chapter 3, was chosen to investigate the guest's tendency to form inclusion complexes. Each substrate was examined in the two standard solvent systems D₂O and D₂O/MeOD (60/40 v/v). In accordance to the studies in Chapter 3, ¹H NMR spectra of solely host or guest as well as spectra of a solution containing both molecules in a 1:1 ratio were measured and compared. The neutral OPEs **162**, **165** and **168** were subjected to an excess of potassium hydroxide, affording the deprotonated OPEs **155**, **156** and **157** and rendering higher solubility in the employed solvents. The observed changes in the chemical shift ($\Delta\delta_{\text{obs}}$) of the guest and also host protons, allowed an estimation about the tendency to form inclusion-complexes. The assignment of the guest signals was primarily performed according to signal integrals and coupling patterns. In general, an upfield shift of the guest protons upon

complexation was expected, as described by Anderson et al.,^[122] and helped in case of doubt to assign the guest signals in the spectra of the 1:1 mixtures. In all spectra, the host protons are designated with a grey dot, while guest protons are labelled with letters and shifts are indicated by arrows.

Analyzing OPE **155**, the strong shift of -2.06 ppm in D₂O and -2.02 ppm in D₂O/MeOD of guest protons C in presence of cyclophane **81** is striking, whereas protons A and B show a significant smaller change of shift (Figure 64). The observed shift of protons C are in accord with the expected $\Delta\delta_{\text{obs}}$ for saturated complexation and indicate that the cyclophane is located on the “middle” phenyl ring. Additionally, the downfield shift of the cyclophane protons (0.24 and 0.28 ppm, respectively) further underpin that an inclusion complex is formed.

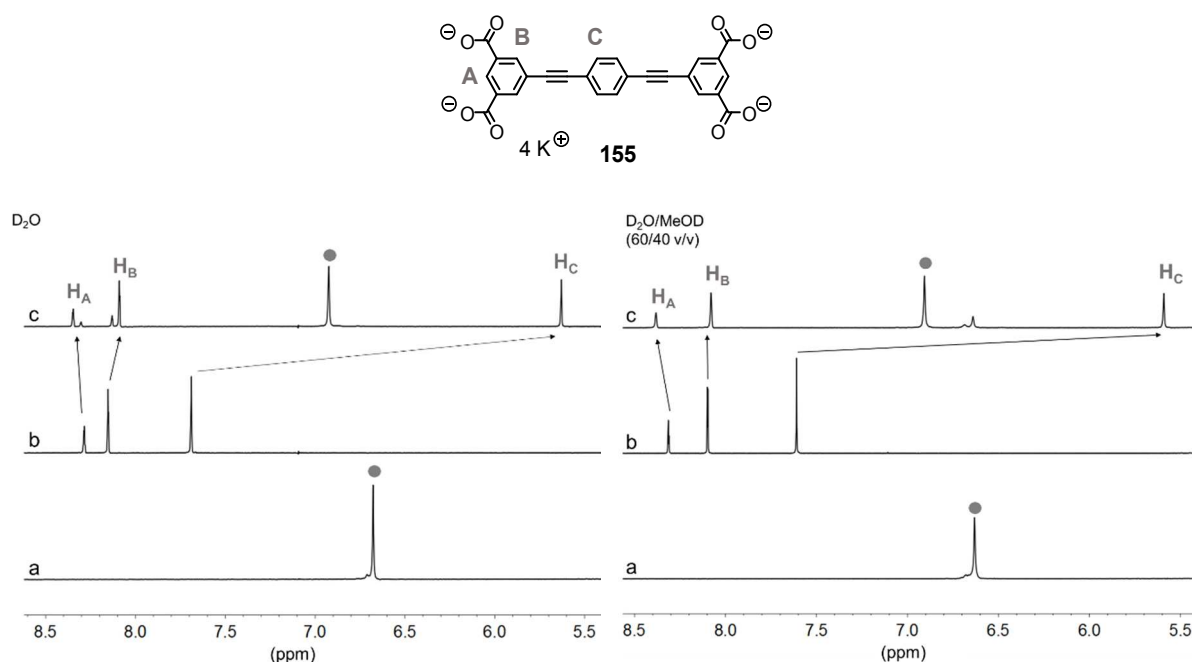


Figure 64. Aromatic region of ¹H NMR spectra in D₂O (left) and D₂O/MeOD (60/40 v/v) (right) of cyclophane **81** only (a), OPE **155** (b) and a 1:1 mixture of both compounds each in a concentration of 0.5 mM (c).

The corresponding study with the smaller cyclophane clearly shows much smaller changes in the chemical shifts (Figure 65), leading to the conclusion that OPE **155** only threads macrocycle **109** to minor extent. The nontypical downfield shift of protons A and B in D₂O/MeOD rather indicates other aggregation modes of the OPE rod with the cyclophane.

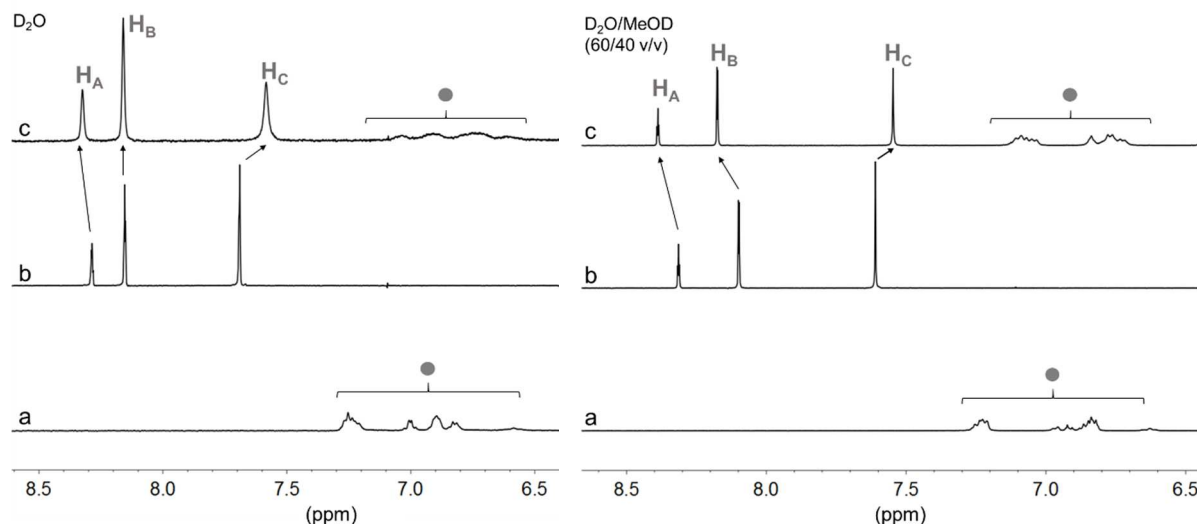


Figure 65. Aromatic region of ^1H NMR spectra in D_2O (left) and $\text{D}_2\text{O}/\text{MeOD}$ (60/40 v/v) (right) of cyclophane **109** only (a), OPE **155** (b) and a 1:1 mixture of both compounds each in a concentration of 0.5 mM (c).

The ^1H NMR spectrum of the host-guest mixture containing OPE **156**, which comprises only two solubilizing groups, shows broad peaks of low intensity in D_2O (Figure 66). Hence, definite assignment of protons A and B in this spectrum proved to be impossible. Based on the well-resolved peaks of the spectrum in $\text{D}_2\text{O}/\text{MeOD}$ (spectrum (c)), the amount of dissolved guest could be quantified and revealed a host-guest ratio of only 4:1. Nevertheless, the experiments allowed some general conclusions. For example, protons C exhibit the strongest shifts ($\Delta\delta_{\text{obs}} = -0.79$ in D_2O and -0.76 ppm in $\text{D}_2\text{O}/\text{MeOD}$), which is in line with the results obtained for OPE **155**. In both cases, the cyclophane is mainly encircling the “middle” phenyl ring. Protons B show a smaller change of $\Delta\delta_{\text{obs}} = -0.43$ and -0.23 ppm, while the shift of protons A, adjacent to the carboxylate groups, is negligible.

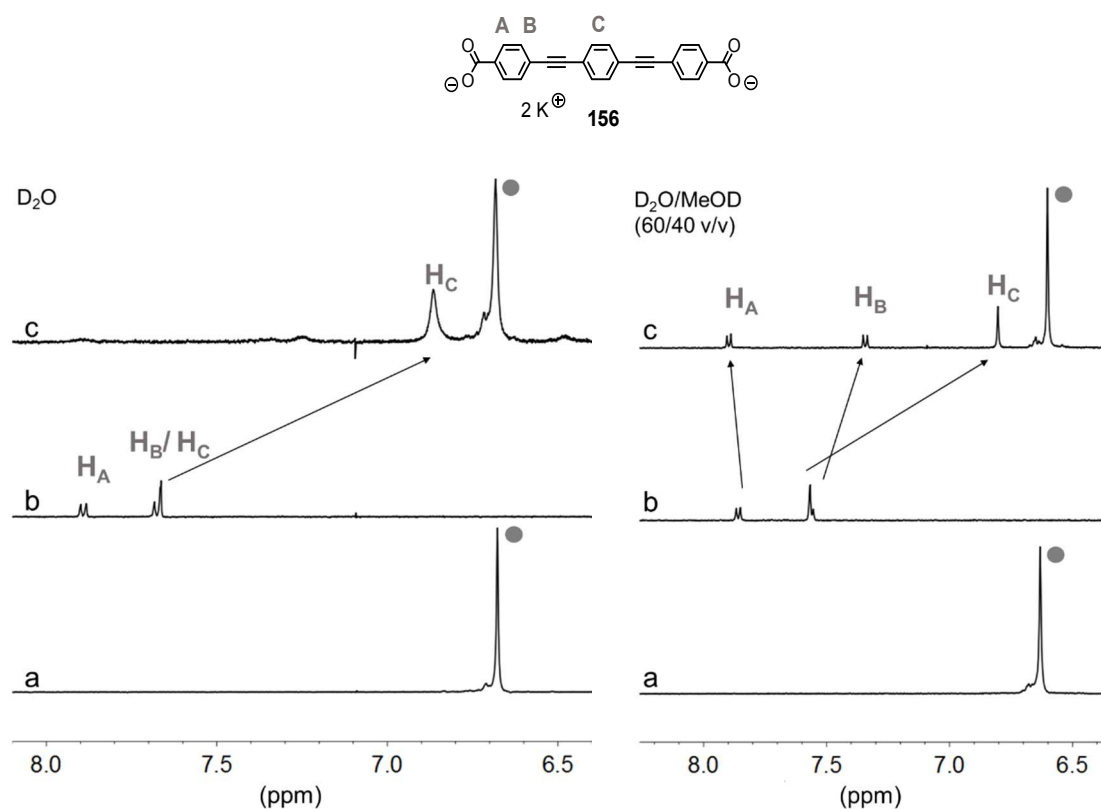


Figure 66. Aromatic region of ^1H NMR spectra in D_2O (left) and $\text{D}_2\text{O}/\text{MeOD}$ (60/40 v/v) (right) of cyclophane **81** only (a), OPE **156** (b) and a 1:1 mixture of both compounds each in a concentration of 0.5 mM (c).

The experiments with cyclophane **109** (Figure 67) also demonstrate the low solubility of OPE **156** and additionally absence of inclusion-complexation can be assumed due to the very small shift of guest protons in $\text{D}_2\text{O}/\text{MeOD}$ and also to the peaks of host protons, which do not show any shifting.

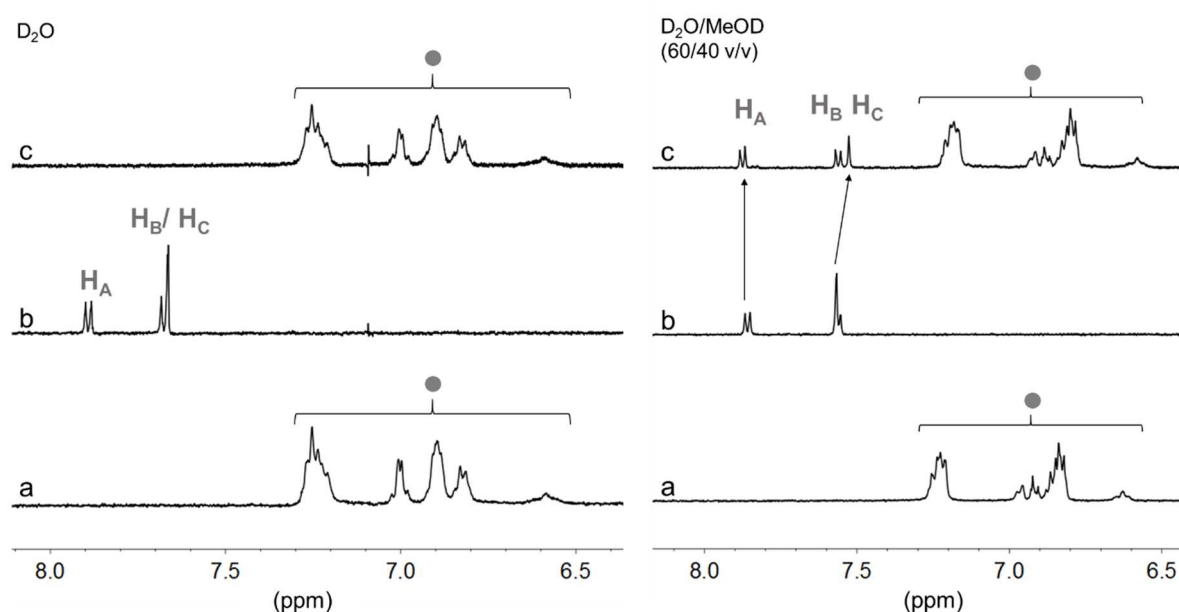


Figure 67. Aromatic region of ^1H NMR spectra in D_2O (left) and $\text{D}_2\text{O}/\text{MeOD}$ (60/40 v/v) (right) of cyclophane **109** only (a), OPE **156** (b) and a 1:1 mixture of both compounds each in a concentration of 0.5 mM (c)

OPE **157**, which comprises two phenylene-ethynylene moieties, shows $\Delta\delta_{\text{obs}}$ values between the other two investigated OPEs with $\Delta\delta_{\text{obs}} = -1.48$ ppm in D_2O and -1.44 ppm in $\text{D}_2\text{O}/\text{MeOD}$ for protons B (Figure 68). Compatible to the guests' shifting, the host protons exhibit intermediate $\Delta\delta_{\text{obs}}$ values of 0.18 ppm in D_2O and 0.16 ppm in $\text{D}_2\text{O}/\text{MeOD}$. Interestingly, the guest protons A and B appear to be split into four signals in the spectra containing host and guest, instead of into two, as observed in the corresponding spectra solely containing OPE. The effect, most likely based on a slow complexation exchange rate in the NMR timescale, is well visible in the binary solvent mixture (indicated by arrows), but also the spectrum in D_2O implies another pair of guest signals. It seems the more shifting and also more intense signals correspond to the complexed guest, while the other signals represent unthreaded OPE. Corroborating this assumption, a comparable low signal corresponding to free uncomplexed cyclophane can be observed in the spectrum in $\text{D}_2\text{O}/\text{MeOD}$ (designated by a second grey dot).

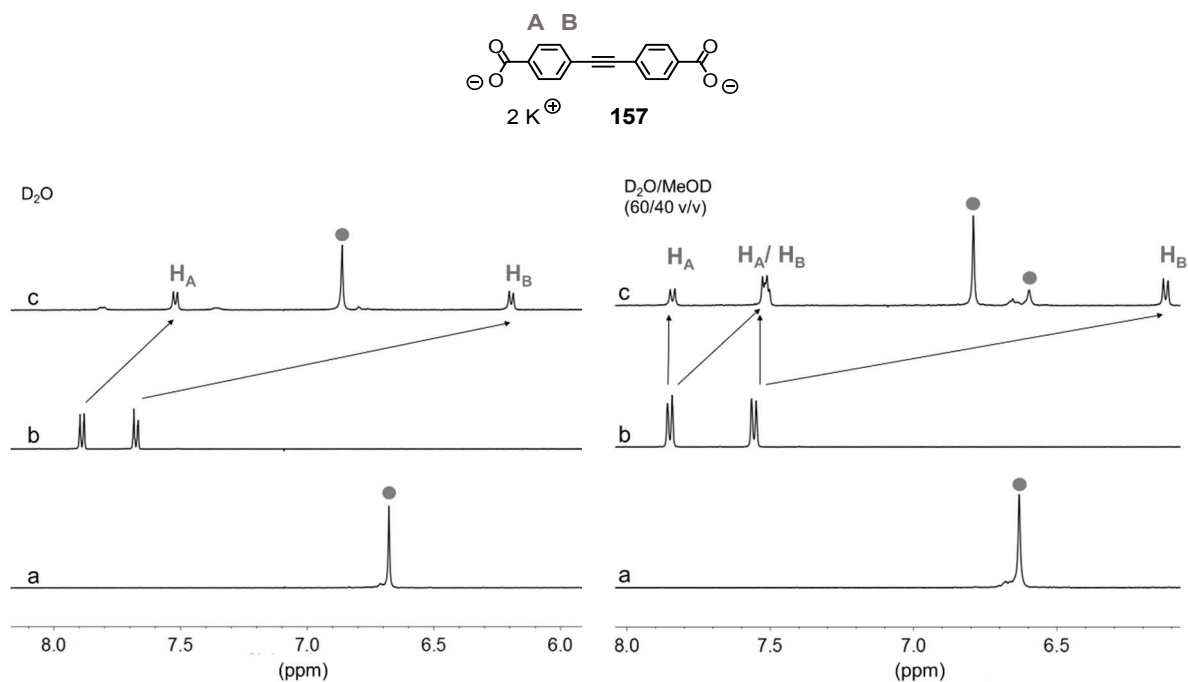


Figure 68. Aromatic region of ^1H NMR spectra in D_2O (left) and $\text{D}_2\text{O}/\text{MeOD}$ (60/40 v/v) (right) of cyclophane **81** only (a), OPE **157** (b) and a 1:1 mixture of both compounds each in a concentration of 0.5 mM (c).

In corresponding experiments with the smaller cyclophane **109** (Figure 69) neither host, nor guest protons of high intensity show a change in the chemical shift. However, a second pair of shifted guest signals with very low intensity is visible in spectrum (c) in $\text{D}_2\text{O}/\text{MeOD}$. The observed result allows the assumption that OPE **157** is capable of threading the smaller Diederich cyclophane **109**, even though in a minor amount. The low quality of the spectrum in D_2O does not permit a conclusion about the threading behavior of OPE **157**.

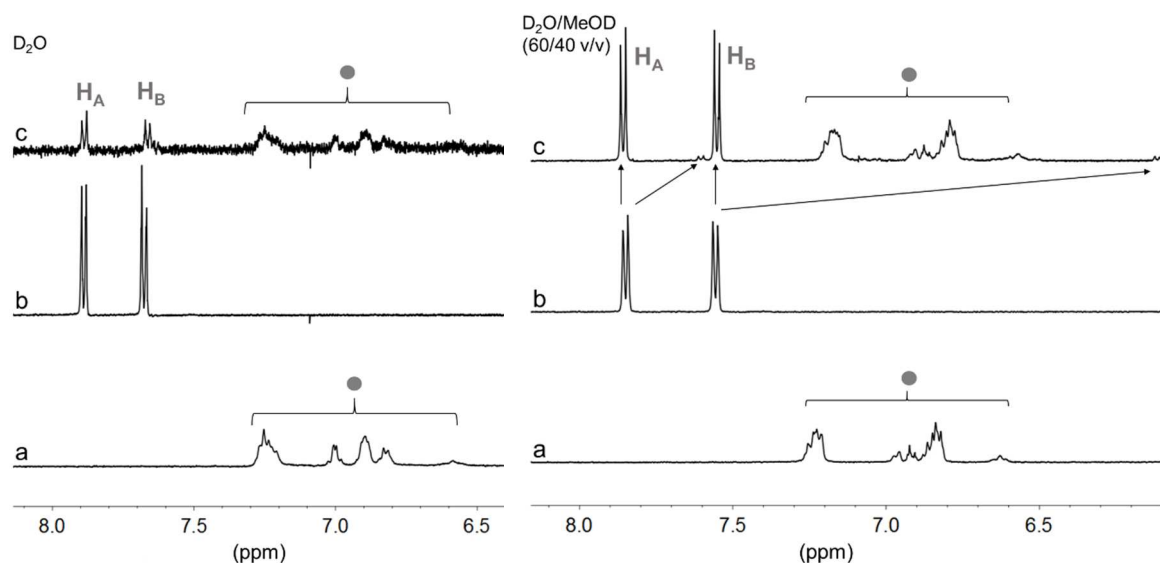


Figure 69. Aromatic region of ^1H NMR spectra in D_2O (left) and $\text{D}_2\text{O}/\text{MeOD}$ (60/40 v/v) (right) of cyclophane **109** only (a), OPE **157** (b) and a 1:1 mixture of both compounds each in a concentration of 0.5 mM (c).

Figure 70 shows the complexation experiments undertaken with naphthalene derivative **158** and cyclophane **81**. Most striking is the dramatically decreasing resolution of the guest protons upon mixing with host in both solvent systems. While spectra b, corresponding to solely **158**, exhibit sharp signals, only one very broad signal can be assigned to the guest in spectra (c). The other signal of low intensity in spectra (c), at 6.7 ppm in D_2O and 6.6 ppm in $\text{D}_2\text{O}/\text{MeOD}$, correspond to the unknown impurity of cyclophane, which does not show any change of the chemical shift. However, in contrast to the poorly soluble OPE **156**, the peak broadening in spectra (c) can presumably be attributed to a slow exchange rate in the NMR timescale of complexed and uncomplexed guest molecules and/or slow interconversion of different inclusion geometries. The most significant proof for complexation demonstrate the host protons, which shift considerably 0.31 ppm in D_2O and 0.16 ppm in $\text{D}_2\text{O}/\text{MeOD}$.

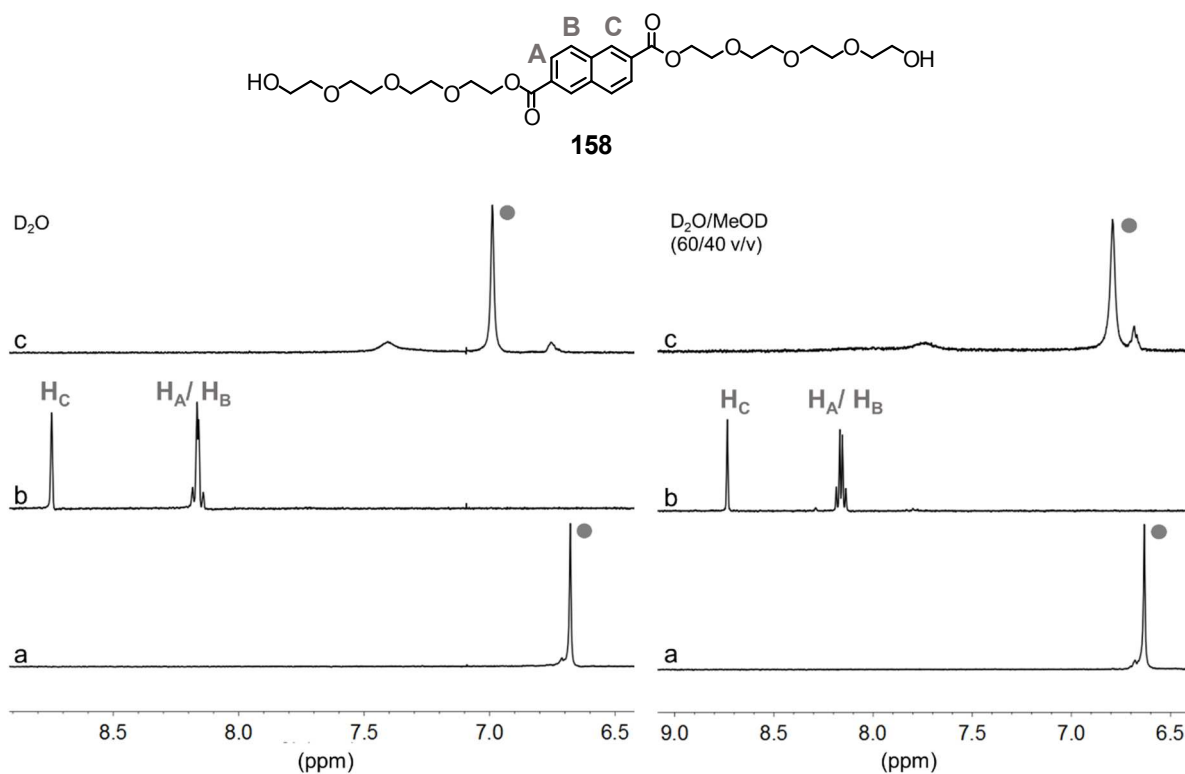


Figure 70. Aromatic region of ¹H NMR spectra in D₂O (left) and D₂O/MeOD (60/40 v/v) (right) of cyclophane **81** only (a), guest **158** (b) and a 1:1 mixture of both compounds each in a concentration of 0.5 mM (c).

While the host-guest spectrum (c) in D₂O/MeOD (Figure 71) looks similar to the spectra of solely **109** and **158** in the same solvent system, the corresponding spectrum (c) in D₂O differs from spectra (a) and (b). The guest protons shift between -0.09 and -0.16 ppm and also the pattern of host protons changed, indicating some kind of aggregation.

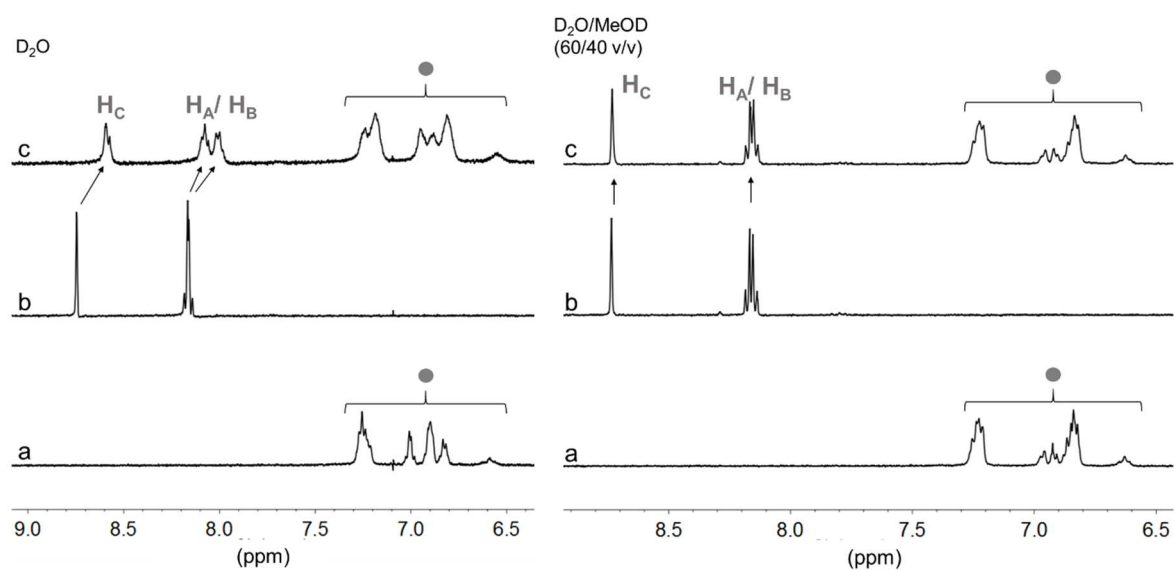


Figure 71. Aromatic region of ¹H NMR spectra in D₂O (left) and D₂O/MeOD (60/40 v/v) (right) of cyclophane **109** only (a), guest **158** (b) and a 1:1 mixture of both compounds each in a concentration of 0.5 mM (c).

Regarding the inclusion-complexation experiment with **159** in D₂O (Figure 72), the guest behaves similar to **158** in presence of host **81**. The broad signals of low intensity indicate slow exchange rates of the host-guest equilibrium. However, the tendency of complexation appears to be less. The protons B corresponding to the benzene ring show an intermediate change in shift ($\Delta\delta_{\text{obs}} = -0.95$ ppm), which is in line with the shift of host (0.14 ppm). The triazole signals shift -0.55 ppm, which gives evidence that cyclophane **81** can be threaded by **159**. Comparing the spectra of D₂O with D₂O/MeOD (Figure 72), the influence of solvent on the host-guest system is significant. The change of chemical shift drops dramatically in the binary solvent mixture and broadening of guest signals is almost negligible.

Figure 73 demonstrates that the smaller cyclophane **109** does not complex compound **159**. Only in D₂O a small degree of aggregation occurs, indicated by the shift of triazole signals while the benzene protons do not change.

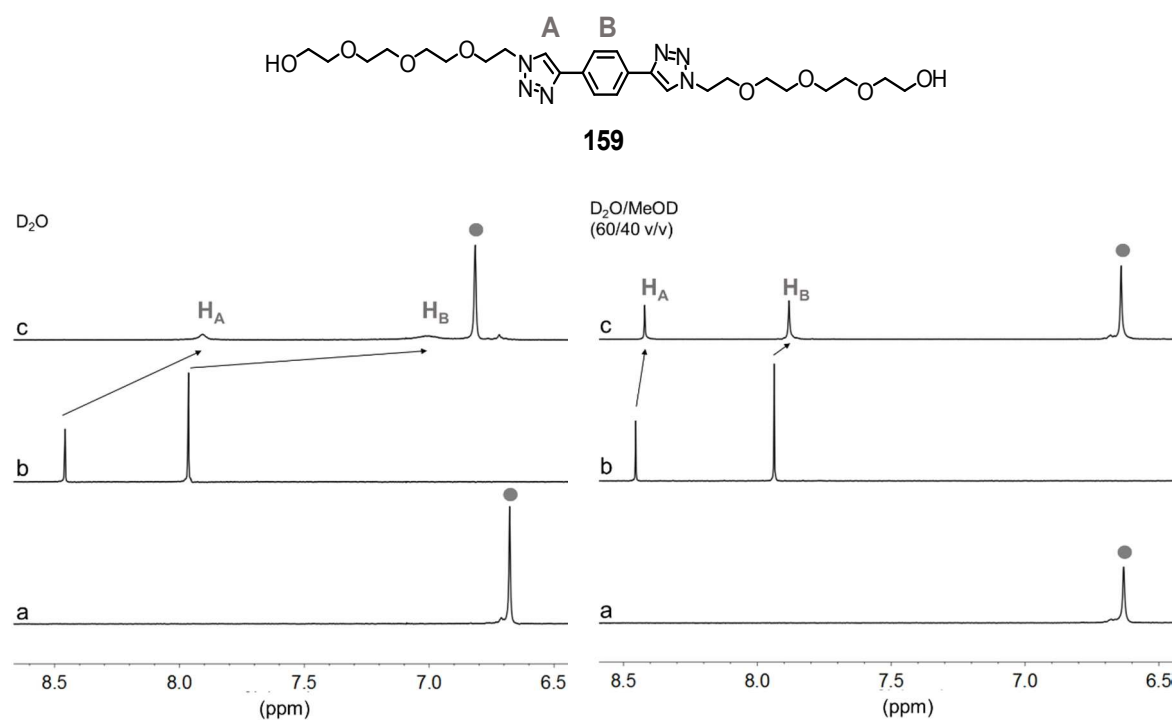


Figure 72. Aromatic region of ¹H NMR spectra in D₂O (left) and D₂O/MeOD (60/40 v/v) (right) of cyclophane **81** only (a), guest **159** (b) and a 1:1 mixture of both compounds each in a concentration of 0.5 mM (c).

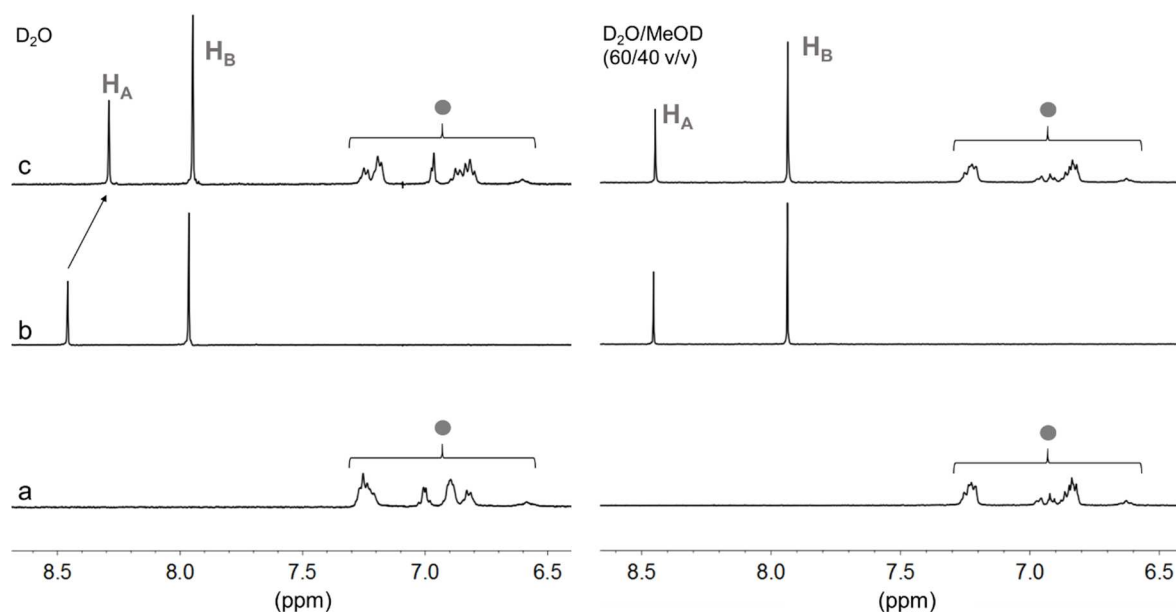


Figure 73. Aromatic region of ^1H NMR spectra in D_2O (left) and $\text{D}_2\text{O}/\text{MeOD}$ (60/40 v/v) (right) of cyclophane **109** only (a), guest **159** (b) and a 1:1 mixture of both compounds each in a concentration of 0.5 mM (c).

4.4 Conclusion

The performed ^1H NMR-based studies gave a deeper insight into the complexation behavior of potential guest molecules with Diederich-type cyclophanes and to further approach the goal of finding a suitable guest moiety for molecular daisy chains. Besides confirming that in D_2O the aggregation is more pronounced than in the $\text{D}_2\text{O}/\text{MeOD}$ mixture and that host **81** with larger and deeper cavity exhibits a higher complexation affinity than the smaller cyclophane **109**, some elucidating information about the guest molecules could be afforded. For example, in case of the carboxylate-functionalized OPEs, the threading tendency revealed to be predominantly dependent on the solubility, otherwise the hydrophobic rod-shaped favorably form other aggregates, as already observed in Chapter 2 and 3. The double amount of solubilizing groups of OPE **155**, compared to OPE **156** with the same molecular backbone, had a significant effect on the complexation and even showed strong inclusion complexation in presence of additive MeOD. A similar solubility-dependent tendency was observed by comparing **156** with the shorter and less hydrophobic OPE **157**. Investigating molecules **158** and **159**, which comprise tetraethylene glycol chains, revealed that the substituents render enough solubility for enabling inclusion-complexation. Both compounds only threaded cyclophane **81**, whereas the naphthalene-based molecule showed greater changes in the

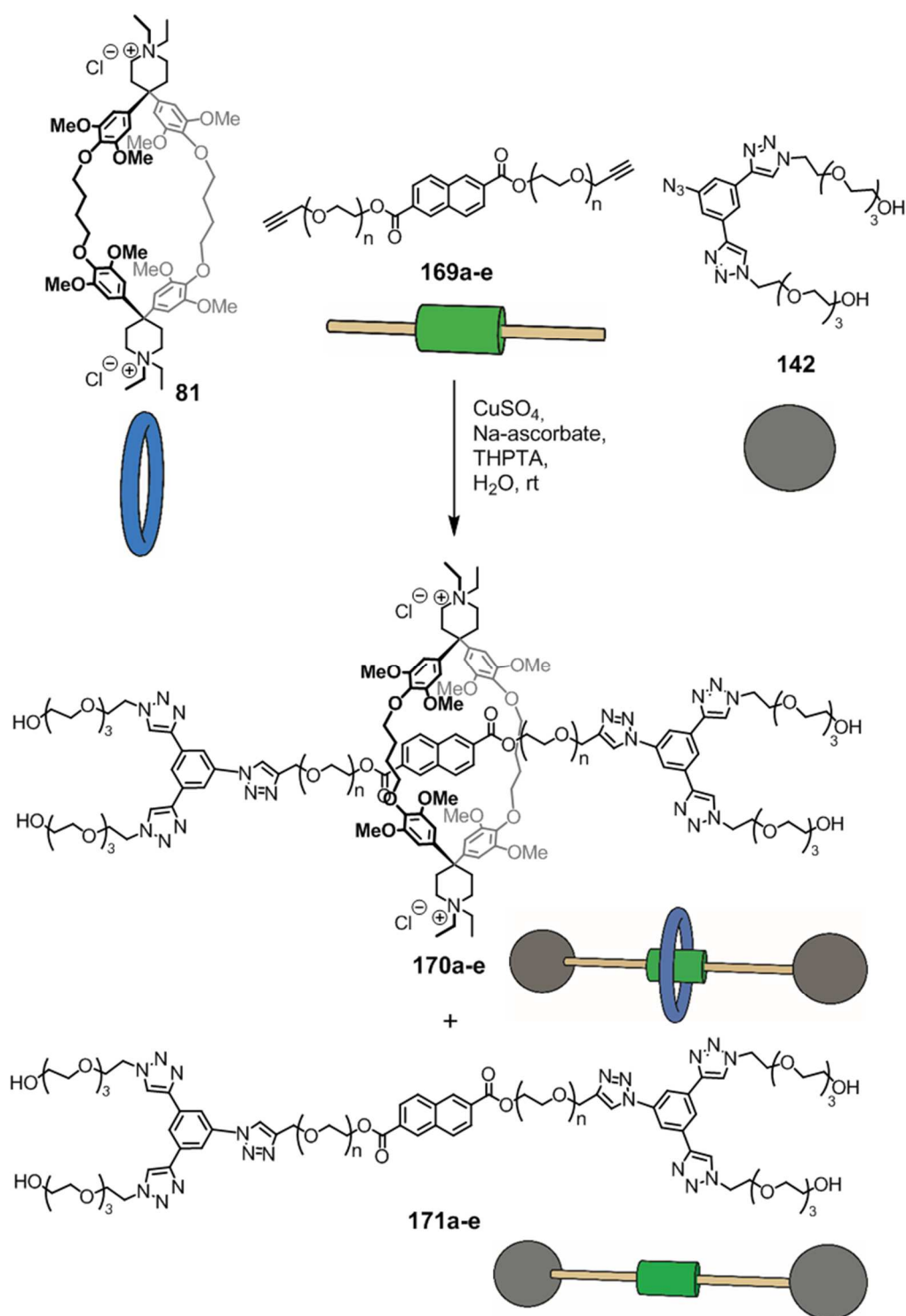
chemical shift than compound **159**. The threading behavior of the latter molecule turned out to be significantly depending on the solvent system. While a certain degree of complexation was observed in D₂O, almost none occurred in the solvent mixture D₂O/MeOD (60/40 v/v). Although the carboxylate equipped OPE **155** appears to exhibit very strong binding affinity towards cyclophane **81**, from a synthetic perspective, naphthalene-based substrates seem to be more facile implementable guests for MIM preparations. Additionally, the zwitterionic character resulting from the negatively charged OPE in combination with the cationic Diederich-type cyclophane might become challenging to handle. Whereas the OPE molecules need to be build up from highly functionalized benzene guests, 2,6-functionalized naphthalene derivatives are commercially available, reducing the synthetic challenges.

5 Assembly of [2]Rotaxanes in Water

Based on the insightful results of the ^1H NMR inclusion-complexation studies of potential guest molecules in presence of the two different Diederich-type cyclophanes **81** and **109** (Chapter 4), a promising host-guest system for the assembly of MIMs in water was found. In line with the stoppering reactions in Chapter 2.9 and Chapter 3, rotaxation was chosen as a direct and simple proof-of-principle method for trapping host-guest complexes and finally enabled the isolation and characterization of a water-soluble [2]rotaxane.

5.1 Introduction

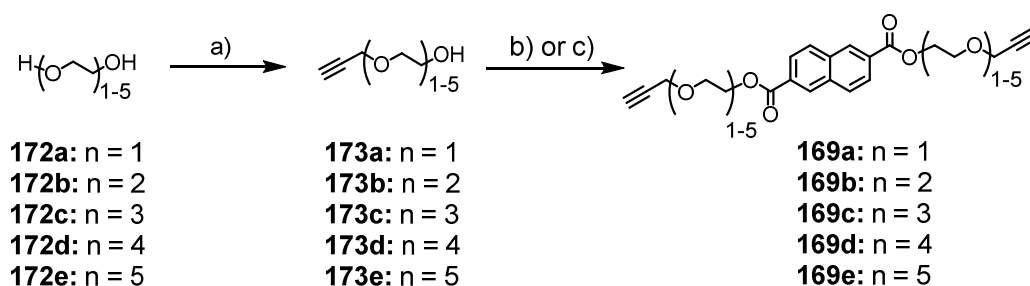
Cyclophane **81**, which proved to be a more suitable host than cyclophane **109**, was used for the rotaxane assembly. The water-soluble naphthalene-based guest **158** was employed as rotaxane axle. By choosing an assembly strategy in pure water, high association constants can be obtained, which is a fundamental requirement to afford high yields of interlocked rotaxanes. The CuAAC reaction is ideally suited for aqueous conditions due to its high functional group tolerance and high reaction rates. Therefore, **158** was equipped with terminal propargyl moieties resulting in molecule **169d**. Additionally, derivatives of **169d**, bearing propargyl terminated oligoethylene glycol esters of different length ($n = 1 - 5$) and hence varying in their hydrophilic character, were prepared and investigated as potential rotaxane axles (Scheme 46). Azide-functionalized stopper **142** was used to capture interlocked rotaxanes. Screening reactions under three different reaction conditions were performed with each guest molecule and analyzed semi-quantitatively by HPLC-ESI-MS. Binding constants of cyclophane **81** towards guests **169c-e** could be determined by fluorescence quenching titrations.



Scheme 46. Syntheses of the [2]rotaxanes **170a-e** from cyclophane **81**, axles **169a-e** and stopper **142** via CuAAC in water and dumbbell **171a-e** formation as byproducts ($n = 1$: **a**; $n = 2$: **b**; $n = 3$: **c**; $n = 4$: **d**; $n = 5$: **e**).

5.2 Syntheses of Rotaxane Axles

Axles **169a-e** were synthesized starting from the appropriate ethylene glycol **172a-e** (Scheme 47), which was monosubstituted by alkylation with propargyl bromide in presence of base, following slightly modified previously reported protocols.^[159–163] Monopropargyl oligoethylene glycol ethers **173a-b** reacted with 2,6-naphthalenedicarboxylic dimethyl ester via transesterification to afford the shorter axles **169a-b**. However, a considerable excess of the corresponding compounds **173a-b** were essential and high reaction temperatures (130 °C) were required to drive methanol out of the equilibrium while simultaneously distilling off the solvent. It turned out that for the axles **169c-e**, which comprise longer ethylene glycol chains ($n = 3 - 5$), a Mitsunobu reaction^[164,165] starting from 2,6-naphthalenedicarboxylic acid and **173c-e** resulted in higher yields.



Scheme 47. Synthesis of axles **169a-e**. a) 1.) base, 0 °C, THF, then rt, 20 min; 2.) propargyl bromide, rt, 18 h; **173a** 66%, **173b** 11%, **173c** 78%, **173d** 90%, **173e** 41%; b) 2,6-naphthalenedicarboxylic dimethyl ester, NaH, THF, 130 °C, 45 min, **169a** 42%, **169b** 14%; c) 2,6-naphthalenedicarboxylic acid, PPh₃, DEAD, r.t., 16 h, **169c** 82%, **169d** 64%, **169e** 43%.

5.3 Binding Studies

Fluorescence quenching titrations with cyclophane **81** were only conducted for axles **169c-e** ($n = 3 - 5$), since axles **169a-b** revealed to be insoluble in water. Aliquots of a host **81** solution (0.0 – 20 eq) to the respective naphthalene derivative **169c-e** solution were added and the changes in fluorescence intensity were recorded. As representative example the quenching of the fluorescence of the naphthalene axle **169d** with the addition of the cyclophane **81** is displayed in Figure 74. The association constants in water for **81·169c**, **81·169d** and **81·169e** were obtained from nonlinear regression of the titration curves (see exemplary Figure 75) as

$K_a = 1.67 (\pm 0.056) \times 10^5 \text{ M}^{-1}$, $K_a = 1.44 (\pm 0.052) \times 10^5 \text{ M}^{-1}$ and $K_a = 1.18 (\pm 0.023) \times 10^5 \text{ M}^{-1}$, respectively.

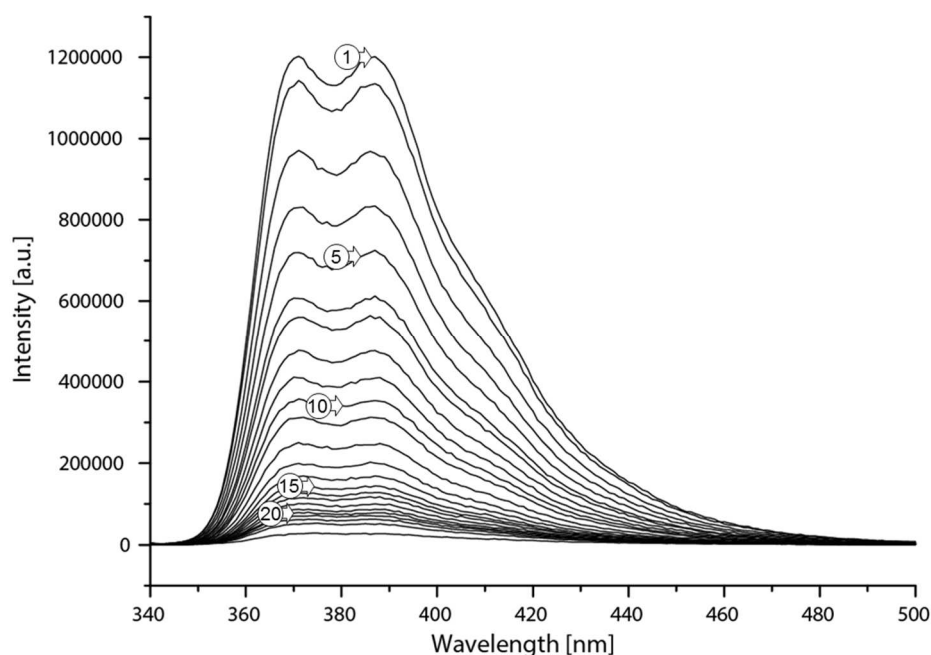


Figure 74. Titration of 20.0 μM **169d** with cyclophane **81** in water at 22 $^\circ\text{C}$ ($\lambda_{\text{exc}} = 333 \text{ nm}$). Fluorescence spectra correspond to added host equivalents, top down: 1) 0.0 eq; 2) 0.1 eq; 3) 0.3 eq; 4) 0.5 eq; 5) 0.7 eq; 6) 0.9 eq; 7) 1.0 eq; 8) 1.2 eq; 9) 1.4 eq; 10) 1.6 eq; 11) 1.8 eq; 12) 2.2 eq; 13) 2.6 eq; 14) 3.0 eq; 15) 3.4 eq; 16) 3.8 eq; 17) 4.2 eq; 18) 5.0 eq; 19) 5.5 eq; 20) 6.0 eq; 21) 7.0 eq; 22) 8.0 eq; 23) 10 eq and 24) 20 eq.

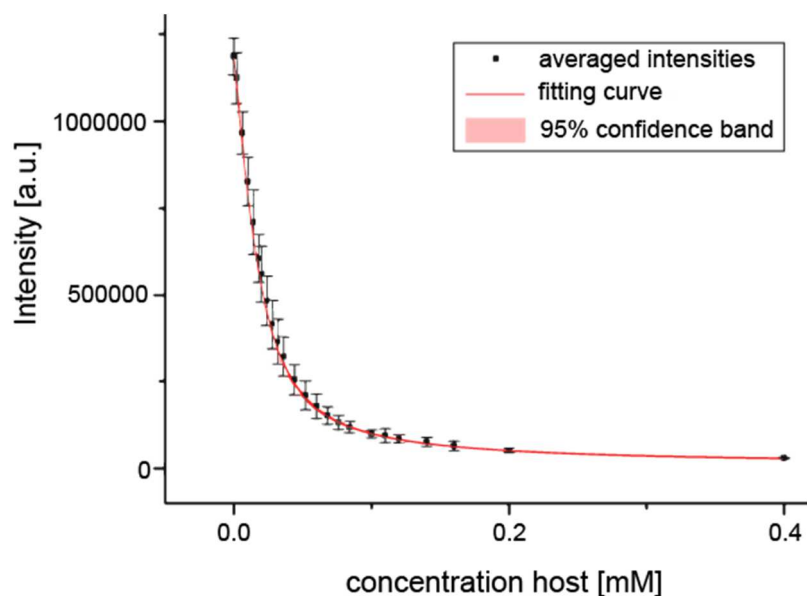


Figure 75. Fitting curve of fluorescence titration with guest **169d**.

The three association constants of the supramolecular host-guest systems are of similar dimensions with a trend of decreasing K_a values upon increasing oligo-EG chain lengths of the

guests. Whether this phenomenon is based on the lower apolar character of **169e** compared to **169c** or the entropic cost of complexation cannot be rationalized with the here collected data. The binding strength points at the strong bias that the naphthalene core provides and is comparable with most common recognition motifs used in MIM systems so far (e.g. cyclodextrins·hydrophobic guests with K_a values in water between 10^2 M^{-1} and 10^5 M^{-1} ,^[51,166] macrocyclic dibenzo-crown ethers·dialkylammonium ions with K_a values in dichloromethane between 10^3 M^{-1} and 10^6 M^{-1} ,^[167] and cyclobis(paraquat-*p*-phenylene)·tetrathiafulvalene derivatives with K_a values in acetone between 10^3 M^{-1} and 10^4 M^{-1}).^[168]

5.4 Screening Reactions

In order to screen for suitable reaction conditions, three different conditions were investigated for all five axis compounds (**169a-e**) and the result was evaluated by determining the ratio between formed rotaxane vs. dumbbell. Of particular interest was to elucidate the influence of the ethylene glycol length of axis **169a-e** on the amount of isolated rotaxanes.

5.4.1 Reaction Conditions

In all of the 15 reactions, axle and stopper were used in a 1:2 ratio (Table 1), consequently full consumption of all propargyl groups of **169a-e** and azide groups of **142** can be expected. The reactions performed under condition 1 and 3 contained cyclophane in equimolar amount only, whereas under condition 2 five equivalents of **81** were employed. The solid or respectively oily axes **169a-b** and **169c-e** were directly weighted into the reaction flask, before the appropriate amounts of cyclophane, stopper and catalyst system (Table 1) were added from aqueous stock solutions allowing convenient preparation of the reaction mixtures. As catalyst system for the CuAAC reactions in water, the reagent combination of copper(II) sulfate with the mild reductant sodium ascorbate was utilized. In condition 3, *tris*(3-hydroxypropyl-triazolylmethyl)amine (THPTA)^[169] was additionally employed as the ligand stabilizes the oxidation state of Cu(I) and has shown to increase reaction rates of Cu(I)-catalyzed azide-alkyne cycloadditions^[170]

Table 3. Total concentrations and equivalents of reactants and reagents of the CuAAC screening reactions under three different conditions.*

cond.	cyclophane	axle	stopper	CuSO ₄	Na ascorb.	THPTA
1	0.5 mM (1.0 eq)	0.5 mM (1.0 eq)	1.0 mM (2.0 eq)	0.5 mM (1.0 eq)	0.5 mM (1.0 eq)	–
2	2.5 mM (5.0 eq)	0.5 mM (1.0 eq)	1.0 mM (2.0 eq)	0.5 mM (1.0 eq)	0.5 mM (1.0 eq)	–
3	0.5 mM (1.0 eq)	0.5 mM (1.0 eq)	1.0 mM (2.0 eq)	0.5 mM (1.0 eq)	0.5 mM (1.0 eq)	0.5 mM (1.0 eq)

* All reactions were performed at room temperature and under argon atmosphere.

5.4.2 Analysis of the Screening Reactions

After two hours reaction duration, a sample was taken, diluted with water and analyzed via HPLC-ESI-MS. In case of the longer polyethylene glycol spacers $n = 3 - 5$, stopper **142** was entirely consumed indicating reaction completion, whereas in case of $n = 1$ and 2, the chromatograms exhibit a signal with a retention time (t_R) of 6.5 min corresponding to **142**. The chromatograms recorded of samples taken after 21 hours revealed no further decrease of the stopper signal. Even after prolonged reaction times the stopper was not completely consumed. Furthermore, no signal for the corresponding axles **169a** and **169b**, was observed in the LC-MS traces, which reflects their insolubility in water. Solubilization of **169a** and **169b** in presence of **81** might be expected, which is in fact not the case, as observed by Anderson et al. for lipophilic chromophores of comparable size.^[128] The recorded LC-ESI-MS chromatograms were analyzed by extracting the m/z values of rotaxanes **170a-e** and dumbbells **171a-e** either in the form of their corresponding proton or sodium ion adducts and m/z values for cyclophane from the total ion chromatogram (T.I.C) (see exemplary chromatograms in Figure 76). The peaks were then integrated, the obtained integrals corresponding to the same compound were summed up, e.g. proton and sodium ion adduct of rotaxane (traces b and c in Figure 76), and used for a semiquantitative evaluation.

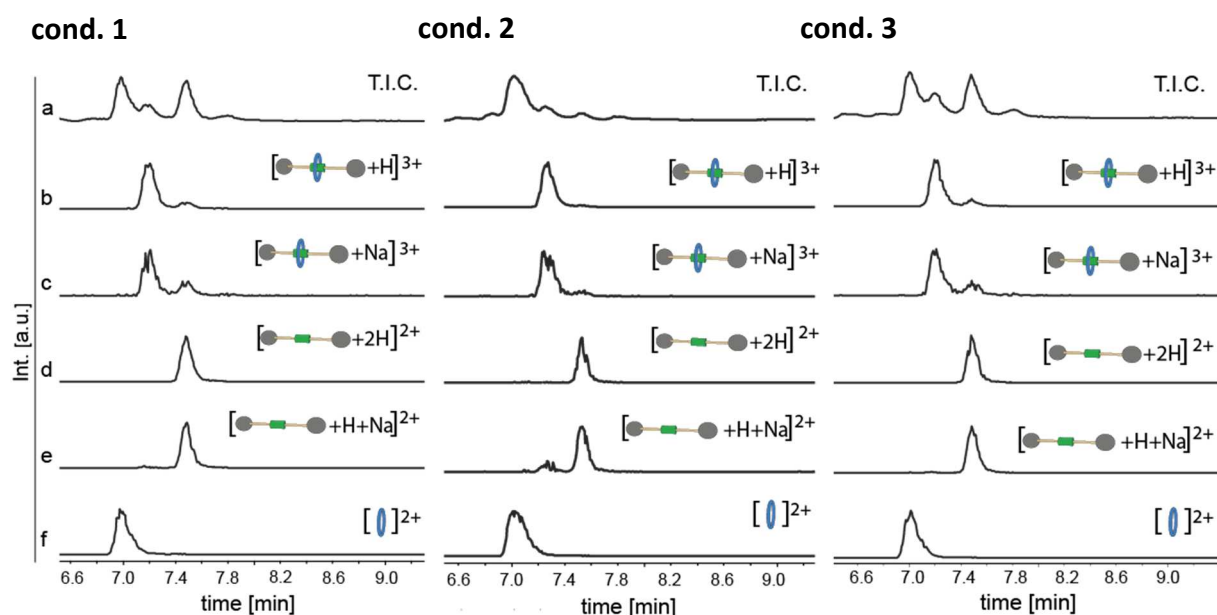


Figure 76. Screening reactions after two hours with *tetra*-EG naphthalene ester axle under the three different conditions 1-3. LC-ESI-MS total ion current trace (a) and extracted ion chromatograms of mainly observed rotaxane (b+c), dumbbell (d+e) and cyclophane (f) adducts (m/z values ± 1). A signal corresponding to either axle **169d** or stopper **142**, respectively, is not observed in either of the three T.I.C.s, which indicates complete conversion of **169d**.

Quantitative analysis based on the recorded UV-chromatograms turned out to be impracticable, since the absorption exhibits only low intensity due to the small concentrations required for the subsequent ESI-MS measurements (about 10^{-5} M). Another advantage using extracted ion chromatograms is that even incompletely separated compounds can be conveniently distinguished and integrated. On the basis of the summed up integrals of corresponding H^+ and Na^+ adducts, the ratios of the respective rotaxane/dumbbell were calculated (see Table 4), allowing a semi-quantitative analysis independent from the injected sample concentration. However, the method allows only to estimate which axle molecules ensues most rotaxane compared to dumbbell and does not give quantitative ratios, as the ionization tendency of rotaxanes most likely differs from dumbbells, which do not comprise an ionic cyclophane unit.

Regarding the determined values of rotaxane/dumbbell, the significantly higher values obtained under condition 2 (with 5.0 equivalents of cyclophane) are striking, pointing at the importance to alter the chemical equilibrium by an excess of cyclophane for an efficient rotaxane synthesis. On average over the screening series with the five different axles, under condition 2 rotaxane compared to dumbbell is formed 5.5 times more than under condition 1.

Remarkable is also the influence of THPTA which increases the CuAAC reaction rate and leads to a higher amount of rotaxane product compared to the reactions lacking the ligand. However, the screening reactions of rotaxane **170c** synthesis differ from this tendency, the **170c/171c** ratio in presence of THPTA (0.31) is slightly lower than in the reaction without THPTA (0.35).

The obtained rotaxane/dumbbell ratios might be rationalized as a combination of two factors, namely the tendency to form the supramolecular complex expressed with the K_a values for pseudorotaxane formation, and the length of the ethylene glycol chains of the axle subunit. The rotaxane formation is favored by an increased K_a value as it is more likely to trap an axle as preformed pseudorotaxane, and it is increased by an increasing length of the axle's ethylene glycol chains which moves the capturing *click* reaction away from the cyclophane ring potentially sterically blocking the reaction center. While under the conditions 1 and 3 the axle **169d** represents the compromise optimizing both effects, under conditions 2 the reduced tendency of axle **169e** to coordinate the cyclophane ring is compensated by an increased cyclophane concentration and thus, the advantage of the longer ethylene glycol chains becomes clearly visible.

Table 4. Summarized results of the binding studies and screening reactions under the three different conditions 1-3, given in calculated rotaxane/dumbbell **170/171** ratios and stopper conversion, both after two hours reaction duration.

n	K_a [x 10⁵ M⁻¹]	170/171 cond. 1	170/171 cond. 2	170/171 cond. 3	stopper 142 conversion ^{a)}
1 (a)	-	0.02	0.15	0.13	incomplete
2 (b)	-	0.14	0.44	0.19	incomplete
3 (c)	1.67	0.35	2.04	0.31	complete
4 (d)	1.44	0.43	1.40	0.56	complete
5 (e)	1.18	0.33	2.63	0.47	complete

a) As the conversion cannot be quantified in our case, the remarks are based on observations of the total ion current chromatograms.

5.5 Isolation and Characterization of [2]Rotaxane 170d

Based on the results of the screening reactions, the synthesis was scaled up to characterize the interlocked product in order to corroborate its rotaxane nature. Despite the encouraging results obtained with compound **169e**, we chose tetraethylene glycol chains for the axle due to easier purification of **169d** and the corresponding rotaxane as well as the wide and inexpensive availability of the corresponding dialcohol **172d** which is required as starting material for **169d**. The reaction comprises a combination of screening condition 2 and 3. Axle **169d** was reacted with 2.0 eq of stopper **142** and 5.0 eq of cyclophane **81** in presence 1.0 eq of Cu(I)-source and 1.0 eq of THPTA. Furthermore, the concentrations of all reactants were quadruplicated compared to the screening reactions, resulting in an (even) higher rotaxane/dumbbell ratio of 9.24 (Figure 77).

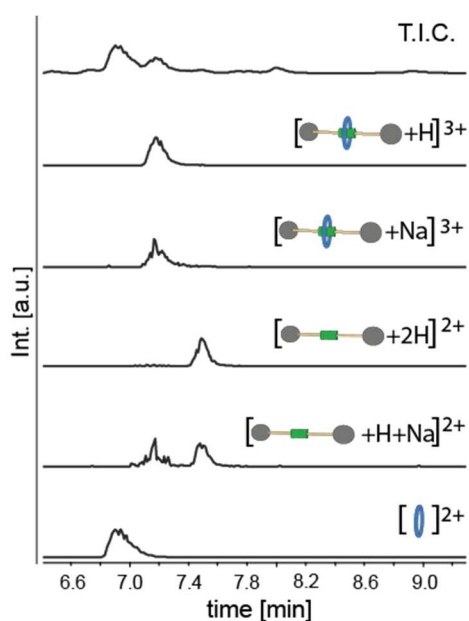


Figure 77. HPLC-ESI-MS measurement of the crude reaction solution of rotaxane synthesis **170d** after 3 hours reaction duration: total ion current trace (a) and extracted ion chromatograms of mainly observed rotaxane (b+c), dumbbell (d+e) and cyclophane (f) adducts (m/z values ± 1).

Rotaxane **170d** was then purified by size exclusion chromatography using Sephadex LH20 beads swelled in methanol. Initial purification attempts applying either normal- or reverse phase silica stationary phases failed. After three size exclusion purification cycles, the uncomplexed dumbbell was completely removed while the eluted product fractions still contained a minor fraction of free cyclophane and a minute amount of an unknown

cyclophane impurity. Further purification by reverse-phase HPLC appeared to be impractical due to the required acid as eluent additive, which leads to ester hydrolysis upon concentration of the product fractions and hence rotaxane decomposition. A yield of 59% for rotaxane **170d** was calculated after subtraction of the 22mol% free cyclophane as determined by ^1H NMR. Interestingly, during the separation of the dumbbell **171d**, its susceptibility to rapid hydrolysis in the absence of an encircling cyclophane became apparent. Even after repeated attempts, the dumbbell could not be isolated in a reasonably pure form.

5.5.1 1D and 2D ^1H NMR Experiments

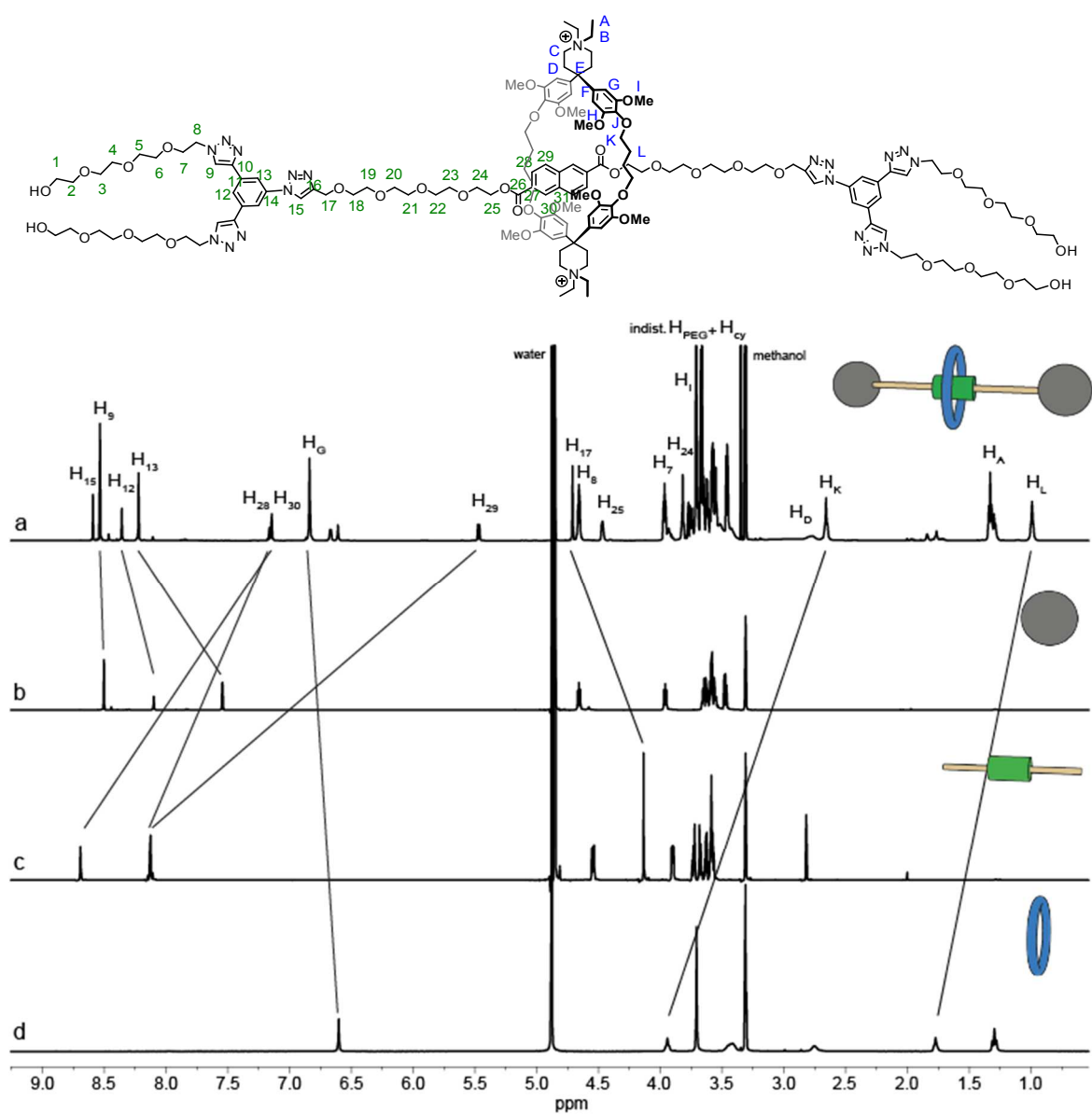


Figure 78. ^1H NMR spectra of rotaxane **170d** (600 MHz, 298 K, methanol- d_4 , (a)), stopper **142** (500 MHz, 298 K, methanol- d_4 , (b)), axle **2d** (500 MHz, 298 K, methanol- d_4 , (c)) and cyclophane **81** (500 MHz, 298 K, methanol- d_4 , (d)).

The rotaxane formation is confirmed by the ^1H NMR spectrum of **170d**, where the effect of the cyclophane on encapsulating the axle becomes clearly visible by comparing the ^1H NMR spectra of the rotaxane **170d** with its starting materials (Figure 78). The strong chemical upfield shift of the naphthalene protons (H_{30} 1.55 ppm; H_{29} 2.65 ppm; H_{28} 0.96 ppm) is induced by their direct orientation into the shielding regions of the cyclophane's diphenylmethane benzene rings.^[122] The chemical shifts of the cyclophane methylene-cavity proton resonances are also significantly moved into the upfield region (H_K 1.28 ppm; H_L 0.79 ppm) compared to the corresponding signals of free cyclophane **81**. Additional evidence for the interlocked structure reveal the distinct NOE crosspeaks (Figure 79) between naphthalene protons with both cyclophane's methylene-cavity and methoxy protons as well as the crosspeaks between the proton of newly formed triazole and the stopper benzene ring.

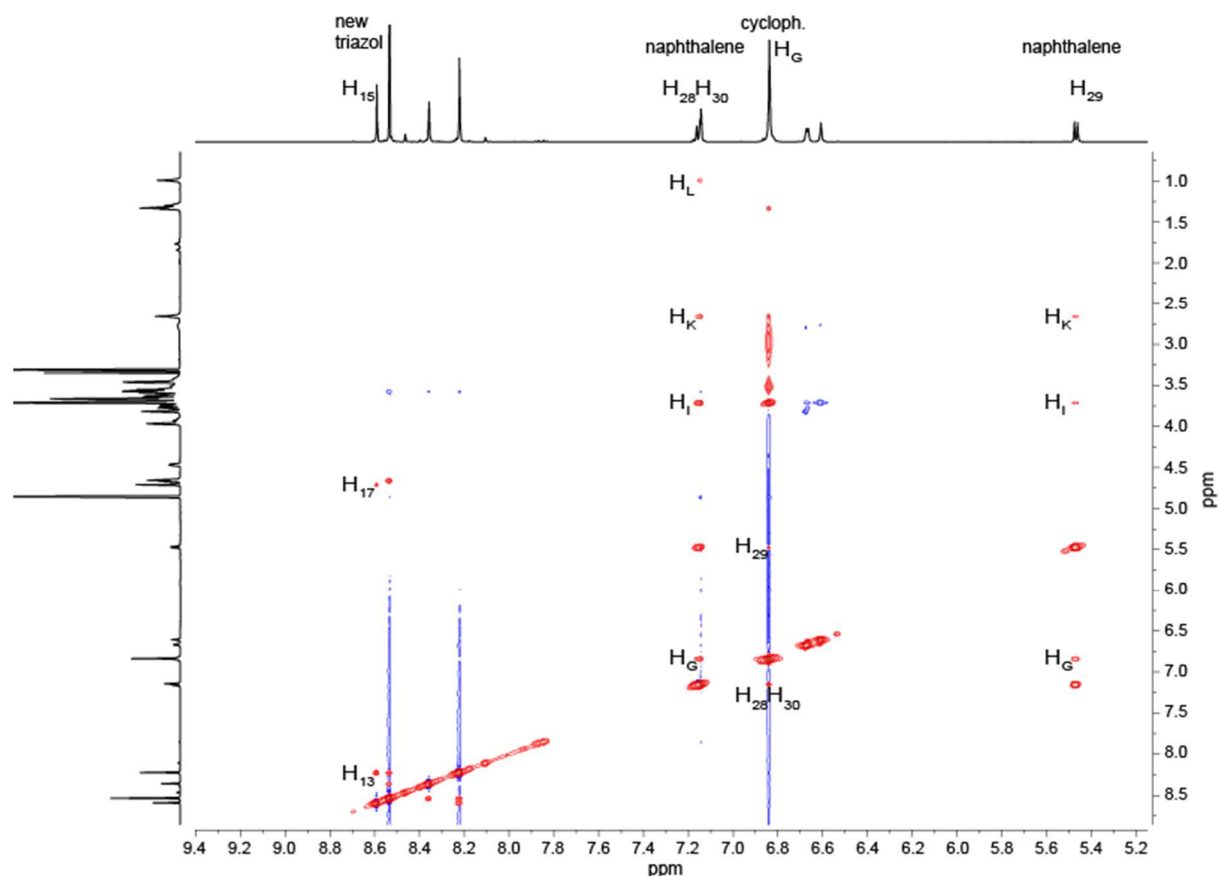


Figure 79. Partial ^1H NOESY spectrum (600 MHz, 298 K, MeOD) of rotaxane **170d** in which the crosspeaks, confirming the formation of the interlocked structure are labeled.

5.5.2 Optical Spectroscopy

Also the optical investigation corroborates the rotaxane formation by displaying a strong fluorescence quenching of the naphthalene emission by the presence of the cyclophane in the rotaxane **170d**. The absorption and emission spectra of rotaxane **170d** and its reactant axle **169d** are displayed in Figure 80. The small bathochromic shift of 4 nm in the UV spectra and the absence of a donor-acceptor absorption band are in accordance to literature for complexes with **81** and naphthalene derivatives.^[171]

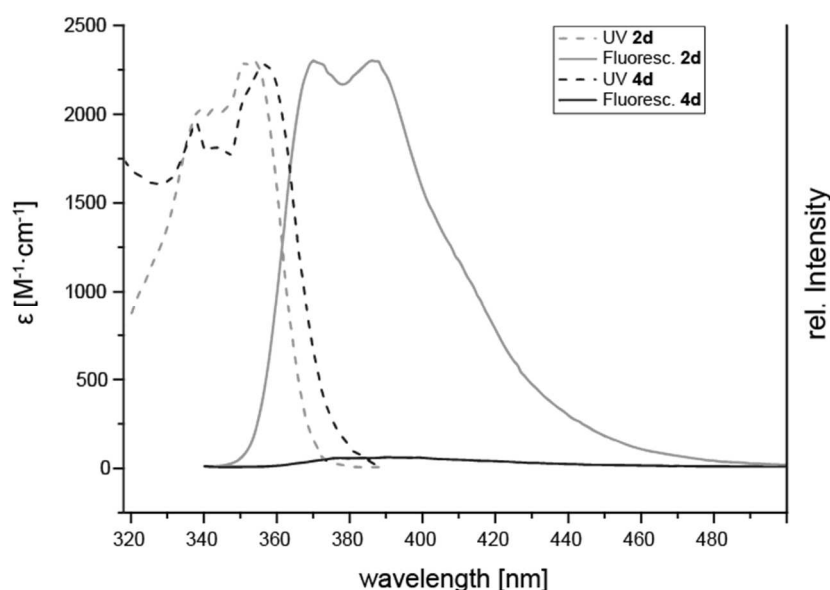


Figure 80: π^* - π transition range of UV/Vis absorption- and emission- (excitation 333 nm) spectra of rotaxane **170d** and axle **169d** in water at 295 K. Both emission spectra were recorded at a concentration of 0.02 mM.

5.6 Stability Test

The thermal stability of rotaxane **170d** was investigated in water with a particular interest to corroborate the stopper character of **142** and examine if **142** is large enough to prevent slipping of cyclophane at elevated temperature. Therefore, a 2.0 mM aqueous solution of rotaxane **170d** was heated at 60 °C for one hour and the temperature was then successively increased every further hour by 10 °C, until 120 °C was reached. A sample was taken after every hour and analyzed via LC-ESI-MS measurements. Until 70 °C neither slippage nor decomposition of the rotaxane was observed. At 80 °C a new signal with low intensity, corresponding to the single hydrolyzed ester, as well as a slight increase of the cyclophane

signal indicated starting of decomposition. Obviously, the chemical stability of the stoppered axle is the thermally most labile component which degrades before the mechanically interlocked supermolecule.

5.7 Conclusion

A series of five 2,6-naphthalenedicarboxylate oligoethylene glycol esters ($n = 1 - 5$) with propargyl termination **169a-e** has been investigated in terms of their efficiency of rotaxane formation from their corresponding inclusion complex with cyclophane **81**. The extent of rotaxane/dumbbell ratio proved to depend on the concentration of supramolecular pseudorotaxane as well as on the length of the ethylene glycol chains, which moves the trapping reaction center away from the complexation site. In view of the relative ease and rapidity with which the potential axle molecules have been investigated, the modular rotaxane synthesis combined with fast analysis revealed to be a convenient strategy which can be applied for testing various axles for rotaxane formation, and thus also for suitability of these subunits for supramolecular systems of increased complexity.

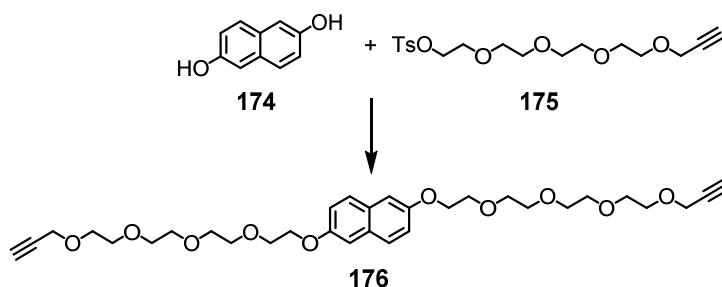
Eventually, the isolation and characterization of a mechanically interlocked molecule, based on a Diederich-type cyclophane and a water-soluble naphthalene guest, could be achieved via CuAAC reaction in water. The interlocked character of the isolated [2]rotaxane could be corroborated by ESI mass spectrometry, as well as ^1H NMR and fluorescence studies.

6 Summary and Outlook

The objective of the thesis was the development of architectures for rotaxane-based mechanically interlocked molecules in water which could pave the way for future applications in functional nanomaterials. Especially molecular [c2]daisy chains are appealing candidates for the implementation in nanomaterials and creation of systems capable of mechanical actuation, such as molecular muscles or potentiometers. The first approach towards daisy chains as functional materials was based on amphiphilic monomers (**91-95**) comprising a Diederich-type cyclophane and an OPE rod. A series of differently functionalized, challenging to synthesize derivatives of the original amphiphile (**91**) was prepared and examined in their aggregation behavior, by means of ^1H NMR dilution studies, diffusion ordered spectroscopy analysis and qualitative fluorescence spectroscopy. In general, a complex aggregation behavior was found, which leaves room to doubt the formation of mechanically linked structures. The attempt to capture daisy chain molecules revealed the absence of interlinked species and rather indicated unthreaded aggregates. Based on these results, the molecular design of components of mechanically interlocked molecules (MIMs) was improved stepwise by analysis of the threading behavior. The first variation was the separation of host and guest moiety of the origin amphiphiles into two individual molecules. A combination of ^1H NMR complexation studies and *click* chemistry based rotaxanation experiments with a water-soluble stopper molecule turned out to be an efficient investigation strategy. Rotaxanes based on OPEs **144** and **146** could be detected, but only in traces which most likely can be ascribed to a low inclusion complexation affinity and poor solubility. Introducing two or four carboxylate units to the OPE backbones increased the solubility, especially in case of four anionic groups (**155**). The threading behavior indeed was found to be strongly dependent on the solubility of the guest molecule in the absence of a host. Furthermore, the 1,4- and 2,6-difunctionalization respectively of a benzene and naphthalene core with tetraethylene glycol chains rendered enough water-solubility for enabling inclusion complexation. The ^1H NMR complexation studies and rotaxanation experiments revealed that the C_4 -bridged octamethoxy-decorated cyclophane (**81**) exhibits a higher binding affinity towards aromatic guests than the smaller and monomethoxy-decorated cyclophane (**109**) and is therefore a more suitable host, which is in accord with the results published by Diederich. The modular rotaxanation strategy was also employed for the screening of a series of synthetically well-

accessible 2,6-functionalized naphthalene guests (**169a-e**), differing in the length of the ethylene glycol substituent and hence water-solubility. The soluble potential rotaxane axles **169c-e** exhibited a rather high binding affinity towards cyclophane **81** with K_a values in the range of 10^5 M^{-1} in water. Applying a semi-quantitative method of analysis based on HPLC-ESI-MS measurements, it was demonstrated that the highest amount of rotaxane was formed with the naphthalene axle exhibiting the highest water-solubility. Finally, based on the optimized host-guest design, a water-soluble [2]rotaxane could be isolated and characterized, corroborating the interlocked nature of the afforded MIM.

Aspiring higher stability of the rotaxane axle and hence facilitating the isolation of pure [2]rotaxane, a new axle molecule **176**, lacking the labile ester moiety of the original component, is currently in preparation. From a synthetic point of view, **176** is potentially well accessible from 2,6-dihydroxy naphthalene (**174**) and propargyltetraethylene glycol tosylate (**175**).



Scheme 48. Synthesis of the new rotaxane axle **176** for the preparation of a stable [2]rotaxane in water.

In close analogy to the OPE rods **155**, **156** and **157** presented in chapter 4, Yves Aeschi enhanced the design of a soluble OPE-rod and could successfully achieve the synthesis of interlocked molecular daisy chains in water (Figure 81). In contrast to the in this work presented approach, the daisy chains were assembled by employing an alkyne-functionalized analogue of azide-functionalized stopper **142** (Figure 82). The required azide group for CuAAC chemistry was attached to the OPE moiety of the amphiphilic daisy chain monomer. Isolation via HPLC and subsequent ^1H NMR analysis revealed the formation of [c2]- and [a2]daisy chains as predominant species besides the stoppered monomer.

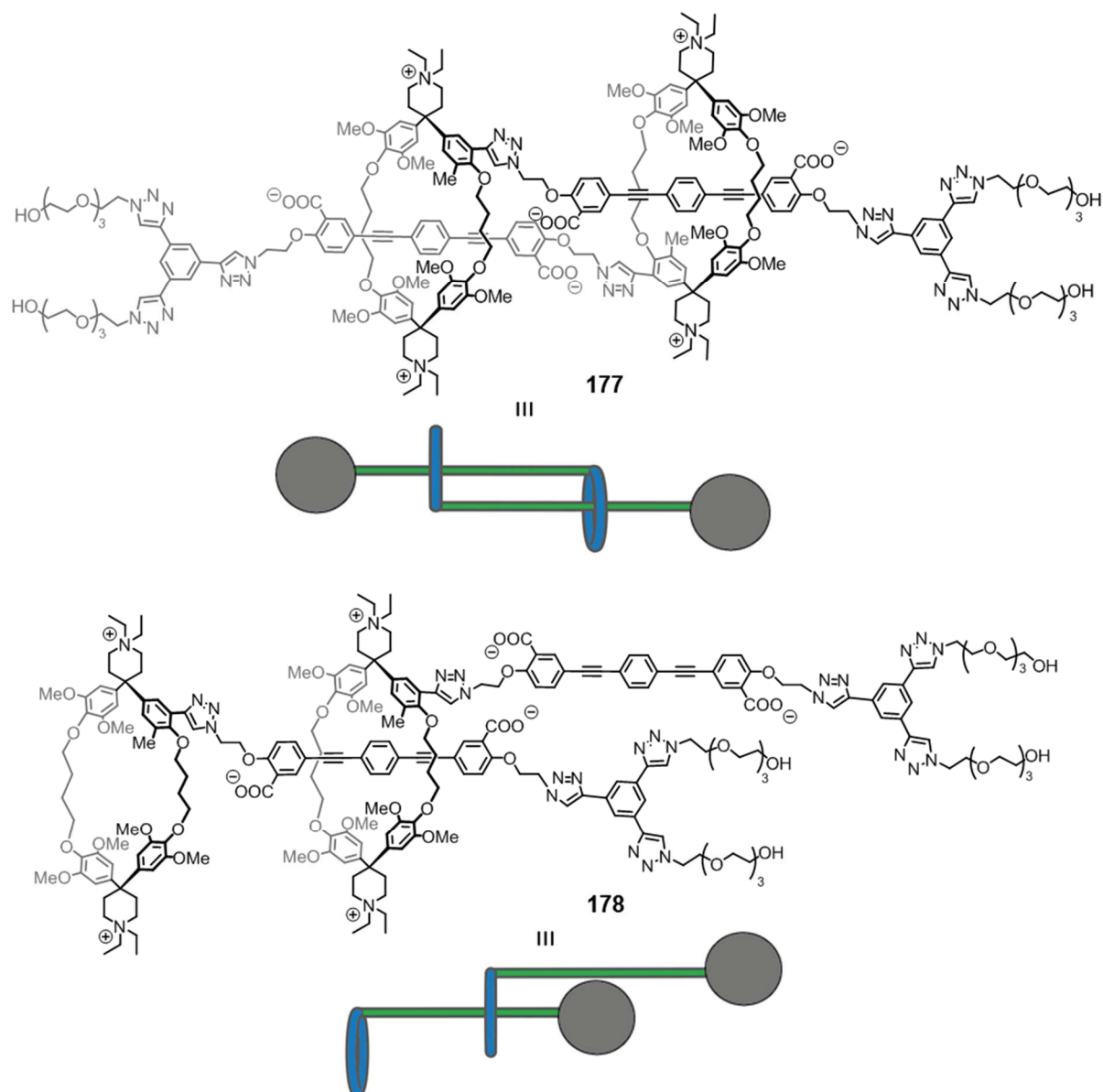


Figure 81. The structure as well as the corresponding cartoon representation of the isolated [c2]- and [a2]daisy chain.

Modifying the water-soluble stopper molecule **179** appears to be a synthetically well feasible approach for the construction of poly[c2]daisy chains and also the realization of a thiol functionalized [c2]daisy chain-based molecular potentiometer. The functionalized stoppers primarily enable the trapping of daisy chains and allow the isolation and characterization of molecular [c2]daisy chains. The interlocked aggregates, comprising a reactive functionality at their two termini, can then be employed for further purposes. Stopper **180** exhibits a second acetylene group, which could be easily cleaved off after the assembly and isolation of [c2]daisy chains. The deprotected acetylene would then render an anchor group for a linker molecule comprising two azide functionalities, connecting the cyclic interlocked structures to a

polymeric chain. With the premise of a stable but also selectively cleavable protecting group (R) for the thiol moiety in **181**, an isolated stoppered [c2]daisy chain could be employed for single molecular conductance measurements.

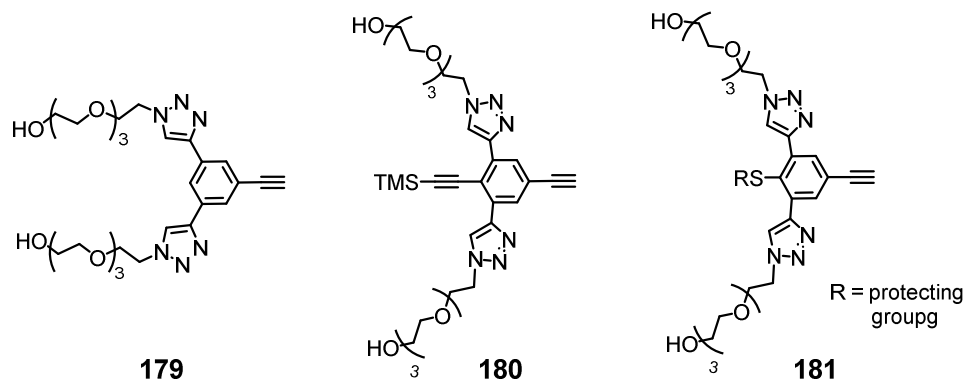


Figure 82. Acetylene-functionalized stopper molecules for the preparation of MIMs in water; **179** was employed for the preparation of interlocked daisy chains **177** and **178**. **180** potentially enables the formation of poly[c2]daisy chains and **181** comprises a thiol anchoring group of a MCBJ setup.

7 Experimental Section

General Remarks

All commercially available compounds were purchased and used as received unless explicitly remarked otherwise. All oxygen- or moisture-sensitive reactions were performed under argon atmosphere.

Chromatographic Purification

For column chromatography either silica gel Siliaflash® p60 (40 – 63 µm) from Silicycle or Alumina from Fluka, activated (basic Brockmann Activity I) neutral was used. Reverse-phase column chromatography was performed with silica gel SiliaBond® C18 R00230B from Silicycle. TLC was performed on silica gel 60 F254 glass plates with a thickness of 0.25 mm purchased from Merck.

Size exclusion chromatography was carried out on Sephadex LH-20, using HPLC grade methanol.

Nuclear Magnetic Resonance

¹H NMR and ¹³C NMR spectra were recorded either on an Oxford 400 MHz NMR equipped with an Avance III 400 spectrometer and with a BBFO⁺ probe head, respectively, on a Bruker UltraShield 500 MHz Avance III equipped with a BBO⁺ probe head with Z-gradients or on a Bruker Ascend 600 MHz Avance III HD equipped with a 1.7 mm TCI cryo probe head. 2D Spectra were either recorded on a Bruker UltraShield 500 MHz Avance III equipped with a BBO⁺ probe head with Z-gradients or on a Bruker Ascend 600 MHz Avance III HD equipped with a 1.7 mm TCI cryo probe head. The chemical shifts are reported in parts per million (ppm) relative to tetramethylsilane or a residual solvent peak and the *J* values are given in Hz. The order of coupling constants was specified by a superscript number (^{*n*}*J*). Deuterated NMR solvents were obtained from *Cambridge Isotope Laboratories, Inc. (Andover, MA, USA)*. All spectra were recorded at 298 K.

Mass Spectrometry

Low-resolution mass spectra were either recorded on a Bruker amaZon™ X for Electro Spray Ionization (ESI) or on a Shimadzu GCMS-QP2010 SE gas chromatography system with a ZB-5HT inferno column (30 m x 0.25 mm x 0.25 mm) at 1 mL/min He-flow rate (split = 20:1) with a Shimadzu electron ionization (EI 70 eV) mass detector. High-resolution mass spectra (HRMS) were measured as HR-ESI-ToF-MS with a Maxis 4G instrument from Bruker.

High-Performance Liquid Chromatography

Analytical and semi-preparative HPLC measurements were performed on a Shimadzu LC-20AT HPLC equipped with a diode array UV/Vis detector (SPD-M10A VP from Shimadzu, $\lambda = 200 - 600$ nm). For analytical HPLC, either a Reprosil, 100 C18, 5 μm , 250 x 4.6 mm; Dr. Maisch GmbH column or in case of HPLC-ESI-MS a Reprospher, 100 C18 Aqua, 5 μm , 125 x 2 mm; Dr. Maisch GmbH column was used. Semi-prep HPLC was performed on a Reprosil, 100 C18, 5 μm , 250 x 16 mm; Dr. Maisch GmbH column. Water filtered over a Millipak^R Express 40 Filter, 0.22 μm from Merck Milipore, subsequently charged with 0.01% vv formic acid and HPLC grade acetonitrile from Avantor also charged with 0.01% vv formic acid were used as HPLC solvents. The HPLC method for subsequent ESI-MS was composed of a solvent gradient starting from 10% vv water, 90% vv acetonitrile and changing to 5% vv water, 95% vv acetonitrile within 10 min at a constant flow rate of 0.5 mL/min.

UV/Vis and Fluorescence Spectroscopy

UV/Vis measurements were performed on a Shimadzu UV spectrometer UV-1800 and fluorescence measurements were recorded on a Horiba FluoroMax-4 spectrofluorometer using 10 x 10 mm 111-QS Hellma cuvettes at room temperature. The extinction coefficient ϵ values were determined based on UV spectra at different concentrations. All solutions were prepared and measured under air saturated conditions.

¹H NMR dilution studies

Stock solution of amphiphiles **92-95** in D₂O/CD₃OD (60/40 v/v) were prepared. These solutions were diluted stepwise and ¹H NMR spectra (500 MHz) of the corresponding samples were recorded. The samples were locked on CD₃OD.

DOSY

Self-diffusion measurements were performed with the bipolar gradient pulse sequence of Wu et al.^[172], by using a Bruker Avance III NMR spectrometer, operating at 600 MHz and equipped with a 5 mm BBFO smart probe with a shielded z-gradient coil and a GAB gradient amplifier.^[133] All samples were dissolved in a mixture of D₂O and CD₃OD (60/40 v/v). The diffusion experiments were performed at 298 K and the temperature was calibrated by using a methanol standard to an accuracy of 0.2 K. The gradient strength was calibrated by using a Shigemitsu tube filled with H₂O to a height of 4.0 mm and imaging this water cylinder.^[173] The resulting gradient calibration was validated by determining the diffusion coefficient of water at 298 K, which reproduced the literature value within 5%. Twelve single diffusion experiments with constant diffusion times (40 ms) and gradient lengths (2.5 ms) were performed, and the gradient strength was varied between 5 and 95% of the maximum strength. The decrease in the intensity of the signal of interest was determined and fitted with the Bruker t1/t2 software package suitable for DOSY experiments, which is included in the instrument software (TOPSPIN 3.0, Bruker Biospin GmbH, Software Dept., Rheinstetten, Germany).

¹H NMR Host-Guest Complexation Studies

A 1.0 mM stock solutions of the relevant guest molecule and also of cyclophanes **109** (3.24 mg in 4.00 mL solvent) and **81** (4.28 mg in 4.00 mL solvent) was prepared in D₂O as well as in D₂O/CD₃OD (60/40 v/v). 0.5 mM solutions of each host and guest were prepared by dilution in both solvent systems and ¹H NMR spectra were recorded. Furthermore, 1:1 mixtures of respective host and guest (*c* = 0.5 mM/0.5 mM) were prepared by mixing 0.3 mL of host stock solution and 0.3 mL of guest stock solution. The mixtures in both solvent systems were measured by ¹H NMR spectroscopy. The change of the observed chemical shift of substrate and also cyclophane was determined by comparing the spectra of the respective host and guest with the spectrum of the 1:1 mixture of host and guest.

Host-Guest Fluorescence Titrations of Naphthalene Ester Axles **169c-e**

Binding studies were performed by adding aliquots of a host **81** solution to the respective naphthalene derivative **169c-e** solution and recording the changes in fluorescence intensity. Therefore, a 66.6 μM stock solution of **169c** was prepared by dissolving 1.00 μmol (0.556 mg) in 15.0 mL water. Naphthalene derivative stock solutions of **169d** and **169e** with a concentration of 0.10 mM were prepared by dissolving 1.00 μmol of **169d** (0.645 mg) and **169e** (0.733 mg), respectively in 10.0 mL water. Each guest stock solution was diluted to the measurement concentration $c = 20.0 \mu\text{M}$ solutions with a starting volume $V = 2.00 \text{ mL}$. To keep the guest concentration constant, the host solution contained the same concentration of guest. To obtain the host solution with a concentration of 400 μM (20 eq) and 20.0 μM of the relevant guest, 1.07 mg of **81** were dissolved in 2.5 mL of a 20.0 μM guest solution. The fluorescence spectra were recorded in a quartz cuvette with the excitation wavelength of 333 nm. Following instrumental parameters were used: excitation slit width 2.00 nm (front entrance and exit); emission slit width 1.00 nm (front entrance and exit); integration time 0.100 s. As for each series the independent variables (total concentration of host $[H]_0$) were identical, the association constants (K_a) were determined from nonlinear regression analysis with concatenate fitting. The applied fit function was derived from an equation described by Thordarson^[174]:

$$F_{obs} = F_0 + \frac{\Delta F}{2[G]_0} \left([H]_0 + [G]_0 + \frac{1}{K_a} - \sqrt{\left([H]_0 + [G]_0 + \frac{1}{K_a} \right)^2 - 4[H]_0[G]_0} \right)$$

F_{obs} the observed fluorescence; $F_{obs} \hat{=} y$; dependent variable

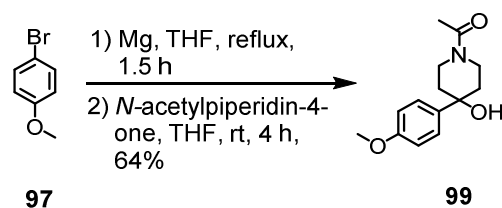
F_0 fluorescence of guest solution before the guest is added; constant

ΔF maximal fluorescence quench, here $\Delta F \hat{=} F_0$, negative value; parameter

$[G]_0$ total concentration of the guest; constant

$[H]_0$ total concentration of the host; $[H]_0 \hat{=} x$; independent variable

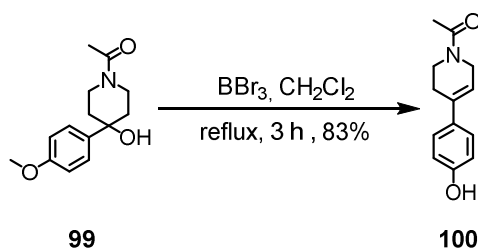
K_a association constant; parameter

1-(4-Hydroxy-4-(4-methoxyphenyl)piperidin-1-yl)ethanone (99)

In an oven-dried 500 mL two-neck flask magnesium turnings (1.89 g, 77.9 mmol, 0.920 eq) were stirred neat for 10 min under argon-atmosphere. After addition of dry THF (15 mL), 4-bromoanisole (**97**, 16.0 g, 84.7 mmol, 10.7 mL, 1.00 eq) was added dropwise via a dropping funnel until the reaction started. The remaining 4-bromoanisole in the dropping funnel was then diluted with dry THF (60 mL) and the solution was added dropwise by keeping the reaction mixture under a continuous reflux. After stirring for 1.5 hrs at reflux, the Grignard solution was cooled to 0 °C and while vigorously stirred, a solution of N-acetyl-4-piperidone (10.2 g, 70.0 mmol, 8.94 mL, 0.826 eq) in dry THF (65 mL) was added dropwise. After stirring the resulting milky suspension for 4 hrs at room temperature the reaction mixture was carefully quenched with sat. ammonium chloride solution (100 mL) and the mixture was stirred for 17 hrs at room temperature. THF was removed *in vacuo* and the remaining pale yellow oil was suspended in water and extracted with dichloromethane. The combined organic layers were dried over sodium sulfate, filtered and concentrated under reduced pressure. The resulting residue was washed with plenty of diethyl ether to afford alcohol **99** (11.2 g, 64%) as a colorless solid.

¹H NMR (400 MHz, CDCl₃): δ = 7.38 (d, ³J(H,H) = 8.8 Hz, 2H, *H_{ar}*), 6.90 (d, ³J(H,H) = 8.8 Hz, 2H, *H_{ar}*), 4.57 – 4.52(m, 1H), 3.81 (s, 3H, OCH₃), 3.72 – 3.67 (m, 1H), 3.63-3.55 (m, 1H), 3.10 (td, ³J(H,H) = 12.9, ²J(H,H) = 3.0 Hz, 1H, *H_{piperidine}*), 2.13 (s, 3H, C=OCH₃), 2.04 – 1.89 (m, 2H), 1.96 (s, 1H, OH), 1.85-1.75 (m, 2H) ppm; **¹³C-NMR (101 MHz, CDCl₃):** δ = 169.0 (C_q, 1C, C=O), 158.9 (C_q, 1C, C_{ar}OCH₃), 139.9 (C_q, 1C, C_{ar}), 125.8 (C_t, 2C, C_{ar}), 113.9 (C_t, 2C, C_{ar}), 71.2 (C_q, 1C, COH), 55.4 (C_p, 1C, OCH₃), 42.9 (C_s, 1C), 39.1 (C_s, 1C), 38.0 (C_s, 1C), 37.9 (C_s, 1C), 21.6 (C_p, 1C, COCH₃) ppm; **GC-MS (EI +, 70 eV):** m/z (%) = 56 (23), 57 (20), 72 (15), 77 (15), 87 (19), 114 (19), 135 (100), 206 (40), 231 (19), 249 (19) [M]⁺.

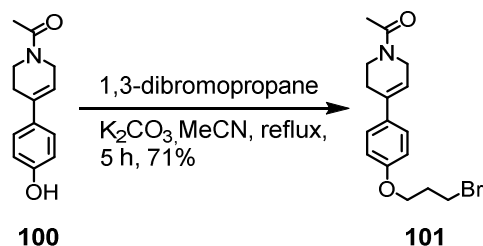
The spectroscopic data are in agreement with those previously reported.^[133]

1-(4-(4-Hydroxyphenyl)-5,6-dihydropyridin-1(2H)-yl)ethanone (100)

1-(4-hydroxy-4-(4-methoxyphenyl)piperidin-1-yl)ethan-1-one (**99**, 6.34 g, 27.4 mmol, 1.00 eq) was dissolved in dry dichloromethane (200 mL) under argon atmosphere. Boron tribromide solution (1.0 M in dichloromethane, 101 g, 68.6 mmol, 1.00 eq) was added dropwise and the resulting brown reaction-mixture was heated to reflux for three hrs. After cooling to 0 °C, the reaction mixture was carefully quenched with methanol (100 mL). The solvents were evaporated under reduced pressure and the resulting residue was washed with demin. water and a small amount of diethylether (product is soluble in diethylether) affording alkene **100** (4.95 g) in 83% yield.

¹H NMR (400 MHz, MeOD): δ = 6.80 – 6.73 (m, 2H, *H_{ar}*), 6.29 – 6.26 (m, 2H, *H_{ar}*), 5.50 – 5.48 (m, 1H, C=CHCH₂), 3.71 – 3.68 (m, 2H), 3.30, 3.24 (2t, ³*J_(H,H)* = 6.7 Hz, 2H), 2.12 – 2.00 (2m, 2H), 1.70, 1.66 (2s, 3H, C=OCH₃) ppm; **¹³C NMR (101 MHz, CDCl₃):** δ = 171.9 (C_q, 1C, C=O), 158.1 (C_q, 1C, C_{ar}), 136.4 (C_q, 1C, C_{ar}), 133.0 (C_q, 1C, C=CCH₂), 127.2, 127.1 (C_t, 2C, CH_{ar}), 118.8, 118.2 (C_t, 1C, C=CCH₂), 116.1 (C_t, 2C, CH_{ar}), 46.9, 44.7 (C_s, 1C), 39.8 (C_s, 1C), 28.1 (C_s, 1C), 21.2 (C_s, 1C, C=OCH₃) ppm; **GC-MS (EI +, 70 eV):** *m/z* (%) = 78 (15), 89(16), 92(20), 108(23), 115(23), 118(23), 131(30), 140(20), 146(45), 158(25), 174(70), 175(27), 217(100) [M]⁺.

The spectroscopic data are in agreement with those previously reported.^[133]

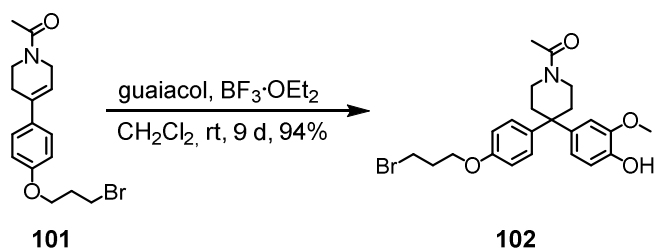
1-(4-(4-(3-Bromopropoxy)phenyl)-5,6-dihydropyridin-1(2H)-yl)ethanone (101)

Alkene **100** (7.29 g, 33.6 mmol, 1.00 eq) was suspended in dry MeCN (220 mL). 1,3-dibromopropane (69.2 g, 336 mmol, 35 mL, 10.0 eq) and potassium carbonate (23.5 g, 168 mmol, 5.01 eq) were added and the resulting reaction mixture heated to reflux for five hrs. The precipitate was filtered off and washed with plenty of diethyl ether. The filtrate was concentrated and the crude product was purified by column chromatography (SiO₂; dichloromethane, 5% MeOH) yielding **101** (8.10 g, 71%) as a colorless solid.

¹H NMR (400 MHz, CDCl₃): δ = 7.32 – 7.28 (m, 2H, *H*_{ar}), 6.89 – 6.86 (m, 2H, *H*_{ar}), 6.00 – 5.91 (2m, 1H, CCHCH₂), 4.23 – 4.21 (m, 1H), 4.12 – 4.09 (m, 3H), 3.82 – 3.79 (m, 1H), 3.67 – 3.64 (m, 1H), 3.61 (t, ³*J*_(H,H) = 5.3 Hz, 2H, CH₂CH₂Br), 2.57 – 2.49 (m, 2H), 2.32 (quint, ³*J*_(H,H) = 4.8 Hz, 2H, CH₂CH₂CH₂), 2.16, 2.14 (2s, 3H, C=OCH₃) ppm; **¹³C NMR (101 MHz, CDCl₃):** δ = 169.3 (C_q, 1C, C=O), 158.4 (C_q, 1C, C_{ar}), 136.2, 134.4 (C_q, 1C), 133.3 (C_q, 1C), 126.2 (C_t, 2C, CH_{ar}), 117.9 (C_t, 1C, C=CHCH₂), 114.6 (C_t, 2C, CH_{ar}), 65.5 (C_s, 1C, OCH₂CH₂), 45.9, 43.5 (C_s, 1C), 42.3, 38.4 (C_s, 1C), 32.5 (C_s, 1C, CH₂CH₂CH₂), 30.1 (C_s, 1C, CH₂CH₂Br), 28.1, 27.3 (C_s, 1C), 22.0, 21.6 (C_p, 1C, C=OCH₃) ppm; **GC-MS (EI +, 70 eV):** *m/z* (%) = 87 (23), 91 (26), 115 (37), 131 (26), 145 (42), 146 (42), 158 (65), 174 (63), 200 (33), 294 (50), 296 (40), 337 (100) [M]⁺, 339 (95) [M]⁺.

The spectroscopic data are in agreement with those previously reported.^[133]

**1-(4-(4-(3-Bromopropoxy)phenyl)-4-(4-hydroxy-3-methoxyphenyl)piperidin-1-yl)ethanone
(102)**



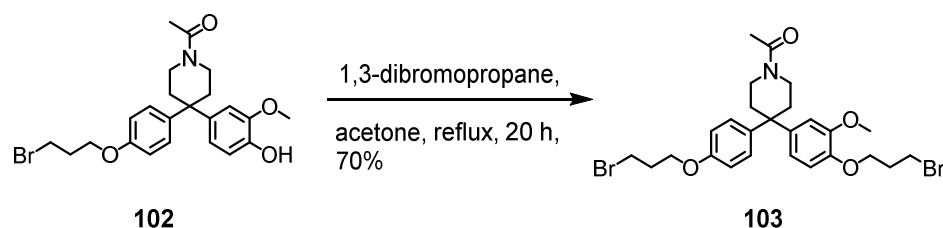
In an oven-dried Schlenk tube alkene **101** (10.8 g, 31.9 mmol, 1.00 eq) was dissolved in dry dichloromethane (50 mL). Boron trifluoride diethyl etherate (32.4 g, 224 mmol, 29.0 mL, 7.02 eq) was added dropwise and caused an immediate color change of the reaction mixture from pale yellow to red-brown. After stirring the mixture for 9 days at room temperature, the solution was cooled to 0 °C and was carefully quenched with methanol (5 mL). The mixture was then poured into demin. water (40 mL) and was three times extracted with ethyl acetate. The combined organic layers were dried over sodium sulfate, filtered and concentrated under reduced pressure. The resulting red oil was purified by column chromatography (SiO₂; dichloromethane, 5% MeOH) to afford compound **102** (13.8 g, 94%) as a colorless solid.

¹H NMR (400 MHz, CDCl₃): δ = 7.14 (d, ³J_(H,H) = 8 Hz, 2H), 6.85 – 6.86 (m, 3H), 6.73 (dd, ³J_(H,H) = 8 Hz, ⁴J_(H,H) = 2 Hz, 1H, H6 (4-hydroxy-3-methoxyphenyl)), 6.66 (d, ⁴J_(H,H) = 2 Hz, 1H, H2(4-hydroxy-3-methoxyphenyl)), 5.50 (s, 1H, OH), 4.07 (t, ³J_(H,H) = 6 Hz, 2H, OCH₂CH₃), 3.81 (s, 3H, OCH₃), 3.69 – 3.58 (m, 4H), 3.51 – 3.47 (m, 2H), 2.35 – 2.25 (m, 6H), 2.09 (s, 3H, C=OCH₃) ppm;

¹³C NMR (101 MHz, CDCl₃): δ = 169.0 (C_q, 1C, C=O), 157.0 (C_q, 1C, C4(bromopropoxyphenyl)), 146.7 (C_q, 1C), 144.0 (C_q, 1C), 138.9 (C_q, 1C), 138.8 (C_q, 1C), 128.1 (C_t, 2C), 119.8 (C_t, 1C), 114.6 (C_t, 2C), 114.6 (C_t, 1C), 109.8 (C_t, 1C), 65.3 (C_s, 1C, OCH₂CH₂), 56.0 (C_p, 1C), 44.4 (C_s, 1C), 43.8 (C_q, 1C), 38.8 (C_s, 1C), 37.3 (C_s, 1C), 36.3 (C_s, 1C), 32.5 (C_s, 1C), 30.2 (C_s, 1C), 21.6 (C_p, 1C, C=OCH₃) ppm.

The spectroscopic data are in agreement with those previously reported.^[133]

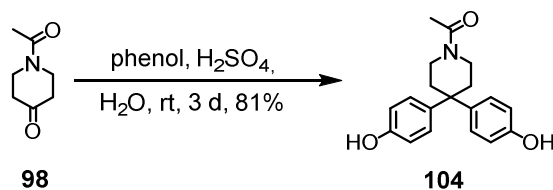
1-(4-(4-(3-Bromopropoxy)-3-methoxyphenyl)-4-(4-(3-bromopropoxy)phenyl)piperidin-1-yl)ethanone (103)



Phenol **102** (9.99 g, 21.6 mmol, 1.00 eq) was dissolved in acetone (120 mL) under argon atmosphere in an oven-dried flask. 1,3-dibromopropane (22.2 g, 108 mmol, 11.2 mL, 5.00 eq) and potassium carbonate (9.06 g, 64.9 mmol, 3.00 eq) were consecutively added and the resulting reaction mixture was heated at reflux for 20 hrs. After cooling to room temperature, the suspension was filtered and the solid was washed several times with acetone. The filtrate was concentrated and the residue purified by column chromatography (SiO₂; dichloromethane, 5% MeOH). Subsequent purification by HPLC using a 22.5 min gradient starting from 50/50 (v/v) H₂O/MeCN and finishing at 5% H₂O/ 95% MeCN afforded compound **103** (8.85 g) in 70% yield.

¹H NMR (400 MHz, CDCl₃): δ = 7.14 (d, ³J_(H,H) = 8 Hz, 2H), 6.86 – 6.79 (m, 3H), 6.77 – 6.74 (m, 1H, H₆(4-hydroxy-3-methoxyphenyl)), 6.71 (d, ⁴J_(H,H) = 2 Hz, 1H, H₂(4-hydroxy-3-methoxyphenyl)), 4.13 – 4.06 (m, 4H, OCH₂CH₂), 3.82 – 3.76 (m, 3H, -OCH₃), 3.63 – 3.48 (m, 8H), 2.37 – 2.27 (m, 8H), 2.09 (s, 3H, C=OCH₃) ppm; ¹³C NMR (101 MHz, CDCl₃): δ = 168.9 (C_q, 1C, C=O), 156.9 (C_q, 1C, C₄(bromopropoxyphenyl)), 149.5 (C_q, 1C), 146.5 (C_q, 1C), 140.0 (C_q, 1C), 138.6 (C_q, 1C), 128.0 (C_t, 2C), 119.2 (C_t, 1C), 114.5 (C_t, 2C), 113.3 (C_t, 1C), 111.4 (C_t, 1C), 66.6 (C_s, 1C, OCH₂CH₂), 65.2 (C_s, 1C, OCH₂CH₂), 56.2 (C_p, 1C), 44.2 (C_s, 1C), 43.7 (C_q, 1C), 38.7 (C_s, 1C), 37.0 (C_s, 1C), 36.1 (C_s, 1C), 32.4 (C_s, 1C), 30.3 (C_s, 1C), 30.1 (C_s, 1C), 21.5 (C_p, 1C, C=OCH₃) ppm.

The spectroscopic data are in agreement with those previously reported.^[133]

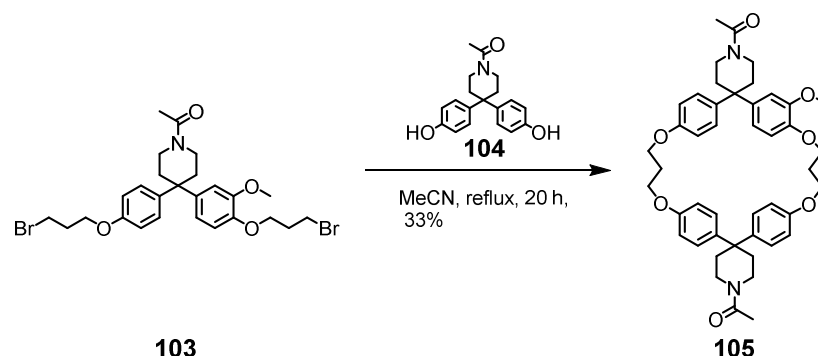
1-(4,4-Bis(4-hydroxyphenyl)piperidin-1-yl)ethanone (104)

To a solution of phenol (17.0 g, 181 mmol, 2.06 eq) in demin. water (7.3 mL) *N*-acetyl-4-piperidone (**98**, 12.5 g, 87.7 mmol, 11.0 mL, 1.00 eq) was added. Afterwards, the solution was cooled to 0 °C and conc. sulfuric acid (32.5 g, 325 mmol, 17.7 mL, 3.71 eq) was added. The yellow, highly viscous reaction mixture was left standing at room temperature for three d. The reaction mixture was then dissolved in a mixture of acetone/methanol (7:3; 180 mL) and the resulting solution was neutralized by addition of sodium carbonate solution (1.0 N; 304 mL). Demin water (190 mL) was added to a total volume of 720 mL and the mixture was cooled at 0 °C for one h until precipitation was completed. The precipitate was filtered and washed with plenty of demin. water. The solid was recrystallized from ethanol to afford **104** as colorless solid (22.0 g, 81%).

¹H NMR (400 MHz, DMSO-*d*₆): δ = 9.18 (s, 2H, OH), 7.06 (d, $^3J_{(H,H)}$ = 8.7 Hz, 4H, *H*_{ar}), 6.65 (d, $^3J_{(H,H)}$ = 8.6 Hz, 4H, *H*_{ar}), 3.41 – 3.34 (m, 4H, *H*_{piperidine}), 2.27 – 2.25 (m, 2H, *H*_{piperidine}), 2.18 – 2.15 (m, 2H, *H*_{piperidine}), 1.97 (s, 3H, C=OCH₃) ppm, **¹³C NMR (101 MHz, DMSO-*d*₆):** δ = 168.0 (C_q, 1C), 155.0 (C_q, 2C), 137.4 (C_q, 2C), 127.6 (C_t, 4C), 115.0 (C_t, 4C), 43.0 (C_s, 1C), 38.1 (C_s, 1C), 42.9 (C_s, 1C), 38.1 (C_s, 1C), 36.0 (C_s, 1C), 35.4 (C_s, 1C), 21.3 (C_p, 1C) ppm.

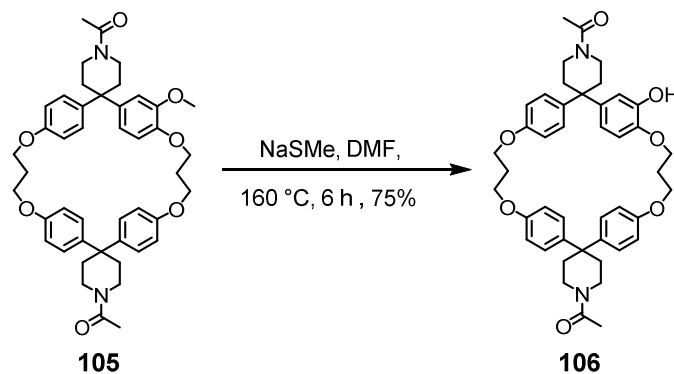
The spectroscopic data are in agreement with those previously reported.^[133]

1,1''-Diacteyl-5'-methoxy-dispiro[piperidine-4,2'-[7,11,21,25]-tetraoxacyclopenta-[24.2.2.2^{3,6}.2^{12,15}.2^{17,20}]hexatriaconta[3,5,12,14,17,19,26,28,29,31,33,35]dodecaene-16,4''-piperidine] (105)



A mixture of cesium carbonate (11.3 g, 34.3 mmol, 10.0 eq), bisphenol **104** (1.07 g, 3.43 mmol, 1.00 eq) and dialkyl bromide **103** (2.00 g, 3.43 mmol, 1.00 eq) were suspended in acetonitrile (1.20 L) and heated to reflux for 20 hrs. After allowing the mixture to cool down to room temperature, the precipitate was filtered off and the filtrate was concentrated. The residue was taken up in dichloromethane and the insoluble white solid was filtered off again. The filtrate was concentrated and the remaining crude was purified by column chromatography (SiO₂; dichloromethane, 5% MeOH). The colorless solid product was precipitated with ethanol, filtered and washed with some ethanol and a small amount of diethylether to afford cyclophane **105** (829 mg, 33%).

¹H NMR (400 MHz, CDCl₃): δ = 7.14 – 7.10 (m, 6H, *H_{ar}*), 6.74 – 6.68 (m, 8H, *H_{ar}*), 6.61 – 6.60 (m, 1H, *H_{ar}*), 4.04 – 4.03 (m, 8H), 3.82 – 3.77 (m, 1H), 3.63 – 3.53 (m, 5H, including OCH₃), 2.39 – 2.36 (m, 8H), 2.20 – 2.15 (m, 4H), 2.07 (ds, 6H, C=OCH₃) ppm; ¹³C NMR (101 MHz, CDCl₃): δ = 168.9 (C_q, 2C, C=O), 157.2 (C_q, 1C), 157.1 (C_q, 1C), 157.1 (C_q, 1C), 149.3 (C_q, 1C), 146.9 (C_q, 1C), 139.9 (C_q, 1C), 138.8 (C_q, 1C), 138.6 (C_q, 1C), 127.1 (C_t, 2C), 126.8 (C_t, 4C), 117.9 (C_t, 1C), 115.0 (C_t, 2C), 114.7 (C_t, 2C), 114.7 (C_t, 2C), 113.0 (C_t, 1C), 110.2 (C_t, 1C), 64.6 (C_s, 1C), 63.5 (C_s, 1C), 63.3 (C_s, 1C), 63.3 (C_s, 1C), 55.9 (C_p, 1C, OCH₃), 43.6 (C_q, 1C), 43.5 (C_s, 2C), 43.0 (C_q, 1C), 38.6 (C_s, 1C), 38.5 (C_s, 1C), 35.7 (C_s, 1C), 35.0 (C_s, 1C), 29.5 (C_s, 1C), 21.5 (C_p, 2C, C=OCH₃) ppm. The spectroscopic data are in agreement with those previously reported.^[133]

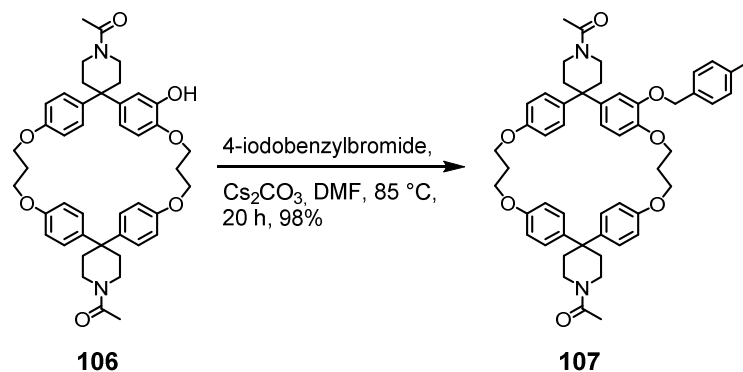
1,1''-Diacteyl-5'-hydroxy-dispiro[piperidine-4,2'-[7,11,21,25]-tetraoxacyclopenta[24.2.2.-2^{3,6}.2^{12,15}.2^{17,20}]hexatriaconta[3,5,12,14,17,19,26,28,29,31,33,35]dodecaene-16,4''-piperidine] (106)

Cyclophane **105** (500 mg, 0.682 mmol, 1.00 eq) and sodium thiomethoxide (266 mg, 3.41 mmol, 5.00 eq) were dissolved in dry DMF (60 mL) and stirred at 160 °C for five hrs. Afterwards, aq. hydrochloric acid (1 M, 35 mL) was added and the solvents were removed *in vacuo*. The remaining pale beige solid was washed once with diethylether. The crude solid was then purified by column chromatography (SiO₂; dichloromethane, 5% MeOH) (286 mg, 75%).

¹H NMR (400 MHz, CDCl₃): δ = 7.15 – 7.03 (m, 6H, *H_{ar}*), 6.77 – 6.61 (m, 9H, *H_{ar}*), 5.56 (s, 1H, OH), 4.10 (t, ³*J_{H,H}* = 5.1 Hz, 2H, phenol-O-CH₂), 4.01 (t, ³*J_{H,H}* = 5.2 Hz, 6H, OCH₂), 3.67 – 3.60 (m, 4H), 3.50 – 3.46 (m, 4H), 2.41 – 2.31 (m, 8H), 2.25 – 2.09 (m, 4H), 2.07 (s, 3H, C=OCH₃), 2.06 (s, 3H, C=OCH₃) ppm.

The spectroscopic data are in agreement with those previously reported.^[133]

1,1''-Diacteyl-5'-(1-iodo-4-phenoxyethylbenzene)-dispiro[piperidine-4,2'-[7,11,21,25]-tetraoxacyclopenta[24.2.2.2^{3,6}.2^{12,15}.2^{17,20}]hexatriaconta[3,5,12,14,17,19,26,28,29,31,33,-35]dodecaene-16,4''-piperidine] (107)

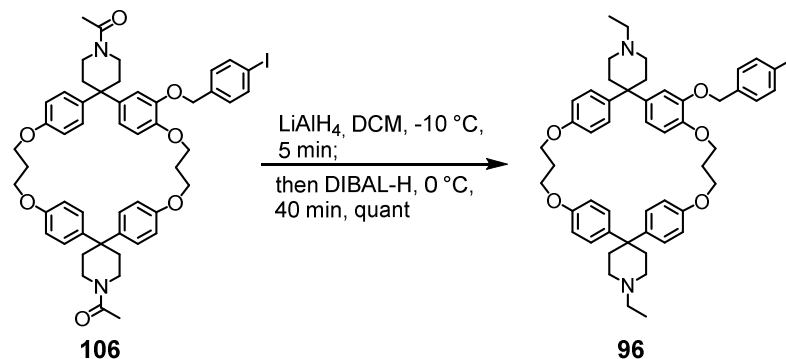


A mixture of cyclophane **106** (263 mg, 0.366 mmol, 1.00 eq), 4-iodobenzyl bromide (172 mg, 0.549 mmol, 1.50 eq) and cesium carbonate (241 mg, 0.732 mmol, 2.00 eq) were suspended in dry DMF (20 mL) under argon atmosphere. The reaction mixture was stirred at 85 °C for 20 hrs. Afterwards, the solvent was evaporated by vacuum distillation and the residue was then taken up in dichloromethane and demin. water. The layers were separated and the aqueous one was extracted three times with dichloromethane. The combined organic layers were washed with demin. water and brine, dried over sodium sulfate, filtered and concentrated under reduced pressure. The crude was purified by column chromatography (SiO₂; dichloromethane, 5% MeOH) yielding solid compound **107** (340 mg, 98%).

¹H NMR (400 MHz, CDCl₃): δ = 7.66 – 7.61 (m, 2H, *H_{ar}*), 7.11 – 7.06 (m, 4H, *H_{ar}*), 7.00 – 6.95 (m, 2H, *H_{ar}*), 6.95 – 6.90 (m, 2H, *H_{ar}*), 6.75 – 6.67 (m, 8H, *H_{ar}*), 6.45 (d, ³*J_{H,H}* = 2.0 Hz, 1H, *H_{ar}*), 4.73 (s, 2H, CH₂O), 4.08 – 4.01 (m, 8H, C_qOCH₂), 3.73 – 3.60 (m, 3H), 3.51 – 3.37 (m, 5H), 2.37 (dt, ³*J_{H,H}* = 12.2, 5.4 Hz, 4H), 2.30 – 2.13 (m, 8H), 2.06 (ds, 6H, CH₂CH₃) ppm.

The spectroscopic data are in agreement with those previously reported.^[133]

1,1''-Diethyl-5'-(1-iodo-4-phenoxyethylbenzene)-dispiro[piperidine-4,2'-[7,11,21,25]-tetraoxacyclopenta[24.2.2.2^{3,6}.2^{12,15}.2^{17,20}]hexatriaconta[3,5,12,14,17,19,26,28,29,31,33,-35]dodecaene-16,4''-piperidine] (96)

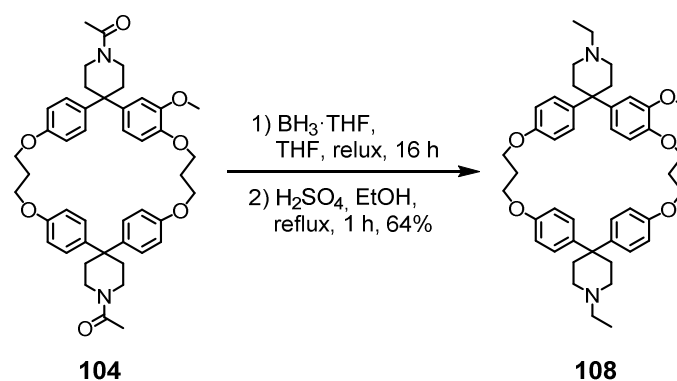


Cyclophane **96** was synthesized according to a slightly modified literature-known procedure^[133]: In an oven-dried Schlenk tube **106** (100 mg, 0.107 mmol, 1.00 eq) was suspended in dry dichloromethane (5 mL). After cooling to $-10\text{ }^\circ\text{C}$, lithium aluminium hydride in THF (1 M, 0.428 mL, 0.428 mmol, 4.00 eq) was added slowly. After 5 minutes of stirring, diisobutyl aluminium hydride in hexane (1 M, 165 mg, 0.235 mmol, 0.235 mL, 2.20 eq) in hexanes was added dropwise over the course of one min stirring for 40 min at $0\text{ }^\circ\text{C}$. The reaction was quenched by addition of sat. aq. sodium hydrogen carbonate solution (2 mL). Insoluble aluminium salts were filtered off and the aqueous phase was extracted with dichloromethane three times. The combined organic layers were dried over sodium sulfate, filtered and concentrated under reduced pressure. Purification by column chromatography (SiO_2 ; ethyl acetate, 1% MeOH, 5% NEt_3) afforded cyclophane **96** (97.0 mg, quant.) as a colorless solid. Regioisomers of **96** caused by the regioisomer formation in the synthesis of **102** were separated by semi-preparative HPLC with a Reprosil 100 Si, $5\text{ }\mu\text{m}$, $250 \times 4.6\text{ mm}$ column (ethyl acetate, 2% MeOH, 0.5% NEt_3 , isocratic flow). The predominant and also desired isomer was eluted at a retention time of 45 min (77%).

$^1\text{H NMR}$ (400 MHz, CDCl_3): $\delta = 7.66 - 7.60$ (m, 2H, H_{ar}), $7.14 - 7.05$ (m, 4H, H_{ar}), $7.02 - 6.90$ (m, 4H, H_{ar}), $6.77 - 6.63$ (m, 8H, H_{ar}), 6.49 (s, 1H, H_{ar}), 4.73 (s, 2H, CH_2O), $4.09 - 3.99$ (m, 8H, C_qOCH_2), $2.62 - 2.23$ (m, 8H, NCH_2CH_2 , 8H, NCH_2CH_2 ; 4H, NCH_2CH_3), $2.23 - 2.10$ (m, 4H, OCH_2CH_2), 1.04 (td, $J = 7.2, 3.7\text{ Hz}$, 7H) ppm; **$^{13}\text{C NMR}$ (101 MHz, CDCl_3):** $\delta = 156.9$ (C_q , 1C, COCH_2CH_2), 156.8 (C_q , 1C, COCH_2CH_2), 156.8 (C_q , 1C, COCH_2CH_2), 147.6 (C_q , 1C, $\text{CHCOCH}_2\text{CCH}$), 147.2 (C_q , 1C, COCH_2CH_2), 137.6 (C_q , 1C, C_qC_q , piperid), 137.5 (C_t , 2C, CHC_qI ; C_q , 3C, C_qC_q , piperid),

129.1 (C_t, 2C, CHCHC_ql), 127.4 (C_t, 2C, CHC_qC_q,piperid), 127.1 (C_t, 4C, CHC_q C_q,piperid), 114.5 (C_t, 3C, OC_qCHCHC_q C_q,piperid), 114.5(C_t, 2C, OC_qCHCHC_qC_q,piperid), 114.4 (C_t, 2C, OC_qCHCHC_q C_q,piperid), 93.0 (C_q, 1C, C_ql), 70.4 (C_s, 1C, CH₂,benzyl), 64.8 (C_s, 1C, OCH₂CH₂), 63.4 (C_s, 1C, OCH₂CH₂), 63.3 (C_s, 1C, OCH₂CH₂), 63.3 (C_s, 1C, OCH₂CH₂), 52.5 (C_s, 2C, NCH₂CH₃), 50.2 (C_s, 4C, NCH₂CH₂), (C_q, 1C, C_q,spiro), 42.8 (C_q, 1C, C_q,spiro), 35.5 (C_s, 2C, NCH₂CH₂), 35.3 (C_s, 2C, NCH₂CH₂), 29.8 (C_s, 1C, OCH₂CH₂), 29.7 (C_s, 1C, OCH₂CH₂), 12.3 (C_p, 2C, NCH₂CH₃) ppm. Two signals two tertiary C-atoms at the threefold substituted benzene ring (C_qCHCHC_qO, expected at approx. 119.2 ppm and C_qCHCHC_qO, expected at approx. 113.8 ppm) were not observed.

1,1''-Diethyl-5'-methoxy-dispiro[piperidine-4,2'-[7,11,21,25]-tetraoxacyclopenta-[24.2.2.^{23,6}.2^{17,20}]hexatriaconta[3,5,12,14,17,19,26,28,29,31,33,35]dodecane-16,4''-piperidine] (108)

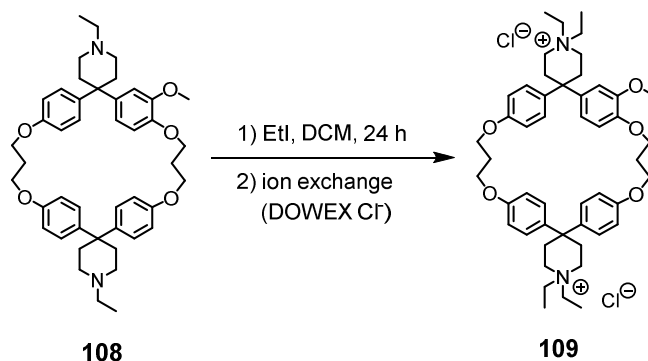


The hydroxyl decorated cyclophane **108** was synthesized according to a procedure reported in literature.^[128] To a solution of cyclophane **105** (50.0 mg, 0.0682 mmol, 1.00 eq) in 3.5 mL THF borane-tetrahydrofuran complex (1.02 mL (1 M in THF), 911 mg, 1.02 mmol, 15.0 eq) was added under argon atmosphere. After heating the mixture at reflux for 16 hrs, excess borane was quenched with 5 mL methanol. The solvent was removed *in vacuo* and the residue was treated with 25 mL ethanol and concentrated sulfuric acid (0.75 mL, 1.38 mg, 14.1 mmol, 206 eq). The suspension was refluxed until the solid was completely dissolved (about 1 h). The acid was then neutralized with aqueous sodium hydroxide solution (1 M). Afterwards ethanol was removed *in vacuo* and the remaining aqueous colorless suspension was made basic with 10 mL aqueous sodium hydroxide solution (1 M). The aqueous layer was extracted three times with dichloromethane and the combined organic layers were dried with sodium sulfate,

filtered and concentrated. The residue was purified by column chromatography (SiO₂; EtOAc, 5% MeOH, 5% NEt₃) and recrystallization in acetonitrile to afford diamine **108** as a colorless solid (64%).

¹H NMR (400 MHz, CDCl₃): δ = 7.14-7.10 (m, 6H, *H_{ar}*), 6.72-6.65 (m, 9H, *H_{ar}*), 4.05-4.03 (m, 8H, OCH₂), 3.62 (s, 3H, OCH₃), 2.45 (broad s, 16H), 2.32 (q, ³*J_{H,H}* = 7 Hz, 4H, NCH₂CH₃), 2.21-2.12 (m, 4H, OCH₂CH₂), 1.04 (t, ³*J_{H,H}* = 6 Hz, NCH₂CH₃) ppm; **¹³C NMR (101 MHz, CDCl₃):** δ = 156.9 (C_q, 1C), 156.8 (C_q, 2C), 156.8 (C_q, 2C), 149.1 (C_q, 2C), 146.5 (C_q, 2C), 127.1 (C_t, 2C), 127.1 (C_t, 4C), 118.3 (C_t, 1C), 114.5 (C_t, 2C), 114.5 (C_t, 2C), 114.4 (C_t, 2C), 113.1 (C_t, 1C), 110.6 (C_t, 1C), 63.5 (C_s, 1C), 63.4 (C_s, 1C), 63.3 (C_s, 1C), 63.3 (C_s, 1C), 55.8 (C_s, 1C), 52.5 (C_s, 2C), 50.3 (C_s, 2C), 50.2 (C_s, 2C), 43.4 (C_q, 1C), 42.9 (C_q, 1C), 35.6 (C_s, 2C), 35.3 (C_s, 2C), 29.7 (C_s, 1C), 29.7 (C_s, 1C), 12.3 (C_p, 2C, CH₂CH₃) ppm; **MS (ESI, +, MeCN):** *m/z* = 705 ([M+H]⁺), 353 ([M+2H]²⁺).

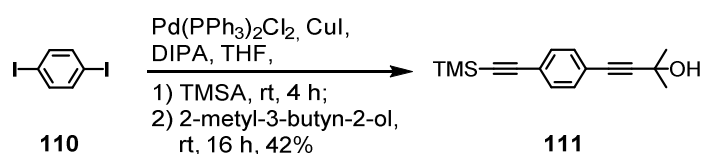
1,1,1'',1''-Diethyl-5'-methoxy-dispiro[piperidine-4,2'-[7,11,21,25]-tetraoxacyclopenta-[24.2.2.^{23,6}.2^{17,20}]hexatriaconta[3,5,12,14,17,19,26,28,29,31,33,35]dodecane-16,4''-piperidine] (109)



Diamine **108** (34.3 mg, 0.0487 mmol, 1.00 eq) was treated with freshly distilled iodoethane (0.5 mL) under argon atmosphere and 2 mL dry dichloromethane were added to dissolve the whole starting material. After stirring the mixture in the dark for 24 hrs the solvent was removed *in vacuo* and the crude was purified by column chromatography (SiO₂; acetone:1 M aqueous ammonium chloride solution:MeCN 7:1:1). The eluent was evaporated and then the white solid was extracted with dichloromethane (Soxhlet) for 30 hrs. After removing the solvent *in vacuo*, the obtained white solid was subjected to an ion exchange column (DOWEX 1X8 200-400 mesh Cl⁻) eluting with MeCN:H₂O 1:1. The obtained pale yellow solid was recrystallized from a MeOH:Et₂O 1:1 mixture to obtain cyclophane **109** as a colorless solid (54%).

¹H NMR (400 MHz, acetonitrile-*d*₃): δ = 7.19-7.14 (m, 6H, *H*_{ar}), 6.84-6.67 (m, 9H, *H*_{ar}), 4.07-4.03 (m, 8H, OCH₂), 3.65 (broad s, 3H, OCH₃), 3.27 (broad s, 14H), 2.63 (broad s, 8H), 2.14-2.10 (m, 4H, OCH₂CH₂), 1.30-1.16 (m, 12H, NCH₂CH₃) ppm; **MS (ESI, +, MeCN):** *m/z* = 381 ([M-2Cl]²⁺), 374 ([M-2Cl-CH₂]²⁺), 367 ([M-2Cl-2CH₂]²⁺).

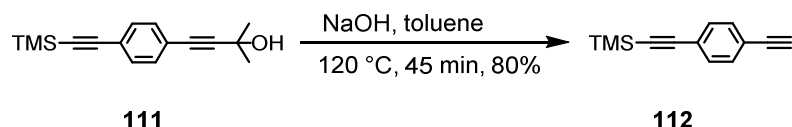
2-methyl-4-(4-((trimethylsilyl)ethynyl)phenyl)but-3-yn-2-ol (**111**)



In an oven-dried 250 mL Schlenk tube, 1,4-diiodobenzene (**110**, 10.0 g, 30.0 mmol, 1.00 eq) was dissolved in dry THF (50 mL) under argon atmosphere. Bis(triphenylphosphine)palladium(II) chloride (1.28 g, 1.80 mmol, 6 mol%), copper iodide (345 mg, 1.80 mmol, 6 mol%) and diisopropyl amine (21.5 g, 210 mmol, 30.0 mL 76.00 eq) were added and the yellow solution was degassed with argon for 10 min. Afterwards, it was slowly treated with TMS-acetylene (2.95 g, 30.0 mmol, 4.27 mL, 1.00 eq). The inhomogeneous reaction mixture was stirred for 4 hrs at room temperature before 2-methyl-3-butyn-2-ol (5.15 g, 60.0 mmol, 5.98 mL, 2.00 eq) was added dropwise. The resulting dark brown reaction mixture was stirred for another 16 hrs at room temperature. Afterwards, the solvent was removed *in vacuo* and the residue was subjected to demin. water and extracted with dichloromethane three times. The combined organic layers were washed with water and brine, dried over sodium sulfate, filtered and evaporated to dryness. The dark brown residue was purified by flash column chromatography (SiO₂; hexane: dichloromethane 3:7, then dichloromethane) to obtain the product as a pale yellow solid (3.20 g, 42%).

¹H NMR (400 MHz, CDCl₃): δ = 7.39 (d, ³*J*_{H,H} = 8.5 Hz, 2H), 7.34 (d, ³*J*_{H,H} = 8.5 Hz, 2H), 1.61 (s, 6H), 0.24 (s, 9H) ppm; **¹³C NMR (101 MHz, CDCl₃):** δ = 131.9 (C_t, 2C), 131.6 (C_t, 2C), 123.0 (C_q, 1C), 122.9 (C_t, 1C), 104.7 (C_q, 1C), 96.3 (C_q, 1C), 95.7 (C_q, 1C), 81.9 (C_q, 1C), 65.8 (C_q, 1C), 31.6 (C_p, 2C), 0.1 (C_p, 3C) ppm; **GC-MS (EI +, 70 eV):** *m/z* (%) = 241 (100), 256 (23) [M]⁺.

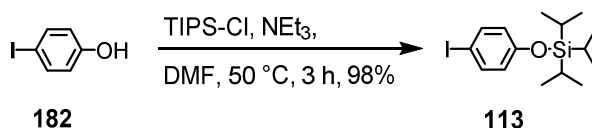
The spectroscopic data are in agreement with those previously reported.^[175]

((4-ethynylphenyl)ethynyl)trimethylsilane (112)

111 (750 mg, 2.92 mmol, 1.00 eq) was dissolved in dry toluene (12 mL) under argon atmosphere and was then charged with powdered sodium hydroxide (129 mg, 3.22 mmol, 1.10 eq). After stirring the reaction mixture at 120 °C for 45 min, it was allowed to cool down to room temperature and the solvent was removed under reduced pressure. The resulting crude solid was subjected to aqueous sat. ammonium chloride solution and extracted three times with dichloromethane. The combined organic layers were washed with brine, dried over sodium sulfate, filtered and the solvent was evaporated *in vacuo*. The dark brown crude product was purified by column chromatography (SiO₂; pentane: ethyl acetate 10:1) and product **112** was isolated as a pale yellow solid (381 mg, 76%).

¹H NMR (400 MHz, CDCl₃): δ = 7.41 (s, 4H, *H_{ar}*), 3.16 (s, 1H, C≡CH), 0.25 (s, 9H, SiCH₃) ppm; GC-MS (EI +, 70 eV): *m/z* (%) = 91.6 (7), 129.1 (7), 153.0 (9), 183.0 (100), 184.0 (18), 185.0 (5), 198.0 (25) [M]⁺.

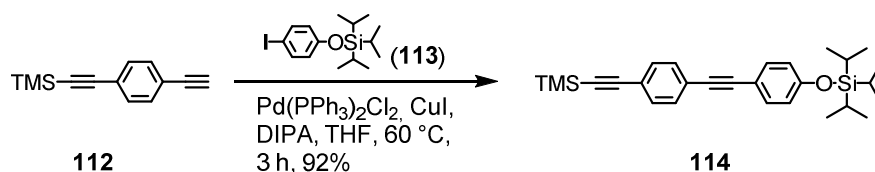
The spectroscopic data are in agreement with those previously reported.^[175]

(4-iodophenoxy)triisopropylsilane (113)

In an oven-dried Schlenk tube 4-iodophenol (**182**, 100 mg 0.45 mmol, 1.00 eq) and triethylamine (138 mg, 1.35 mmol, 0.192 mL, 3.00 eq) were dissolved in dry DMF (3 mL) under argon atmosphere. The solution was stirred for five min, before triisopropyl chloride (224 mg, 1.13 mmol, 0.248 mL, 2.50 eq) was added. The reaction mixture was stirred for 3 hours at 50 °C and was then poured into cold demin. water and extracted with dichloromethane three times. The organic layer was washed with brine, dried over sodium sulfate and filtered. The concentrated filtrate was purified by column chromatography (SiO₂; cyclohexane: ethyl acetate 5:1) to afford the target compound as a colorless liquid (161 mg, 95%).

¹H NMR (400 MHz CDCl₃): δ = 7.48 (d, $^3J_{H,H}$ = 8.8 Hz, 2H, *H_{ar}*), 6.65 (d, $^3J_{H,H}$ = 8.8 Hz, 2H, *H_{ar}*), 1.28 – 1.17 (m, 3H, SiCH), 1.08 (d, $^3J_{H,H}$ = 7.3 Hz, 18H, SiCH(CH₃)₂) ppm; **¹³C NMR (101 MHz, CDCl₃):** δ = 138.4 (C_t, 2C), 122.5 (C_t, 2C), 18.0 (C_p, 6C), 12.8 (C_t, 3C) ppm; **GC-MS (EI +, 70 eV):** m/z (%) = 76.0 (21), 77.0 (13), 121.0 (31), 135.0 (30), 136.0 (36), 138.5 (42), 150.0 (41), 163.0 (18), 164.0 (17), 178.0 (19), 206.1 (23), 246.8 (17), 262.9 (29), 276.9 (69), 304.9 (49), 333.0 (100), 334.0 (17), 376.0 (35).

Triisopropyl(4-((4-((trimethylsilyl)ethynyl)phenyl)ethynyl)phenoxy)silane (**114**)

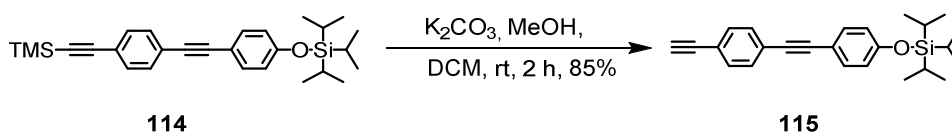


Aryl iodide **113** (107 mg, 0.283 mmol, 1.00 eq) and acetylene **112** (73.0 mg, 0.368 mmol, 1.30 eq) and copper iodide (1.65 mg, 0.00849 mmol, 3 mol%) were dissolved in dry THF (10 mL) in an oven-dried 25 mL Schlenk tube under argon atmosphere. The mixture was degassed with argon for five min and diisopropylamine (0.7 mL) was added followed by further degassing for two min. Afterwards, bis(triphenylphosphine)palladium(II) chloride (6.02 mg, 0.00849 mmol, 3 mol%) was added and the reaction mixture was stirred for three hrs at 60 °C. After evaporating the solvent under reduced pressure, the crude was taken up in demin. water and dichloromethane. The phases were separated and the aqueous one was extracted twice with dichloromethane. The combined organic layers were washed with brine, dried over sodium sulfate, filtered and concentrated. The crude was purified by column chromatography (SiO₂; cyclohexane: dichloromethane 10:1) yielding a colorless oil (116 mg, 92%).

¹H NMR (400 MHz, CDCl₃): δ = 7.42 (s, 4H, *H_{ar}*), 7.39 (d, $^3J_{H,H}$ = 8.6 Hz, 2H, *H_{ar}*), 6.85 (d, $^3J_{H,H}$ = 8.6 Hz, 2H, *H_{ar}*), 1.30 – 1.19 (m, 3H, SiCH(CH₃)₂), 1.10 (d, $^3J_{H,H}$ = 7.3 Hz, 18H, SiCH(CH₃)₂), 0.25 (s, 9H, SiCH₃) ppm; **¹³C NMR (101 MHz, CDCl₃):** δ = 133.2 (C_t, 2C), 132.0 (C_t, 2C), 131.3 (C_t, 2C), 123.9 (C_q, 1C), 122.6 (C_q, 1C), 120.3 (C_t, 2C), 115.5 (C_q, 1C), 104.9 (C_q, 1C), 96.2 (C_q, 1C), 91.7 (C_q, 1C), 88.0 (C_q, 1C), 18.0 (C_p, 6C), 12.8 (C_t, 3C), 0.1 (C_t, 3C) ppm; **GC-MS (EI +, 70 eV):** m/z (%) = 59.0 (12), 73.1 (40), 75.0 (16), 151.1 (18), 159.0 (55), 166.0 (100), 167.0 (19), 333.0 (47),

334.0 (15), 347.0 (69), 348.0 (22), 361.0 (13), 375.0 (42), 376.0 (15), 403.1 (51), 404.1 (19), 446.1 (83) [M]⁺, 447.1 (32), 448.1 (12).

(4-((4-ethynylphenyl)ethynyl)phenoxy)triisopropylsilane (115)

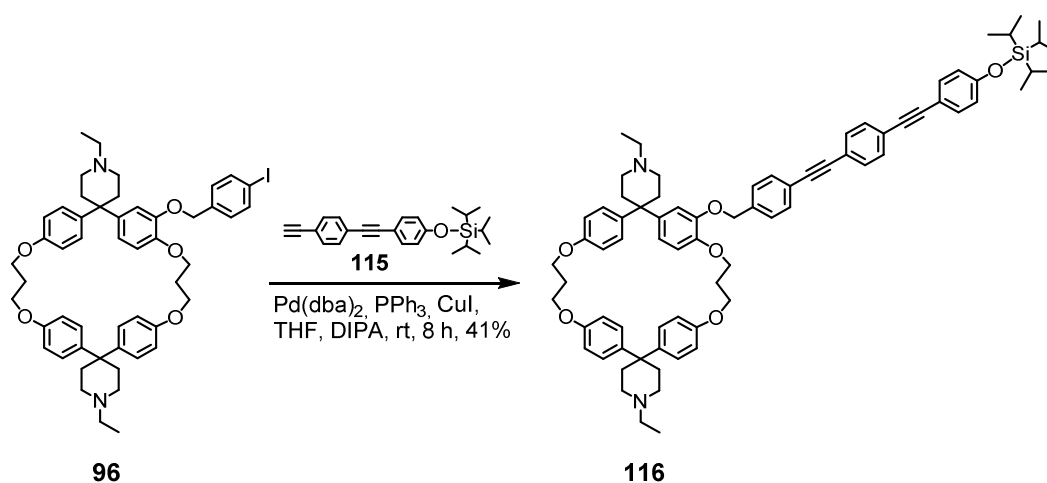


Reactant **114** (318 mg, 0.712 mmol, 1.00 eq) was dissolved in dichloromethane (2 mL). Methanol (0.2 mL) was added, the solution was charged with potassium carbonate (299 mg, 2.14 mmol, 3.01 eq) and was stirred at room temperature for six hrs. GC-MS indicated full conversion.

The reaction mixture was treated with demin. water and extracted three times with dichloromethane, washed with brine, dried over sodium sulfate, filtered and the solvents were evaporated under reduced pressure. After purification via column chromatography (SiO₂; cyclohexane: ethyl acetate 5:1) OPE **115** was obtained as a colorless solid (227 mg, 85%).

¹H NMR (400 MHz, CDCl₃): δ = 7.45 (s, 4H, *H_{ar}*), 7.43 – 7.37 (m, 2H, *H_{ar}*), 6.88 – 6.83 (m, 2H, *H_{ar}*), 3.16 (s, 1H, C≡CH), 1.32 – 1.21 (m, 3H, SiCH(CH₃)₂), 1.11 (s, 18H, SiCH(CH₃)₂) ppm. ¹³C NMR (101 MHz, CDCl₃): δ = 156.8 (C_q, 1C), 133.2 (C_t, 1C), 132.2 (C_t, 1C), 131.4 (C_t, 1C), 124.3 (C_q, 1C), 121.6 (C_q, 1C), 120.3, 115.5, 91.8 (C_q, 1C), 87.8 (C_q, 1C), 83.5 (C_q, 1C), 78.8 (C_t, 1C), 18.0 (C_s, 6C), 12.8 (C_t, 3C) ppm GC-MS (EI +, 70 eV): m/z (%) = 59.1(16), 75.1(35), 122.6(11), 130.6(28), 130.6(32), 137.6(65), 137.6(98), 200.0(28), 201.0(15), 202.0(17), 261.0(63), 262.0(15), 275.0(100), 276.0(24), 289.0(14), 303.1(51), 304.1(14), 331.1(68), 332.1(20), 374.1(82) [M]⁺, 375.1(27).

1,1''-diethyl-3'-((4-((4-((triisopropylsilyloxy)phenyl)ethynyl)phenyl)ethynyl)benzyl)-oxy)dispiro[piperidine-4,2'-4,8,12,16-tetraoxa-1,3,9,11(1,4)-tetrabenzenacyclohexadecaphane-10',4''-piperidine] (116)

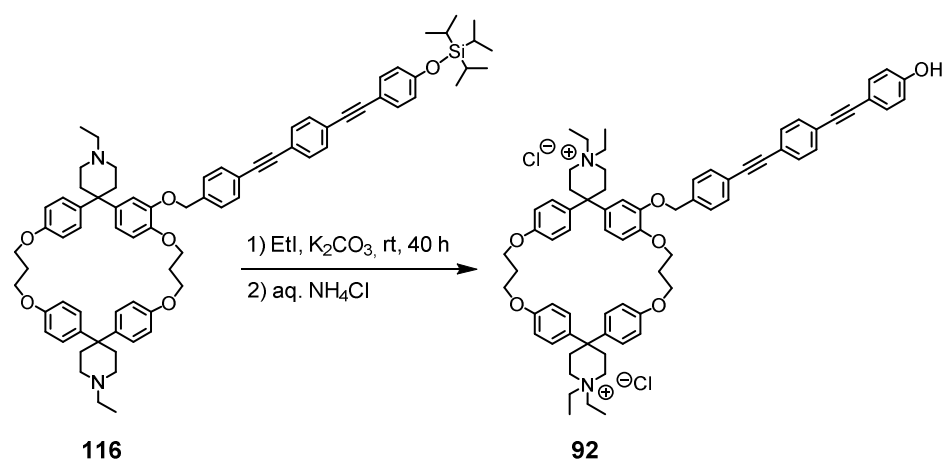


In an oven-dried Schlenk tube, cyclophane **96** (102 mg, 0.112 mmol, 1.00 eq) and OPE **115** (78.7 mg, 0.354 mmol, 1.00 eq) were dissolved in dry THF (11 mL) and diisopropylamine (3 mL) under argon atmosphere. The mixture was degassed by flushing with argon for 10 min. Afterwards, copper iodide (1.08 mg, 5.62 μ mol, 5 mol%), bis(dibenzylideneacetone)-palladium(0) (3.23 mg, 5.62 μ mol, 5 mol%) and triphenylphosphine (22.3 mg, 0.0843 mmol, 0.75 eq) were added and the reaction mixture was stirred at room temperature for eight hrs. The solvents were removed under reduced pressure, the crude mixture was then taken up in demin. water and was extracted three times with dichloromethane. The combined organic layers were washed with brine, dried over sodium sulfate, filtered and the solvents were removed *in vacuo*. Purification via column chromatography (SiO_2 ; ethyl acetate, 5% methanol, 5% NEt_3) yielded product **116** as a pale yellow solid (53.2 mg, 41%).

$^1\text{H NMR}$ (600 MHz, CDCl_3): δ = 7.55 (d, $^3J_{\text{H,H}}$ = 8.0 Hz, 2H, $H_{\text{ar,OPE}}$), 7.49 (d, $^3J_{\text{H,H}}$ = 8.0 Hz, 2H, $H_{\text{ar,OPE}}$), 7.42 (d, $^3J_{\text{H,H}}$ = 8.4 Hz, 2H, $H_{\text{ar,OPE}}$), 7.41 (d, $^3J_{\text{H,H}}$ = 8.4 Hz, 2H, $H_{\text{ar,OPE}}$), 7.12 – 7.07 (m, 2H, $H_{\text{ar,OPE}}$; 4H, $H_{\text{ar,cyclophane}}$), 6.90 (d, $^3J_{\text{H,H}}$ = 8.5 Hz, 2H, $H_{\text{ar,cyclophane}}$), 6.86 (d, $^3J_{\text{H,H}}$ = 8.1 Hz, 2H, $H_{\text{ar,OPE}}$), 6.78 – 6.64 (m, 8H, $H_{\text{ar,cyclophane}}$), 6.45 (s, 1H, $H_{\text{ar,cyclophane}}$), 4.85 (s, 2H, $\text{OCH}_2\text{-C}_{\text{q,ar}}$), 4.10 (t, $^3J_{\text{H,H}}$ = 5.3 Hz, 2H, OCH_2CH_2), 4.07 (t, $^3J_{\text{H,H}}$ = 5.3 Hz, 2H, OCH_2CH_2), 4.03 – 4.00 (m, 4H, OCH_2CH_2), 2.80 – 2.29 (m, 16H, NCH_2CH_2 , NCH_2CH_2 ; 4H, NCH_2CH_3), 2.24 – 2.17 (m, 2H, $\text{OCH}_2\text{CH}_2\text{CH}_2$), 2.09 – 2.08 (m, 2H, $\text{OCH}_2\text{CH}_2\text{CH}_2$), 1.32 – 1.23 (m, 3H, SiCH), 1.11 – 1.10 (m, 6H, NCH_2CH_3 , 18H, $\text{SiCH}(\text{CH}_3)_2$) ppm; **$^{13}\text{C NMR}$ (126 MHz, CDCl_3):** δ = 156.9 (C_{q} , 1C), 156.9 (C_{q} , 2C), 156.8 (C_{q} , 1C), 147.3 (C_{q} , 1C), 146.3 (C_{q} , 1C), (139.7), 138.2 (C_{q} , 1C), 133.2 (C_{t} , 2C), 131.8 (C_{t} ,

2C), 131.7 (C_t, 2C), 131.5 (C_t, 2C), 127.1 (C_t, 6C), 127.1 (C_t, 2C), 123.7 (C_q, 1C), 122.7 (C_q, 1C), 122.3 (C_q, 1C), 120.2 (C_t, 2C), 118.9 (C_t, 1C), 115.5 (C_q, 1C), 114.6 (C_t, 6C), 114.4 (C_t, 1C), 113.8 (C_t, 1C) 91.7 (C_q, 1C), 91.2 (C_q, 1C), 89.6 (C_q, 1C), 88.0 (C_q, 1C), 70.6 (C_s, 1C), 64.5 (C_s, 1C), 63.5 (C_s, 1C), 63.3 (C_s, 1C), 63.1 (C_s, 1C), 52.4 (C_s, 2C), 50.0 (C_s, 4C), 43.0 (C_q, 1C), 42.7 (C_q, 1C), 34.8 (C_s, 4C), 29.7 (C_s, 1C), 29.6 (C_s, 1C), (25.5), 18.0 (C_s, 6C), 12.8 (C_t, 3C), 11.9 (C_s, 2C) ppm. No signals for C_q next to the spiro centre (4C) were observed in the spectrum. The signals in brackets correspond to impurity; **HRMS (ESI, +)**: calc. for C₇₆H₉₀N₂O₆Si 1153.6484 [M+H]⁺, found 1153.6487.

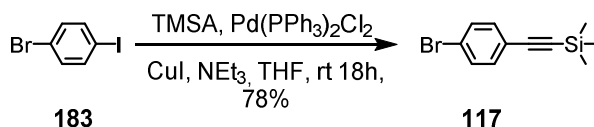
1,1,1'',1''-tetraethyl-3'-((4-((4-((4-hydroxyphenyl)ethynyl)phenyl)ethynyl)benzyl)oxy)di-spiro[piperidine-4,2'-4,8,12,16-tetraoxa-1,3,9,11(1,4)-tetrabenzenacyclohexadecaphane-10',4''-piperidine]-1,1''-dium dichloride (92)



Diamine **116** (30.0 mg, 0.026 mmol, 1.00 eq) was subjected to freshly distilled iodoethane (6.82 mg, 43.3 mmol, 3.5 mL, 1,666 eq) and potassium carbonate (18.1 mg, 0.13 mmol, 5.00 eq). The resulting suspension was stirred in the dark at room temperature. After 40 hrs, LC-ESI-MS indicated full conversion of **116** and iodoethane was then removed *in vacuo*. The obtained pale yellow solid was taken up in methanol and the insoluble potassium carbonate was filtered off. Impurities were separated by reversed phase column chromatography (SiO₂-C18, acetonitrile, 10% water). For the elution of the target compound a change to a charged eluent (acetonitrile, 5% water, 5% 1 M aq. ammonium chloride solution) was inevitable. After evaporation of the solvents under reduced pressure, the resulting mixture of target

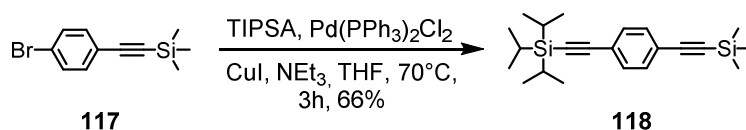
compound **92** and ammonium salts was subjected to a small amount of demin. water (0.5 mL). The dissolved ammonium salts were removed by filtration, the solid product was washed twice with some water and was then taken up in methanol. Evaporation of methanol afforded the pure target diammonium salt **92** as a pale yellow solid (13.2 mg, 45%).

¹H NMR (600 MHz, CD₃CN: D₂O 1:1): δ = 7.57 (d, $^3J_{H,H}$ = 8.4 Hz, 2H, *H*_{ar,OPE}), 7.49 (d, $^3J_{H,H}$ = 8.4 Hz, 2H, *H*_{ar,OPE}), 7.36 (d, $^3J_{H,H}$ = 8.6 Hz, 2H, *H*_{ar,OPE}), 7.34 (d, $^3J_{H,H}$ = 8.2 Hz, 2H, *H*_{ar,OPE}), 7.16 – 7.07 (m, 2H, *H*_{ar,OPE}; 4H, *H*_{ar,cyclophane}), 6.85 (d, $^3J_{H,H}$ = 8.5 Hz, 2H, *H*_{ar,cyclophane}), 6.83 – 6.80 (m, 2H, *H*_{ar,OPE}), 6.80 – 6.76 (m, 4H, *H*_{ar,cyclophane}), 6.74 (d, $^3J_{H,H}$ = 8.6 Hz, 2H, *H*_{ar,cyclophane}), 6.61 (d, $^3J_{H,H}$ = 8.4 Hz, 2H, *H*_{ar,cyclophane}), 6.52 (s, 1H, *H*_{ar,cyclophane}), 5.10 – 5.00 (m, 2H, OCH₂-C_{q,ar}), 4.07 (t, $^3J_{H,H}$ = 5.3 Hz, 2H, OCH₂CH₂), 4.03 (t, $^3J_{H,H}$ = 5.3 Hz, 2H, OCH₂CH₂), 3.93 (t, $^3J_{H,H}$ = 5.3 Hz, 2H, OCH₂CH₂), 3.89 (t, $^3J_{H,H}$ = 5.3 Hz, 2H, OCH₂CH₂), 3.17 (bs, 8H, NCH₂CH₃; 8H, NCH₂CH₂), 2.53 (bs, 8H, NCH₂CH₂), 2.17 – 2.11 (m, 2H, OCH₂CH₂), 1.91 – 1.89 (m, 2H, OCH₂CH₂), 1.15 – 1.05 (m, 12H, NCH₂CH₃) ppm; **¹³C NMR (151 MHz, CD₃CN):** δ = 157.2 (C_q, 1C), 156.9 (C_q, 1C), 156.8 (C_q, 1C), 156.6 (C_q, 1C), 147.0 (C_q, 1C), 146.1 (C_q, 1C), 137.9 (C_q, 1C), 132.9 (C_t, 2C), 131.4 (C_t, 2C), 131.2 (C_t, 2C), 131.0 (C_t, 2C), 127.5 (C_t, 2C), 127.4 (C_t, 2C), 127.1 (C_t, 2C), 126.8 (C_t, 2C), 123.3 (C_q, 1C), 121.9 (C_q, 1C), 121.5 (C_q, 1C), 118.3 (C_q, 1C), 115.4 (C_t, 2C), 114.2 (C_t, 4C), 114.0 (C_t, 2C), 113.8 (C_q, 1C), 112.9 (C_q, 1C), 112.1 (C_q, 1C), (99.6), 91.6 (C_q, 1C), 90.6 (C_q, 1C), 89.1 (C_q, 1C), 86.6 (C_q, 1C), 69.1 (C_s, 1C), 63.5 (C_s, 1C), 63.2 (C_s, 1C), 63.0 (C_s, 1C), 62.8 (C_s, 1C), 54.7 (C_s, 8C), 41.1 (C_q, 1C), 41.0 (C_q, 1C), 28.2 (C_s, 1C), 28.1 (C_s, 1C), 28.1 (C_s, 2C), 27.8 (C_s, 2C), 6.0 (C_p, 4C) ppm. No signals for C_q adjacent to the spiro centre (4C) were observed in the spectrum. The signals in brackets could not be assigned and correspond most likely to impurity; **HRMS (ESI, +):** calc. for C₇₁H₇₈N₂O₆ 527.2924 [M – 2Cl]²⁺, found 527.2931.

((4-bromophenyl)ethynyl)trimethylsilane (117)

In an oven-dried Schlenk tube, 1-bromo-4-iodobenzene (**183**, 1.00 g, 3.53 mmol, 1.00 eq), bis-(triphenylphosphine)palladium(II) chloride (125 mg, 0.177 mmol, 5 mol%) and copper iodide (20.3 mg, 0.106 mmol, 3 mol%) were dissolved in dry THF (5 mL) and triethylamine (5 mL) under argon atmosphere. The solution was degassed by flushing with argon for 10 min. Afterwards ethynyltrimethylsilane (417 mg, 4.24 mmol, 0.604 mL, 1.20 eq) was added. Thereupon the color changed from yellow to dark green and slight warming occurred. After stirring at room temperature for 18 hrs, the solvents were removed under reduced pressure. The target compound was isolated by column chromatography (SiO₂; pentane) resulting in a colorless solid (700 mg, 78%).

¹H NMR (400 MHz, CDCl₃): δ = 7.47 – 7.39 (m, 2H, *H*_{ar}), 7.35 – 7.28 (m, 2H, *H*_{ar}), 0.25 (s, 9H, CH₃) ppm; **¹³C NMR (101 MHz, CDCl₃):** δ = 133.5 (C_t, 2C), 131.6 (C_t, 2C), 122.9 (C_q, 1C), 122.2 (C_q, 1C), 104.0 (C_q, 1C), 95.7 (C_q, 1C), 0.03 (C_s, 3C) ppm; **GC-MS (EI +, 70 eV):** *m/z* (%) = 53.0 (10), 79.1 (13), 115.1 (12), 119.6 (11), 128.1 (15), 142.1 (10), 143.1 (16), 237.1 (100), 238.1 (15), 239.1 (93), 240.1 (14), 252.1 (21) [M]⁺, 254.1 (21) [M]⁺.

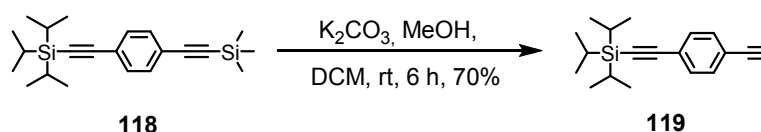
Triisopropyl((4-((trimethylsilyl)ethynyl)phenyl)ethynyl)silane (118)

In an oven-dried Schlenk tube, **117** (562 mg, 2.22 mmol, 1.00 eq), bis(triphenylphosphine)-palladium(II) chloride (47.2 mg, 0.0666 mmol, 3 mol%) and copper iodide (12.7 mg, 0.0666 mmol, 3 mol%) were suspended in triethylamine (4 mL) and dry THF (3 mL) under argon atmosphere. The mixture was degassed by flushing with argon for 10 min. After heating up to 70 °C triisopropylsilylacetylene (500 mg, 2.66 mmol, 0.615 mL, 1.20 eq) was added

dropwise over a time of 5 min. The color of the reaction mixture turned from yellow to dark red. After 2 hrs 45 min TLC indicated full conversion of **118**. The solvents were removed *in vacuo* and the crude product was purified by column chromatography (SiO₂; pentane) resulting in a colorless solid target compound (520 mg, 66%).

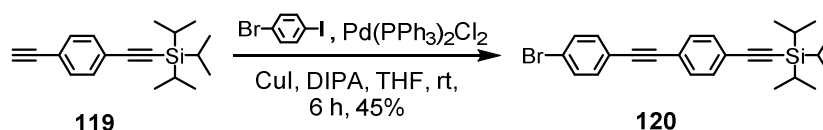
¹H NMR (400 MHz, CDCl₃): δ = 7.39 (s, 4H, *H_{ar}*), 1.12 (s, 21H, SiCH(CH₃)₂), 0.25 (s, 9H, SiCH₃) ppm; **¹³C NMR (101 MHz, CDCl₃):** δ = 132.0, 131.9, 123.7, 123.1, 106.7, 104.8, 96.3, 92.9, 18.8, 11.5, 0.1 ppm; **GC-MS (EI +, 70 eV):** *m/z* (%) = 73.0 (32), 105.0 (12), 106.0 (14), 113.0 (63), 120.1 (84), 121.0 (14), 183.0 (15), 211.0 (10), 225.0 (12), 227.0 (15), 241.1 (95), 242.1 (32), 243.0 (13), 255.1 (83), 256.1 (24), 257.1 (12), 269.1 (78), 270.1 (23), 283.1 (48), 284.1 (14), 311.0 (100), 311.9 (63), 313.2 (21), 339.2 (19), 354.2 (29) [M]⁺, 355.2 (10).

((4-ethynylphenyl)ethynyl)triisopropylsilane (**119**)



Reactant **118** (302 mg, 0.815 mmol, 1.00 eq) was dissolved in a mixture of dichloromethane and wet methanol (3:1, 4 mL). The solution was charged with potassium carbonate (131 mg, 0.937 mmol, 1.10 eq) and was stirred at room temperature for 6 hrs. GC-MS indicated full conversion. The reaction mixture was treated with demin. water and was extracted three times with dichloromethane, washed with brine, dried over sodium sulfate, filtered and the solvent was evaporated under reduced pressure. Compound **119** was obtained as a colorless solid (145 mg, 60%).

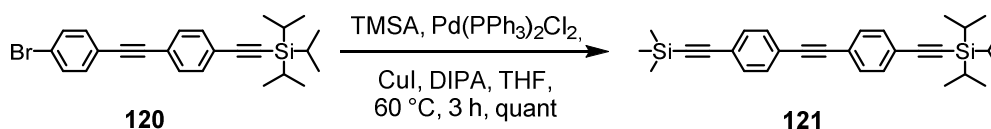
¹H NMR (400 MHz, CDCl₃): δ = 7.42 (s, 4H, *H_{ar}*), 3.16 (s, 1H, C \equiv CH), 1.13 (s, 21H, SiCH(CH₃)₂) ppm; **¹³C NMR (101 MHz, CDCl₃):** δ = 132.0 (C_t, 2C), 131.9 (C_t, 2C), 123.7 (C_q, 1C), 123.1 (C_q, 1C), 106.7 (C_q, 1C), 104.8 (C_q, 1C), 96.3 (C_q, 1C), 92.9 (C_q, 1C), 18.8 (C_s, 6C), 11.5 (C_t, 3C), 0.1 (C_s, 3C) ppm; **GC-MS (EI +, 70 eV):** *m/z* (%) = 53.0 (12), 59.0 (15), 84.6 (12), 91.6 (32), 91.6 (13), 103.0 (12), 129.0 (32), 145.1 (10), 153.1 (48), 154.1 (13), 155.1 (25), 159.1 (13), 169.2 (100), 169.9 (29), 183.1 (88), 184.1 (20), 197.1 (74), 198.1 (15), 211.1 (53), 212.1 (11), 239.3 (100), 239.9 (51), 241.1 (11), 282.2 (24) [M]⁺.

((4-((4-bromophenyl)ethynyl)phenyl)ethynyl)triisopropylsilane (120)

An oven-dried Schlenk tube was charged with **119** (284 mg, 1.01 mmol, 1.30 eq) and 1-bromo-4-iodobenzene (223 mg, 0.773 mmol, 1.00 eq) which was dissolved in dry THF (20 mL) and diisopropylamine (3 mL) in argon atmosphere. The mixture was degassed by flushing with argon for 10 min. Afterwards, copper iodide (4.44 mg, 0.0232 mmol, 3 mol%) and bis(triphenylphosphine)palladium chloride (16.4 mg, 0.0232 mmol, 3 mol%) were added and the reaction mixture was stirred at room temperature for six hrs. The solvents were removed under reduced pressure, the crude mixture was then taken up in demin. water and was extracted three times with dichloromethane. The combined organic layers were washed with brine, dried over sodium sulfate, filtered and the solvents were removed in *vacuo*. Purification via column chromatography (SiO₂; cyclohexane) afforded product **120** as a colorless solid (153 mg) in 45% yield.

¹H NMR (400 MHz, CDCl₃): δ = 7.51 – 7.47 (m, 2H, *H_{ar}*), 7.45 – 7.44 (m, 4H, *H_{ar}*), 7.41 – 7.36 (m, 2H, *H_{ar}*), 1.13 (m, 3H, SiCH, 18H, SiCH(CH₃)₂) ppm; ¹³C NMR (101 MHz, CDCl₃): δ = 133.2 (C_t, 2C), (132.4), 132.2 (C_t, 2C), 131.8 (C_t, 2C), 131.5 (C_t, 2C), 129.1 (C_q, 1C), 123.8 (C_q, 1C), 122.9 (C_q, 1C), 122.9 (C_q, 1C), 122.2 (C_q, 1C), 106.7 (C_q, 1C), 93.2 (C_q, 1C), 90.4 (C_q, 1C), 90.2 (C_q, 1C), 18.8 (C_s, 6C), 11.5 (C_t, 3C) ppm.

The spectroscopic data are in agreement with those previously reported.^[176]

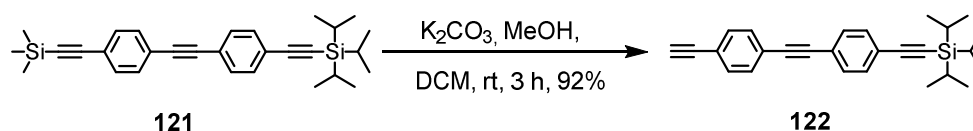
Triisopropyl((4-((4-((trimethylsilyl)ethynyl)phenyl)ethynyl)phenyl)ethynyl)silane (121)

This compound was prepared by a modification of the previously reported procedure^[177] in order to use starting material **120** available from other synthesis. OPE **120** (134 mg, 0.306 mmol, 1.00 eq) and trimethylsilylacetylene (39.1 mg, 0.398 mmol, 1.30 eq) and copper iodide (1.76 mg, 9.19 μmol , 3 mol%) were dissolved in dry THF (4 mL) in an oven-dried 25 mL Schlenk tube under argon atmosphere. The mixture was degassed with argon for five min and diisopropylamine (0.7 mL) was added followed by further degassing for two min. Afterwards, *bis*(triphenylphosphine)palladium(II) chloride (6.02 mg, 9.19 μmol , 3 mol%) was added and the reaction mixture was stirred for four hrs at 60 °C. After evaporating the solvent under reduced pressure, the crude was taken up in demin. water and dichloromethane. The phases were separated and the aqueous one was extracted twice with dichloromethane. The combined organic layers were washed with brine, dried over sodium sulfate, filtered and concentrated. The crude was purified by column chromatography (SiO_2 ; cyclohexane) yielding OPE **121** as a pale yellow solid (139 mg, quant.).

$^1\text{H NMR}$ (400 MHz, CDCl_3): δ = 7.45 (s, 8H, H_{ar}), 1.13 – 1.12 (m, 3H, SiCH, 18H, $\text{SiCH}(\text{CH}_3)_2$), 0.26 (s, 9H, $\text{Si}(\text{CH}_3)_3$) ppm.

The spectroscopic data are in agreement with those previously reported.^[177]

((4-((4-ethynylphenyl)ethynyl)phenyl)ethynyl)triisopropylsilane (**122**)

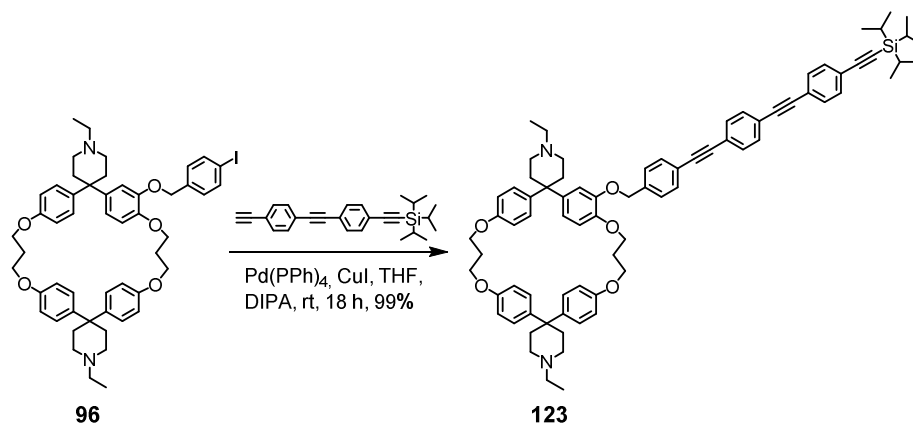


Reactant **121** (127 mg, 0.279 mmol, 1.00 eq) was dissolved in a mixture of dichloromethane (3 mL) and wet methanol (1 mL). The resulting solution was charged with potassium carbonate (117 mg, 0.837 mmol, 3.00 eq) and was stirred at room temperature for three hrs. GC-MS indicated full conversion. The reaction mixture was treated with demin. water and was extracted with dichloromethane three times. The combined organic layers were washed with brine, dried over sodium sulfate, filtered and the solvents were evaporated under reduced pressure. The solid, colorless target OPE **122** could be afforded in 92% yield (98.0 mg).

¹H NMR (400 MHz, CDCl₃): δ = 7.47 (s, 4H, *H_{ar}*), 7.45 (s, 4H, *H_{ar}*), 3.18 (s, 1H, C≡CH), 1.13 (s, 3H, SiCH₃, 18H, SiCH(CH₃)₂) ppm. **¹³C NMR (101 MHz, CDCl₃):** δ = 132.2 (C_t, 2C), 132.1 (C_t, 2C), 131.6 (C_t, 2C), 131.5 (C_t, 2C), 123.8 (C_q, 1C), 123.7 (C_q, 1C), 122.9 (C_q, 1C), 122.2 (C_q, 1C), 106.7 (C_q, 1C), 93.2 (C_q, 1C), 91.2 (C_q, 1C), 90.7 (C_q, 1C), 83.4 (C_q, 1C), 79.2 (C_t, 1C), 18.8 (C_t, 3C), 11.5 (C_p, 6C) ppm.

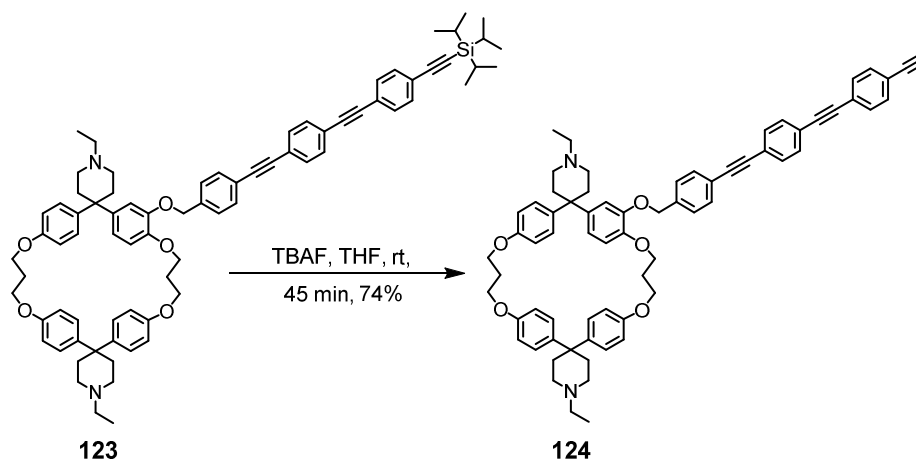
The spectroscopic data, obtained by a slightly modified procedure, are in agreement with those previously reported.^[178]

1,1''-diethyl-3'-((4-((4-((triisopropylsilyl)ethynyl)phenyl)ethynyl)phenyl)ethynyl)benzyl)oxy)dispiro[piperidine-4,2'-4,8,12,16-tetraoxa-1,3,9,11(1,4)-tetrabenzenacyclohexadecaphane-10',4''-piperidine] (123**)**



An oven-dried Schlenk tube was charged with cyclophane **96** (40.0 mg, 0.0441 mmol, 1.00 eq) and OPE **122** (33.7 mg, 0.0882 mmol, 2.00 eq) which were dissolved in dry THF (3 mL) and diisopropylamine (0.5 mL) under argon atmosphere. The mixture was degassed by flushing with argon for 10 min. Afterwards, copper iodide (0.506 mg, 2.65 μmol, 6 mol%) and tetrakis-(triphenylphosphine)palladium(0) (3.09 mg, 2.65 μmol, 6 mol%) were added and the reaction mixture was stirred at room temperature for 18 hrs. The solvents were removed under reduced pressure, the crude mixture was then taken up in demin. water and was extracted three times with dichloromethane. The combined organic layers were washed with brine, dried over sodium sulfate, filtered and the solvents were removed in *vacuo*. Without further purification, amine **123** (51.0 mg, 99%) was directly used in the next step.

1,1''-diethyl-3'-((4-((4-((4-ethynylphenyl)ethynyl)phenyl)ethynyl)benzyl)oxy)dispiro[piperidine-4,2'-4,8,12,16-tetraoxa-1,3,9,11(1,4)-tetrabenzenacyclohexadecaphane-10',4''-piperidine] (124)

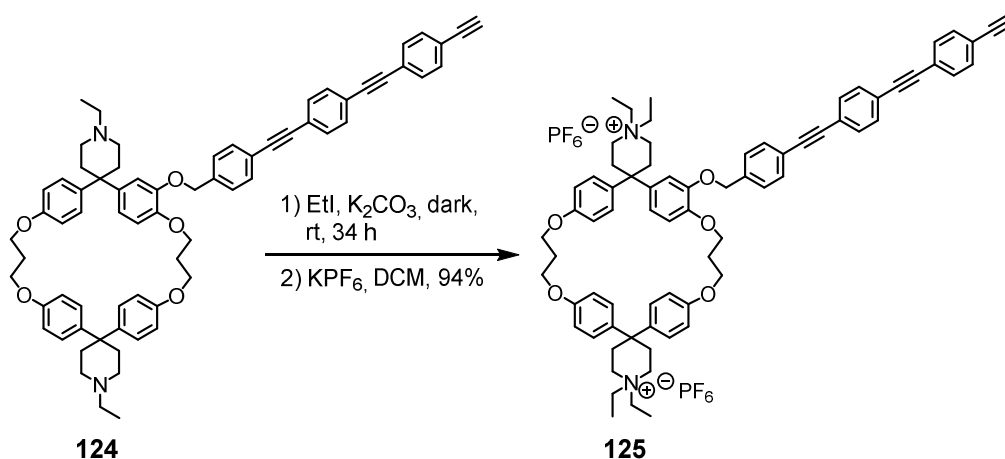


In an oven-dried Schlenk-tube **123** (38.3 mg, 0.0330 mmol, 1.00 eq) was dissolved in dry tetrahydrofuran (1.5 mL) under argon atmosphere. Tetrabutylammonium fluoride solution (1 M in THF, 34.8 mg, 0.0396 mmol, 1.20 eq) was added and the reaction mixture was stirred at room temperature for 45 min. TLC (SiO_2 ; ethyl acetate, 5% NEt_3 , 5% MeOH) indicated full conversion of the reactant. After removing the solvent under reduced pressure, the crude was taken up in demin. water and dichloromethane. The layers were separated and the aqueous one was extracted twice with dichloromethane. The combined organic layers were washed with brine, dried over sodium sulfate, filtered and concentrated *in vacuo*. The crude product was purified by column chromatography (SiO_2 ; ethyl acetate, 5% NEt_3 , 5% MeOH) to afford target compound **124** as a colorless solid (24.6 mg, 74%).

$^1\text{H NMR}$ (500 MHz, CDCl_3): δ = 7.57 – 7.56 (m, 2H, $H_{ar, OPE}$), 7.53 – 7.51 (m, 2H, $H_{ar, OPE}$), 7.48 (s, 4H, $H_{ar, OPE}$), 7.45 – 7.39 (m, 2H, $H_{ar, OPE}$), 7.15 – 7.09 (m, 2H, $H_{ar, OPE}$), 7.08 – 7.04 (m, 4H, $H_{ar, cyclo}$), 6.88 (d, $^3J_{H,H}$ = 8.7 Hz, 2H, $H_{ar, cyclo}$), 6.77 – 6.61 (m, 8H, $H_{ar, cyclo}$), 6.41 (s, 1H, $H_{ar, cyclo}$), 4.84 (s, 2H, OCH_2C_q), 4.11 – 4.06 (m, 4H, $\text{OCH}_2\text{CH}_2\text{CH}_2$), 4.03 – 4.00 (m, 4H, $\text{OCH}_2\text{CH}_2\text{CH}_2$), 3.19 (s, 1H, $\equiv\text{CH}$), 3.18 – 2.01 (broad m, 20H, NCH_2 , NCH_2CH_2), 2.25 – 2.15 (m, 2H, $\text{OCH}_2\text{CH}_2\text{CH}_2$), 2.1 – 2.08 (m, 2H, $\text{OCH}_2\text{CH}_2\text{CH}_2$), 1.21– 1.17 (m, 6H, NCH_2CH_3) ppm; **$^{13}\text{C NMR}$ (126 MHz, CDCl_3):** δ = 157.2 (C_q , 3C, COCH_2CH_2), 147.6 (C_q , 1C, $\text{CHCOCH}_2\text{CCH}$), 147.6 (C_q , 1C, $\text{CHCOCH}_2\text{CCH}$), 147.6 (C_q , 1C, $\text{CHCOCH}_2\text{CCH}$), 138.2 (C_q , 1C, $\text{OCH}_2\text{C}_q, OPE$), 132.2 (C_t , 2C, CH_{OPE}), 131.8 (C_t , 2C, $\text{CH}_{ar, OPE}$), 131.7 (C_t , 2C, $\text{CH}_{ar, OPE}$), 131.6 (C_t , 2C, $\text{CH}_{ar, OPE}$), 127.1 (C_t , 2C, $\text{CH}_{ar, OPE}$), 127.0 (C_t , 1C, $\text{C}_{q, spiro}\text{C}_q\text{CH}$), 126.9 (C_t , 1C, $\text{C}_{q, spiro}\text{C}_q\text{CH}$), 126.8 (C_t , 1C, $\text{C}_{q, spiro}\text{C}_q\text{CH}$), 123.5 (C_q , 1C,

CHC_{q, OPE}), 123.3 (C_q, 1C, CHC_{q, OPE}), 123.0 (C_q, 1C, CHC_{q, OPE}), 122.3 (C_q, 1C, CHC_{q, OPE}), 122.2 (C_q, 1C, CHC_{q, OPE}), 117.7 (hmqc, C_t, 1C, C_{q, spiro}C_qCHCH) 114.8 – 114.7 (C_t, 8C, CH_{cyclo}), 91.4 (C_q, 1C, C_qC≡C), 91.1 (C_q, 1C, C_qC≡C), 90.9 (C_q, 1C, C_qC≡C), 89.6 (C_q, 1C, C_qC≡C), 83.3 (C_q, 1C, C_qC≡C), 79.2 (C_q, 1C, C≡CH), 70.5 (C_s, 1C, OCH₂C_{q, OPE}), 63.5 (C_s, 1C, OCH₂CH₂CH₂), 63.5 (C_s, 1C, OCH₂CH₂CH₂), 63.3 (C_s, 1C, OCH₂CH₂CH₂), 63.2 (C_s, 1C, OCH₂CH₂CH₂), 58.9, 52.3 (C_s, 2C, NCH₂CH₃), 49.6 (C_s, 4C, NCH₂CH₂), 42.7 (C_q, 1C, C_{q, spiro}), 42.4 (C_q, 1C, C_{q, spiro}), 33.6 (C_s, 4C, NCH₂CH₂), 29.6 (C_s, 2C, NCH₂CH₂), 29.6 (C_s, 4C, NCH₂CH₂), 10.8 (C_p, 2C, NCH₂CH₃) ppm. C_q adjacent to the spiro center could not be detected, neither in ¹³C NMR spectrum, nor in spectra of 2D NMR experiments; **HRMS (ESI, +)**: calc. for C₆₉H₆₉N₂O₅ 1005.5201 [M+H]⁺, found 1005.5191.

1,1,1'',1''-tetraethyl-3'-((4-((4-((4-ethynylphenyl)ethynyl)phenyl)ethynyl)benzyl)oxy)di-spiro[piperidine-4,2'-4,8,12,16-tetraoxa-1,3,9,11(1,4)-tetrabenzenacyclohexadecaphane-10',4''-piperidine]-1,1''-dium potassium di-hexafluorophosphate (125)

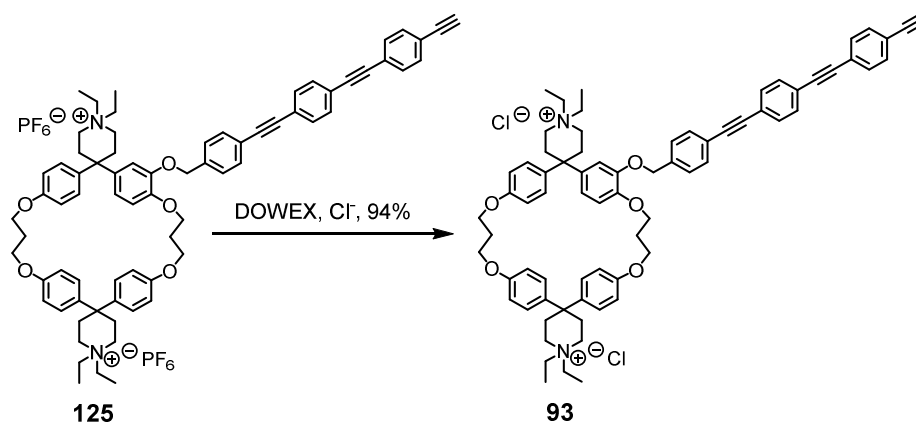


In a 10 mL one-neck flask amine **124** (21.3 mg, 0.0212 mmol, 1.00 eq) was charged with potassium carbonate (11.8 mg, 0.0848 mmol, 4.00 eq) and freshly distilled iodoethane (2.54 g, 16.1 mmol, 1.30 mL, 759 eq). After stirring the suspension room temperature for 34 hrs in the dark, excess iodoethane was removed under reduced pressure. Potassium hexafluorophosphate (39.8 mg, 0.212 mmol, 10.0 eq) and dichloromethane (5 mL) were added to the yellow crude mixture and stirred for five min. at room temperature, before

demin. water was added. The layers were separated and the aqueous one was extracted twice with dichloromethane. The combined organic layers were filtered over cotton and the solvent was removed *in vacuo* to obtain the hexafluorophosphate salt **125** (27.0 mg, 94%) as a yellow solid.

¹H NMR (500 MHz, CD₂Cl₂): δ = 7.61 (d, $^3J_{H,H}$ = 7.9 Hz, 2H, $H_{ar,OPE}$), 7.58 – 7.45 (m, 8H, $H_{ar,OPE}$), 7.30 (d, $^3J_{H,H}$ = 7.9 Hz, 2H, $H_{ar,OPE}$), 7.11 – 7.08 (m, 4H, $H_{ar,cyclo}$), 6.95 (d, $^3J_{H,H}$ = 8.4 Hz, 2H, $H_{ar,cyclo}$), 6.81 – 6.69 (m, 8H, $H_{ar,cyclo}$), 6.56 (s, 1H, $H_{ar,cyclo}$), 5.02 (s, 2H, OCH₂C_q), 4.07 (bs, 4H, OCH₂CH₂CH₂), 4.01 – 3.99 (m, 4H, OCH₂CH₂CH₂), 3.30 – 3.19 (m, 1H, C \equiv CH, 8H, NCH₂CH₃, 8H, NCH₂CH₂), 2.65 (bs, 8H, NCH₂CH₂), 2.20 – 2.18 (m, 2H, OCH₂CH₂), 2.08 – 2.06 (m, 2H, OCH₂CH₂), 1.30 – 1.25 (m, 12H, NCH₂CH₃) ppm; **¹³C NMR (126 MHz, CD₂Cl₂):** δ = 158.1 (C_q, 1C, COCH₂CH₂), 158.0 (C_q, 1C, COCH₂CH₂), 157.9 (C_q, 1C, COCH₂CH₂), 148.6 (C_q, 1C, CHCOCH₂CCH), 148.3 (C_q, 1C, CHCOCH₂CCH), 138.7 (C_q, 1C, OCH₂C_{q,OPE}), 132.5 (C_t, 2C, CH_{OPE}), 132.1 (C_t, 2C, CH_{OPE}), 132.1 (C_t, 4C, CH_{OPE}), 131.9 (C_t, 2C, CH_{OPE}), 127.7 (C_t, 2C, CH_{OPE}), 126.5 (C_t, 3C, C_{q,spiro}C_qCH), 123.8 (C_q, 1C, CHC_{q,OPE}), 123.6 (C_q, 1C, CHC_{q,OPE}), 123.3 (C_q, 1C, CHC_{q,OPE}), 122.6 (C_q, 1C, CHC_{q,OPE}), 122.5 (C_q, 1C, CHC_{q,OPE}), 117.7 (hmqc, C_t, 1C, C_{q,spiro}C_qCHCH), 115.2 (C_t, 4C, CH_{cyclo}), 115.0 (C_t, 2C, CH_{cyclo}), 113.4 (C_t, 1C, CH_{cyclo}), 113.1 (C_t, 1C, CH_{cyclo}), 91.7 (C_q, 1C, C_qC \equiv C), 91.2 (C_q, 1C, C_qC \equiv C), 91.1 (C_q, 1C, C_qC \equiv C), 89.7 (C_q, 1C, C_qC \equiv C), 83.3 (C_q, 1C, C_qC \equiv C), 79.5 (C_q, 1C, C \equiv CH), 70.8 (C_s, 1C, OCH₂C_{q,OPE}), 64.3 (C_s, 1C, OCH₂CH₂CH₂), 63.7 (C_s, 1C, OCH₂CH₂CH₂), 63.5 (C_s, 1C, OCH₂CH₂CH₂), 63.4 (C_s, 1C, OCH₂CH₂CH₂), 56.0 (C_s, 8C, NCH₂), 41.8 (C_q, 1C, C_{q,spiro}), 41.7 (C_q, 1C, C_{q,spiro}), (32.3), (32.0), (30.1), 29.6 (C_s, 1C, NCH₂CH₂CH₂), 29.5 (C_s, 1C, NCH₂CH₂CH₂), 29.0 (C_s, 2C, NCH₂CH₂CH₂), 29.0 (C_s, 2C, NCH₂CH₂CH₂), 23.0, 14.3, 7.6, 7.4 (C_p, 4C, NCH₂CH₃) ppm. C_q adjacent to the spiro center could not be detected, neither in ¹³C spectrum, nor in spectra of 2D NMR experiments. The signals in brackets correspond to impurity; **HRMS (ESI, +):** calc. for C₇₃H₇₈N₂O₅ 531.2950 [M – 2PF₆⁻]²⁺, found 531.2954.

**1,1,1'',1''-tetraethyl-3'-((4-((4-((4-ethynylphenyl)ethynyl)phenyl)ethynyl)benzyl)oxy)di-
spiro[piperidine-4,2'-4,8,12,16-tetraoxa-1,3,9,11(1,4)-tetrabenzenacyclohexadecaphane-
10',4''-piperidine]-1,1''-dium chloride (93)**

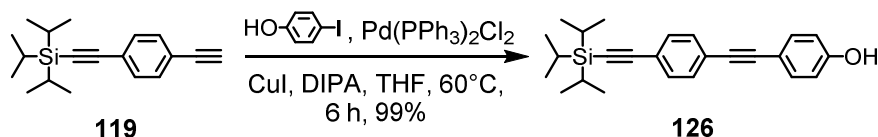


Hexafluorophosphate salt **125** (21.7 mg, 0.0160 mmol, 1.00 eq) was dissolved in acetonitrile (2 mL) and was subjected to an ion exchange column (Dowex 1X8, 200-400 mesh Cl⁻) eluting with acetonitrile: water 7:1. Complete ion exchange was indicated by ¹⁹F NMR experiment. The eluate was dried *in vacuo* yielding the target chloride salt **93** (17.1 mg, 94%) as a pale yellow solid.

¹H NMR (500 MHz, CD₂Cl₂): $\delta = 7.63 - 7.58$ (m, 2H, $H_{ar,OPE}$), $7.58 - 7.53$ (m, 2H, $H_{ar,OPE}$), $7.53 - 7.45$ (m, 6H, $H_{ar,OPE}$), 7.31 (d, $^3J_{H,H} = 8.1$ Hz, 2H, $H_{ar,OPE}$), $7.14 - 7.10$ (m, 4H, $H_{ar,OPE}$), 6.98 (d, $^3J_{H,H} = 8.9$ Hz, 2H, $H_{ar,OPE}$), $6.79 - 6.77$ (m, 4H, $H_{ar,cyclo}$), $6.75 - 6.73$ (m, 2H, $H_{ar,cyclo}$), $6.71 - 6.66$ (m, 2H, $H_{ar,cyclo}$), $6.64 - 6.60$ (m, 1H, $H_{ar,cyclo}$), 5.05 (s, 2H, OCH₂C_q), 4.06 (t, $^3J_{H,H} = 5.3$ Hz, 4H, OCH₂CH₂CH₂), 3.99 (t, $^3J_{H,H} = 5.2$ Hz, 4H, OCH₂CH₂CH₂), 3.53 (bs, 8H, NCH₂CH₃, 8H, NCH₂CH₂), 3.30 (s, 1H, C \equiv CH), $2.85 - 2.48$ (m 8H, NCH₂CH₂), (2.41 (d, $J = 11.0$ Hz, 3H)), 2.19 (q, $^3J_{H,H} = 5.3$ Hz, 2H, $^3J_{H,H}$), $2.11 - 2.03$ (m, 2H, $^3J_{H,H}$), $1.32 - 1.25$ (m, 12H, NCH₂CH₃) ppm; **¹³C NMR (126 MHz, CD₂Cl₂):** $\delta = 158.1$ (C_q, 1C, COCH₂CH₂), 158.1 (C_q, 1C, COCH₂CH₂), 158.0 (C_q, 1C, COCH₂CH₂), 148.6 (C_q, 1C, CHCOCH₂CCH), 148.4 (C_q, 1C, CHCOCH₂CCH), 138.8 (C_q, 1C, OCH₂C_{q,OPE}), 132.6 (C_t, 2C, CH_{OPE}), 132.2 (C_t, 2C, CH_{OPE}), 132.2 (C_t, 4C, CH_{OPE}), 132.0 (C_t, 2C, CH_{OPE}), 127.8 (C_t, 2C, CH_{OPE}), 126.8 (C_t, 3C, C_{q,spiro}C_qCH), 123.9 (C_q, 1C, CHC_{q,OPE}), 123.8 (C_q, 1C, CHC_{q,OPE}), 123.4 C_q, 1C, CHC_{q,OPE}), 122.7 (C_q, 1C, CHC_{q,OPE}), 122.6 (C_q, 1C, CHC_{q,OPE}), 117.7 (hmqc, C_t, 1C, C_{q,spiro}C_qCHCH), 115.3 (C_t, 4C, CH_{cyclo}), 115.2 (C_t, 1C, CH_{cyclo}), 115.1 (C_t, 1C, CH_{cyclo}), 113.8 (C_t, 1C, CH_{cyclo}), 113.1 (C_t, 1C, CH_{cyclo}), 91.8 (C_q, 1C, C_qC \equiv C), 91.4 (C_q, 1C, C_qC \equiv C), 91.2 (C_q, 1C, C_qC \equiv C), 89.8 (C_q, 1C, C_qC \equiv C), 83.5 (C_q, 1C, C_qC \equiv C), 79.7 (C_q, 1C, C \equiv CH), 71.1 (C_s, 1C, OCH₂C_{q,OPE}), 152

64.4 (C_s, 1C, OCH₂C_{q, OPE}), 63.8 (C_s, 1C, OCH₂CH₂CH₂), 63.6 (C_s, 1C, OCH₂CH₂CH₂), 63.5 (C_s, 1C, OCH₂CH₂CH₂), 55.6 (C_s, 4C, NCH₂), 55.5 (C_s, 4C, NCH₂), 42.1 (C_q, 1C, C_{q, spiro}), 41.9 (C_q, 1C, C_{q, spiro}), 29.8 (C_s, 1C, NCH₂CH₂ CH₂), 29.7 (C_s, 2C, NCH₂CH₂CH₂), 29.3 (C_s, 2C, NCH₂CH₂CH₂), 8.0 (C_p, 4C, NCH₂CH₃) ppm. C_q next to the spiro center could not be detected, neither in ¹³C spectrum, nor in spectra of 2D NMR experiments; **HRMS (ESI, +)**: calc. for C₇₃H₇₈N₂O₅ 531.2950 [M – 2Cl]²⁺, found 531.2957.

4-((4-((triisopropylsilyl)ethynyl)phenyl)ethynyl)phenol (**126**)

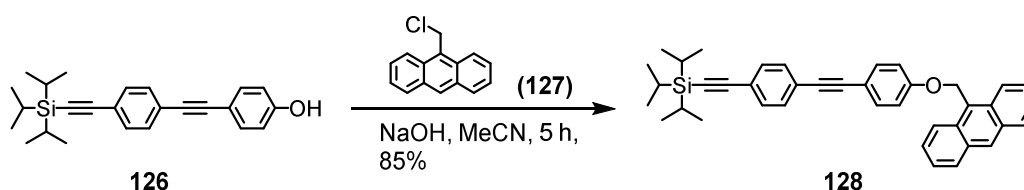


An oven-dried Schlenk tube was charged with **119** (130 mg, 0.460 mmol, 1.30 eq) and 4-iodophenol (78.7 mg, 0.354 mmol, 1.00 eq) which was dissolved in dry THF (20 mL) and diisopropylamine (3 mL) in argon atmosphere. The mixture was degassed by flushing with argon for 10 min. Afterwards, copper iodide (2.03 mg, 0.0106 mmol, 3 mol%) and bis(triphenylphosphine)-palladium chloride (7.52 mg, 0.0106 mmol, 3 mol%) were added and the reaction mixture was stirred at 60 °C for six hrs. The solvents were removed under reduced pressure, the crude mixture was then taken up in demin. water and was extracted three times with dichloromethane. The combined organic layers were washed with brine, dried over sodium sulfate, filtered and the solvents were removed in *vacuo*. Purification via column chromatography (SiO₂; ethyl acetate: methanol 5:2) afforded the pure product as a colorless solid (132 mg) in 99% yield.

¹H NMR (400 MHz, CDCl₃): δ = 7.47 – 7.39 (m, 6H, *H_{ar}*), 6.81 (d, ³*J_{H,H}* = 8.7 Hz, 2H, *H_{ar}*), 4.91 (s, 1H, *OH*), 1.13 (m, 21H, SiCH(CH₃)₂) ppm; **¹³C NMR (101 MHz, CDCl₃)**: δ = 156.0 (C_q, 1C, COH), 133.5 (C_t, 2C, *C_{ar}*), 132.1 (C_t, 2C, *C_{ar}*), 131.3 (C_t, 2C, *C_{ar}*), 123.6 (C_t, 2C, *C_{ar}*), 123.1 (C_q, 1C, *C_{ar}*), 115.7 (C_q, 1C, *C_{ar}*), 115.5 (C_t, 2C, *C_{ar}*), 106.9 (C_q, 1C, C≡C-Si), 92.7 (C_q, 1C, C≡C), 91.2 (C_q, 1C, C≡C), 88.0 (C_q, 1C, C≡C), 18.8 (C_s, 6C, CH), 11.5 (C_t, 3C, CH) ppm. **GC-MS (EI +, 70 eV)**: *m/z* (%) = 59.1 (13), 110.6 (14), 121.1 (14), 123.5 (13), 130.7 (69), 137.7 (100), 207.1 (10), 245.1 (12),

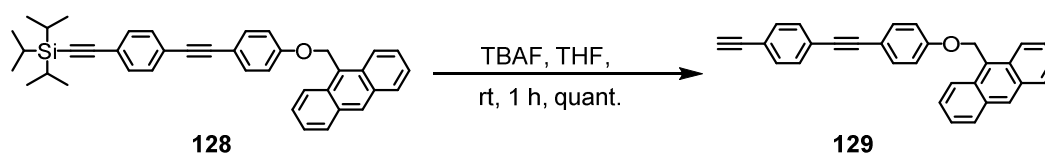
247.1 (12), 261.2 (97), 262.2 (22), 275.2 (68), 276.2 (16), 289.2 (58), 290.2 (15), 303.2 (27), 331.3 (79), 332.3 (22), 374.3 (45) $[M]^+$, 375.3 (14).

((4-((4-(anthracen-9-ylmethoxy)phenyl)ethynyl)phenyl)ethynyl)triisopropylsilane (128)



OPE **126** (108 mg, 0.288 mmol, 1.00 eq) was dissolved in dry acetonitrile (5 mL) under argon atmosphere and was then charged with sodium hydroxide (17.3 mg, 0.432 mmol, 1.50 eq). The resulting suspension was vigorously stirred for 45 min at 45 °C. Afterwards 9-(chloromethyl)anthracene (**127**, 65.3 mg, 0.288 mmol, 1.00 eq) was added. The mixture was stirred for four hrs at 45 °C and was then quenching with aq. ammonium chloride solution (0.1 M, 5 mL). The aqueous layer was extracted three times with dichloromethane, washed with brine, dried over sodium sulfate, filtered and the solvents were evaporated under reduced pressure. Column chromatography (SiO₂; cyclohexane: ethyl acetate 4:1) was performed to obtain **128** (138 mg, 85%) as a pale yellow solid.

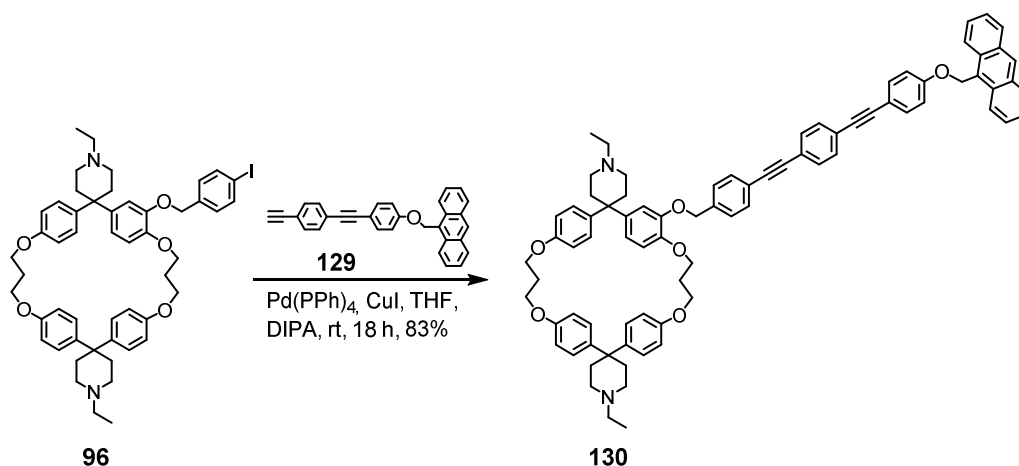
¹H NMR (400 MHz, CDCl₃): δ = 8.55 (s, 1H, C_q-CH-C_q), 8.28 (d, ³J_{H,H} = 9.0 Hz, 2H, CH_{ar,anthra}), 8.09 – 8.03 (m, 2H, CH_{ar,anthra}), 7.59 – 7.43 (m, 10H, 4 x CH_{ar,anthra}, 6 x CH_{ar,OPE}), 7.14 (d, ³J_{H,H} = 8.8 Hz, 2H, CH_{ar,OPE}), 6.00 (s, 2H, CH₂), 1.14 (bs, 21H, SiCH(CH₃)₂) ppm. **¹³C NMR (101 MHz, CDCl₃):** δ = 159.6 (C_q, 1C, O-C), 133.4 (C_t, 2C, C_{ar,OPE}), 132.1 (C_t, 2C, C_{ar,OPE}), 131.6 (C_q, 2C, C_{ar,anthra}), 131.4 (C_t, 2C, C_{ar,OPE}), 131.2 (C_q, 2C, C_{ar,anthra}), 129.3 (C_t, 1C, C_{ar,anthra}), 129.3 (C_t, 2C, C_{ar,anthra}), 126.8 (C_t, 2C, C_{ar,anthra}), 126.5 (C_q, 1C, C_{ar,anthra}), 125.3 (C_t, 2C, C_{ar,anthra}), 124.0 (C_t, 2C, C_{ar,anthra}), 123.6 (C_q, 1C, C_{ar,OPE}), 123.1 (C_q, 1C, C_{ar,OPE}), 115.8 (C_q, 1C, C_{ar,OPE}), 115.1 (C_t, 2C, C_{ar,OPE}), 106.9 (C_q, 1C, C≡C), 92.7 (C_q, 1C, C≡C), 91.4 (C_q, 1C, C≡C), 88.3 (C_q, 1C, C≡C), 63.0 (C_s, 1C, CH₂), 18.8 (C_p, 6C, CH₃), 11.5 (C_t, 3C, CH-CH₃) ppm. **GC-MS (EI +, 70 eV):** m/z (%) = 111 (14), 121 (11), 122 (10), 123 (12), 131 (68), 131 (11), 138 (90), 138 (26), 207 (18), 245 (11), 247 (12), 261 (100), 262 (24), 275 (69), 276 (17), 289 (63), 290 (16), 303 (29), 331 (87), 332 (25), 374 (52) $[M - \text{CH}_2\text{-anthracene} + \text{H}]^+$, 375 (17).

9-((4-((4-ethynylphenyl)ethynyl)phenoxy)methyl)anthracene (**129**)

In an oven-dried Schlenk tube OPE **128** (56.9 mg, 0.101 mmol, 1.00 eq) was dissolved in dry THF (1.4 mL). Tetrabutylammonium fluoride solution (1 M in THF, 106 mg, 0.120 mmol, 0.12 mL, 1.20 eq) was added and the reaction mixture was stirred at room temperature for 45 min. TLC (SiO₂; ethyl acetate, 5% NEt₃, 5% MeOH) showed full conversion of the reactant. After removing the solvent under reduced pressure, the crude was taken up in demin. water and dichloromethane. The layers were separated and the aqueous one was extracted twice with dichloromethane. The combined organic layers were washed with brine, dried over sodium sulfate, filtered and concentrated *in vacuo*. The crude was purified by column chromatography (SiO₂; cyclohexane: ethyl acetate 10:1) to afford product **129** as colorless solid (41.2 mg, 100%).

¹H NMR (400 MHz, CDCl₃): δ = 8.55 (s, 1H, C_q-CH-C_q), 8.27 (d, ³J_{H,H} = 8.8 Hz, 2H, CH_{ar,anthra}), 8.06 (d, ³J_{H,H} = 8.3 Hz, 2H, CH_{ar,anthra}), 7.60 – 7.41 (m, 10H, 4 x CH_{ar,anthra}, 6 x CH_{ar,OPE}), 7.17 – 7.08 (m, 2H, CH_{ar,OPE}), 5.99 (s, 2H, CH₂), 3.18 (s, 1H, C≡CH) ppm; ¹³C NMR (101 MHz, CDCl₃): δ = 159.6 (C_q, 1C, O-C), 133.4 (C_t, 2C, C_{ar,OPE}), 132.2 (C_t, 2C, C_{ar,OPE}), 131.6 (C_q, 2C, C_{ar,anthra}), 131.5 (C_t, 2C, C_{ar,OPE}), 131.2 (C_q, 2C, C_{ar,anthra}), 129.4 (C_t, 1C, C_{ar,anthra}), 129.3 (C_t, 2C, C_{ar,anthra}), 126.8 (C_t, 2C, C_{ar,anthra}), 126.5 (C_q, 1C, C_{ar,anthra}), 125.3 (C_t, 2C, C_{ar,anthra}), 124.3 (C_q, 1C, C_{ar,OPE}), 124.0 (C_t, 2C, C_{ar,anthra}), 121.7 (C_q, 1C, C_{ar,OPE}), 115.7 (C_q, 1C, C_{ar,OPE}), 115.1 (C_t, 2C, C_{ar,OPE}), 91.6 (C_q, 1C, C≡C), 88.0 (C_q, 1C, C≡C), 83.5 (C_q, 1C, C≡C), 78.9 (C_t, 1C, C≡CH), 63.1 (C_s, 1C, CH₂) ppm.

3'-((4-((4-((4-(anthracen-9-ylmethoxy)phenyl)ethynyl)phenyl)ethynyl)benzyl)oxy)-1,1''-diethyldispiro[piperidine-4,2'-4,8,12,16-tetraoxa-1,3,9,11(1,4)-tetrabenzenacyclohexadecaphane-10',4''-piperidine] (130)

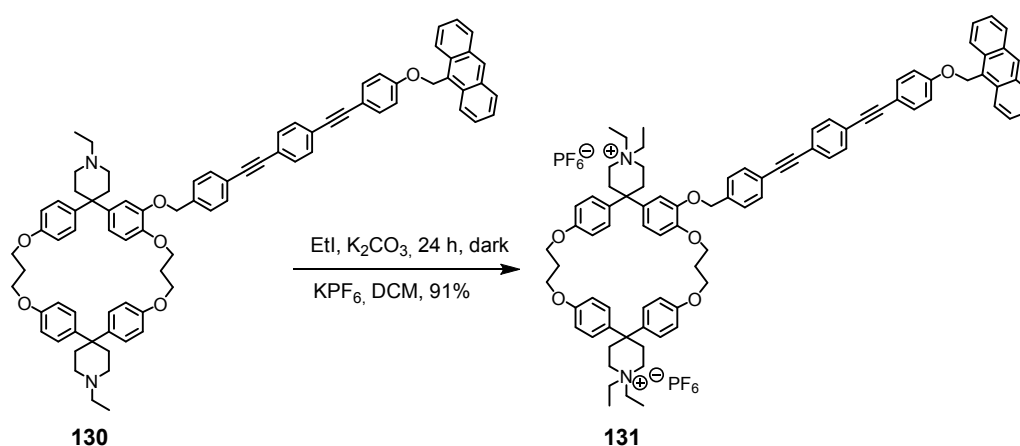


An oven-dried Schlenk tube was charged with cyclophane **96** (46.0 mg, 0.0507 mmol, 1.00 eq) and OPE **129** (43.5 mg, 0.106 mmol, 2.10 eq) which were dissolved in dry THF (4 mL) and diisopropylamine (1 mL) in argon atmosphere. The mixture was degassed by flushing with argon for 10 min. Afterwards, copper iodide (0.631 mg, 0.00330 mmol, 6 mol%) and tetrakis-(triphenylphosphine)palladium(0) (3.55 mg, 0.00330 mmol, 6 mol%) were added and the reaction mixture was stirred at room temperature for 18 hrs. The solvents were removed under reduced pressure, the crude mixture was then taken up in demin. water and was extracted three times with dichloromethane. The combined organic layers were washed with brine, dried over sodium sulfate, filtered and the solvents were removed in *vacuo*. Purification via column chromatography (SiO₂; ethyl acetate, 5% methanol, 4% NEt₃) afforded **130** as a colorless solid (50.0 mg, 83%).

¹H NMR (500 MHz, CDCl₃): δ = 8.55 (s, 1H, C_q-CH-C_{q,anthra}), 8.31 – 8.24 (m, 2H, H_{ar,anthra}), 8.10 – 8.02 (m, 2H, H_{ar,anthra}), 7.59 – 7.47 (m, 10H, H_{ar}), 7.43 (d, ³J_{H,H} = 8.1 Hz, 2H, H_{ar,cyclophane}), 7.17 – 7.01 (m, 8H, H_{ar}), 6.90 (d, ³J_{H,H} = 8.8 Hz, 2H, H_{ar,OPE}), 6.78 – 6.62 (m, 8H, H_{ar,cyclophane}), 6.44 (s, 1H, C_q-CH₂-C_q-O), 6.00 (s, 2H, OCH₂-C_{q,anthra}), 4.85 (s, 2H, OCH₂-C_{q,OPE}), 4.12– 4.09 (m, 2H, O-CH₂-CH₂), 4.07 (t, J = 5.3 Hz, 2H, O-CH₂-CH₂), 4.04 – 4.01 (m, 4H, O-CH₂-CH₂), 2.80 – 2.46 (m, 20H, CH_{2,piperidine}, NCH₂CH₃), 2.25 – 2.15 (m, 2H, O-CH₂-CH₂-CH₂), 2.15 – 2.03 (m, 2H, O-CH₂-CH₂-CH₂), 1.18 – 1.06 (m, 6H, NCH₂CH₃) ppm; **¹³C NMR (151 MHz, CDCl₃):** δ = 159.6 (C_q, 1C), 157.1 (C_q, 1C), 157.1 (C_q, 1C), 157.1 (C_q, 1C), 147.6 (C_q, 1C), 147.4 (C_q, 1C), 138.2 (C_q, 1C), (133.4), 133.4 (C_t, 2C), (132.6), 131.8 (C_q, 2C), 131.7 (C_t, 2C), 131.6 (C_t, 2C), 131.6 (C_t, 2C), 131.2

(C_q, 2C), 129.4 (C_t, 1C), 129.3 (C_t, 2C), 127.1 (C_t, 2C), 126.9 (C_t, 6C), 126.8 (C_t, 2C), 126.5 (C_q, 1C), (125.7), 125.3 (C_t, 2C), 124.0 (C_t, 1C), 123.8 (C_q, 1C), 122.7 (C_q, 1C), 122.3 (C_q, 1C), 115.7 (C_q, 1C), 115.1 (C_t, 2C), 114.7 (C_t, 6C), 114.6 (C_t, 3C), 91.6 (C_q, 1C), 91.2 (C_q, 1C), 89.7 (C_q, 1C), 88.2 (C_q, 1C), 70.6 (C_s, 1C), 63.5 (C_s, 1C), 63.3 (C_s, 1C), 63.2 (C_s, 1C), 63.0 (C_s, 1C), 59.2 (C_s, 1C), 52.4 (C_s, 4C), 49.8 (C_s, 1C), 49.8 (C_s, 1C), 42.8 (C_q, 1C), 42.5 (C_q, 1C), (34.2), (30.5), 29.8 (C_s, 1C), 29.7 (C_s, 1C), 29.7 (C_s, 2C), 29.6 (C_s, 2C), (18.8), (11.4), 8.6 (C_p, 2C) ppm. No signals for C_q next to the spiro centre (4C) were observed in the spectrum. The signals put into brackets could not be assigned; **HRMS (ESI, +)**: calc. for C₈₂H₈₀N₂O₆ 594.3003 [M+2H]²⁺, found 594.3010.

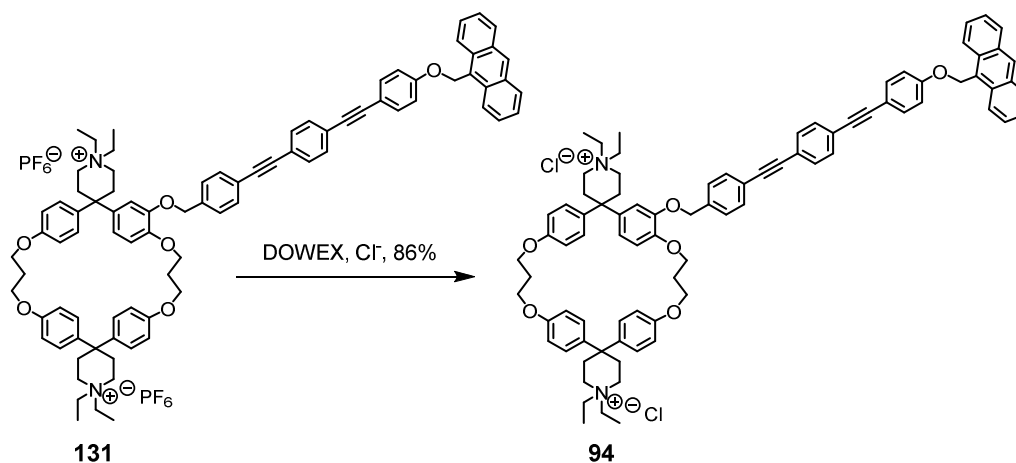
3'-((4-((4-((4-(anthracen-9-ylmethoxy)phenyl)ethynyl)phenyl)ethynyl)benzyl)oxy)-1,1,1',1''-tetraethylspiro[piperidine-4,2'-4,8,12,16-tetraoxa-1,3,9,11(1,4)-tetrabenzene-cyclohexadecaphane-10',4''-piperidine]-1,1''-dium di-hexafluorophosphate (131)



Amine **130** (35.0 mg, 0.0296, 1.00 eq) was charged with freshly distilled iodoethane (6.14 g, 39 mmol, 3.15 mL, 1320 eq) and potassium carbonate (16.5 mg, 0.118 mmol, 4.00 eq). The mixture was stirred in the dark at room temperature for 24 hrs. LC-ESI-MS indicated full conversion of the amine and excess iodoethane was distilled off. The crude product was first subjected to potassium hexafluorophosphate (111 mg, 0.590 mmol, 20.0 eq) and then dichloromethane (15 mL) was added. After stirring the mixture for 10 min, demin. water was added and the aqueous layer was extracted with dichloromethane three times. The combined organic phases were dried by filtration over dry cotton. Remaining insoluble particles were filtered off to obtain the target compound as a pale yellow solid 41.0 mg, 91%).

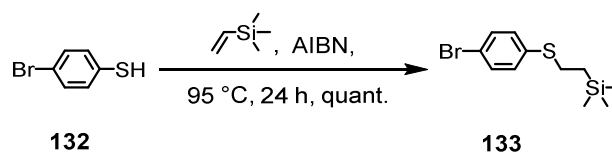
¹H NMR (600 MHz, CD₂Cl₂): δ = 8.58 (s, 1H, *H*_{ar,anthra}), 8.29 (d, ³*J*_{H,H} = 8.8 Hz, 2H, *H*_{ar,anthra}), 8.09 (d, ³*J*_{H,H} = 8.4 Hz, 2H, *H*_{ar,anthra}), 7.61–7.50 (m, 4H, *H*_{ar,anthra}; 8H, *H*_{ar,OPE}), 7.29 (d, ³*J*_{H,H} = 7.9 Hz, 2H, *H*_{ar,OPE}), 7.15 (d, ³*J*_{H,H} = 8.8 Hz, 2H, *H*_{ar,OPE}), 7.11–7.08 (m, 4H, *H*_{ar,cycloph}), 6.94 (d, ³*J*_{H,H} = 8.8 Hz, 2H, *H*_{ar,cycloph}), 6.81 (d, ³*J*_{H,H} = 8.6 Hz, 2H, *H*_{ar,cycloph}), 6.78 – 6.74 (m, 4H, *H*_{ar,cycloph}), 6.71 (d, ³*J*_{H,H} = 8.6 Hz, 2H, *H*_{ar,cycloph}), 6.54 (s, 1H, *H*_{ar,cycloph}), 6.02 (s, 2H, OCH₂-C_{q,anthra}), 5.02 (s, 2H, OCH₂-C_{q,OPE}), 4.08 – 4.06 (m, 4H, O-CH₂-CH₂), 4.02 – 4.00 (m, 4H, O-CH₂-CH₂) 3.44 – 3.06 (m, 16H, NCH₂), 2.60 (bs, 8H, NCH₂CH₂), 2.24 – 2.17 (m, 2H, O-CH₂-CH₂), 2.11 – 2.05 (m, 2H, O-CH₂-CH₂), 1.30 – 1.22 (m, 12H, CH₃) ppm; **¹³C NMR (151 MHz, CD₂Cl₂):** δ = 160.0 (C_q, 1C, O-C_{q,OPE}), 158.1 (C_q, 1C, COCH₂CH₂), 158.1 (C_q, 1C, COCH₂CH₂), 158.0 (C_q, 1C, COCH₂CH₂), 148.6 (C_q, 1C, CHCOCH₂CCH), 148.3 (C_q, 1C, COCH₂CH₂), 138.6 (C_q, 1C, OCH₂C_{q,OPE}), 133.7 (C_q, 1C), 133.6 (C_t, 2C, CH_{OPE}), 132.9 (C_q, 1C), 132.1 (C_t, 2C, CH_{OPE}), 132.0 (C_t, 2C, CH_{OPE}), 131.8 (C_t, 2C, CH_{OPE}), 131.8 (C_t, 2C, CH_{OPE}), 131.8 (C_q, 2C, C_{q,anthra}), 131.3 (C_q, 2C, C_{q,anthra}), 129.5 (C_t, 3C, CH₄,CH₅, CH₁₀_{anthra}), 127.7 (C_t, 2C, CH_{OPE}), 127.1 (C_t, 2C, CH_{OPE}; C_t, 2C, CH₂,CH₇_{anthra}), 127.0 (C_q, 1C, C_{q,anthra}), 126.5–126.2 (C_t, 3C, C_{q,spiro}C_qCH), 125.6 (C_t, 2C, CH₃,CH₆_{anthra}), 124.2 (C_t, 2C, CH₁,CH₈_{anthra}), 124.1 (C_q, 1C, CHC_{q,OPE}), 123.0 (C_q, 1C, CHC_{q,OPE}), 122.6 (C_q, 1C, CHC_{q,OPE}), 117.6 (hmbc, C_t, 1C, CH_{cyclo}) 115.8 (C_q, 1C, CHC_{q,OPE}), 115.4 (C_t, 2C, CH_{OPE}), 115.3– 115.1 (C_t, 6C, C_{q,spiro}C_qCHCH), 113.4 (C_t, 1C, C_qCHC_q), 113.1 (C_t, 1C, CH_{cyclo}), 91.9 (C_q, 1C, C_qC≡C), 91.4 (C_q, 1C, C_qC≡C), 89.9 (C_q, 1C, C_qC≡C), 88.2 (C_q, 1C, C_qC≡C), 70.9 (C_s, 1C, C_{q,cyclo}OCH₂C_q), 64.3 (C_s, 1C, OCH₂CH₂CH₂), 63.7 (C_s, 1C, OCH₂CH₂CH₂), 63.6 (C_s, 1C, OCH₂CH₂CH₂), 63.4 (C_s, 1C, OCH₂CH₂CH₂), 63.2 (C_s, 1C, OCH₂C_{q,anthra}), 56.0 (C_s, 8C, NCH₂), 41.9 (C_q, 1C, C_{q,spiro}), 41.7 (C_q, 1C, C_{q,spiro}), 32.3 (C_s, 2C, NCH₂CH₂), 30.1 (C_s, 2C, NCH₂CH₂), 29.6 (C_s, 1C, OCH₂CH₂CH₂), 29.6 (C_s, 1C, OCH₂CH₂CH₂), 29.1 (C_s, 2C, NCH₂CH₂), 29.0 (C_s, 2C, NCH₂CH₂), (23.1), (18.8), (14.3), (11.7), (9.4), (8.1), (7.6), 7.4 (C_p, 4C, NCH₂CH₃) ppm. C_q (4C) next to the spiro centre could not be detected, neither in ¹³C spectrum nor in the spectra of 2D experiments; The signals put into brackets could not be assigned; **HRMS (ESI, +):** calc. for C₈₆H₈₈N₂O₆ 622.3316 [M – 2PF₆]²⁺, found 622.3325.

3'-((4-((4-((4-(anthracen-9-ylmethoxy)phenyl)ethynyl)phenyl)ethynyl)benzyl)oxy)-1,1,1'',1''-tetraethyldispiro[piperidine-4,2'-4,8,12,16-tetraoxa-1,3,9,11(1,4)-tetrabenzene-cyclohexadecaphane-10',4''-piperidine]-1,1''-dium dichloride (94**)**



The hexafluorophosphate salt **131** (8.31 mg, 0.00541 mmol, 1.00 eq) was dissolved in acetonitrile (2 mL) and was subjected to an ion exchange column (Dowex 1X8, 200-400 mesh Cl⁻) eluting with acetonitrile: water 7:1. The eluate was dried *in vacuo*. The resulting yellow solid was dissolved in dichloromethane and remaining insoluble particles were filtered off yielding the target chloride salt **94** (6.10 mg, 86%).

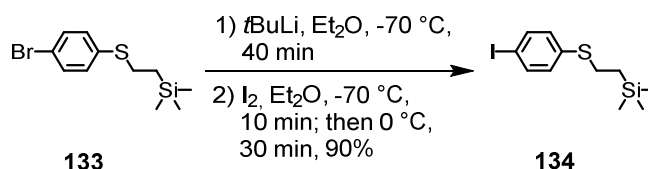
¹H NMR (500 MHz, CD₂Cl₂): δ = 8.58 (s, 1H, CH_{ar,anthra}), 8.31 – 8.28 (m, 2H, CH_{ar,anthra}), 8.10 – 8.08 (m, 2H, CH_{ar,anthra}), 7.61 – 7.46 (m, 4H, CH_{ar,anthra}; 8H, CH_{ar,OPE}), 7.29 (d, ³J_{H,H} = 8.0 Hz, 2H, CH_{ar,OPE}), 7.18 – 7.05 (m, 2H, CH_{ar,OPE}, 4H, CH_{ar,cycloph}), 6.97 (d, ³J_{H,H} = 8.9 Hz, 2H, CH_{ar,cycloph}), 6.82 – 6.67 (m, 2H, CH_{ar,cycloph}, 4H, CH_{ar,cycloph}, 2H, CH_{ar,cycloph}), 6.59 (d, ⁴J_{H,H} = 2.1 Hz, 1H, CH_{ar,cycloph}), 6.02 (s, 2H, OCH₂-C_{q,anthra}), 5.04 (s, 2H, OCH₂-C_{q,OPE}), 4.10 – 4.04 (m, 4H, O-CH₂-CH₂), 4.01 (t, ³J_{H,H} = 5.2 Hz, 4H, O-CH₂-CH₂), 3.63 – 3.33 (m, 16H, NCH₂), 2.68 (bs, 8H, NCH₂CH₂), 2.21 (t, ³J_{H,H} = 5.5 Hz, 2H, O-CH₂-CH₂), 2.08 (t, ³J_{H,H} = 5.5 Hz, 2H, O-CH₂-CH₂), 1.33 – 1.23 (m, 12H, CH₃) ppm; **HRMS (ESI, +):** calc. for C₈₆H₈₈N₂O₆ 622.3316 [M – 2Cl]²⁺, found 622.3321.

(2-((4-bromophenyl)thio)ethyl)trimethylsilane (133)

A 25 mL pressure tube was subjected to 4-bromothiophenol (**132**, 1.60 g, 8.29 mmol, 1.00 eq), vinyltrimethylsilane (3.43 g, 33.2 mmol, 4.97 mL, 4.00 eq) and AIBN (69.5 g, 0.415 mmol, 5 mol%), the pressure tube was sealed and was heated to 95 °C for 24 hrs. After allowing the reaction mixture to cool down to room temperature, excess vinyltrimethylsilane was evaporated under reduced pressure. The resulting crude brown liquid was purified by column chromatography (SiO₂; cyclohexane: ethyl acetate 5:1) to obtain a colorless liquid (2.44 g, quant.).

¹H NMR (400 MHz, CDCl₃): δ = 7.39 (d, ³J_{H,H} = 8.5 Hz, 2H, *H_{ar}*), 7.16 (d, ³J_{H,H} = 8.5 Hz, 2H, *H_{ar}*), 2.97 – 2.89 (m, 2H, CH₂), 0.95 – 0.87 (m, 2H, CH₂), 0.04 (s, 9H, CH₃) ppm; **¹³C NMR (101 MHz, CDCl₃):** δ = 136.6 (C_q, 1C), 132.0 (C_t, 2C), 130.6 (C_t, 2C), 119.5 (C_q, 1C), 29.8 (C_s, 1C), 16.9 (C_s, 1C), -1.6 (C_q, 3C) ppm; **GC-MS (EI +, 70 eV):** m/z (%) = 58 (8), 59 (5), 63 (3), 69 (3), 73 (100), 74 (12), 75 (8), 101 (11), 108 (13), 151 (3), 165 (4), 166 (5), 245 (4), 247 (4), 260 (5), 262 (5), 288 (3) [M]⁺, 290 (3) [M]⁺.

The spectroscopic data are in agreement with those previously reported.^[147]

(2-((4-iodophenyl)thio)ethyl)trimethylsilane (134)

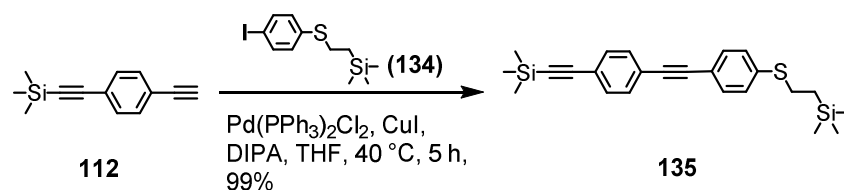
In an oven-dried 100 mL-Schlenk tube, aryl bromide **133** (510 mg, 1.76 mmol, 1.00 eq) was dissolved in dry diethyl ether (30 mL) under argon atmosphere. The solution was cooled to -70 °C via a dry ice/acetone cooling bath and the cooled solution was then slowly charged with a *tert*-butyllithium solution (1.9 M, in pentane; 1.47 g, 4.23 mmol, 2.23 mL, 2.40 eq). In

another Schlenk tube iodine (582 mg, 2.29 mmol, 1.30 eq) was dissolved in dry diethyl ether (30 mL) under argon atmosphere and was cooled to -70°C . The cooled iodine solution was then slowly cannulated to the Schlenk tube containing the reaction mixture of aryl bromide and *t*-BuLi. After stirring for another 10 min at -70°C , the mixture was allowed to warm up to room temperature and was stirred for further 30 min. The crude mixture was then washed with a conc. aq. sodium thiosulfate solution in a separation funnel. The organic layer was washed with brine and dried over sodium sulfate to afford aryl iodide **134** (531 mg, 90%) as a brown liquid.

$^1\text{H NMR}$ (400 MHz, CDCl_3): δ = 7.58 (d, $^3J_{\text{H,H}} = 8.5$ Hz, 2H, H_{ar}), 7.03 (d, $^3J_{\text{H,H}} = 8.5$ Hz, 2H, H_{ar}), 2.96 – 2.90 (m, 2H, CH_2), 0.94 – 0.88 (m, 2H, CH_2), 0.04 (s, 9H, $\text{Si}(\text{CH}_3)_3$) ppm.

The spectroscopic data are in agreement with those previously reported.^[148]

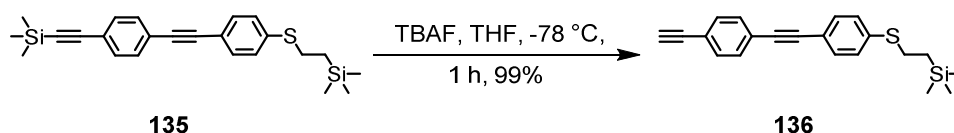
Trimethyl((4-((4-((2-(trimethylsilyl)ethyl)thio)phenyl)ethynyl)phenyl)ethynyl)silane (**135**)



An oven-dried Schlenk tube was charged with **112** (97.0 mg, 0.489 mmol, 1.70 eq) and iodo-aryl **134** (96.9 mg, 0.288 mmol, 1.00 eq) which was dissolved in dry THF (8 mL) and diisopropylamine (0.7 mL) under argon atmosphere. The mixture was degassed by flushing with argon for 10 min. Afterwards, copper iodide (1.68 mg, 8.63 μmol , 3 mol%) and bis(triphenylphosphine)palladium chloride (6.12 mg, 8.63 μmol , 3 mol%) were added and the reaction mixture was stirred at 40°C for five hrs. The solvents were removed under reduced pressure, the crude mixture was then taken up in demin. water and was extracted three times with dichloromethane. The combined organic layers were washed with brine, dried over sodium sulfate, filtered and the solvents were removed in *vacuo*. Purification via column chromatography (SiO_2 ; cyclohexane: ethyl acetate 10:1) afforded the pure product as a colorless solid (117 mg) in 99% yield.

$^1\text{H NMR}$ (400 MHz, CDCl_3): δ = 7.44 (s, 4H, H_{ar}), 7.43 – 7.40 (m, 2H, H_{ar}), 7.26 – 7.20 (m, 2H, H_{ar}), 3.07 – 2.91 (m, 2H, CH_2), 1.01 – 0.88 (m, 2H, CH_2), 0.26 (s, 9H, $\text{C}\equiv\text{CSi}(\text{CH}_3)_3$) 0.06 (s, 9H, $\text{CH}_2\text{Si}(\text{CH}_3)_3$) ppm; **$^{13}\text{C NMR}$ (101 MHz, CDCl_3):** δ = 138.8 (C_q , 1C, S- C_q), 132.0 (C_t , 2C, CH_{ar}), 132.0 (C_t , 2C, CH_{ar}), 131.5 (C_t , 2C, CH_{ar}), 127.9 (C_t , 2C, CH_{ar}), 123.5 (C_q , 1C, $\text{C}_{q,ar}$), 123.0 (C_q , 1C, $\text{C}_{q,ar}$), 119.8 (C_q , 1C, $\text{C}_{q,ar}$), 104.8 (C_q , 1C, $\text{C}\equiv\text{CC}_q$), 96.4 (C_q , 1C, $\text{C}\equiv\text{CC}_q$), 91.3 (C_q , 1C, $\text{C}\equiv\text{CC}_q$), 89.4 (C_q , 1C, $\text{C}\equiv\text{CC}_q$), 29.0 (C_s , 1C, CH_2), 16.8 (C_s , 1C, CH_2), 0.1 (C_p , 3C, $\text{C}\equiv\text{C-Si}(\text{CH}_3)_3$), -1.6 (C_p , 3C, $\text{CH}_2\text{Si}(\text{CH}_3)_3$) ppm; **GC-MS (EI +, 70 eV):** m/z (%) = 73.1 (100), 378.0 (22), 406.0 (14) $[\text{M}]^+$.

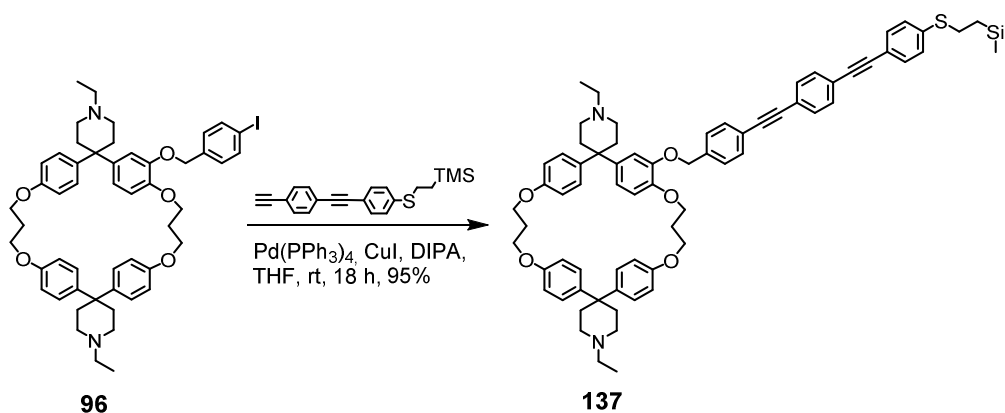
(2-((4-((4-ethynylphenyl)ethynyl)phenyl)thio)ethyl)trimethylsilane (136)



In a 10 mL-Schlenk tube, OPE **135** (126 mg, 0.310 mmol, 1.00 eq) was dissolved in dry THF (4 mL) under argon atmosphere. The solution was cooled to -78°C via a dry ice/isopropanol cooling bath. Afterwards, tetrabutylammonium fluoride solution (1 M in THF, 273 mg, 0.310 mol, 0.310 mL, 1.00 eq) was added and the resulting yellow reaction mixture was stirred for one h at -78°C . The mixture was treated with dichloromethane and water and the aqueous layer was extracted with dichloromethane three times. The combined organic layers were washed with brine, dried over sodium sulfate, filtered and the solvents were evaporated *in vacuo*. The crude yellow solid was further purified by column chromatography (SiO_2 ; cyclohexane: ethyl acetate 10:1) to obtain a colorless solid (104 mg, 99%).

$^1\text{H NMR}$ (400 MHz, CDCl_3): δ = 7.46 (s, 4H, H_{ar}), 7.43 (d, $^3J_{H,H} = 8.4$ Hz, 2H, H_{ar}), 7.24 (d, $^3J_{H,H} = 8.4$ Hz, 2H, H_{ar}), 3.17 (s, 1H, $\text{C}\equiv\text{CH}$), 3.03 – 2.94 (m, 2H, CH_2), 0.99 – 0.91 (m, 2H, CH_2), 0.06 (s, 9H, $\text{CH}_2\text{Si}(\text{CH}_3)_3$) ppm; **$^{13}\text{C NMR}$ (101 MHz, CDCl_3):** δ = 138.9 (C_q , 1C, S- C_q), 132.2 (C_t , 2C, CH_{ar}), 132.0 (C_t , 2C, CH_{ar}), 131.5 (C_t , 2C, CH_{ar}), 127.9 (C_t , 2C, CH_{ar}), 123.9 (C_q , 1C, $\text{C}_{q,ar}$), 121.9 (C_q , 1C, $\text{C}_{q,ar}$), 119.8 (C_q , 1C, $\text{C}_{q,ar}$), 91.4 (C_q , 1C, $\text{C}_q\equiv\text{C}$), 89.2 (C_q , 1C, $\text{C}_q\equiv\text{C}$), 83.4 (C_q , 1C, $\text{C}_q\equiv\text{C}$), 79.0 (C_t , 1C, $\text{C}\equiv\text{CH}$), 29.0 (C_s , 1C, CH_2), 16.8 (C_s , 1C, CH_2), -1.6 (C_p , 3C, $\text{Si}(\text{CH}_3)_3$) ppm; **GC-MS (EI +, 70 eV):** m/z (%) = 73.1 (100), 306.0 (23), 334.0 (13) $[\text{M}]^+$.

1,1''-diethyl-3'-((4-((4-((2-(trimethylsilyl)ethyl)thio)phenyl)ethynyl)phenyl)ethynyl)phenyl)ethynyl)-benzyl)oxy)dispiro[piperidine-4,2'-4,8,12,16-tetraoxa-1,3,9,11(1,4)-tetrabenzenacyclohexadecaphane-10',4''-piperidine] (137)

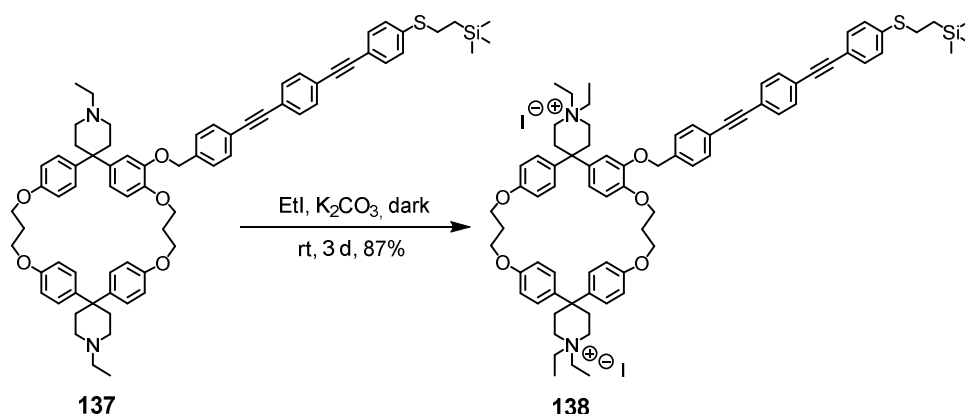


In an oven-dried Schlenk tube cyclophane **96** (58.3 mg, 0.0643 mmol, 1.00 eq) and OPE **136** (43.0 mg, 0.129 mmol, 2.00 eq) were dissolved in dry THF (4 mL) and diisopropylamine (0.7 mL) under argon atmosphere. The mixture was degassed by flushing with argon for 10 min. Afterwards, copper iodide (1.23 mg, 6.43 μmol , 10 mol%) and tetrakis(triphenylphosphine)palladium(0) (4.50 mg, 3.86 μmol , 6 mol%) were added and the reaction mixture was stirred at room temperature for 18 hrs. The solvents were removed under reduced pressure, the crude mixture was then taken up in demin. water and was extracted three times with dichloromethane. The combined organic layers were washed with brine, dried over sodium sulfate, filtered and the solvents were removed in *vacuo*. Purification via column chromatography (SiO_2 ; ethyl acetate, 5% MeOH, 1% NEt_3) yielded amine **137** (68.0 mg, 95%).

$^1\text{H NMR}$ (500 MHz, CDCl_3): δ = 7.71 – 7.67 (m, 2H, $H_{ar,OPE}$), 7.60 – 7.44 (m, 8H, $H_{ar,OPE}$, 4H), 7.31 – 7.25 (m, 2H, $H_{ar,OPE}$), 7.17 – 7.06 (m, 4H, $H_{ar,cycloph}$), 6.95 – 6.88 (m, 2H, $H_{ar,cycloph}$), 6.79 – 6.64 (m, 8H, $H_{ar,cycloph}$), 6.48 (s, 1H, $H_{ar,cycloph}$), 4.88 (s, 2H, $\text{OCH}_2\text{-C}_{q,ar}$), 4.13 – 4.05 (m, 4H, OCH_2CH_2), 4.04 – 4.01 (m, 4H, OCH_2CH_2), 3.04 – 2.97 (m, 2H, SCH_2), 2.91 – 2.24 (m, 16H, NCH_2CH_2 , NCH_2CH_2 ; 4H, NCH_2CH_3), 2.24 – 2.16 (m, 2H, $\text{OCH}_2\text{CH}_2\text{CH}_2$), 2.12 – 2.07 (m, 2H, $\text{OCH}_2\text{CH}_2\text{CH}_2$), 1.11 – 1.06 (m, 6H, NCH_2CH_3), 0.99 – 0.93 (m, 2H, SCH_2CH_2), 0.08 (s, 9H, $\text{Si}(\text{CH}_3)_3$) ppm; **$^{13}\text{C NMR}$ (126 MHz, CDCl_3):** δ = (177.2), 156.9 (C_q , 1C), 156.9 (C_q , 1C), 156.8 (C_q , 1C), 147.4 (C_q , 1C), 147.3 (C_q , 1C), 138.8 (C_q , 4C), 138.2 (C_q , 1C), (133.0), 132.2 (C_t , 2C), 132.1 (C_t , 2C), (132.0), 132.0 (C_t , 2C), 132.0 (C_t , 2C), (131.7), 131.7 (C_t , 2C), (131.6), 128.6 (C_t , 2C), 128.5 (C_t , 2C), 127.8 (C_t , 2C), 127.0 (C_t , 2C), 123.3 (C_q , 1C), 123.0 (C_q , 1C), 122.2 (C_q , 1C), 119.7 (C_q , 1C), 114.5 (C_t , 6C), 114.4 (C_t , 2C), 91.3 (C_q , 1C), 91.3 (C_q , 1C), 89.5 (C_q , 1C), 89.4 (C_q , 1C), 70.6 (C_s , 1C), 63.4 (C_s ,

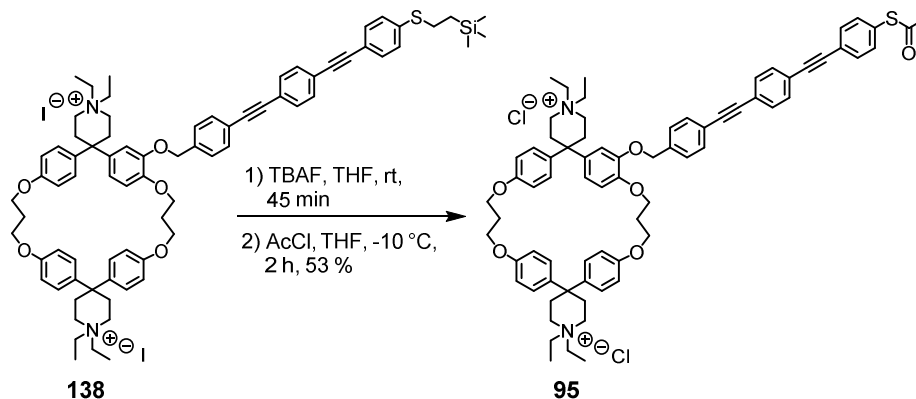
1C), 63.2 (C_s, 1C), 63.1 (C_s, 1C), 58.7 (C_s, 1C), 52.2 (C_s, 2C), 49.7 (C_s, 2C), 49.7 (C_s, 2C), 42.8 (C_q, 1C), 42.5 (C_q, 1C), 34.6 (C_s, 2C), 34.5 (C_s, 2C), (29.8), 29.6 (C_s, 1C), 29.6 (C_s, 1C), 28.9 (C_s, 1C), (23.5), (22.8), 16.7 (C_s, 1C), 11.6 (C_s, 1C), 11.6 (C_s, 1C), (8.4), -1.7 (C_p, 3C) ppm. This assignment is not based on 2D NMR experiments, it was derived from the spectra of derivatives of amine **137**. The signal of one C_t at the threefold substituted aromatic ring, which would be expected at ~ 120 ppm, was not observed in the spectrum. The signals in brackets correspond to impurity.

1,1,1'',1''-tetraethyl-3'-((4-((4-((4-((2-(trimethylsilyl)ethyl)thio)phenyl)ethynyl)phenyl)ethynyl)benzyl)oxy)dispiro[piperidine-4,2'-4,8,12,16-tetraoxa-1,3,9,11(1,4)-tetrabenzenacyclohexadecaphane-10',4''-piperidine]-1,1''-dium iodide (138)



In a one-neck flask, amine **137** (68.0 mg, 0.0611 mmol, 1.00 eq) was charged with freshly distilled iodoethane (2.47 mL, 30.6 mmol, 500 eq) and potassium carbonate (17.9 mg, 0.128 mmol, 2.10 eq). The resulting suspension was stirred in the dark for 3 days at room temperature. Afterwards, the excessive iodoethane was removed under reduced pressure. The resulting yellow crude mixture was then taken up in THF and the insoluble solid was filtered off. The solution was dried *in vacuo* and the resulting product (75.4 mg, 87%) was directly used in the next step without further purification.

3'-((4-((4-((4-(acetylthio)phenyl)ethynyl)phenyl)ethynyl)benzyl)oxy)-1,1,1',1''-tetraethyl-di-spiro[piperidine-4,2'-4,8,12,16-tetraoxa-1,3,9,11(1,4)-tetrabenzenacyclohexadecaphane-10',4''-piperidine]-1,1''-dium chloride (95)

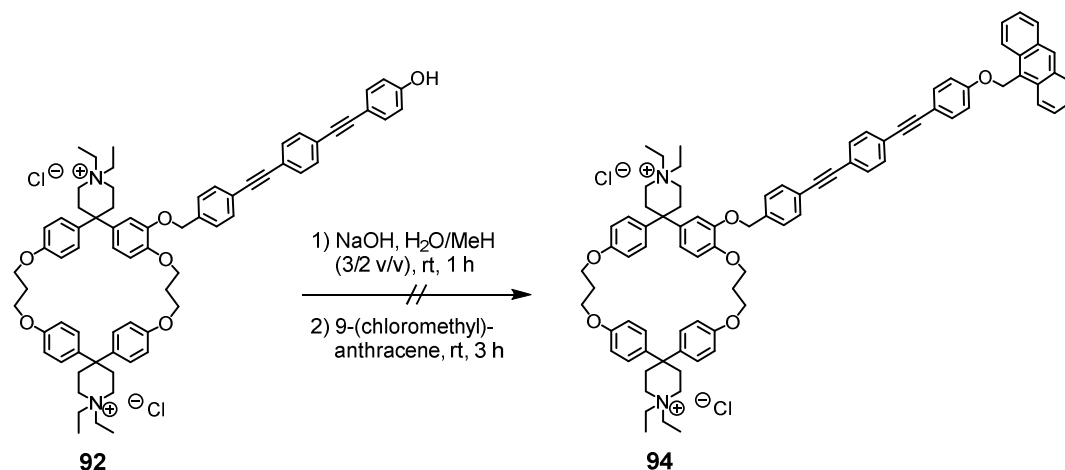


An oven-dried Schlenk tube was charged with the quaternary ammonium salt **138** (45.0 mg, 0.0316 mmol, 1.00 eq) which was dissolved in dry THF (2.5 mL) in an inert atmosphere. The solution was rigorously degassed by flushing with argon, before tetrabutylammonium fluoride (1 M in THF, 2.48 mg, 0.0947 mmol, 2.81 mL, 3.00 eq) was added, which caused the former colorless solution to turn orange immediately. After 45 min of stirring at room temperature, the reaction mixture was cooled down to $-10\text{ }^\circ\text{C}$ and afterwards, previously degassed acetyl chloride (55.0 mg, 0.694 mmol, 0.050 mL, 22.0 eq), was added dropwise which caused a subsequent color change to yellow. After further two hrs in the cooling bath, the reaction was cautiously quenched by the addition of saturated NaHCO_3 solution (0.6 mL). The solvents were evaporated under reduced pressure. The resulting crude product was further purified three times by column chromatography (SiO_2 -C18; acetonitrile, 10% water; then acetonitrile 10% water, 2% 1 M NH_4Cl solution), the fractions containing target compound were concentrated and the resulting solid was then taken up in some demin. water. The poorly soluble target compound was separated from the aqueous ammonium salt solution by centrifugation affording **95** (20.0 mg) as a pale yellow solid in 53% yield.

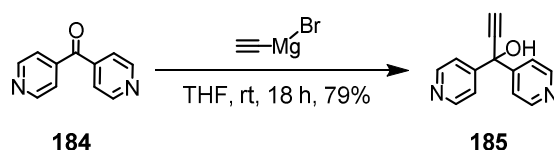
^1H NMR (700 MHz, Deuterium Oxide): δ = 7.72 (d, $^3J_{\text{H,H}} = 8.2$ Hz, 2H, $H_{\text{ar,OPE}}$), 7.71 – 7.65 (m, 4H, $H_{\text{ar,OPE}}$), 7.55 (d, $^3J_{\text{H,H}} = 8.2$ Hz, 2H, $H_{\text{ar,OPE}}$), 7.49 (d, $^3J_{\text{H,H}} = 8.0$ Hz, 2H, $H_{\text{ar,OPE}}$), 7.28 (d, $^3J_{\text{H,H}} = 7.9$ Hz, 2H, $H_{\text{ar,OPE}}$), 7.25 – 7.22 (m, 4H, $H_{\text{ar,cycloph}}$), 7.00 (d, $^3J_{\text{H,H}} = 8.5$ Hz, 2H, $H_{\text{ar,cycloph}}$), 6.90 (d, $^3J_{\text{H,H}} = 8.4$ Hz, 4H, $H_{\text{ar,cycloph}}$), 6.86 (d, $^3J_{\text{H,H}} = 8.3$ Hz, 2H, $H_{\text{ar,cycloph}}$), 6.75 (d, $^3J_{\text{H,H}} = 8.3$ Hz, 2H, $H_{\text{ar,cycloph}}$), 6.64 (s, 1H, $H_{\text{ar,cycloph}}$), 5.15 (s, 2H, $\text{OCH}_2\text{-C}_{\text{q,ar}}$), 4.07 (t, $^3J_{\text{H,H}} = 5.3$ Hz, 2H, OCH_2CH_2),

4.04 (t, $^3J_{H,H} = 5.3$ Hz, 2H, OCH₂CH₂), 3.33 (bs, 8H, NCH₂CH₃, 8H, NCH₂CH₂), 2.66 (bs, 8H, NCH₂CH₂), 2.50 (s, 3H, C=OCH₃), 1.23 (t, $^3J_{H,H} = 6.7$ Hz, 12H, NCH₂CH₃) ppm. The signals for the two OCH₂ protons are located below the water signal at 4.17 ppm; HRMS (ESI, +): calc. for C₇₃H₈₀N₂O₆S 556.2863 [M – 2Cl]²⁺, found 556.2867.

Experiment to Stopper Aggregates of Amphiphile **92**



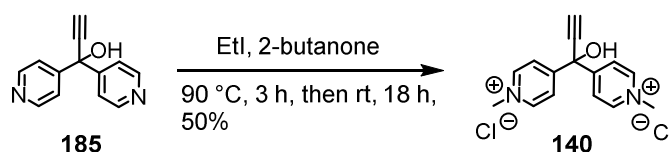
Amphiphile **92** (1.30 mg, 1.15 μmol, 1.00 eq) was placed into a 10 mL flask and dissolved in 5.0 mL of water/methanol (60/40 v/v). Sodium hydroxide (0.06 mg, 1.38 μmol, 1.30 eq) was added and the resulting yellow suspension was stirred for 1 hour at room temperature. The mixture was charged with 9-(chloromethyl)anthracene (0.782 mg, 0.00345 mmol, 3.00 eq) and the mixture was stirred for additional three hours at room temperature. Reaction control via HPLC-ESI-MS only showed a signal corresponding to amphiphile **92** (*m/z* = 527). Neither stoppered aggregates or stoppered monomer (**94**), nor 9-(chloromethyl)anthracene was detected.

1,1-Di-4-pyridylprop-2-yn-1-ol (185)

Ethynylmagnesium bromide (0.5 mM in THF, 0.117 mmol, 0.234 mL, 1.20 eq) was added under argon atmosphere to a 10 mL Schlenk tube containing in 1.8 mL dry THF dissolved di-4-pyridylmethanone (**184**, 18.0 mg, 0.0977 mmol, 1.00 eq). After stirring overnight, the reaction mixture was quenched with aqueous 2 M ammonium chloride solution. The product was extracted three times with dichloromethane, the combined organic layers were washed with brine, dried over sodium sulfate, filtered and the solvent was removed under reduced pressure. The pale brown solid was recrystallized from methanol:chloroform 1:1 by layered addition of light petroleum to afford product **185** as a light beige colored solid in 79% yield.

¹H NMR (400 MHz, Methanol-*d*₄): δ = 8.51 (m, 4H, *H_{ar}*), 7.71 – 7.66 (m, 4H, *H_{ar}*), 3.50 (s, 1H, C≡CH) ppm; ¹³C NMR (101 MHz, MeOD): δ = 155.7 (C_q, 2C), 150.4 (C_t, 4C), 122.4 (C_t, 4C), 85.1 (C_q, 1C), 78.2 (C_t, 1C), 73.0 (C_q, 1C) ppm.

The spectroscopic data are in agreement with those previously reported.^[128]

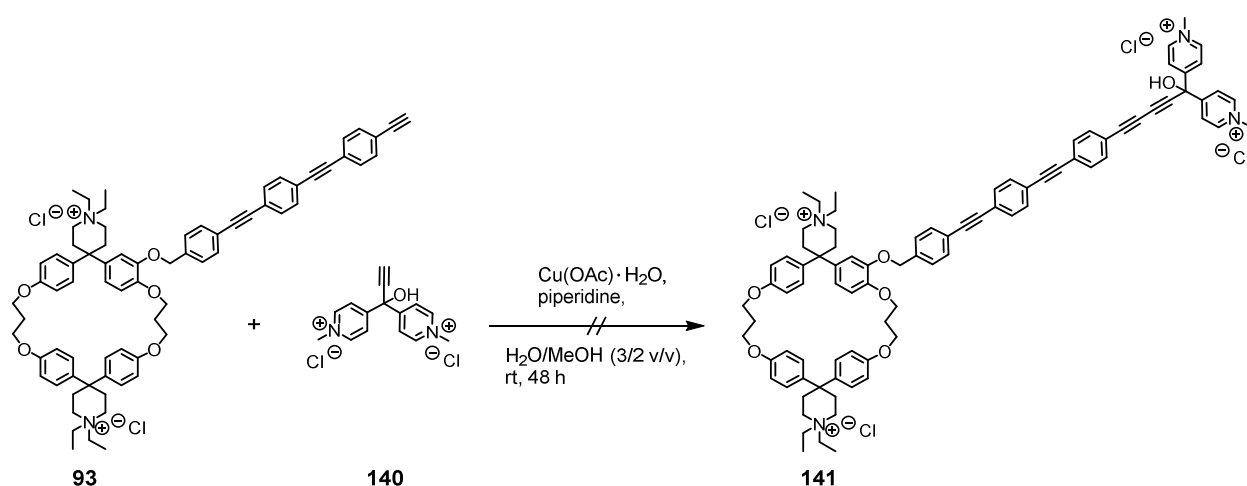
4,4'-(1-hydroxyprop-2-yne-1,1-diyl)bis(1-methylpyridin-1-ium) (140)

Stopper **140** was synthesized according to a slightly modified synthetic procedure for the analogue of **140** comprising a phenylene ethynylene unit:^[128] In a two-neck flask equipped with a reflux condenser, methyl iodide (0.17 mL, 381 mg, 2.66 mmol, 100 eq) was added to a solution of **185** (5.59 mg, 0.0266 mmol, 1.00 eq) in 3.0 mL 2-butanone. The mixture was left at 90 °C for three hours and was then stirred at room temperature overnight. After filtering the resulting dark purple precipitate, the solid was dissolved in water:methanol (1:1 v/v) and

passed through an ion exchange column (DOWEX 1X8, 200-400 mesh, Cl⁻) with the same binary solvent mixture as eluent. Recrystallization from methanol by layer addition of diisopropyl ether yielded 4.1 mg of dark red compound **140** (50%).

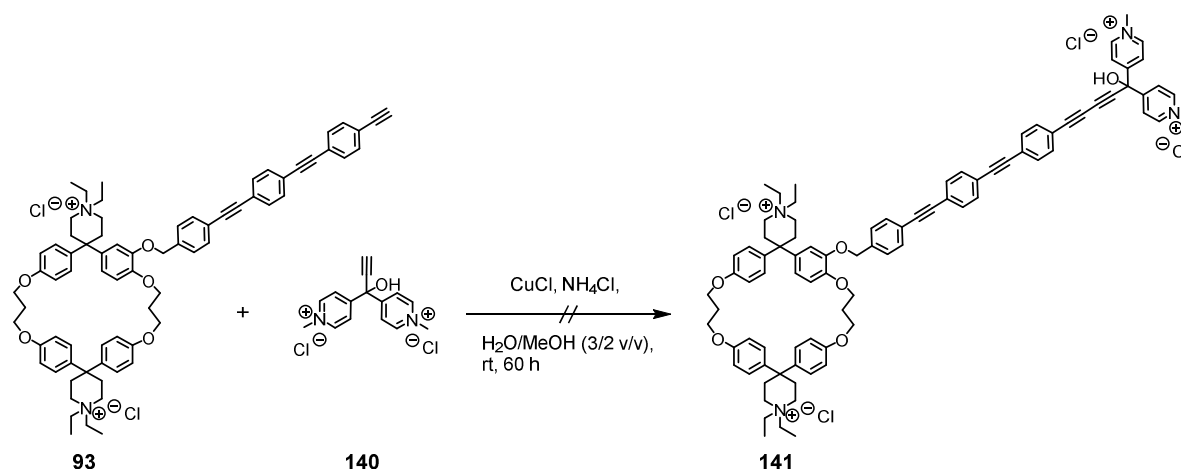
¹H NMR (400 MHz, Methanol-*d*₄): δ = 8.98 – 8.92 (m, 4H, *H_{ar}*), 8.42 – 8.37 (m, 4H, *H_{ar}*), 4.40 (s, 6H, NCH₃), 3.94 (s, 1H, C≡CH) ppm.

Experiment to Stopper Aggregates of Amphiphile **93** via Glaser Coupling Using Copper(II) Acetate



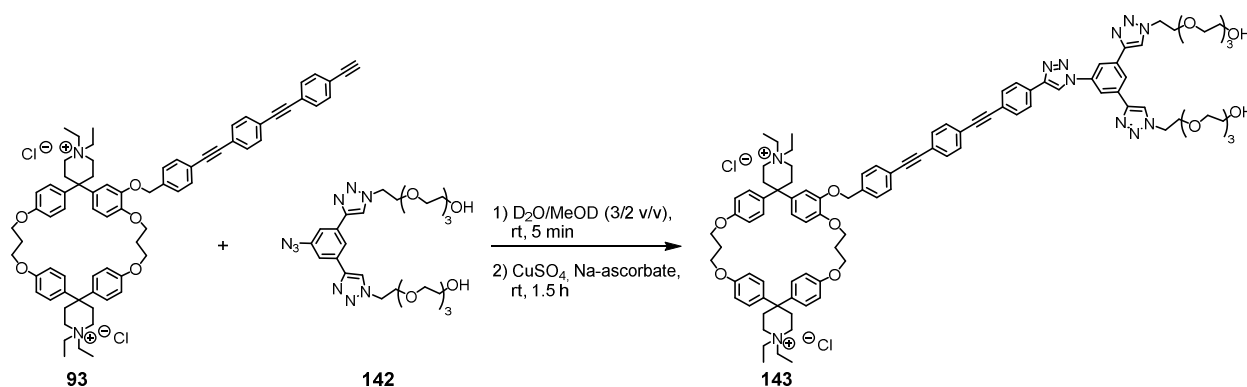
The stoppering experiment was performed according to a modified previously reported synthetic protocol for Glaser coupling:^[153] In a 10 mL flask amphiphile **93** (1.50 mg, 0.00132 mmol, 1.00 eq) was dissolved in 1.3 mL of a H₂O/MeOH (60/40 v/v) (resulting c = 1 mM). Stopper **140** (4.11 mg, 0.0132 mmol, 10.0 eq) was added, the solution was charged with copper(II) acetate monohydrate (0.054 mg, 0.264 μmol, 0.20 eq) and piperidine (0.227 mg, 2.64 μmol, 2.00 eq) and was stirred at 25 °C under air for two days. The recorded HPLC-ESI-MS chromatogram did not show conversion of **93**.

Experiment to Stopper Aggregates of Amphiphile **93** via Glaser-Hay Coupling Using Copper(I) Chloride



The stoppering experiment was performed according to a modified, previously reported synthetic protocol for Glaser coupling:^[128] A solution of amphiphile **93** (1.50 mg, 1.32 μmol , 1.00 eq) and stopper **140** (1.50 mg, 1.32 μmol , 1.00 eq) in 1.3 mL $\text{H}_2\text{O/MeOH}$ (60/40 v/v) was charged with copper(I) chloride (26.9 mg, 0.264 mmol, 200 eq) and ammonium chloride (14.3 mg, 0.264 mmol, 200 eq). The mixture was vigorously stirred at room temperature under air. After 60 hrs reaction duration, reaction control via HPLC-ESI-MS was performed, whereas only a signal corresponding to unreacted amphiphile **93** ($m/z = 531$) could be identified in the chromatogram of low intensity. Neither m/z values corresponding to stopper, nor to trapped monomer (**141**), dimer or trimer could be observed.

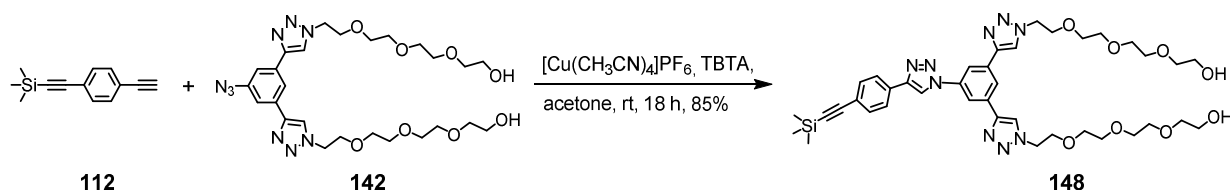
Experiment to Stopper Aggregates of Amphiphile **93** via *Click* Chemistry



In a NMR tube free acetylene-substituted monomer **93** (0.50 mg, 4.41×10^{-4} mmol, 1.00 eq) was dissolved in 0.8 mL of a D_2O/CD_3OD (60/40 v/v) mixture, resulting in a concentration of $c = 0.55$ mM. After degassing with argon for five min at room temperature, stopper **142** (0.40 mg, 6.61×10^{-4} mmol, 1.50 eq) was added and the resulting yellow suspension was charged with copper(II) sulfate (0.07 mg, 4.41×10^{-4} mmol, 1.00 eq) and L(+)-ascorbic acid sodium salt (0.09 mg, 4.41×10^{-4} mmol, 1.00 eq) and was degassed again for two min. The solution was stirred for 1.5 hrs, when the HPLC-ESI-MS chromatogram indicated full conversion of free acetylene **93** to the stoppered monomer **143**.

LC-MS (ESI, +): $m/z = 557.0$ (48), 606.4 (26) [**142**+H]⁺, 628.4 (18) [**142**+Na]⁺, 834.6 (75), 835.0 (100) [**143**+H]⁺, 835.4 (59).

2,2'-((((((((5-(4-(4-((trimethylsilyl)ethynyl)phenyl)-1H-1,2,3-triazol-1-yl)-1,3-phenylene)-bis(1H-1,2,3-triazole-4,1-diyl))bis(ethane-2,1-diyl))bis(oxy))bis(ethane-2,1-diyl))bis(oxy))-bis(ethane-2,1-diyl))bis(oxy))bis(ethan-1-ol) (148**)**

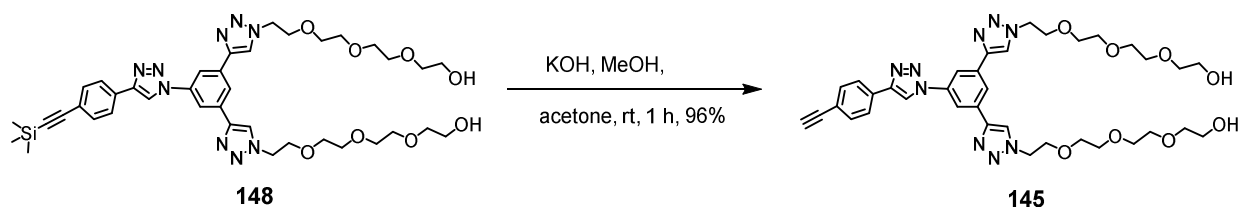


In a 10 mL Schlenk tube OPE precursor **112** (90.1 mg, 0.454 mmol) and stopper **142** (250 mg, 0.413 mmol) were dissolved in acetone (3.5 mL). After flushing argon into the orange solution for 10 min, $[Cu(CH_3CN)_4]PF_6$ (61.6 mg, 0.165 mmol, 0.4 eq) and TBTA (87.7 mg, 0.165 mmol, 0.4 eq) were added. The mixture was degassed again for 2 min and was stirred at room temperature for 18 hrs. LC-ESI-MS indicated full conversion of stopper **142**. Without previous workup of the reaction mixture column chromatography (SiO_2 ; ethyl acetate: methanol 5:2) was performed. The eluents were evaporated *in vacuo*, resulting in a mixture of target compound and silica which was then dissolved in ethyl acetate and the insoluble silica was filtered off to yield **148** as a colorless oil (281 mg, 85%).

¹H NMR (400 MHz, CD_3CN): $\delta = 8.83$ (s, 1H, $H_{triazol}$), $8.40 - 8.39$ (m, 3H, $H_{triazol}$, H_{ar}), $8.29 - 8.28$ (m, 2H, H_{ar}), 7.93 (d, $^3J_{H,H} = 8.3$, 2H, H_{ar}), $7.57 - 7.50$ (m, 2H, H_{ar}), 4.59 (dd, $^3J_{H,H} = 5.7, 4.4$ Hz,

4H, CH₂), 3.92 (dd, ³J_{H,H} = 5.7, 4.4 Hz, 4H, CH₂), 3.63 – 3.45 (m, 20H, CH₂), 3.40 (dd, ³J_{H,H} = 5.4, 4.1 Hz, 4H, CH₂), 2.89 (t, ³J_{H,H} = 5.8 Hz, 2H, CH₂), 0.26 (s, 9H, Si(CH₃)₃) ppm. **¹³C NMR (101 MHz, CD₃CN):** δ = 148.0, 146.5, 139.1, 134.5, 133.3, 131.8, 126.5, 123.5, 123.4, 123.0, 120.7, 117.0, 105.7, 95.9, 73.2, 71.1 (2 signals), 71.0, 71.0, 69.9, 61.9, 51.3, -0.1 ppm; **LC-MS (ESI, +):** m/z (%) = 804.4 (23.4) [M + H]⁺, 805.4 (11.2), 826.4 (100), 827.4 (46.1) [M + Na]⁺, 828.4 (13.9); **HRMS (ESI, +):** calc. for C₃₉H₅₄N₉O₈Si 804.3859 [M+H]⁺, found 804.3864.

2,2'-((((((((5-(4-(4-ethynylphenyl)-1H-1,2,3-triazol-1-yl)-1,3-phenylene)bis(1H-1,2,3-triazole-4,1-diyl))bis(ethane-2,1-diyl))bis(oxy))bis(ethane-2,1-diyl))bis(oxy))bis(ethane-2,1-diyl))bis(oxy))bis(ethane-1-ol) (145)

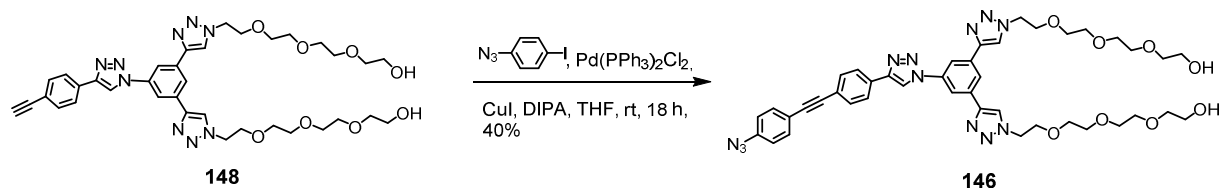


148 (93.0 mg, 0.116 mmol) was dissolved in a 1:1 mixture of acetone: methanol (5 mL). Potassium hydroxide (9.19 mg, 0.139 mmol) was added and the resulting suspension was stirred at room temperature for 1 hour. The mixture was filtered and the filtrate was diluted with ethyl acetate (20 mL) and charged with demin. water (5 mL), the aqueous layer was extracted three times with each 20 mL of ethyl acetate. The combined organic layers were washed with brine, dried over sodium sulfate, filtered and the solvents were evaporated under reduced pressure. **145** was obtained as a pale yellow oil (81.3 mg, 96%).

¹H NMR (400 MHz, CD₃CN): δ = 8.88 (s, 1H, *H*_{triazol}), 8.43 (t, ⁴J_{H,H} = 1.5 Hz, 1H, *H*_{ar}), 8.42 (s, 2H, *H*_{triazol}), 8.33 (d, ⁴J_{H,H} = 1.5 Hz, 2H, *H*_{ar}), 7.97 (d, ³J_{H,H} = 8.5 Hz, 1H, *H*_{ar}), 7.62 (d, ³J_{H,H} = 8.4 Hz, 1H, *H*_{ar}), 4.60 (t, ³J_{H,H} = 5.1 Hz, 4H, CH₂), 3.93 (t, ³J_{H,H} = 5.1 Hz, 4H, CH₂), 3.63 – 3.59 (m, 4H, CH₂), 3.58 – 3.54 (m, 4H, CH₂), 3.54 – 3.48 (m, 12H, CH₂), 3.41 (dd, ³J_{H,H} = 5.5, 4.1 Hz, 4H, CH₂), 3.28 (s, 1H, C≡CH) ppm; **¹³C NMR (101 MHz, CD₃CN):** δ = 148.0, 146.5, 139.1, 134.6, 133.6, 132.1, 126.5, 123.5, 123.1, 122.7, 120.8, 118.3, 117.0, 84.0, 79.7, 73.2, 71.1 (2 signals), 71.0, 70.9, 69.9, 61.9, 51.3 ppm; **LC-MS (ESI, +):** m/z (%) = 732.4 (100) [M+H]⁺, 733.4 (46), 734.4 (12),

754.4 (54) $[M+Na]^+$, 755.4 (25), 1463.7 (18), 1464.7 (15), 1485.6 (10); **HRMS (ESI, +)**: calc. for $C_{36}H_{46}N_9O_8$ 732.3464 $[M+H]^+$, found 732.3465.

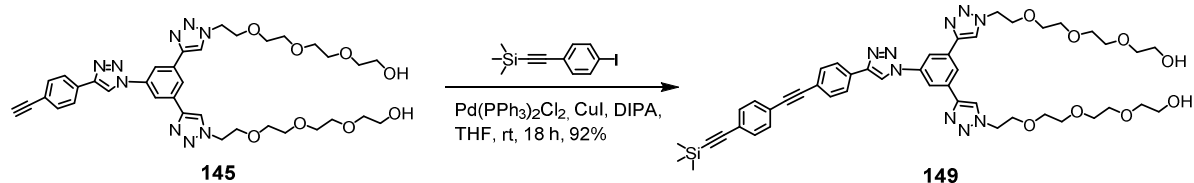
2,2'-((((((((5-(4-(4-((4-azidophenyl)ethynyl)phenyl)-1H-1,2,3-triazol-1-yl)-1,3-phenylene)-bis(1H-1,2,3-triazole-4,1-diyl))bis(ethane-2,1-diyl))bis(oxy))bis(ethane-2,1-diyl))bis(oxy))-bis(ethane-2,1-diyl))bis(oxy))bis(ethan-1-ol) (146)



In an oven-dried Schlenk tube, **148** (40 mg, 0.0547 mmol) and 1-azido-4-iodobenzene (0.109 mL of a 0.5 M in *tert*-butyl methyl ether, 0.0547 mmol) were dissolved in dry THF (2 mL) and diisopropylamine (0.7 mL) in argon atmosphere. The mixture was degassed by flushing with argon for 10 min. Afterwards, copper iodide (0.314 mg, 1.64 μ mol, 3 mol%) and bis-(triphenylphosphine)palladium chloride (1.16 mg, 1.64 μ mol, 3 mol%) were added and the reaction mixture was stirred at room temperature for 18 hrs. TLC (SiO_2 ; ethyl acetate: methanol 5:2) indicated full conversion of **148**. Column chromatography (SiO_2 ; ethyl acetate: methanol 5:2) was performed, by subjecting the crude reaction mixture without previous workup to the column. A yellow solid (18.5 mg) was obtained in a yield of 40%.

1H NMR (400 MHz, CD_3CN): δ = 8.91 (s, 1H, $CH_{triazole}$), 8.45 (t, $^4J_{H,H}$ = 1.5 Hz, 1H, CH_{ar}), 8.44 (s, 2H, $CH_{triazole}$), 8.35 (d, $^4J_{H,H}$ = 1.5 Hz, 2H, CH_{ar}), 8.01 (d, $^3J_{H,H}$ = 8.3 Hz, 2H, CH_{ar}), 7.66 (d, $^3J_{H,H}$ = 8.3 Hz, 2H, CH_{ar}), 7.58 (d, $^3J_{H,H}$ = 8.6 Hz, 2H, CH_{ar}), 7.12 (d, $^3J_{H,H}$ = 8.6 Hz, 2H, CH_{ar}), 4.62 (t, $^3J_{H,H}$ = 5.5 Hz, 4H, NCH_2), 3.93 (t, $^3J_{H,H}$ = 5.5 Hz, 4H, NCH_2CH_2), 3.65 – 3.47 (m, 20H, OCH_2), 3.44 – 3.41 (m, 4H, OCH_2), 2.97 (s, 2H, OH) ppm; **^{13}C NMR (101 MHz, CD_3CN)**: δ = 148.1, 146.5, 141.4, 139.0, 134.5, 134.0, 133.0, 131.5, 126.6, 123.5, 123.5, 123.0, 120.6, 120.3, 116.9, 100.9, 90.3, 90.1, 73.1, 71.0, 71.0, 70.9, 70.8, 69.9, 61.8, 51.2 ppm; **LC-MS (ESI, +)**: m/z = 837.4 (27), 838.4 (15), 849.5 (57) $[M+H]^+$, 850.4 (31), 853.4 (24), 854.4 (13), 859.4 (53), 860.4 (30), 861.4 (11), 871.5 (100) $[M+Na]^+$, 872.4 (54), 873.4 (17), 875.4 (42), 876.4 (23); **HRMS (ESI, +)**: calc. for $C_{42}H_{48}N_{12}NaO_8$ 871.3610 $[M+Na]^+$, found 871.3608.

2,2'-((((((((5-(4-(4-((4-((trimethylsilyl)ethynyl)phenyl)ethynyl)phenyl)-1H-1,2,3-triazol-1-yl)-1,3-phenylene)bis(1H-1,2,3-triazole-4,1-diyl))bis(ethane-2,1-diyl))bis(oxy))bis(ethane-2,1-diyl))bis(oxy))bis(ethane-2,1-diyl))bis(oxy))bis(ethane-2,1-diyl))bis(oxy))bis(ethan-1-ol) (149)



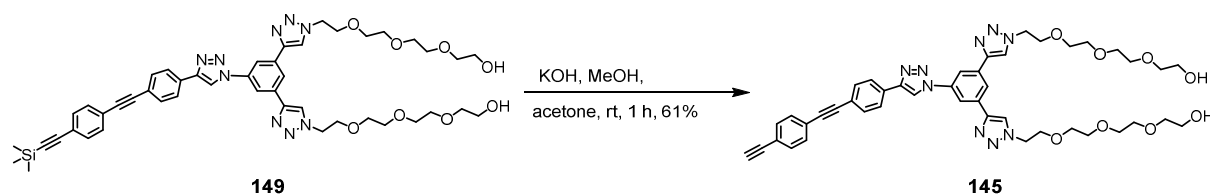
An oven-dried Schlenk tube was charged with **145** (11.0 mg, 0.0150 mmol, 1.00 eq) and (4-iodophenylethynyl)trimethylsilane (4.64 mg, 0.0150 mmol, 1.00 eq) which was dissolved in dry THF (10 mL) and diisopropylamine (3 mL) in argon atmosphere. The mixture was degassed by flushing with argon for 10 min. Afterwards, copper iodide (0.0861 mg, 0.45 μmol , 3 mol%) and bis(triphenylphosphine)palladium chloride (0.319 mg, 0.45 μmol , 3 mol%) were added and the reaction mixture was stirred at room temperature for 18 hrs. The solvents were removed under reduced pressure, the crude mixture was then taken up in demin. water and was extracted three times with ethyl acetate. The combined organic layers were washed with brine, dried over sodium sulfate, filtered and the solvents were removed in *vacuo*. Purification via column chromatography (SiO_2 ; ethyl acetate: methanol 5:2), dissolving the solvent-freed product fractions in ethyl acetate separation and filtering off silica afforded the pure product as a yellow solid (39.3 mg) in 92% yield.

$^1\text{H NMR}$ (400 MHz, CD_3CN): δ = 9.06 (s, 1H, $\text{CH}_{\text{triazole}}$), 8.57 (s, 2H, $\text{CH}_{\text{triazole}}$), 8.42 (t, $^4J_{\text{H,H}}$ = 1.5 Hz, 1H, CH_{ar}), 8.33 (d, $^4J_{\text{H,H}}$ = 1.5 Hz, 2H, CH_{ar}), 8.05 – 7.98 (m, 2H, CH_{ar}), 7.63 (d, $^3J_{\text{H,H}}$ = 7.0 Hz, 2H, CH_{ar}), 7.58 – 7.51 (m, 2H, CH_{ar}), 7.51 – 7.46 (m, 2H, CH_{ar}), 4.63 (t, $^3J_{\text{H,H}}$ = 5.0 Hz, 4H, OCH_2), 3.97 (t, $^3J_{\text{H,H}}$ = 5.1 Hz, 4H, OCH_2), 3.71 – 3.46 (m, 24H, OCH_2), 2.93 (s, 2H, OH), 0.27 (s, 9H, C) ppm;

$^{13}\text{C NMR}$ (101 MHz, CD_3CN): δ = 148.0, 146.5, 139.0, 134.3, 133.1, 132.8, 132.5, 131.8, 126.6, 124.2, 123.8, 123.8, 123.2, 122.9, 120.9, 116.9, 105.2, 97.3, 92.1, 90.3, 72.8, 70.9, 70.7, 70.6, 70.5, 70.0, (68.7), (68.3), 61.5, 51.2, (30.3), (21.3), (21.1), (19.5), (18.7), (14.5), -0.2 ppm. The signals in brackets correspond to impurity; **LC-MS (ESI, +):** m/z = 904.5 (57) $[\text{M}+\text{H}]^+$, 905.5 (37),

906.5 (15), 926.5 (100) $[M+Na]^+$, 927.5 (64), 928.5 (25); **HRMS (ESI, +)**: calc. for $C_{47}H_{57}N_9NaO_8Si$ 926.3992 $[M+Na]^+$, found 926.3990.

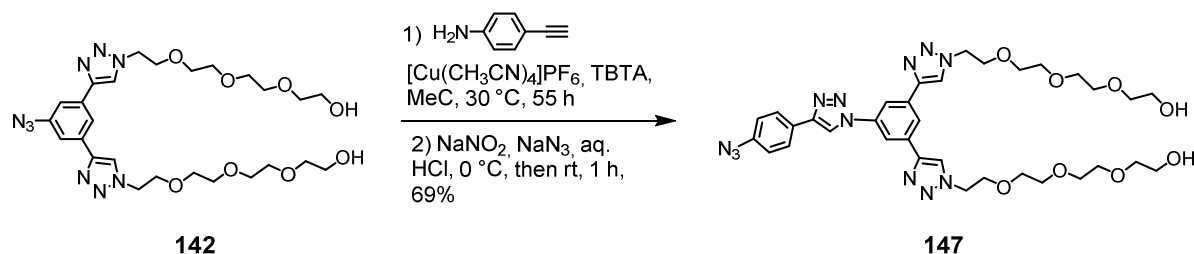
2,2'-((((((((5-(4-(4-((4-ethynylphenyl)ethynyl)phenyl)-1H-1,2,3-triazol-1-yl)-1,3-phenylene)-bis(1H-1,2,3-triazole-4,1-diyl))bis(ethane-2,1-diyl))bis(oxy))bis(ethane-2,1-diyl))bis(oxy))-bis(ethane-2,1-diyl))bis(oxy))bis(ethan-1-ol) (144)



In a 10 mL round-neck flask reactant **149** (12.5 mg, 0.0138 mmol, 1.00 eq) was dissolved in a mixture of acetone (3.0 mL) and methanol (1.5 mL). The solution was charged with potassium carbonate (3.81 mg, 0.0276 mmol, 2.00 eq) and was stirred at room temperature. According to HPLC-ESI-MS, the reaction was completed after one hour. Excess potassium carbonate was filtered off and was washed with methanol. The solvents of the filtrate were removed under reduced pressure yielding a yellow solid (7.00 mg, 61%).

1H NMR (400 MHz, CD_3CN): δ = 9.21 (s, 1H, $CH_{triazole}$), 8.67 (s, 2H, $CH_{triazole}$), 8.49 (t, $^4J_{H,H}$ = 1.5 Hz, 1H, CH_{ar}), 8.41 (d, $^4J_{H,H}$ = 1.5 Hz, 2H, CH_{ar}), 8.10 – 8.05 (m, 2H, CH_{ar}), 7.66 (d, $^3J_{H,H}$ = 8.4 Hz, 2H, CH_{ar}), 7.54 (d, $^3J_{H,H}$ = 3.9 Hz, 4H, CH_{ar}), 4.69 – 4.62 (m, 4H, OCH_2), 3.97 – 3.95 (m, 4H, OCH_2), 3.68 – 3.46 (m, 24H, OCH_2), 2.91 (s, 2H, OH) ppm; **^{13}C NMR (101 MHz, CD_3CN)**: δ = 148.1, 146.6, 139.1, 134.4, 133.1, 133.1, 132.5, 131.9, 126.7, 124.4, 124.1, 124.1, 123.3, 123.0, 121.2, 117.1, 100.9, 83.6 (2 signals), 80.9, 72.4, 70.7, 70.4, 70.2, 68.6, 61.2, 51.1, (19.5), (19.2) ppm; **LC-MS (ESI, +)**: m/z (%) = 416.7 (88), 417.2 (48), 417.7 (15), 427.7 (11), 832.5 (100) $[M+H]^+$, 833.4 (55), 834.4 (16), 854.4 (59) $[M+Na]^+$, 855.4 (33); **HRMS (ESI, +)**: calc. for $C_{44}H_{49}N_9NaO_8$ 854.3596 $[M+Na]^+$, found 854.3607.

2,2'-((((((((5-(4-(4-azidophenyl)-1H-1,2,3-triazol-1-yl)-1,3-phenylene)bis(1H-1,2,3-triazole-4,1-diyl))bis(ethane-2,1-diyl))bis(oxy))bis(ethane-2,1-diyl))bis(oxy))bis(ethane-2,1-diyl))-bis(oxy))bis(ethane-1-ol) (147)



A 10 mL Schlenk tube was charged with 4-ethynylaniline (15.0 mg, 0.124 mmol) and stopper molecule **142** (75.1 mg, 0.124 mmol) and were dissolved in acetonitrile (3.0 mL) under argon atmosphere. After flushing argon into the solution for 10 min, $[\text{Cu}(\text{CH}_3\text{CN})_4]\text{PF}_6$ (9.24 mg, 0.0248 mmol, 0.2 eq) and TBTA (13.2 mg, 0.0248 mmol, 0.2 eq) were added. The mixture was degassed again for 2 min and was stirred at room temperature over the weekend (55 hrs). The reaction mixture was diluted with ethyl acetate (30 mL), treated with demin. water (10 mL) and the aqueous layer was extracted three times with ethyl acetate (30 mL each). The combined organic phases were washed with brine, dried over sodium sulfate, filtered and the solvents were removed in *vacuo*. The formed amine was dissolved in half concentrated aq. hydrochloric acid (4 mL) and cooled to 0 °C. Sodium nitrite was added in small portions. The reaction mixture was stirred at 0 °C for 20 min, before sodium azide was added portion-wise at 0 °C. When the addition was complete, the reaction was allowed to warm to room temperature and further stirred for 1 h. The reaction mixture was then neutralized with solid NaHCO_3 , diluted with demin. water (5 mL) and extracted three times with ethyl acetate (25 mL each). The combined organic layers were dried over sodium sulfate, filtered and evaporated. The crude product was obtained as an amber oil (50 mg, 69%). According to ^1H NMR the product contained 13 mol% TBTA.

^1H NMR (400 MHz, CD_3CN): δ = 8.80 (s, 1H, H_{triazole}), 8.42 – 8.41 (m, 3H, H_{triazole} (2H), H_{ar} (2H)), 8.31 (d, $^4J_{\text{H,H}} = 1.5$ Hz, 2H, H_{ar}), 8.00 – 7.94 (m, 2H, H_{ar}), 7.73 (s, 0.4 H, H_{triazole} TBTA), 7.40 – 7.31 (m, 1.2H, H_{ar} TBTA), 7.30 – 7.25 (m, 0.8H, H_{ar} TBTA), 7.20 – 7.18 (m, 2H, H_{ar}), 5.51 (s, 0.8H, $\text{CH}_{2,\text{triazole}}$), 4.61 – 4.59 (m, 4H, NCH_2), 3.96 – 3.89 (m, 4H, OCH_2), 3.65 – 3.47 (m, 21H, OCH_2 (20H), NCH_2 TBTA(0.8H)), 3.44 – 3.39 (m, 4H, OCH_2), 2.92 (s, 2H, OH) ppm;

^{13}C NMR (101 MHz, CD_3CN): δ = 148.1, 146.6, 140.9, 139.2, 134.5, 129.8, 129.2, 128.8, 128.4, 128.0, 124.7, 123.5, 123.0, 120.6, 120.1, 117.0, 73.2, 71.1, 71.1, 70.9, 70.9, 69.9, 61.9, 51.3 ppm, ^{13}C NMR spectrum contains four signals in the down field region (between 150 – 115 ppm) corresponding to TBTA; **LC-MS (ESI, +):** m/z (%) = 370.2 (100), 370.7 (46), 371.2 (12), 375.2 (35), 375.7 (16), 381.2 (14), 531.3 (59), 532.3 (23), 553.3 (19), 749.4 (20) $[\text{M}+\text{H}]^+$, 771.4 (10) $[\text{M}+\text{Na}]^+$; **HRMS (ESI, +):** calc. for $\text{C}_{34}\text{H}_{45}\text{N}_{12}\text{O}_8$ 749.3478 $[\text{M}+\text{H}]^+$, found 749.3477.

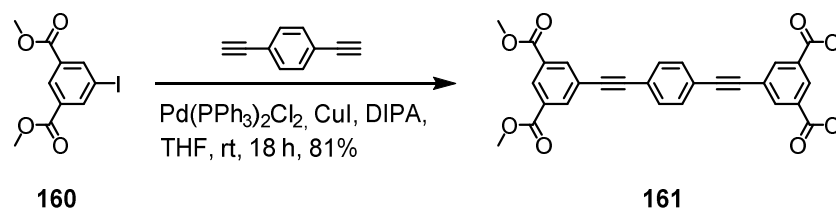
General Procedure for the OPE-based Rotaxane Test Systems

A test series composed of the two mono-stoppered OPE molecules **144** and **145** and the three stopper molecules **142**, **146** and **147** was performed by investigating various combinations of the reactants in their ability to form rotaxanes with cyclophane **81** via *click* chemistry:

OPE **144** and respectively **145** (1.00 μmol) was subjected to a 10 mL two-neck flask and 1.00 mL of a 1.00 mM solution of an azide-functionalized stopper (**142**, **146** or **147**) in water (1.00 μmol in 1.00 mL water) was added. The mixture was charged with cyclophane **81** (2.00 mg, 2.00 μmol). After flushing with argon for five min, copper(II)sulfate (0.08 mg, 0.50 μmol) and L(+)-ascorbic acid sodium salt (0.10 mg, 0.50 μmol) was added. The solution was put under argon again and was stirred at room temperature. Samples were taken and analyzed by HPLC-ESI-MS measurements, until the recorded chromatograms did not show any changes, typically after 15 hours.

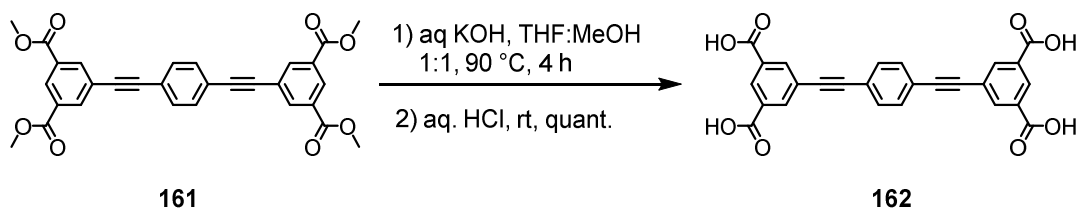
The reaction mixture comprising the combination of OPE **144** and stopper **142** was measured by high-resolution ESI-MS, confirming [2]rotaxane (M) formation:

HRMS (ESI, +): calc. for $\text{C}_{128}\text{H}_{172}\text{N}_{20}\text{NaO}_8$ 820.0844 $[\text{M}+\text{Na}]^{3+}$, found 820.0853.

Tetramethyl 5,5'-(1,4-phenylenebis(ethyne-2,1-diyl))diisophthalate (161)


In an oven-dried Schlenk tube dimethyl 5-iodoisophthalate (**160**) (558 mg, 1.74 mmol) and 1,4-diethynylbenzene (100 mg, 0.793 mmol) were dissolved in dry THF (10 mL) and diisopropylamine (3 mL) under argon atmosphere. The mixture was degassed by flushing with argon for 10 min. Afterwards, copper iodide (4.55 mg, 0.0238 mmol, 3 mol%) and bis-(triphenylphosphine)palladium chloride (16.9 mg, 0.0238 mmol, 2 mol%) was added and the reaction mixture was stirred at room temperature for 18 hrs. After one hour the solution was already cloudy due to a formed pale yellow precipitate. Tlc (SiO₂; dichloromethane) showed full conversion of the diacetylene and the ester (**160**). The precipitate was separated from the solvent by filtration, was washed with THF and then dissolved in DCM. The solution was extracted twice with demin. water. The combined organic layers were washed with brine, dried over sodium sulfate, filtered and the solvents were removed under reduced pressure. The product was obtained as an orange solid (327 mg, 81%).

¹H NMR (400 MHz, CDCl₃): δ = 8.64 (t, ⁴J_{H,H} = 1.6 Hz, 2H, *H_{ar}*), 8.37 (d, ⁴J_{H,H} = 1.7 Hz, 4H, *H_{ar}*), 7.55 (s, 4H, *H_{ar}*), 3.97 (s, 6H, CH₃) ppm; **¹³C NMR (101 MHz, CDCl₃):** δ = 165.7 (C_q, 4C, COOMe), 136.6 (C_t, 4C, CH_{ar}), 131.9 (C_t, 4C, CH_{ar}), 131.2 (C_t, 2C, CH_{ar}), 130.4 (C_q, 4C, CCOOMe), 124.2 (C_q, 2C, C_{q,ar}), 123.0 (C_q, 2C, C_{q,ar}), 90.9 (C_q, 2C, C≡C), 89.5 (C_q, 2C, C≡C), 52.7 (C_q, 4C, CH₃) ppm; **LC-MS (ESI, -):** m/z (%) = 453.3 (100) [M-H]⁻, 454.1 (32), 680.2 (16), 907.3 (46), 908.2 (26).

5,5'-(1,4-phenylenebis(ethyne-2,1-diyl))diisophthalic acid (162**)**

162 was synthesized according to a slightly modified procedure described in literature.^[156] Tetramethyl-5,5'-(1,4-phenylenebis(ethyne-2,1-diyl))diisophthalate (150 mg, 0.294 mmol) was dissolved in a mixture of MeOH/THF (1:1, 3 mL). After addition of aq. KOH (3 M, 6 mL, 18.0 mmol), the reaction mixture was heated under reflux for 4 hrs. Afterward, the solvent was evaporated under reduced pressure and the aq. solution was acidified with aq. HCl (6 M) to give a precipitate, which was filtered and dried in *vacuo*. Product **162** was obtained as a pale orange solid (133 mg, quant.).

¹H NMR (400 MHz, DMSO-*d*₆): δ = 13.59 (s, 4H, COOH), 8.46 (t, ⁴J_{H,H} = 1.6 Hz, 2H, *H*_{ar}), 8.28 (d, ⁴J_{H,H} = 1.6 Hz, 4H, *H*_{ar}), 7.71 (s, 4H, *H*_{ar}) ppm.

The spectroscopic data are in agreement with those previously reported.^[156]

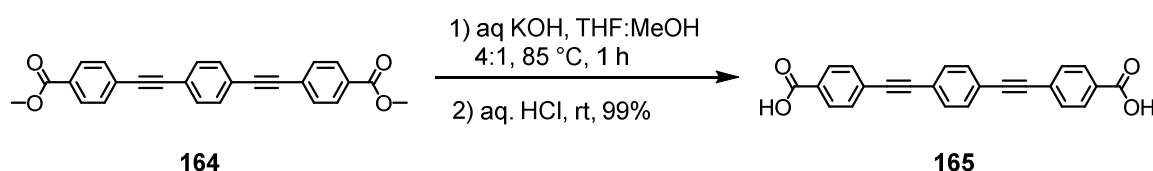
Dimethyl 4,4'-(1,4-phenylenebis(ethyne-2,1-diyl))dibenzoate (164**)**

An oven-dried Schlenk tube was charged with methyl 4-bromobenzoate (**163**, 114 mg, 0.524 mmol) and 1,4-diethynylbenzene (30.0 mg, 0.238 mmol) which were then dissolved in dry THF (5 mL) and diisopropylamine (1 mL) under argon atmosphere. The mixture was degassed by flushing with argon for 10 min. Afterwards, copper iodide (1.37 mg, 7.14 μ mol, 3 mol%) and bis(triphenylphosphine)palladium chloride (5.06 mg, 7.14 μ mol, 3 mol%) was added and the reaction mixture was stirred at 60 °C for 18 hrs. THF was removed under reduced pressure and the resulting solid was dissolved in DCM and charged with demin. water

(10 ml). In a separation funnel the layers were separated and the aqueous one was extracted with DCM twice. The combined organic layers were washed with brine, dried over sodium sulfate, filtered and the solvents were removed under reduced pressure. The brown crude product was purified by column chromatography (SiO₂; DCM) to obtain product **164** as a yellow solid (83.5 mg, 89%).

¹H NMR (500 MHz, CD₂Cl₂): δ = 8.05 – 8.00 (m, 4H, *H_{ar}*), 7.64 – 7.60 (m, 4H, *H_{ar}*), 7.57 – 7.55 (m, 4H, *H_{ar}*), 3.91 (s, 6H, CH₃) ppm; **¹³C NMR (126 MHz, CD₂Cl₂):** δ = 166.2 (C_q, 2C, C=O), 131.5 (C_t, 4C, CH_{ar}), 129.5 (C_t, 4C, CH_{ar}), 127.5 (C_q, 2C), 123.0 (C_t, 4C, CH_{ar}), 91.5 (C_q, 2C, C≡C), 90.6 (C_q, 2C, C≡C), 52.1 (C_p, 2C, CH₃) ppm. 2 x C_{q,ar} could not be observed.

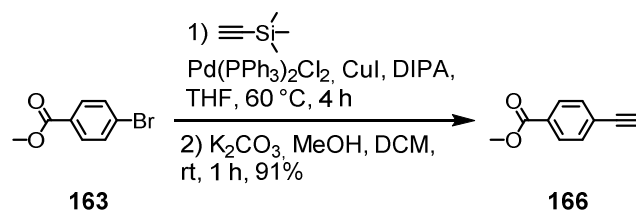
4,4'-(1,4-phenylenebis(ethyne-2,1-diyl))dibenzoic acid (**165**)



OPE **164** (11.0 mg, 0.0279 mmol) was dissolved in 2.5 mL of THF/methanol (4:1 v/v). Aqueous potassium hydroxide solution (3.0 M, 0.30 mL, 0.90 mmol) was added and the mixture was stirred at 85 °C for one hour. The reaction mixture was allowed to cool down to room temperature and was then charged dropwise with conc. hydrochloric acid, until the precipitation process was finished. The resulting colorless solid was filtered and dried *in vacuo*, affording **165** (10.1 mg) in a yield of 99%.

¹H NMR (400 MHz, DMSO-*d*₆): δ = 13.19 (s, 2H, COOH), 8.02 – 7.95 (m, 4H, *H_{ar}*), 7.75 – 7.68 (m, 4H, *H_{ar}*), 7.66 (s, 4H, *H_{ar}*) ppm; **¹³C NMR (101 MHz, DMSO):** δ = 166.6 (C_q, 2C, COOH), 131.9 (C_t, 4C, CH_{ar}), 131.6 (C_t, 4C, CH_{ar}), 130.8 (C_q, 2C, C_{ar}), 129.6 (C_t, 4C, CH_{ar}), 126.2 (C_q, 2C, C_{ar}), 122.4 (C_q, 2C, C_{ar}), 91.4 (C_q, 2C, C≡C), 90.8 (C_q, 2C, C≡C) ppm.

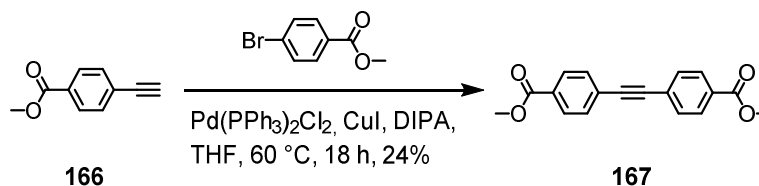
The spectroscopic data are in agreement with those reported previously.^[179]

Methyl 4-ethynylbenzoate (166)

166 was synthesized according to a slightly modified procedure described in literature.^[157] In an oven-dried Schlenk-tube, reactant **163** (93.0 mg, 0.428 mmol, 1.00 eq) was dissolved in 2 mL dry THF and 0.7 mL DIPA under argon atmosphere. The mixture was degassed by flushing with argon for 10 min. Afterwards, trimethylsilylacetylene (73.1 μL , 50.4 mg, 0.514 mmol, 1.20 eq), copper iodide (2.46 mg, 0.0128 mmol, 3 mol%) and bis(triphenylphosphine)-palladium chloride (9.10 mg, 0.0128 mmol, 3 mol%) were added and the reaction mixture was stirred for 4 hours at 60 °C. The solvents were removed under reduced pressure. Short column chromatography (SiO_2 ; dichloromethane) was performed. The dried product was dissolved in 1 mL dichloromethane and 0.3 mL methanol and was charged with potassium carbonate (119 mg, 0.86 mmol, 2.00 eq). After 1 hour stirring at room temperature, the solid was filtered off and column chromatographic purification was performed (SiO_2 ; dichloromethane), affording **166** (62.7 mg) in 91% yield.

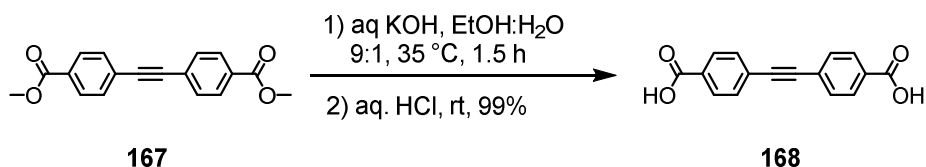
$^1\text{H NMR}$ (400 MHz, CDCl_3): δ = 7.92 – 7.87 (m, 2H, H_{ar}), 7.47 – 7.42 (m, 2H, H_{ar}), 3.82 (s, 3H, CH_3), 3.13 (s, 1H, $\text{C}\equiv\text{CH}$) ppm; $^{13}\text{C NMR}$ (101 MHz, CDCl_3): δ = 166.6 (C_q , 1C, $\text{C}=\text{O}$), 132.2 (C_t , 2C, CH_{ar}), 130.3 (C_q , 1C), 129.6 (C_t , 2C, C_{Har}), 126.9 (C_q , 1C), 82.9 (C_q , 1C, $\text{C}\equiv\text{CH}$), 80.2 (C_t , 1C, $\text{C}\equiv\text{CH}$), 52.4 (C_s , 1C, CH_3) ppm.

The spectroscopic data are in agreement with those reported previously.^[157]

Dimethyl 4,4'-(ethyne-1,2-diyl)dibenzoate (**167**)

In an oven-dried Schlenk tube, methyl 4-bromobenzoate (12.2 mg, 0.0562 mmol), acetylene **166** (9.00 mg, 0.0562 mmol) and bis(triphenylphosphine)palladium chloride (1.20 mg, 1.69 μmol , 3 mol%) were dissolved in dry THF (2 mL) and diisopropylamine (0.5 mL) under argon atmosphere. The mixture was degassed by flushing with argon for 10 min. Afterwards, copper iodide (0.716 mg, 1.69 μmol , 3 mol%) was added and the reaction mixture was stirred at 60 $^\circ\text{C}$ for 18 hrs. The solvents were evaporated and the resulting brown crude product was dissolved in dichloromethane and demin. water (10 mL) was added. The aqueous layer was extracted three times with dichloromethane (20 mL each). The combined organic layers were washed with brine, dried over sodium sulfate and the solvents were removed under reduced pressure. The brown solid was purified by column chromatography (SiO_2 ; dichloromethane) to obtain **167** in a yield of 24% (4.00 mg).

$^1\text{H NMR}$ (400 MHz, CDCl_3): δ = 8.08 – 7.99 (m, 4H, H_{ar}), 7.66 – 7.55 (m, 4H, H_{ar}), 3.94 (s, 6H, CH_3) ppm; $^{13}\text{C NMR}$ (101 MHz, CDCl_3): δ = 166.6 (C_q , 2C, $\text{C}=\text{O}$), 131.8 (C_t , 4C, CH_{ar}), 130.1 (C_q , 2C, C_{ar}), 129.7 (C_t , 4C, CH_{ar}), 127.5 (C_q , 2C, C_{ar}), 91.5 (C_q , 2C, $\text{C}\equiv\text{C}$), 52.4 (C_s , 2C, CH_3) ppm.

4,4'-(ethyne-1,2-diyl)dibenzoic acid (**168**)

4,4'-(ethyne-1,2-diyl)dibenzoic acid (**168**) was prepared according to a literature-known procedure.^[158] Compound **167** (3.50 mg, 0.0119 mmol, 1.00 eq) was dissolved in 1 mL of an ethanol/ mixture (9:1 v/v) and charged with potassium hydroxide (3.34 mg, 0.0595 mmol,

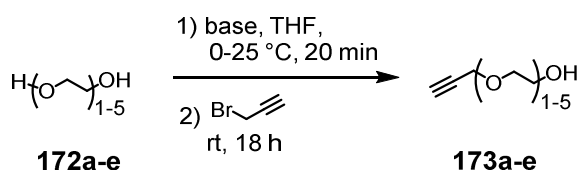
5.00 eq). The mixture was heated to 35 °C for 1.5 hours. Ethanol was removed under reduced pressure and 0.2 mL demin. water were added. The resulting aqueous solution was washed with dichloromethane and then acidified with conc. hydrochloric acid, until no more solid precipitated. The solid was filtered, washed with demin. water and dried *in vacuo*, affording product **168** (3.12 mg) in 99% yield.

The ^1H NMR sample was previously charged with 2 eq of KOH to form the potassium salt of **168**.

^1H NMR (400 MHz, Deuterium Oxide): $\delta = 7.89 - 7.81$ (m, 4H, H_{ar}), $7.66 - 7.59$ (m, 4H, H_{ar}) ppm.

The spectroscopic data are in agreement with those reported previously.^[158]

General procedure for the syntheses of **173a-e**



A 100 mL Schlenk tube was charged with the appropriate ethylene glycol derivative which was then diluted with dry THF (10% vv) under argon atmosphere. The solution was cooled to 0 °C with an ice-bath and base was then added portion-wise at 0 °C. Afterwards, the solution was allowed to warm up to room temperature and was stirred at this temperature for 20 min. Propargyl bromide solution (80% in toluene, 1.0 eq) was added dropwise and the reaction mixture was stirred for 18 hrs at room temperature. The solvent was removed under reduced pressure and the crude oil was purified via column chromatography.

2-(prop-2-yn-1-yloxy)ethan-1-ol (**173a**)

Ethylene glycol (7.76 g, 125 mmol, 6.99 mL, 5.0 eq), potassium hydroxide (3.30 g, 50.0 mmol, 2.0 eq), propargyl bromide solution (3.71 g, 25.9 mmol, 2.69 mL, 1.0 eq); column chromatography (SiO_2 ; dichloromethane: methanol 96:4); 66% yield (1.64 g); colorless oil.

^1H NMR (400 MHz, CDCl_3): $\delta = 4.21$ (d, $^4J_{H,H} = 2.4$ Hz, 2H, $\text{CH}_2\text{C}\equiv\text{CH}$), $3.80 - 3.75$ (m, 2H, CH_2), $3.69 - 3.64$ (m, 2H, CH_2), 2.46 (t, $^4J_{H,H} = 2.4$ Hz, 1H, $\text{C}\equiv\text{CH}$), 2.08 (s, 1H, OH) ppm.

The spectroscopic data are in agreement with those previously reported.^[159]

2-(2-(prop-2-yn-1-yloxy)ethoxy)ethan-1-ol (173b)

Diethylene glycol (9.65 g, 90.0 mmol, 8.69 mL, 2.0 eq), potassium *tert*-butoxide (5.26 g, 45.4 mmol, 1.01 eq), propargyl bromide solution (6.69 g, 45.0 mmol, 4.85 mL, 1.0 eq); column chromatography (SiO₂; ethyl acetate); 11% yield (700 mg); colorless oil.

¹H NMR (400 MHz, CDCl₃): δ = 4.20 (d, ⁴J_{H,H} = 2.4 Hz, 2H, CH₂C≡CH), 3.78 – 3.66 (m, 6H, CH₂), 3.64 – 3.57 (m, 2H, CH₂), 2.44 (t, ⁴J_{H,H} = 2.4 Hz, 1H, C≡CH) ppm.

The spectroscopic data are in agreement with those previously reported.^[160]

2-(2-(2-(prop-2-yn-1-yloxy)ethoxy)ethoxy)ethan-1-ol (173c)

Triethylene glycol (9.01 g, 59.4 mmol, 8.04 mL, 3.0 eq), sodium hydride 60% dispersion in mineral oil (800 mg, 20.0 mmol, 1.01 eq), propargyl bromide solution (2.94 g, 19.8 mmol, 2.13 mL, 1.0 eq); column chromatography (SiO₂; ethyl acetate); 78% yield (2.92 g); colorless oil.

¹H NMR (400 MHz, CDCl₃): δ = 4.20 (d, ⁴J_{H,H} = 2.4 Hz, 2H, CH₂C≡C), 3.75 – 3.64 (m, 10H, CH₂), 3.64 – 3.58 (m, 2H, CH₂OH), 2.43 (t, ⁴J_{H,H} = 2.4 Hz, 1H, C≡CH) ppm. The spectroscopic data are in agreement with those previously reported.^[161]

3,6,9,12-tetraoxapentadec-14-yn-1-ol (173d)

Tetraethylene glycol (25.0 g, 129 mmol, 22.3 mL, 2.80 eq), sodium hydride 60% dispersion in mineral oil (1.00 g, 41.7 mmol, 2.24 eq), propargyl bromide solution (2.76 g, 18.6 mmol, 2.00 mL, 1.00 eq); column chromatography (SiO₂; ethyl acetate); 90% yield (3.90 g); colorless oil.

¹H NMR (400 MHz, CDCl₃): δ = 4.21 (d, ⁴J_{H,H} = 2.4 Hz, 2H, CH₂C≡C), 3.77 – 3.64 (m, 14H, CH₂), 3.64 – 3.59 (m, 2H, CH₂), 2.64 (s, 1H, OH), 2.43 (t, ⁴J_{H,H} = 2.4 Hz, 1H, C≡CH) ppm.

The spectroscopic data are in agreement with those previously reported.^[162]

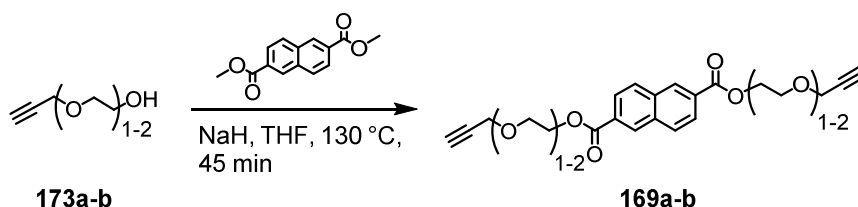
3,6,9,12,15-pentaaoctadec-17-yn-1-ol (173e)

Pentaethylene glycol (1.70 g, 7.11 mmol, 1.50 mL, 2.8 eq), sodium hydride 60% dispersion in mineral oil (101 mg, 2.51 mmol, 0.99 eq), propargyl bromide solution (378 mg, 2.54 mmol, 0.274 mL, 1.0 eq); column chromatography (SiO₂; ethyl acetate, 5% methanol); 41% yield (286 mg); colorless oil.

$^1\text{H NMR}$ (400 MHz, CDCl_3): δ = 4.21 (d, $^4J_{\text{H,H}} = 2.4$ Hz, 2H, $\text{CH}_2\text{C}\equiv\text{CH}$), 3.75 – 3.64 (m, 18H, CH_2), 3.64 – 3.58 (m, 2H, CH_2), 2.43 (t, $^4J_{\text{H,H}} = 2.4$ Hz, 1H, $\text{C}\equiv\text{CH}$) ppm.

The spectroscopic data are in agreement with those previously reported.^[163]

General procedure for the syntheses of 169a and 169b



A 10 mL-Schlenk tube was charged with sodium hydride 60% dispersion in mineral oil under argon atmosphere. A solution of **173a** or respectively **173b** in dry THF was added dropwise and the foaming suspension was stirred at room temperature, until the hydrogen formation stopped (2 min). Then the septum was loosened, 2,6-naphthalenedicarboxylic acid dimethyl ester was added and the reaction mixture was heated to 130 °C while slowly distilling off THF and formed methanol. After 45 min the suspension was allowed to cool to room temperature and was diluted with ethyl acetate and demin. water. The aqueous phase was extracted with ethyl acetate three times. The combined organic layers were washed with brine, dried over sodium sulfate, filtered and the solvents were removed under reduced pressure to afford a colorless solid.

Bis(2-(prop-2-yn-1-yloxy)ethyl) naphthalene-2,6-dicarboxylate (169a): Propargyl-ethylene glycol **173a** (205 mg, 2.05 mmol, 5.0 eq), sodium hydride 60% dispersion in mineral oil (32.7 mg, 818 μmol , 2.0 eq), 2,6-naphthalenedicarboxylic acid dimethyl ester (99.9 mg, 409 μmol , 1.0 eq), THF (50 mL); 42% yield (66.0 mg, 174 μmol); colorless solid.

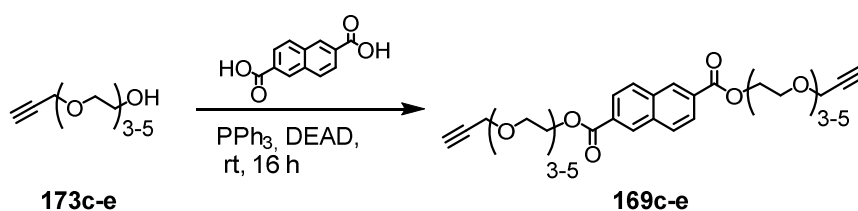
$^1\text{H NMR}$ (400 MHz, CDCl_3): δ = 8.68 – 8.65 (m, 2H, H_{ar}), 8.15 (dd, $^3J_{\text{H,H}} = 8.4$ Hz, $^4J_{\text{H,H}} = 1.6$ Hz, 2H, H_{ar}), 8.01 (d, $^3J_{\text{H,H}} = 8.6$ Hz, 2H, H_{ar}), 4.62 – 4.54 (m, 4H, OCH_2), 4.28 (d, $^3J_{\text{H,H}} = 2.4$ Hz, 4H, OCH_2), 3.97 – 3.91 (m, 4H, $\text{CH}_2\text{C}\equiv\text{CH}$), 2.47 (t, $^4J_{\text{H,H}} = 2.4$ Hz, 2H, $\text{CH}_2\text{C}\equiv\text{CH}$) ppm; $^{13}\text{C NMR}$ (101 MHz, CDCl_3): δ = 166.4 (C_q , 2C, $\text{C}=\text{O}$), 134.8 (C_q , 2C, C_{ar}), 131.0 (C_t , 2C, C_{ar}), 129.7 (C_t , 2C, C_{ar}), 129.6 (C_q , 2C, C_{ar}), 126.2 (C_t , 2C, C_{ar}), 79.4 (C_q , 2C, $\text{C}\equiv\text{CH}$), 75.1 (C_t , 2C, $\text{C}\equiv\text{CH}$), 67.9 (C_s , 2C,

CH₂), 64.4 (C_s, 2C, CH₂), 58.6 (C_s, 2C, CH₂) ppm; **HRMS (ESI, +)**: calc. for C₂₂H₂₀NaO₆ 403.1152 [M+Na]⁺, found 403.1157.

Bis(2-(2-(prop-2-yn-1-yloxy)ethoxy)ethyl) naphthalene-2,6-dicarboxylate (169b): Propargyl-ethylene glycol **173b** (488 mg, 3.38 mmol, 5.0 eq), sodium hydride 60% dispersion in mineral oil (27.1 mg, 677 μmol, 1.00 eq), 2,6-naphthalenedicarboxylic acid dimethyl ester (165 mg, 677 μmol, 1.00 eq), THF (30 mL); 14% yield (45.0 mg, 96 μmol); colorless solid.

¹H NMR (400 MHz, CDCl₃): δ = 8.66 – 8.62 (m, 2H, *H_{ar}*), 8.12 (dd, ³*J_{H,H}* = 8.5, ⁴*J_{H,H}* = 1.6 Hz, 2H, *H_{ar}*), 7.99 (d, ³*J_{H,H}* = 8.6 Hz, 2H, *H_{ar}*), 4.58 – 4.52 (m, 4H, OCH₂), 4.21 (d, ⁴*J_{H,H}* = 2.4 Hz, 4H, CH₂C≡CH), 3.92 – 3.83 (m, 4H, OCH₂), 3.78 – 3.70 (m, 8H, OCH₂), 2.41 (t, ⁴*J_{H,H}* = 2.4 Hz, 2H, CH₂C≡CH) ppm; **¹³C NMR (101 MHz, CDCl₃)**: δ = 166.4 (C_q, 2C, C=O), 134.7 8 (C_q, 2C, *C_{ar}*), 130.9 (C_t, 2C, *C_{ar}*), 129.7 (C_t, 2C, *C_{ar}*), 129.6 (C_q, 2C, *C_{ar}*), 126.2 (C_t, 2C, *C_{ar}*), 79.7 (C_q, 2C, C≡CH), 74.7 (C_t, 2C, C≡CH), 70.6 (C_s, 2C, CH₂), 69.4 (C_s, 2C, CH₂), 69.2 (C_s, 2C, CH₂), 64.5 (C_s, 2C, CH₂), 58.6 (C_s, 2C, CH₂) ppm; **HRMS (ESI, +)**: calc. for C₂₆H₂₉O₈ 469.11857 [M+H]⁺, found 469.1857; calc. for C₂₆H₂₈NaO₈ 491.1676 [M+Na]⁺, found 491.1682.

General procedure for the syntheses of 169c-e



To a suspension of the relevant propargyl ethylene glycol derivative **173c**, **173d** or **173e**, respectively, (2.0 eq), 2,6-naphthalene-dicarboxylic acid (1.0 eq) and triphenylphosphine (2.2 eq) in dry THF, a diethyl azodicarboxylate solution (DEAD) (40% in toluene, 2.2 eq) was slowly added under argon atmosphere. The suspensions turned into a clear, pale yellow solution. After stirring the mixture for 16 hrs, the solvents were removed and the crude yellow oil was subjected to demin. water (10 mL) and was extracted with methyl *tert*-butyl ether (100 mL) three times. The combined organic layers were washed with brine, dried over sodium

sulfate, filtered and the solvents were removed under reduced pressure. The crude product was purified by column chromatography.

Bis(2-(2-(2-(prop-2-yn-1-yloxy)ethoxy)ethoxy)ethyl) naphthalene-2,6-dicarboxylate (169c)

Propargyl-ethylene glycol **173c** (550 mg, 2.92 mmol, 2.0 eq), 2,6-naphthalenedicarboxylic acid (316 mg, 1.46 mmol, 1.0 eq), triphenylphosphine (842 mg, 3.21 mmol, 2.2 eq), DEAD (1.40 g, 3.21 mmol, 1.47 mL, 2.2 eq), dry THF (45 mL); column chromatography (Al₂O₃, basic; ethyl acetate); 82% yield (669 mg, 1.20 mmol); colorless solid.

¹H NMR (400 MHz, CDCl₃): δ = 8.67 – 8.63 (m, 2H, *H_{ar}*), 8.14 (dd, ³*J_{H,H}* = 8.5 Hz, ⁴*J_{H,H}* = 1.5 Hz, 2H, *H_{ar}*), 8.01 (d, *J* = 8.5 Hz, 2H, *H_{ar}*), 4.59 – 4.52 (m, 4H, OCOCH₂), 4.18 (d, ⁴*J_{H,H}* = 2.4 Hz, 4H, CH₂C≡CH), 3.92 – 3.84 (m, 4H, OCOCH₂CH₂), 3.79 – 3.73 (m, 4H, OCH₂), 3.72 – 3.66 (m, 12H, OCH₂), 2.40 (t, ⁴*J_{H,H}* = 2.4 Hz, 2H, C≡CH) ppm; **¹³C NMR (101 MHz, CDCl₃):** δ = 166.5 (C_q, 2C, C=O), 134.7 (C_q, 2C, *C_{ar}*), 130.9 (C_t, 2C, *C_{ar}*), 129.7 (C_t, 2C, *C_{ar}*), 129.6 (C_q, 2C, *C_{ar}*), 126.2 (C_t, 2C, *C_{ar}*), 79.8 (C_q, 2C, C≡CH), 74.7 (C_t, 2C, C≡CH), 70.9 (C_s, 2C, CH₂), 70.8 (C_s, 2C, CH₂), 70.7 (C_s, 2C, CH₂), 69.4 (C_s, 2C, CH₂), 69.3 (C_s, 2C, CH₂), 64.6 (C_s, 2C, CH₂), 58.6 (C_s, 2C, CH₂) ppm; **HRMS (ESI, +):** calc. for C₃₀H₃₆Na₂O₁₀ 301.1046 [M+2Na]²⁺, found 301.1048.

Di(3,6,9,12-tetraoxapentadec-14-yn-1-yl) naphthalene-2,6-dicarboxylate (169d)

Propargyl-ethylene glycol **173d** (729 mg, 3.14 mmol, 2.0 eq), 2,6-naphthalenedicarboxylic acid (339 mg, 1.57 mmol, 1.0 eq), triphenylphosphine (906 mg, 3.45 mmol, 2.2 eq), DEAD (1.50 g, 3.45 mmol, 1.48 mL, 2.2 eq), dry THF (45 mL); column chromatography (rp-SiO₂ C18; water:acetone 5:4); 64% yield (646 mg, 1.00 mmol); colorless solid.

¹H NMR (400 MHz, CDCl₃): δ = 8.68 – 8.63 (m, 2H, *H_{ar}*), 8.14 (dd, ³*J_{H,H}* = 8.4, ⁴*J_{H,H}* = 1.5 Hz, 2H, *H_{ar}*), 8.01 (d, ³*J_{H,H}* = 8.6 Hz, 2H, *H_{ar}*), 4.59 – 4.51 (m, 4H, OCOCH₂), 4.18 (d, ⁴*J_{H,H}* = 2.4 Hz, 4H, CH₂C≡CH), 3.93 – 3.86 (m, 4H, OCOCH₂CH₂), 3.75 – 3.72 (m, 4H, OCH₂), 3.71 – 3.58 (m, 20H, OCH₂), 2.42 (t, ⁴*J_{H,H}* = 2.4 Hz, 2H, C≡CH) ppm; **¹³C NMR (101 MHz, CDCl₃):** δ = 166.6 (C_q, 2C, C=O), 134.8 (C_q, 2C, *C_{ar}*), 131.0 (C_t, 2C, *C_{ar}*), 129.8 (C_t, 2C, *C_{ar}*), 129.7 (C_q, 2C, *C_{ar}*), 126.3 (C_t, 2C, *C_{ar}*), 79.9 (C_q, 2C, C≡CH), 74.8 (C_t, 2C, C≡CH), 71.0 (C_s, 2C, CH₂), 70.9 (C_s, 2C, CH₂), 70.9 (C_s, 2C, CH₂), 70.9 (C_s, 2C, CH₂), 70.7 (C_s, 2C, CH₂), 69.5 (C_s, 2C, CH₂), 69.3 (C_s, 2C, CH₂), 64.7 (C_s, 2C,

CH₂), 58.6 (C_s, 2C, CH₂) ppm; **HRMS (ESI, +)**: calc. for C₃₄H₄₄NaO₁₂ 667.2729 [M+Na]⁺, found 667.2725.

Di(3,6,9,12,15-pentaoxaoctadec-17-yn-1-yl) naphthalene-2,6-dicarboxylate (169e)

Propargyl-ethylene glycol **173e** (558 mg, 2.02 mmol, 2.0 eq), 2,6-naphthalenedicarboxylic acid (218 mg, 1.01 mmol, 1.0 eq), triphenylphosphine (583 mg, 2.22 mmol, 2.2 eq), DEAD (967 mg, 2.22 mmol, 1.02 mL, 2.2 eq), dry THF (30 mL); column chromatography (rp-SiO₂ C18; water:acetone 5:4); 44% yield (322 mg, 439 μmol); colorless solid.

¹H NMR (400 MHz, CDCl₃): δ 8.68 – 8.63 (m, 2H, *H_{ar}*), 8.14 (dd, ³*J_{H,H}* = 8.5, ⁴*J_{H,H}* = 1.6 Hz, 2H, *H_{ar}*), 8.01 (d, ³*J_{H,H}* = 8.6 Hz, 2H, *H_{ar}*), 4.58 – 4.52 (m, 4H, OCOCH₂), 4.19 (d, ⁴*J_{H,H}* = 2.4 Hz, 4H, CH₂C≡CH), 3.92 – 3.86 (m, 4H, OCOCH₂CH₂), 3.77 – 3.72 (m, 4H, OCH₂), 3.72 – 3.58 (m, 28H, OCH₂), 2.42 (t, ⁴*J_{H,H}* = 2.4 Hz, 2H, C≡CH) ppm; **¹³C NMR (101 MHz, CDCl₃)**: δ = 166.5 (C_q, 2C, C=O), 134.7 (C_q, 2C, *C_{ar}*), 130.9 (C_t, 2C, *C_{ar}*), 129.7 (C_t, 2C, *C_{ar}*), 129.6 (C_q, 2C, *C_{ar}*), 126.2 (C_t, 2C, *C_{ar}*), 79.8 (C_q, 2C, C≡CH), 77.4 (C_s, 2C, CH₂), 74.7 (C_t, 2C, C≡CH), 70.9 (C_s, 2C, CH₂), 70.8 (C_s, 2C, CH₂), 70.8 (C_s, 2C, CH₂), 70.8 (C_s, 2C, CH₂), 70.7 (C_s, 2C, CH₂), 70.6 (C_s, 2C, CH₂), 69.4 (C_s, 2C, CH₂), 69.2 (C_s, 2C, CH₂), 64.6 (C_s, 2C, CH₂), 58.5 (C_s, 2C, CH₂) ppm; **HRMS (ESI, +)**: calc. for C₃₈H₅₂NaO₁₄ 755.3249 [M+Na]⁺, found 755.3239.

General Procedure of the Screening Condition 1

A 10 mL two-neck flask was charged with the relevant naphthalene axle (1.00 μmol, 1.00 eq) to which then 1.55 mL of demin. water was added. In case of derivatives **169d** the flask was charged with the relevant substrate solution (1 mM in demin. water; 1.00 mL, 1.00 eq) and was then diluted with 0.55 mL of demin. water. A stock solution of stopper **142** (10 mM in demin. water; 200 μL, 2.00 eq) and cyclophane **81** (20 mM in demin. water; 50.0 μL, 1.00 eq) were added. After flushing with argon for 10 min. under vigorous stirring, the mixture of reactants was subjected to copper(II)sulfate stock solution (10 mM in demin. water; 100 μL, 1.00 eq) and L(+)-ascorbic acid sodium salt solution (10 mM in demin. water; 100 μL, 1.00 eq) and the mixture was again flushed with argon for 10 min. Two hours after addition of catalyst and reducing agent, a sample was taken and measured by HPLC-ESI-MS. In case of an

incomplete conversion of naphthalene rod or stopper, a sample was taken again after three hours, and respectively 21 hrs and analyzed by HPLC-LC-MS. The extracted mass peaks of the cyclophane and the products were integrated and quantitatively analyzed.

Table 5: Total concentrations and equivalents of reactants and reagents of the CuAAc screening under the three different conditions 1-3.

Cond.	cyclophane	axle	stopper	CuSO ₄	Na ascorb.	THPTA
1	1.0 mM (1.0 eq)	1.0 mM (1.0 eq)	2.0 mM (2.0 eq)	1.0 mM (1.0 eq)	1.0 mM (1.0 eq)	–
2	2.5 mM (5.0 eq)	1.0 mM (1.0 eq)	2.0 mM (2.0 eq)	1.0 mM (1.0 eq)	1.0 mM (1.0 eq)	–
3	1.0 mM (1.0 eq)	1.0 mM (1.0 eq)	2.0 mM (2.0 eq)	1.0 mM (1.0 eq)	1.0 mM (1.0 eq)	1.0 mM (1.0 eq)

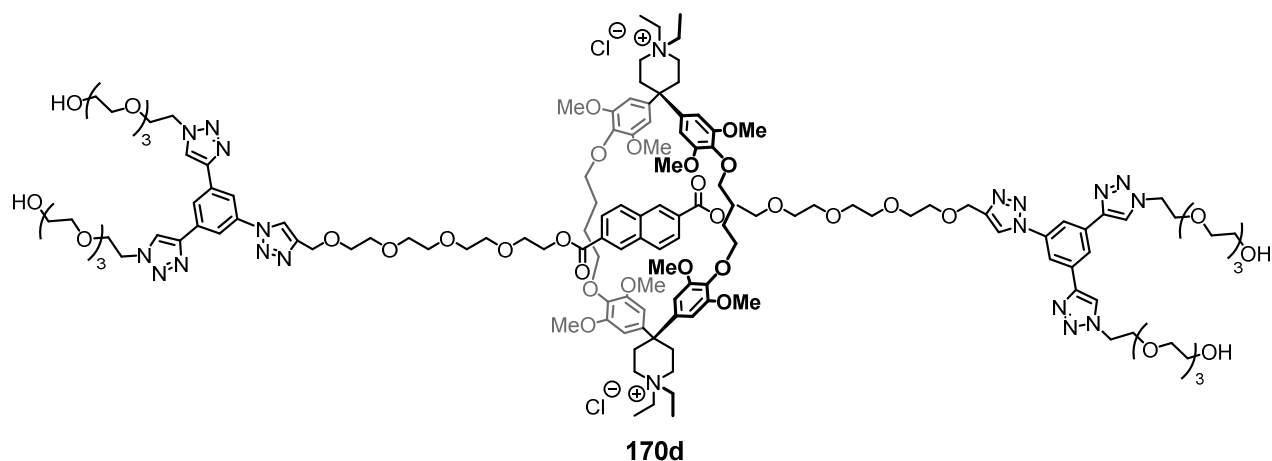
General Procedure of the Screening Condition 2

The procedure of screening conditions 2 resembled the one of variation 1. The difference between both conditions is the amount of cyclophane, the total concentration of the other reactants and reagents stayed the same. The screening reactions were performed with 5.00 eq of cyclophane **81** (20 mM in demin. water; 250.0 μ L) at which the same stock solution as in variation 1 was used. Consequently, the solid naphthalene rods **169a-c** (1.00 μ mol, 1.00 eq) were charged with 1.35 mL demin water, instead of 1.55 mL as in variation 1, whereas the naphthalene rod solutions of **169a-c** (1 mM in demin. water; 1.00 mL, 1.00 eq) were diluted with 0.35 mL demin. water, instead of 0.55 mL. The screening reactions were analyzed as in variation 1.

General Procedure of the Screening Condition 3

The procedure of screening conditions 2 resembled the reactions of variation 1. In contrast to screening variation 1, the reactions were performed with the aid of co-catalyst tris(3-hydroxypropyltriazolylmethyl)amine (10 mM in demin. water; 100 μ L, 1.00 eq). As a stock solution of the co-catalyst was used and to gain the same total concentration of all reactants the same as under conditions 1, the naphthalene rods **169a-c** were charged with 1.45 mL, or in case of **169d-e** diluted with 0.45 mL of demin. water. The screening reactions were analyzed as in variation 1.

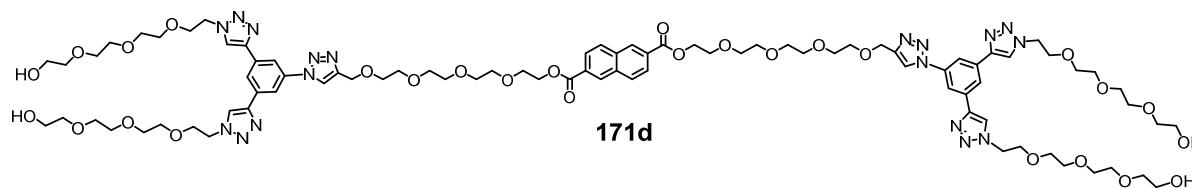
Rotaxane **170d**



In a 50 mL two-neck flask, stopper **142** (36.3 mg, 060 μ mol, 2.0 eq), naphthalene rod **169d** (19.3 mg, 30 μ mol, 1.0 eq) and cyclophane **81** (150 mg, 150 μ mol, 5.0 eq) were dissolved in miliQ water (6.0 mL) under argon atmosphere. The resulting pale orange solution was degassed by flushing with argon for 15 min. Afterwards, a copper(II)sulfate solution (10 mM in water, 3.00 mL, 30 μ mol, 1.0 eq), a L(+)-ascorbic acid sodium salt solution (10 mM in water, 3.00 mL, 30 μ mol, 1.0 eq) and tris(3-hydroxypropyltriazolylmethyl)amine (10 mM in water, 3.00 mL, 30 μ mol, 1.0 eq) were added and the solution was degassed again for 5 min. After stirring at room temperature for 2 hours, HPLC-ESI-MS was recorded which indicated full conversion of stopper **142**. After stirring for 3 hours and 20 minutes, the solvent was removed under reduced pressure. The solid crude product was dissolved in methanol (2.0 mL) and was subjected to a short column (Al_2O_3 , basic; methanol) for separating the copper species salts.

Further purification was performed via size exclusion chromatography (Sephadex LH20, methanol). The fractions containing rotaxane were combined, the eluate was concentrated *in vacuo* and the size exclusion procedure was repeated twice. Remaining twice-stoppered rod (7% according to ^1H NMR spectrum after 3 x size exclusion) was separated from the rotaxane by washing the solid product mixture with a small amount (0.3 mL) of acetone. In the end, the product was dissolved in acetonitrile: water (7:1) and passed through an ion exchange column (DOWEX, 1X8 400 Cl) affording 59.0 mg of product. According to the ^1H NMR spectrum, the product contains 22% of free cyclophane **81** resulting in a calculated yield of 59% for the pure rotaxane.

^1H NMR (600 MHz, Methanol- d_4): δ = 8.59 (s, 2H, H_{15}), 8.53 (s, 4H, H_9), 8.36 (t, $^4J_{H,H}$ = 1.5 Hz, 2H, H_{12}), 8.22 (d, $^4J_{H,H}$ = 1.5 Hz, 4H, H_{13}), 7.17 – 7.15 (m, 2H, H_{28}), 7.14 (s, 2H, H_{30}), 6.84 (s, 8H, H_G), 6.67 (d, J = 4.3 Hz, H_{impurity}), 6.61 (s, H_G , free cycloph), 5.47 (d, $^3J_{H,H}$ = 8.4 Hz, 2H, H_{29}), 4.71 (s, 4H, H_{17}), 4.68 – 4.64 (m, 8H, H_8), 4.49 – 4.45 (m, 4H, H_{25}), 3.97 (t, $^3J_{H,H}$ = 5.0 Hz, 8H, H_7), 3.95 – 3.89 (m, H_K , free cy), 3.83 – 3.81 (m, 4H, H_{24}), 3.78 – 3.39 (m, 112H, H_1 (8H), H_2 (8H), H_3 (8H), H_4 (8H), H_5 (8H), H_6 (8H), H_{18} (4H), H_{19} (4H), H_{20} (4H), H_{21} (4H), H_{22} (4H), H_{23} (4H), H_B (8H), H_C (8H), H_I (24H)), 2.99 (bs (NOESY), 8H, H_D), 2.78 (s, H_D , free cycloph), 2.69 – 2.62 (m, 8H, H_K), 1.77 (s, H_L , free cycloph), 1.33 (t, $^3J_{H,H}$ = 7.2 Hz, 12H, H_A), 1.30 – 1.29 (m, H_A , free cycloph), 1.00 – 0.98 (m, 8H, H_L) ppm; **^{13}C NMR (151 MHz, Methanol- d_4):** δ = 167.0 (C_q , 2C, C_{26}), 155.0 (C_q , 8C, C_H), 154.9 (C_q , 8C, $C_{H,cy}$ free), 147.2 (C_q , 2C, C_{16}), 147.0 (C_q , 4C, C_{10}), 139.4 (C_q , 2C, C_{14}), 136.9 (C_q , 4C, C_J , cy free), 136.5 (C_q , 4C, C_I), 134.9 (C_q , 2C, C_{31}), 134.6 (C_q , 4C, C_{11}), 131.1 (C_t , 2C, C_{30}), 130.6 (C_t , 2C, C_{29}), 129.8 (C_q , 2C, C_{27}), 125.9 (C_t , 2C, C_{28}), 124.2 (C_t , 4C, C_9), 123.5 (C_t , 2C, C_{12}), 123.3 (C_t , 2C, C_{15}), 117.4 (C_t , 4C, C_{13}), 105.4 (C_t , 8C, C_G , cy free), 104.1 (C_t , 8C, C_G), 73.6 (C_s , 4C, C_K), 72.9 (C_s , 4C, C_D), 71.7 (C_s , 2C, C_{19}), 71.7 (C_s , 2C, C_{21}), 71.7 (C_s , 2C, C_{23}), 71.5 (C_s , 8C, C_1 , C_3), 71.5 (C_s , 4C, C_5), 71.4 (C_s , 4C, C_6), 71.4 (C_s , 8C, C_2 , C_4), 71.1 (C_s , 6C, C_{18} , C_{20} , C_{22}), 70.4 (not assigned; corr. in HMQC with rotaxane sign. 3.97 ppm), 70.3 (C_s , 4C, C_7), 65.7 (C_s , 2C, C_{25}), 65.1 (C_s , 2C, C_{17}), 62.2 (not assigned; corr. in HMQC with rotaxane sign. 3.57 ppm), 57.1 (C_s , 4C, C_B), 57.0 (C_s , 4C, C_B , cy free), 56.9 (C_s , 4C, C_C , cy free), 56.9 (C_s , 4C, C_C), 56.8 (C_p , 8C, OCH_3 , C_{24}), 56.6 (C_p , 8C, C_I), 51.7 (C_s , 4C, C_8), (49.8), (45.6), 45.1 (C_q , 2C, C_E , cy free), (45.0), 44.6 (C_q , 2C, C_E), (30.5), 30.4 (not assigned; corr. in HMQC with free cyclophane sign. 1.71 ppm), (30.2), (29.5), (28.4), (27.6), 27.2 (C_s , 4C, C_L , cy free), 26.4 (C_s , 4C, C_L), 7.6 (C_s , 4C, C_A), 7.5 (C_s , 4C, C_A , cy free) ppm. The signal for C_q (expected at \sim 141 ppm) next to the spiro center was not observed; signals in brackets correspond to impurity; **HRMS (ESI, +):** calc. for $\text{C}_{144}\text{H}_{206}\text{N}_{20}\text{NaO}_{40}$ 959.4860 [$\text{M}+\text{Na}-2\text{Cl}$] $^{3+}$, found 959.4876.

Dumbbell 171d

In a 25 mL two-neck flask, stopper **142** (78.7 mg, 30 μmol , 2.70 eq) and axle **169d** (31.0 mg, 48.1 μmol , 1.0 eq) were dissolved in a 5:2 mixture of miliQ water and methanol (3.5 mL). The resulting solution was degassed by flushing with argon gas for 10 min. Afterwards, copper(II)sulfate (7.75 mg, 48.1 μmol , 1.0 eq) and L(+)-ascorbic acid sodium salt (9.53 mg, 48.1 μmol , 1.0 eq) was added and the solution was degassed again for further five min. After stirring at room temperature for 18 hours, LC-ESI-MS indicated full conversion of axle **169d**. The solvents were removed under reduced pressure and the crude product was purified by short column chromatography (Al_2O_3 , basic, EtOAc/MeOH: 7/1). The fractions which contained target compound were concentrated *in vacuo* and were subjected to preparative thin layer chromatography (Al_2O_3 , EtOAc/MeOH: 7/1), and the isolated compound was analyzed by ^1H NMR spectroscopy. One hour after concentration of the pure target compound at the rotary evaporator, the ester bonds of dumbbell **171d** were entirely cleaved, indicated by the single signal in the LC-ESI-MS T.I.C. chromatogram which corresponds to the proton adduct of the decomposition product (m/z 838).

^1H NMR (400 MHz, Methanol- d_4): δ = 8.71 (s, 2H, H_{15}), 8.68 (d, $^4J_{H,H}$ = 1.1 Hz, 2H, H_{30}), 8.61 (s, 4H, H_9), 8.47 (t, $^4J_{H,H}$ = 1.5 Hz, 2H, H_{12}), 8.35 (d, $^4J_{H,H}$ = 1.5 Hz, 4H, H_{13}), 8.12 (d, $^4J_{H,H}$ = 1.0 Hz, 4H, $H_{28}H_{29}$), 4.78 (s, 4H, H_{17}), 4.71 – 4.68 (m, 8H, H_8), 3.99 (s, 4H), 3.99 – 3.97 (m, 8H, H_7), 3.79 – 3.74 (m, 4H, H_{25}), 3.73 – 3.69 (m, 4H, H_{24}), 3.69 – 3.45 (m, 66H), 3.49 – 3.43 (m, 8H) ppm. Due to no available 2D NMR spectra, the peaks of dumbbell **171d** were assigned with the help of the spectra of corresponding reactant axle **169d**, stopper **142** and rotaxane **170d**.

8 Bibliography

- [1] J.-M. Lehn, *Angew. Chem. Int. Ed. Engl.* **1988**, *27*, 89–112.
- [2] G. Barin, R. S. Forgan, J. F. Stoddart, *Proc R Soc A* **2012**, *468*, 2849–2880.
- [3] J. F. Stoddart, *Chem. Soc. Rev.* **2009**, *38*, 1802–1820.
- [4] E. Wasserman, *J. Am. Chem. Soc.* **1960**, *82*, 4433–4434.
- [5] I. T. Harrison, S. Harrison, *J. Am. Chem. Soc.* **1967**, *89*, 5723–5724.
- [6] G. Schill, A. Lüttringhaus, *Angew. Chem. Int. Ed. Engl.* **1964**, *3*, 546–547.
- [7] C. O. Dietrich-Buchecker, J. P. Sauvage, J. P. Kintzinger, *Tetrahedron Lett.* **1983**, *24*, 5095–5098.
- [8] M. Cesario, C. O. Dietrich-Buchecker, J. Guilhem, C. Pascard, J. P. Sauvage, *J. Chem. Soc. Chem. Commun.* **1985**, 244–247.
- [9] E. A. Neal, S. M. Goldup, *Chem. Commun.* **2014**, *50*, 5128–5142.
- [10] P. R. Ashton, I. Baxter, S. J. Cantrill, M. C. T. Fyfe, P. T. Glink, J. F. Stoddart, A. J. P. White, D. J. Williams, *Angew. Chem. Int. Ed.* **1998**, *37*, 1294–1297.
- [11] J. Rotzler, M. Mayor, *Chem. Soc. Rev.* **2012**, *42*, 44–62.
- [12] C. J. Bruns, M. Frasconi, J. Iehl, K. J. Hartlieb, S. T. Schneebeli, C. Cheng, S. I. Stupp, J. F. Stoddart, *J. Am. Chem. Soc.* **2014**, *136*, 4714–4723.
- [13] S.-H. Chiu, S. J. Rowan, S. J. Cantrill, J. F. Stoddart, A. J. P. White, D. J. Williams, *Chem. Commun.* **2002**, 2948–2949.
- [14] H. W. Gibson, N. Yamaguchi, Z. Niu, J. W. Jones, C. Slebodnick, A. L. Rheingold, L. N. Zakharov, *J. Polym. Sci. Part Polym. Chem.* **2010**, *48*, 975–985.
- [15] X. Yan, D. Xu, X. Chi, J. Chen, S. Dong, X. Ding, Y. Yu, F. Huang, *Adv. Mater.* **2012**, *24*, 362–369.
- [16] X. Ji, S. Dong, P. Wei, D. Xia, F. Huang, *Adv. Mater.* **2013**, *25*, 5725–5729.
- [17] X. Ji, J. Li, J. Chen, X. Chi, K. Zhu, X. Yan, M. Zhang, F. Huang, *Macromolecules* **2012**, *45*, 6457–6463.
- [18] L. Fang, M. A. Olson, D. Benítez, E. Tkatchouk, W. A. G. Iii, J. F. Stoddart, *Chem. Soc. Rev.* **2009**, *39*, 17–29.
- [19] X. Yan, M. Zhou, J. Chen, X. Chi, S. Dong, M. Zhang, X. Ding, Y. Yu, S. Shao, F. Huang, *Chem. Commun.* **2011**, *47*, 7086–7088.
- [20] M. Miyauchi, Y. Kawaguchi, A. Harada, *J. Incl. Phenom. Macrocycl. Chem.* **2004**, *50*, 57–62.
- [21] M. C. Jiménez, C. Dietrich-Buchecker, J.-P. Sauvage, *Angew. Chem. Int. Ed.* **2000**, *39*, 3284–3287.
- [22] C. J. Bruns, J. F. Stoddart, *Acc. Chem. Res.* **2014**, *47*, 2186–2199.
- [23] S. Tsuda, Y. Aso, T. Kaneda, *Chem. Commun.* **2006**, 3072–3074.
- [24] L. Fang, M. Hmadeh, J. Wu, M. A. Olson, J. M. Spruell, A. Trabolsi, Y.-W. Yang, M. Elhabiri, A.-M. Albrecht-Gary, J. F. Stoddart, *J. Am. Chem. Soc.* **2009**, *131*, 7126–7134.
- [25] M. Hmadeh, L. Fang, A. Trabolsi, M. Elhabiri, A.-M. Albrecht-Gary, J. F. Stoddart, *J. Mater. Chem.* **2010**, *20*, 3422–3430.
- [26] G. Du, E. Moulin, N. Jouault, E. Buhler, N. Giuseppone, *Angew. Chem. Int. Ed.* **2012**, *51*, 12504–12508.
- [27] M. Xue, Y. Yang, X. Chi, X. Yan, F. Huang, *Chem. Rev.* **2015**, *115*, 7398–7501.
- [28] C. Reuter, W. Wienand, G. M. Hübner, C. Seel, F. Vögtle, *Chem. – Eur. J.* **1999**, *5*, 2692–2697.
- [29] R. Isnin, A. E. Kaifer, *J. Am. Chem. Soc.* **1991**, *113*, 8188–8190.
- [30] J. Yin, S. Dasgupta, J. Wu, *Org. Lett.* **2010**, *12*, 1712–1715.
- [31] A. Affeld, G. M. Hübner, C. Seel, C. A. Schalley, *Eur. J. Org. Chem.* **2001**, *2001*, 2877–2890.
- [32] Z.-J. Zhang, H.-Y. Zhang, H. Wang, Y. Liu, *Angew. Chem. Int. Ed.* **2011**, *50*, 10834–10838.
- [33] V. Aucagne, K. D. Hänni, D. A. Leigh, P. J. Lusby, D. B. Walker, *J. Am. Chem. Soc.* **2006**, *128*, 2186–2187.
- [34] O. A. Bozdemir, G. Barin, M. E. Belowich, A. N. Basuray, F. Beuerle, J. F. Stoddart, *Chem. Commun.* **2012**, *48*, 10401–10403.

- [35] S.-H. Ueng, S.-Y. Hsueh, C.-C. Lai, Y.-H. Liu, S.-M. Peng, S.-H. Chiu, *Chem. Commun.* **2008**, 817–819.
- [36] S. J. Rowan, J. F. Stoddart, *Polym. Adv. Technol.* **2002**, *13*, 777–787.
- [37] M. Zhang, S. Li, S. Dong, J. Chen, B. Zheng, F. Huang, *Macromolecules* **2011**, *44*, 9629–9634.
- [38] C. J. Pedersen, *J. Am. Chem. Soc.* **1967**, *89*, 7017–7036.
- [39] S. J. Cantrill, G. J. Youn, J. F. Stoddart, D. J. Williams, *J. Org. Chem.* **2001**, *66*, 6857–6872.
- [40] B. L. Allwood, H. Shahriari-Zavareh, J. F. Stoddart, D. J. Williams, *J. Chem. Soc. Chem. Commun.* **1987**, 1058–1061.
- [41] N. Yamaguchi, D. S. Nagvekar, H. W. Gibson, *Angew. Chem. Int. Ed.* **1998**, *37*, 2361–2364.
- [42] C. Zhang, S. Li, J. Zhang, K. Zhu, N. Li, F. Huang, *Org. Lett.* **2007**, *9*, 5553–5556.
- [43] B. Zheng, M. Zhang, S. Dong, J. Liu, F. Huang, *Org. Lett.* **2012**, *14*, 306–309.
- [44] X. Yan, D. Xu, X. Chi, J. Chen, S. Dong, X. Ding, Y. Yu, F. Huang, *Adv. Mater.* **2012**, *24*, 362–369.
- [45] M. Zhang, S. Li, S. Dong, J. Chen, B. Zheng, F. Huang, *Macromolecules* **2011**, *44*, 9629–9634.
- [46] S. J. Rowan, J. F. Stoddart, *Polym. Adv. Technol.* **2002**, *13*, 777–787.
- [47] X. Fu, Q. Zhang, S.-J. Rao, D.-H. Qu, H. Tian, *Chem. Sci.* **2016**, *7*, 1696–1701.
- [48] V. V. Rostovtsev, L. G. Green, V. V. Fokin, K. B. Sharpless, *Angew. Chem. Int. Ed.* **2002**, *41*, 2596–2599.
- [49] C. W. Tornøe, C. Christensen, M. Meldal, *J. Org. Chem.* **2002**, *67*, 3057–3064.
- [50] J. E. Hein, V. V. Fokin, *Chem. Soc. Rev.* **2010**, *39*, 1302–1315.
- [51] G. Wenz, B.-H. Han, A. Müller, *Chem. Rev.* **2006**, *106*, 782–817.
- [52] K. Hirotsu, T. Higuchi, K. Fujita, T. Ueda, A. Shinoda, T. Imoto, I. Tabushi, *J. Org. Chem.* **1982**, *47*, 1143–1144.
- [53] S. Tsukagoshi, A. Miyawaki, Y. Takashima, H. Yamaguchi, A. Harada, *Org. Lett.* **2007**, *9*, 1053–1055.
- [54] K. Iwaso, Y. Takashima, A. Harada, *Nat. Chem.* **2016**, *8*, 625–632.
- [55] R. E. Dawson, S. F. Lincoln, C. J. Easton, *Chem. Commun.* **2008**, 3980–3982.
- [56] S. Li, D. Taura, A. Hashidzume, A. Harada, *Chem. – Asian J.* **2010**, *5*, 2281–2289.
- [57] N. Miyaura, K. Yamada, A. Suzuki, *Tetrahedron Lett.* **1979**, *20*, 3437–3440.
- [58] Q.-C. Wang, X. Ma, D.-H. Qu, H. Tian, *Chem. – Eur. J.* **2006**, *12*, 1088–1096.
- [59] P. N. Taylor, M. J. O’Connell, L. A. McNeill, M. J. Hall, R. T. Aplin, H. L. Anderson, *Angew. Chem. Int. Ed.* **2000**, *39*, 3456–3460.
- [60] F. Cacialli, J. S. Wilson, J. J. Michels, C. Daniel, C. Silva, R. H. Friend, N. Severin, P. Samorì, J. P. Rabe, M. J. O’Connell, *Nat. Mater.* **2002**, *1*, 160–164.
- [61] M. T. Stone, H. L. Anderson, *Chem. Commun.* **2007**, 2387–2389.
- [62] C. A. Stanier, S. J. Alderman, T. D. W. Claridge, H. L. Anderson, *Angew. Chem. Int. Ed.* **2002**, *41*, 1769–1772.
- [63] J. Terao, A. Tang, J. J. Michels, A. Krivokapic, H. L. Anderson, *Chem. Commun.* **2004**, 56–57.
- [64] M. J. Frampton, H. L. Anderson, *Angew. Chem. Int. Ed.* **2007**, *46*, 1028–1064.
- [65] J. E. H. Buston, J. R. Young, H. L. Anderson, *Chem. Commun.* **2000**, 905–906.
- [66] K. Kim, *Chem. Soc. Rev.* **2002**, *31*, 96–107.
- [67] Y.-M. Jeon, D. Whang, J. Kim, K. Kim, *Chem. Lett.* **1996**, *25*, 503–504.
- [68] L. Cao, L. Isaacs, *Org. Lett.* **2012**, *14*, 3072–3075.
- [69] T. Ogoshi, S. Kanai, S. Fujinami, T. Yamagishi, Y. Nakamoto, *J. Am. Chem. Soc.* **2008**, *130*, 5022–5023.
- [70] H. Zhang, Y. Zhao, *Chem. – Eur. J.* **2013**, *19*, 16862–16879.
- [71] E. Ador, J. Crafts, *Berichte Dtsch. Chem. Ges.* **1877**, *10*, 2173–2176.
- [72] T. Ogoshi, T. Aoki, K. Kitajima, S. Fujinami, T. Yamagishi, Y. Nakamoto, *J. Org. Chem.* **2011**, *76*, 328–331.
- [73] M. Xue, Y. Yang, X. Chi, Z. Zhang, F. Huang, *Acc. Chem. Res.* **2012**, *45*, 1294–1308.
- [74] N. L. Strutt, H. Zhang, M. A. Giesener, J. Lei, J. F. Stoddart, *Chem. Commun.* **2012**, *48*, 1647–1649.

- [75] C. Li, X. Shu, J. Li, S. Chen, K. Han, M. Xu, B. Hu, Y. Yu, X. Jia, *J. Org. Chem.* **2011**, *76*, 8458–8465.
- [76] X.-B. Hu, L. Chen, W. Si, Y. Yu, J.-L. Hou, *Chem. Commun.* **2011**, *47*, 4694–4696.
- [77] Y. Ma, X. Ji, F. Xiang, X. Chi, C. Han, J. He, Z. Abliz, W. Chen, F. Huang, *Chem. Commun.* **2011**, *47*, 12340–12342.
- [78] N. L. Strutt, H. Zhang, S. T. Schneebeli, J. F. Stoddart, *Acc. Chem. Res.* **2014**, *47*, 2631–2642.
- [79] N. L. Strutt, R. S. Forgan, J. M. Spruell, Y. Y. Botros, J. F. Stoddart, *J. Am. Chem. Soc.* **2011**, *133*, 5668–5671.
- [80] T. Ogoshi, K. Demachi, K. Kitajima, T. Yamagishi, *Chem. Commun.* **2011**, *47*, 7164–7166.
- [81] Z. Zhang, Y. Luo, J. Chen, S. Dong, Y. Yu, Z. Ma, F. Huang, *Angew. Chem. Int. Ed.* **2011**, *50*, 1397–1401.
- [82] Z. Zhang, C. Han, G. Yu, F. Huang, *Chem. Sci.* **2012**, *3*, 3026–3031.
- [83] Z. Zhang, G. Yu, C. Han, J. Liu, X. Ding, Y. Yu, F. Huang, *Org. Lett.* **2011**, *13*, 4818–4821.
- [84] S. Gabriel, *Berichte Dtsch. Chem. Ges.* **1887**, *20*, 2224–2236.
- [85] L. Gao, Z. Zhang, B. Zheng, F. Huang, *Polym. Chem.* **2014**, *5*, 5734–5739.
- [86] A. Arduini, R. Ferdani, A. Pochini, A. Secchi, F. Ugozzoli, *Angew. Chem. Int. Ed.* **2000**, *39*, 3453–3456.
- [87] A. Credi, S. Dumas, S. Silvi, M. Venturi, A. Arduini, A. Pochini, A. Secchi, *J. Org. Chem.* **2004**, *69*, 5881–5887.
- [88] V. Zanichelli, G. Ragazzon, A. Arduini, A. Credi, P. Franchi, G. Orlandini, M. Venturi, M. Lucarini, A. Secchi, S. Silvi, *Eur. J. Org. Chem.* **2016**, *2016*, 1033–1042.
- [89] J. Bügler, N. A. J. M. Sommerdijk, A. J. W. G. Visser, A. van Hoek, R. J. M. Nolte, J. F. J. Engbersen, D. N. Reinhoudt, *J. Am. Chem. Soc.* **1999**, *121*, 28–33.
- [90] F. Vögtle, S. Meier, R. Hoss, *Angew. Chem. Int. Ed. Engl.* **1992**, *31*, 1619–1622.
- [91] C. A. Hunter, *J. Am. Chem. Soc.* **1992**, *114*, 5303–5311.
- [92] G. M. Hübner, J. Gläser, C. Seel, F. Vögtle, *Angew. Chem. Int. Ed.* **1999**, *38*, 383–386.
- [93] P. Ghosh, O. Mermagen, C. A. Schalley, *Chem. Commun.* **2002**, 2628–2629.
- [94] J. A. Wisner, P. D. Beer, M. G. B. Drew, M. R. Sambrook, *J. Am. Chem. Soc.* **2002**, *124*, 12469–12476.
- [95] N. H. Evans, P. D. Beer, *Chem. – Eur. J.* **2011**, *17*, 10542–10546.
- [96] R. H. Grubbs, *Angew. Chem. Int. Ed.* **2006**, *45*, 3760–3765.
- [97] N. L. Kilah, M. D. Wise, C. J. Serpell, A. L. Thompson, N. G. White, K. E. Christensen, P. D. Beer, *J. Am. Chem. Soc.* **2010**, *132*, 11893–11895.
- [98] G. T. Spence, C. J. Serpell, J. Sardinha, P. J. Costa, V. Félix, P. D. Beer, *Chem. – Eur. J.* **2011**, *17*, 12955–12966.
- [99] K. M. Mullen, J. Mercurio, C. J. Serpell, P. D. Beer, *Angew. Chem. Int. Ed.* **2009**, *48*, 4781–4784.
- [100] M. J. Langton, S. W. Robinson, I. Marques, V. Félix, P. D. Beer, *Nat. Chem.* **2014**, *6*, 1039–1043.
- [101] A. G. Johnston, D. A. Leigh, A. Murphy, J. P. Smart, M. D. Deegan, *J. Am. Chem. Soc.* **1996**, *118*, 10662–10663.
- [102] D. A. Leigh, A. Murphy, J. P. Smart, A. M. Z. Slawin, *Angew. Chem. Int. Ed. Engl.* **1997**, *36*, 728–732.
- [103] F. G. Gatti, D. A. Leigh, S. A. Nepogodiev, A. M. Z. Slawin, S. J. Teat, J. K. Y. Wong, *J. Am. Chem. Soc.* **2001**, *123*, 5983–5989.
- [104] S. Erbas-Cakmak, D. A. Leigh, C. T. McTernan, A. L. Nussbaumer, *Chem. Rev.* **2015**, *115*, 10081–10206.
- [105] A. M. Brouwer, C. Frochot, F. G. Gatti, D. A. Leigh, L. Mottier, F. Paolucci, S. Roffia, G. W. H. Wurpel, *Science* **2001**, *291*, 2124–2128.
- [106] M. Asakawa, G. Brancato, M. Fanti, D. A. Leigh, T. Shimizu, A. M. Z. Slawin, J. K. Y. Wong, F. Zerbetto, S. Zhang, *J. Am. Chem. Soc.* **2002**, *124*, 2939–2950.
- [107] M. N. Chatterjee, E. R. Kay, D. A. Leigh, *J. Am. Chem. Soc.* **2006**, *128*, 4058–4073.

- [108] C. Wu, P. R. Lecavalier, Y. X. Shen, H. W. Gibson, *Chem. Mater.* **1991**, *3*, 569–572.
- [109] M. C. Jiménez, C. Dietrich-Buchecker, J.-P. Sauvage, A. De Cian, *Angew. Chem. Int. Ed.* **2000**, *39*, 1295–1298.
- [110] V. Aucagne, J. Berná, J. D. Crowley, S. M. Goldup, K. D. Hänni, D. A. Leigh, P. J. Lusby, V. E. Ronaldson, A. M. Z. Slawin, A. Viterisi, *J. Am. Chem. Soc.* **2007**, *129*, 11950–11963.
- [111] J. D. Crowley, S. M. Goldup, A.-L. Lee, D. A. Leigh, R. T. McBurney, *Chem. Soc. Rev.* **2009**, *38*, 1530–1541.
- [112] J. D. Crowley, K. D. Hänni, A.-L. Lee, D. A. Leigh, *J. Am. Chem. Soc.* **2007**, *129*, 12092–12093.
- [113] D. J. Cram, H. Steinberg, *J. Am. Chem. Soc.* **1951**, *73*, 5691–5704.
- [114] B. Odell, M. V. Reddington, A. M. Z. Slawin, N. Spencer, J. F. Stoddart, D. J. Williams, *Angew. Chem. Int. Ed. Engl.* **1988**, *27*, 1547–1550.
- [115] P. L. Anelli, N. Spencer, J. F. Stoddart, *J. Am. Chem. Soc.* **1991**, *113*, 5131–5133.
- [116] I. Aprahamian, W. R. Dichtel, T. Ikeda, J. R. Heath, J. F. Stoddart, *Org. Lett.* **2007**, *9*, 1287–1290.
- [117] Y. Liu, A. H. Flood, P. A. Bonvallet, S. A. Vignon, B. H. Northrop, H.-R. Tseng, J. O. Jeppesen, T. Huang, B. Brough, M. Baller, *J. Am. Chem. Soc.* **2005**, *127*, 9745–9759.
- [118] F. Diederich, K. Dick, *Tetrahedron Lett.* **1982**, *23*, 3167–3170.
- [119] V. Balzani, L. de Cola, *Supramolecular Chemistry*, Springer Science & Business Media, **2012**.
- [120] F. Diederich, K. Dick, D. Griebel, *Chem. Ber.* **1985**, *118*, 3588–3619.
- [121] F. Diederich, *Angew. Chem. Int. Ed. Engl.* **1988**, *27*, 362, 362–386, 386.
- [122] S. B. Ferguson, E. M. Sanford, E. M. Seward, F. Diederich, *J. Am. Chem. Soc.* **1991**, *113*, 5410–5419.
- [123] S. B. Ferguson, E. M. Seward, F. Diederich, E. M. Sanford, A. Chou, P. Inocencio-Szweda, C. B. Knobler, *J. Org. Chem.* **1988**, *53*, 5593–5595.
- [124] D. R. Benson, J. Fu, C. K. Johnson, S. W. Pauls, D. A. Williamson, *J. Org. Chem.* **1998**, *63*, 9935–9945.
- [125] S. Anderson, H. L. Anderson, *Angew. Chem. Int. Ed. Engl.* **1996**, *35*, 1956–1959.
- [126] W. Eschweiler, *Berichte Dtsch. Chem. Ges.* **1905**, *38*, 880–882.
- [127] H. T. Clarke, H. B. Gillespie, S. Z. Weisshaus, *J. Am. Chem. Soc.* **1933**, *55*, 4571–4587.
- [128] S. Anderson, R. T. Aplin, T. D. W. Claridge, T. G. Iii, A. C. Maciel, G. Rumbles, J. F. Ryan, H. L. Anderson, *J. Chem. Soc. [Perkin 1]* **1998**, 2383–2398.
- [129] C. Glaser, *Ann. Chem. Pharm.* **1870**, *154*, 137–171.
- [130] C. Glaser, *Berichte Dtsch. Chem. Ges.* **1869**, *2*, 422–424.
- [131] P. N. Taylor, A. J. Hagan, H. L. Anderson, *Org. Biomol. Chem.* **2003**, *1*, 3851–3856.
- [132] S. Anderson, T. D. W. Claridge, H. L. Anderson, *Angew. Chem. Int. Ed. Engl.* **1997**, *36*, 1310–1313.
- [133] J. Rotzler, S. Drayss, O. Hampe, D. Häussinger, M. Mayor, *Chem. – Eur. J.* **2013**, *19*, 2089–2101.
- [134] J. S. Meisner, M. Kamenetska, M. Krikorian, M. L. Steigerwald, L. Venkataraman, C. Nuckolls, *Nano Lett.* **2011**, *11*, 1575–1579.
- [135] C. J. Muller, J. M. van Ruitenbeek, L. J. de Jongh, *Phys. C Supercond.* **1992**, *191*, 485–504.
- [136] M. A. Reed, C. Zhou, C. J. Muller, T. P. Burgin, J. M. Tour, *Science* **1997**, *278*, 252–254.
- [137] S. Grunder, R. Huber, V. Horhoiu, M. T. González, C. Schönenberger, M. Calame, M. Mayor, *J. Org. Chem.* **2007**, *72*, 8337–8344.
- [138] S. Wu, M. T. González, R. Huber, S. Grunder, M. Mayor, C. Schönenberger, M. Calame, *Nat. Nanotechnol.* **2008**, *3*, 569–574.
- [139] K. Sonogashira, Y. Tohda, N. Hagihara, *Tetrahedron Lett.* **1975**, *16*, 4467–4470.
- [140] S.-W. Tam-Chang, L. Jimenez, F. Diederich, *Helv. Chim. Acta* **1993**, *76*, 2616–2639.
- [141] P. Mattei, F. Diederich, *Helv. Chim. Acta* **1997**, *80*, 1555–1588.
- [142] T. Marti, B. R. Peterson, A. Fürer, T. Mordasini-Denti, J. Zarske, B. Jaun, F. Diederich, V. Gramlich, *Helv. Chim. Acta* **1998**, *81*, 109–144.
- [143] Grignard, V. C. R., *Acad. Sci* **1900**, *130*, 1322–1324.

- [144] Grignard, V., *Ann. Chim.* **1901**, *7*, 433–490.
- [145] X. Huang, Y. Han, Y. Wang, Y. Wang, *J. Phys. Chem. B* **2007**, *111*, 12439–12446.
- [146] C. J. Yu, Y. Chong, J. F. Kayyem, M. Gozin, *J. Org. Chem.* **1999**, *64*, 2070–2079.
- [147] F. Foucoin, C. Caupene, J.-F. Lohier, J. S. D. O. Santos, S. Perrio, P. Metzner, *Synthesis* **2007**, 1315–1324.
- [148] A. K. Flatt, S. M. Dirk, J. C. Henderson, D. E. Shen, J. Su, M. A. Reed, J. M. Tour, *Tetrahedron* **2003**, *59*, 8555–8570.
- [149] M. Iwamura, C. Hodota, M. Ishibashi, *Synlett* **1991**, *1991*, 35–36.
- [150] A. K. Singh, P. K. Khade, *Tetrahedron Lett.* **2005**, *46*, 5563–5566.
- [151] “Nanoelectronics - Uni Basel - Research in molecular electronics,” can be found under <https://nanoelectronics.unibas.ch/research/molecular.php>, **n.d.**
- [152] N. Agraït, A. L. Yeyati, J. M. van Ruitenbeek, *Phys. Rep.* **2003**, *377*, 81–279.
- [153] K. Balaraman, V. Kesavan, *Synthesis* **2010**, *2010*, 3461–3466.
- [154] T. Sandmeyer, *Berichte Dtsch. Chem. Ges.* **1884**, *17*, 2650–2653.
- [155] T. Sandmeyer, *Berichte Dtsch. Chem. Ges.* **1884**, *17*, 1633–1635.
- [156] D. Frahm, F. Hoffmann, M. Fröba, *Cryst. Growth Des.* **2014**, *14*, 1719–1725.
- [157] J. Li, J. Zhang, H. Tan, D. Z. Wang, *Org. Lett.* **2015**, *17*, 2522–2525.
- [158] T. Gadzikwa, B.-S. Zeng, J. T. Hupp, S. T. Nguyen, *Chem. Commun.* **2008**, 3672–3674.
- [159] T. Mayer, M. E. Maier, *Eur. J. Org. Chem.* **2007**, *2007*, 4711–4720.
- [160] V. Percec, P. Leowanawat, H.-J. Sun, O. Kulikov, C. D. Nusbaum, T. M. Tran, A. Bertin, D. A. Wilson, M. Peterca, S. Zhang, *J. Am. Chem. Soc.* **2013**, *135*, 9055–9077.
- [161] D. Mertz, C. J. Ochs, Z. Zhu, L. Lee, S. N. Guntari, G. K. Such, T. K. Goh, L. A. Connal, A. Blencowe, G. G. Qiao, *Chem. Commun.* **2011**, *47*, 12601–12603.
- [162] S. Asano, J. Gavriilyuk, D. R. Burton, C. F. Barbas, *ACS Med. Chem. Lett.* **2014**, *5*, 133–137.
- [163] J. Diot, M. I. García-Moreno, S. G. Gouin, C. O. Mellet, K. Haupt, J. Kovensky, *Org. Biomol. Chem.* **2008**, *7*, 357–363.
- [164] O. Mitsunobu, M. Yamada, T. Mukaiyama, *Bull. Chem. Soc. Jpn.* **1967**, *40*, 935–939.
- [165] O. Mitsunobu, M. Yamada, *Bull. Chem. Soc. Jpn.* **1967**, *40*, 2380–2382.
- [166] G. Chen, M. Jiang, *Chem. Soc. Rev.* **2011**, *40*, 2254–2266.
- [167] P. R. Ashton, R. Ballardini, V. Balzani, M. Gómez-López, S. E. Lawrence, M. V. Martínez-Díaz, M. Montalti, A. Piersanti, L. Prodi, J. F. Stoddart, *J. Am. Chem. Soc.* **1997**, *119*, 10641–10651.
- [168] M. B. Nielsen, J. O. Jeppesen, J. Lau, C. Lomholt, D. Damgaard, J. P. Jacobsen, J. Becher, J. F. Stoddart, *J. Org. Chem.* **2001**, *66*, 3559–3563.
- [169] T. R. Chan, R. Hilgraf, K. B. Sharpless, V. V. Fokin, *Org. Lett.* **2004**, *6*, 2853–2855.
- [170] V. Hong, S. I. Presolski, C. Ma, M. G. Finn, *Angew. Chem. Int. Ed.* **2009**, *48*, 9879–9883.
- [171] D. B. Smithrud, T. B. Wyman, F. Diederich, *J. Am. Chem. Soc.* **1991**, *113*, 5420–5426.
- [172] D. H. Wu, A. D. Chen, C. S. Johnson, *J. Magn. Reson. A* **1995**, *115*, 260–264.
- [173] M. Holz, H. Weingartner, *J. Magn. Reson.* **1969** **1991**, *92*, 115–125.
- [174] P. Thordarson, in *Supramol. Chem.* (Eds.: P.A. Gale, J.W. Steed), John Wiley & Sons, Ltd, Chichester, UK, **2012**.
- [175] S. Goeb, R. Ziessel, *Org. Lett.* **2007**, *9*, 737–740.
- [176] T. Weil, E. Reuther, C. Beer, K. Müllen, *Chem. – Eur. J.* **2004**, *10*, 1398–1414.
- [177] O. Lavastre, L. Ollivier, P. H. Dixneuf, S. Sibandhit, *Tetrahedron* **1996**, *52*, 5495–5504.
- [178] T. Peterle, P. Ringler, M. Mayor, *Adv. Funct. Mater.* **2009**, *19*, 3497–3506.
- [179] L. M. Ballesteros, S. Martín, J. Cortés, S. Marqués-González, S. J. Higgins, R. J. Nichols, P. J. Low, P. Cea, *Chem. – Eur. J.* **2013**, *19*, 5352–5363.

9 Appendix

9.1 Abbreviations

δ_{agg}	chemical shift of aggregate
δ_{mon}	chemical shift of monomer
δ_{obs}	observed chemical shift
δ	chemical shift
ΔG°	Gibbs free energy
λ	wavelength
Å	Ångström
AFM	atomic force microscopy
ar	aryl
B21C7	benzo-21-crown-7
BIPY	bipyridine
BMP32C10	bis(<i>m</i> -phenylene)-32-crown-10
<i>c</i>	concentration
C_{agg}	concentration of aggregate
<i>cac</i>	critical aggregation concentration
CB	cucurbituril
CBPQT ⁴⁺	tetracationic cyclobis(paraquat- <i>p</i> -phenylene)
CD	cyclodextrin
C_{mon}	concentration of monomer
C_p	primary carbon
C_q	quaternary carbon
C_s	secondary carbon
C_t	tertiary carbon
C_{tot}	total concentration
CuAAC	copper(I)-catalyzed alkyne-azide cycloaddition
CV	cyclic voltammetry
DB24C8	dibenzo-24-crown-8
<i>D</i>	diffusion coefficient

DCM	dichloromethane
DIPA	diisopropylamine
DMSO	dimethyl sulfoxide
DOSY	diffusion ordered spectroscopy
dpp	2,9-diphenyl-1,10-phenanthroline
EG	ethylene glycol
EPR	electron paramagnetic resonance
eq	equivalents
ESI	electrosprays
<i>G</i>	conductance
h	hour
HH	head-head
HOP	dimethylpropargyl alcohol
HPLC	high-performance liquid chromatography
HT	head-tail
hrs	hours
K	Kelvin
K_a	association constant
LC	liquid chromatography
m	multiplett
M	molar
m/z	mass-to-charge ratio
MCBJ	mechanically controllable break junction
MIM	mechanically interlocked molecule
min	minute
MS	mass spectrometry
n	number
N	aggregation number
nm	nanometer
NMR	nuclear magnetic resonance
NOESY	nuclear Overhauser effect spectroscopy
NP	naphthalene

OPE	oligophenylene ethynylene
ppm	parts per million
quant.	quantitative
R	residual group
r_H	hydrodynamic radius
rt	room temperature
s	singlet
SEM	single electron microscopy
SEtTMS	S-ethyl trimethylsilyl
t	triplet
TBAF	tetrabutylammonium fluoride
TBAH	tetrabutylammonium hydroxide
TEM	transmission electron microscopy
THF	tetrahydrofuran
TIPS	triisopropylsilyl
TIPSA	triisopropylsilylacetylene
T.I.C.	total ion current
TLC	thin layer chromatography
TMS	trimethylsilyl
TMSA	trimethylsilylacetylene
TT	tail-tail
TTF	tetrathiafulvalene
UV	ultraviolet
V_{agg}	volume of aggregate
VIS	visible
V_{mon}	volume of monomer
z	distance

9.2 Contributions

My colleague Yves Aeschi synthesized important compounds, as indicated at the relevant passages in this thesis. During his “Wahlpraktikum” Rajesh Mannancherry helped to prepare building blocks for the synthesis of amphiphiles **92-95** and did a scale-up of the cyclophane **96** preparation. During their “Nanopraktikum” or “Schlussversuche” Niels Burzan, Lukas Gubser and Severin Freud supported the preparation of building blocks of amphiphiles **92-95**. The MCBJ conductance measurements were performed by Anton Vladyka from the group of Prof. Dr. Michel Calame at the University of Basel. PD Dr. Daniel Häussinger performed the DOSY measurements, determined the corresponding diffusion coefficients and helped to develop the indirect evaluation method described in Chapter 2. The compound for the diffusion-based analysis of amphiphile **92** was prepared by Dr. Jürgen Rotzler. 2D-NMR spectra were recorded by PD Dr. Daniel Häussinger and Kaspar Zimmermann, who did the full assignment of the signals of amphiphile **92** and the nonquaternized precursor **116**. The NMR signals of rotaxane **170d** were assigned by Felix Raps. All high-resolution ESI-MS spectra were recorded by Dr. Heinz Nadig. The basic structure for all pictures were made by Dr. Michel Rickhaus.

9.3 Chromatograms of Screening Reactions

Penta-EG naphthalene ester axle (169e):

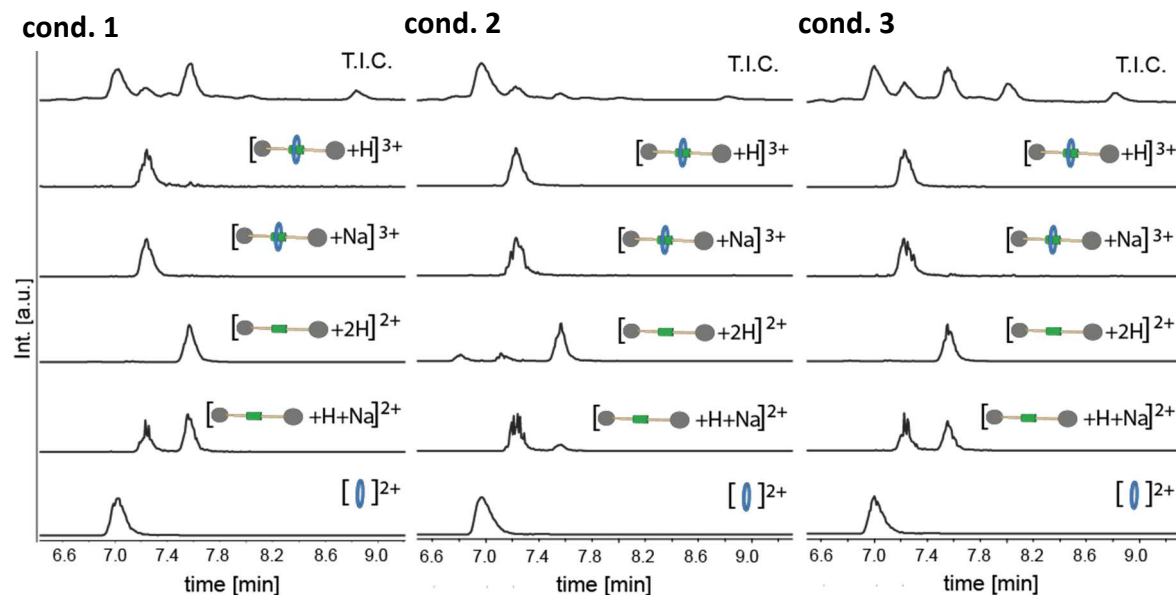


Figure 83. Screening reactions after **two hours** with *penta*-EG naphthalene ester axle **169e** under the three different conditions 1-3. A signal for stopper **142** is not observed; the low signals with retention time $t_R = 8.0$ min and $t_R = 8.9$ min corresponds to some single-stoppered and unconsumed axle **169e**, respectively.

Tri-EG naphthalene ester axle (169c), after 2 hours:

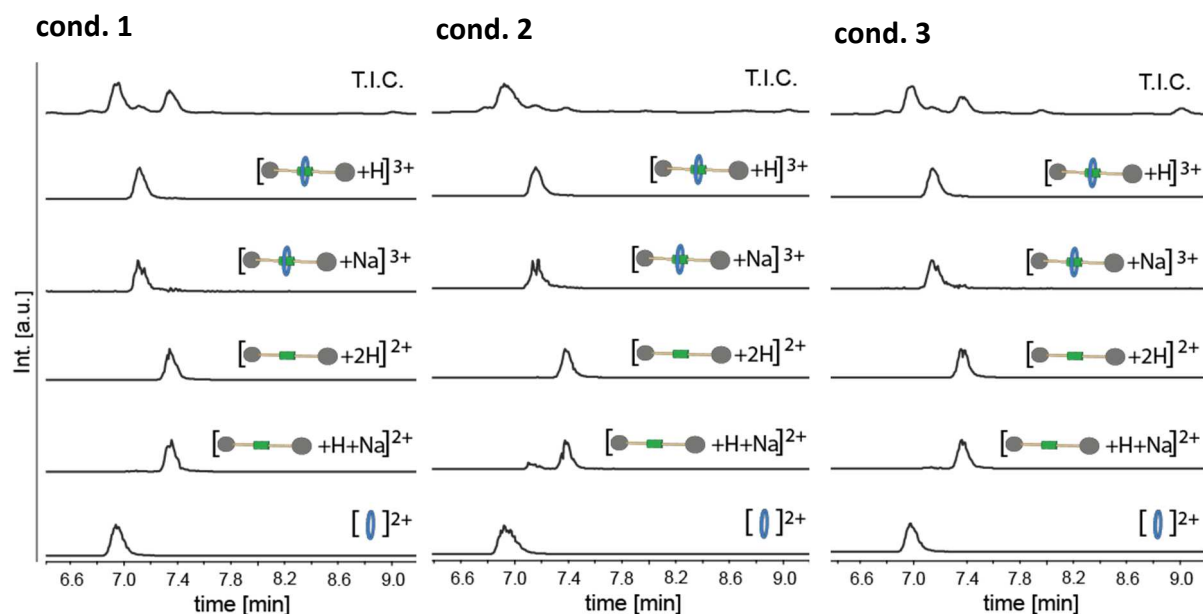


Figure 84. Screening reactions after **two hours** with *tri*-EG naphthalene ester axle **169c** under the three different conditions 1-3. A signal corresponding to stopper **142** ($t_R = 6.5$ min) is not observed in neither of the three T.I.C.s, whereas the low signal under condition 3 indicates some unconsumed axle **169c** ($t_R = 9.0$ min).

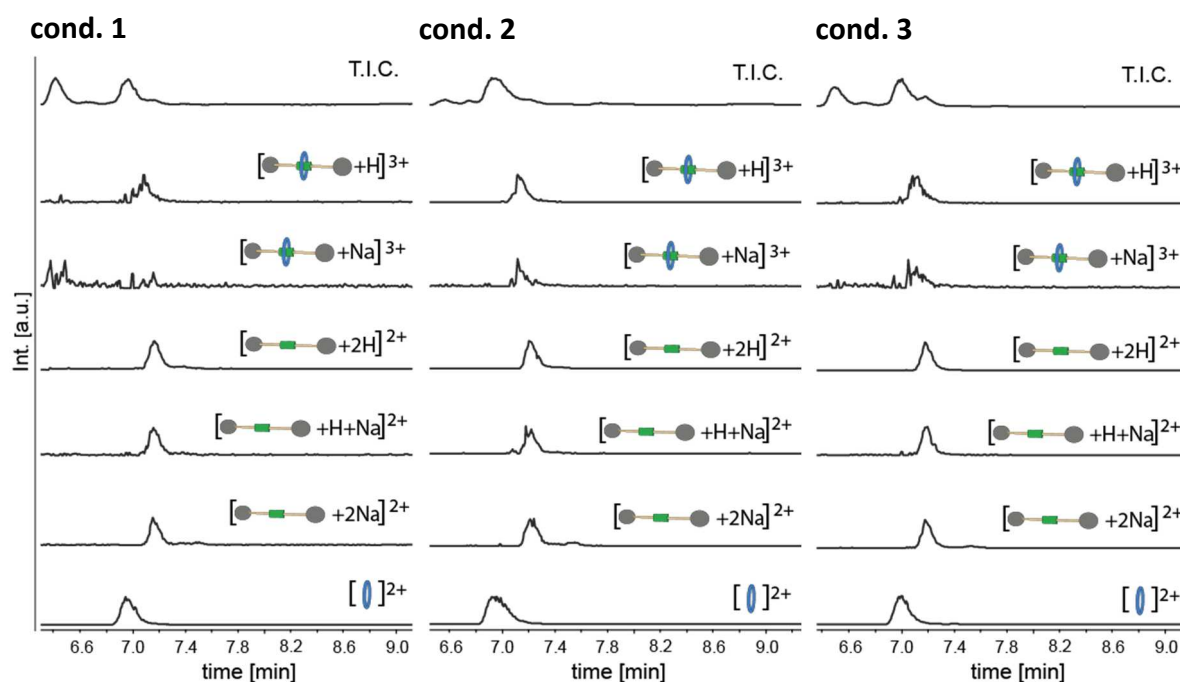
Di-EG naphthalene ester axle (169b), after 2 hours:

Figure 85. Screening reactions after **two hours** with *di*-EG naphthalene ester axle **169b** under the three different conditions 1-3. The signal at $t_R = 6.5$ min in each T.I.C. corresponds to stopper **142** and indicates incomplete conversion after two hours; axle **169b** cannot be observed due to its insolubility in pure water.

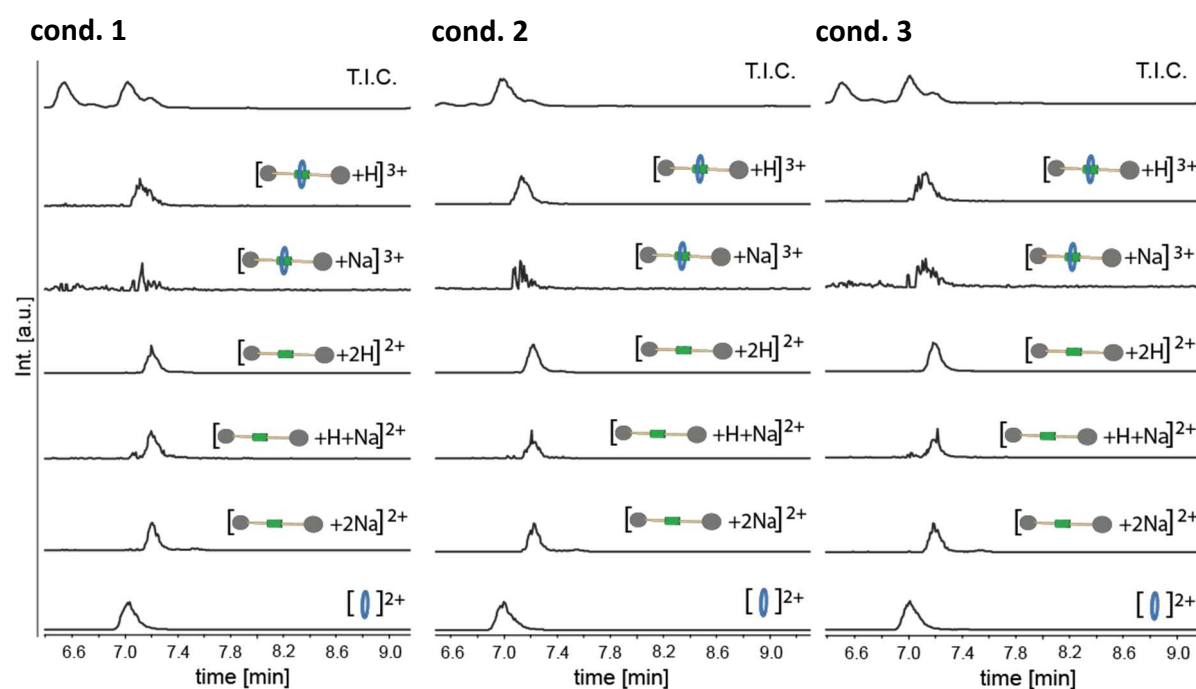
Di-EG naphthalene ester axle (169b), after 21 hours:

Figure 86. Screening reactions after **21 hours** with *di*-EG naphthalene ester axle **169b** under the three different conditions 1-3. The signal at $t_R = 6.5$ min in each T.I.C. corresponds to stopper **142** and indicates incomplete conversion after two hours; axle **169b** cannot be observed due to its insolubility in pure water.

Mono-EG naphthalene ester axle (169a), after 2 hours:

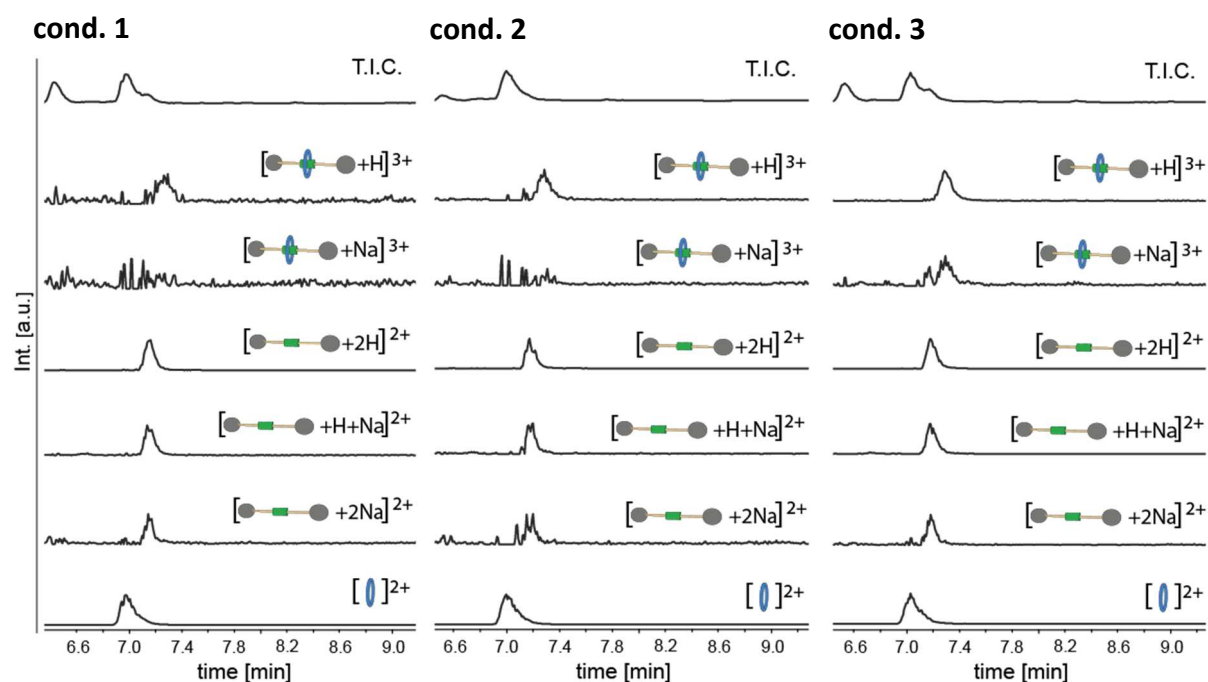


Figure 87. Screening reactions after **two hours** with **mono-EG naphthalene ester axle 169a** under the three different conditions 1-3. The signal at $t_R = 6.5$ min in each T.I.C. corresponds to stopper **142** and indicates incomplete conversion after two hours; axle **169a** cannot be observed due to its insolubility in pure water.

Mono-EG naphthalene ester axle (169a), 21 hours:

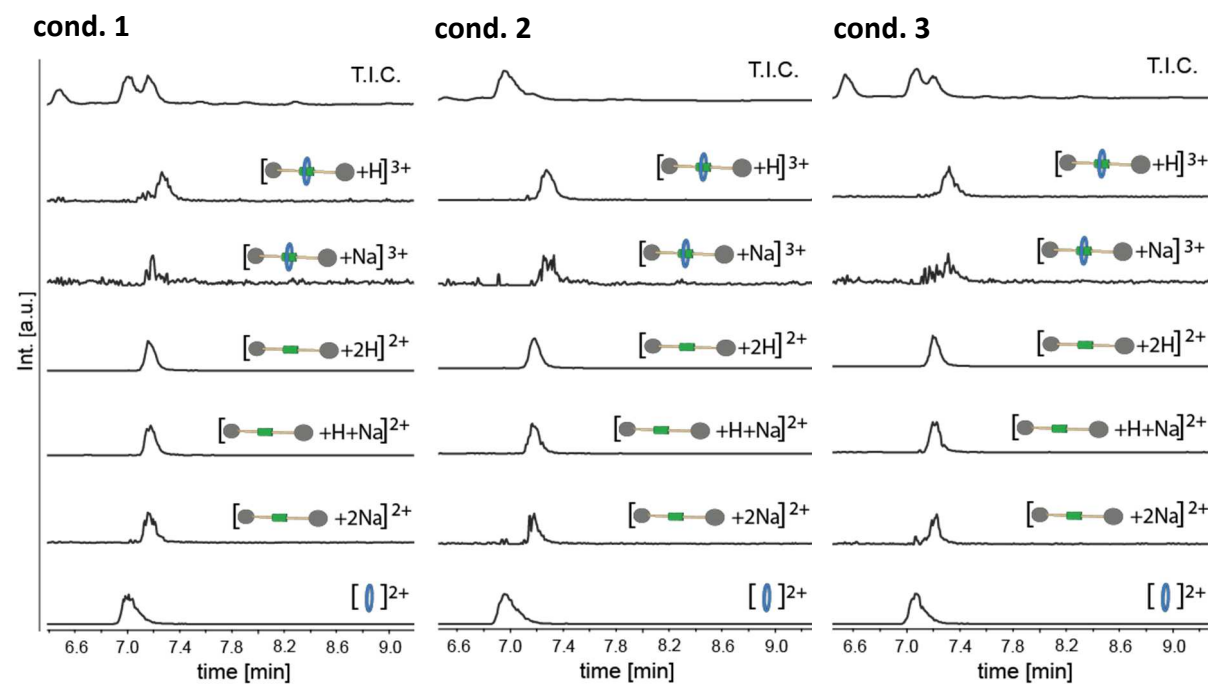


Figure 88. Screening reactions after **two hours** with **mono-EG naphthalene ester axle 169a** under the three different conditions 1-3. The signal at $t_R = 6.5$ min in each T.I.C. corresponds to stopper **142** and indicates incomplete conversion after two hours; axle **169a** cannot be observed due to its insolubility in pure water.